LOWERING OF THE WATER TABLE, IRRIGATION POLICY CHANGE AND ITS INFLUENCE ON THE GROUNDWATER ARSENIC CONTAMINATION PROBLEM IN BANGLADESH

By

Md. Nazrul Islam

A DISSERTATION

Submitted to

Michigan State University

In partial fulfillment of the requirements

For the degree of

DOCTOR OF PHILOSOPHY

Biosystem Engineering

Agricultural Engineering Department

2003

ABSTRACT

LOWERING OF THE WATER TABLE, IRRIGATION POLICY CHANGE AND ITS INFLUENCE ON THE GROUNDWATER ARSENIC CONTAMINATION PROBLEM IN BANGLADESH

By

Md. Nazrul Islam

This study is based on the hypothesis that shortage of dissolved oxygen at and below the water table and extraction of groundwater by irrigation wells at a rate greater than the aquifer recharge rate are the main causes of arsenic release in the groundwater of Bangladesh. The main purpose of this study was to identify the processes that produce high arsenic concentrations in the groundwater system and to formulate a quantitative irrigation development policy for Bangladesh. This dissertation evaluated the currently existing oxidation and reduction theories of arsenic release from the context of dissolved oxygen shortage in recharging groundwater. This study also conducted both numerical and thermodynamic analyses to demonstrate how the oxidation theory of arsenic release was not adequate to explain the cause of arsenic release in the groundwater system and how shortage of dissolved oxygen in recharging groundwater at and below the water table produces high arsenic concentrations.

This study focused on quantitative analysis of the oxygen diffusion rate in deeper layers of the arsenic-contaminated aquifer and the variations in redox potentials over the aquifer's depths in order to evaluate the oxidation and reduction theory of arsenic release. This study also computed the amount of

shallow aquifer recharge (SAR) available and the amount of groundwater flow passing through the deeper layers of the aquifer in order to establish a relation between lowering of the water table, the tube well extraction rate, and the likelihood of arsenic migration from the currently contaminated layers to uncontaminated deeper layers of the aquifer.

Based on the dissertation's main findings, it can be concluded that variable management decisions such as the tube well extraction rate, increased irrigation system efficiencies, shifted and adjusted cropping patterns and seasons, rainwater harvesting, and avoidance of pumping from the top layers of the aquifer can improve the control of the system and reduce the risk of arsenic migration.

ACKNOWLEDGEMENTS

Committee chairman Dr. R.D. von Bernuth deserves special recognition for generously taking me under his wings and expertly guiding me throughout all stages of my coursework and dissertation. Dr. Bernuth's exceptional intelligence, humanity, patience and calming influence were especially helpful and appreciated throughout my dissertation period. He is real teacher and I am very much grateful to him for his major contribution to complete this dissertation.

Committee member Dr. S. Davies deserves special recognition for his valuable guidance on the complicated geochemical issues and thermodynamic analysis of this dissertation. Committee member Dr. William Northcott deserves special recognition for offering me excellent advice on handling the GIS issues. Committee member Dr. Karen Chow also deserves my special appreciation for helping me understand the extent of the toxicological issues of arsenic-contaminated groundwater. I value Dr. Larry J. Segerlind's and Dr. Shuguang Li's help understanding the oxygen diffusion modeling by finite element solution techniques and groundwater modeling with the interactive groundwater model respectively.

The Government of the People's Republic of Bangladesh, the World Bank, and the Bangladesh Rice Research Institute (BRRI) also deserve my special appreciation for helping me fund my doctoral course, giving me the opportunity to study at Michigan State University.

My heartiest gratitude is also deserved by the Surface Water Modeling Center (SWMC), the Bangladesh Water Development Board (BWDB), and the British Geological Survey (BGS). I must acknowledge the contribution of Dr. Sadiqul Islam Bhuyian and Dr. Habib Chowdhury for their strong support to keep my sprit high. I also thank Mr. Abdullah, Mr. Monir Hossain, Mr. Nurul Islam, Dr. M.A. Ghani, Dr. M. A. Sattar, Dr. M.k. Mondal, Mr. H.R. Molla, my youngest sister Mrs. Shamima Sultana Ruby and her husband , and all of those who helped collecting field data from Bangladesh . I also acknowledge Miss Tina Urbain' s help during the dissertation formatting process.

DEDICATION

This dissertation is dedicated to my parents, my wife *"Khuku,"* my two lovely daughters (*Nitu & Jibu*) and those who were brutally killed by the occupied force and their local associates during the liberation war of Bangladesh in 1971.

TABLE OF CONTENTS

LIST OF TABLES

LIST OF FIGURES

APPENDICES

1. INTRODUCTION

Bangladesh is in the midst of what the World Health Organization calls the "largest mass poisoning of a population in history". Some 35 million of its 126 million people are drinking arsenic-contaminated water, the poison accumulating within them day by day, sip by sip. High concentrations of naturally occurring arsenic have already been found in water from thousands of tubewells, the main source of potable water, in 59 out of Bangladesh's 64 administrative districts. "It seems like nonsense to people, telling them the water is killing them when it looks so clean and nice," said Dr.Allan H. Smith, an epidemiologist at the University of California at Berkeley, and he has called the situation in Bangladesh "the highest environmental cancer risk ever found," worse than Bhopal or Chernobyl. However, the exact cause of the arsenic release that is poisoning the groundwater is still poorly understood.

Moreover, there are divergences in opinions about the exact cause of arsenic release and strong disagreements on the source of arsenic in the groundwater of Bangladesh. The explanations as to the origin of the arsenic contamination in the ground water can be grouped into two camps. According to one explanation, the arsenic adsorbed by the iron hydroxide is released and reduced to its soluble lethal forms from the reduction of arsenic laden iron hydroxides flushed from Pleistocene-Holocene sediments (Nickson, et al., 1998. This is known as the reduction theory of arsenic release.

Another explanation is that the arsenic contamination in drinking water is a recent phenomenon. Expansion of the vadose zone due to irrigation withdrawal

caused arseno-pyrite (FeAsS) oxidation and eventually arsenic to be released into the groundwater system. This is known as the oxidation theory of arsenic release. However, neither of these two theories is unequivocally accepted by all, and from the chemical point of view, these two theories are oppositional and insufficient to explain the exact cause of groundwater arsenic contamination in Bangladesh. Neither of these theories considers the impact of upstream withdrawal of river water and shortage of groundwater recharge on the process of arsenic release.

This study presents an explanation of arsenic release that is based on the intuitive idea of lack of oxygenated recharging water at and below the water table after extension of the unsaturated zone due to large-scale irrigation withdrawal both from ground and surface water resources. Groundwater withdrawal and upstream water withdrawal from the major river systems have jointly contributed to the lowering of the water table and the shortage of aquifer recharge water. Consequently, they have reduced the dissolved oxygen content in recharging groundwater.

The hypothesis presented in this study completely contradicts the oxidation theory of arsenic release and partially supports the oxyhydroxide reduction theory. It is acknowledged that, in the presence of dissolved oxygen in recharging groundwater, arsenic will be scavenged by iron hydroxide, which is supportive to the existing reduction theory. However, this study is mainly focused on the dissolved oxygen shortage in recharging groundwater, the influence of groundwater withdrawal at a rate greater than the amount of available recharging

water, and the influence of this on the groundwater flow dynamics in the deeper layers of the aquifer and on the likelihood of arsenic migration.

1.1 Statement of the problem

Before the introduction of a large number of irrigation wells in Bangladesh and of upstream water diversion in the major river systems, the water table elevation was in close proximity to the ground surface. As a result, the dissolved oxygen content in the recharging groundwater was in equilibrium with the atmospheric oxygen content (0.21 atm). Therefore, it was assumed that the redox potential values were controlled by the dissolved oxygen present in the aquifer system. The abundant supply of oxygenated water was favorable to oxidation reactions during which iron oxides scavenge arsenic and stay in solid particulate form. Therefore, before introducing well fields, the groundwater ecosystem was oxic, redox potential values were high, and amorphous iron oxides (Fe_2O_3, $Fe(OH)_3$) were precipitated as solid form.

After 1970, because of large-scale irrigation withdrawal and upstream diversion of river water, the depth to groundwater was increased. The redox potential values (p^e) decrease and were no longer controlled by the dissolved oxygen content because dissolved oxygen is consumed by the supply of electron donors (organic carbons) in the system. As a result, the system redox potential values were decreased to zero or less and a mild reducing condition developed.

Due to the low oxygen concentration in the aquifer, the chemical equilibrium has shifted from oxic to suboxic states, which eventually favors the dissolution of iron hydroxides and the release of arsenic into the groundwater. Present irrigation withdrawal policy (or unlimited abstraction policy) would promote further lowering of the water table and changing of shallow aquifer recharge (SAR) and groundwater movements through the deeper layers.

Because reducing the pumping rates and increasing the present irrigation system efficiencies of the lift irrigation projects in Bangladesh could achieve improvements in controls, a quantitative irrigation withdrawal policy could stop further degradation of Bangladesh's groundwater by arsenic contamination.

1.2 Scale of the groundwater arsenic problem

The most serious groundwater arsenic problem appears in much of the southern and eastern part of Bangladesh (Fig.1.1). Recent findings of the British Geological Survey (BGS) showed that the groundwater of 61 surveyed districts out of a total of 64 is contaminated with arsenic (BGS, 1999). Preliminary reports submitted by the BGS to the government of Bangladesh (GOB) indicated that out of 2,022 samples analyzed in 1998, 51% of the samples were contaminated with arsenic above 0.010 mg/L (10 ppb) [the WHO guideline value], 35% were above 0.050 mg/L (50 ppb) [the Bangladesh drinking water standard], 25% were above 0.10 mg/L (100 ppb), 8.4% were above 0.30 mg/L (300 ppb) and 0.1% were above 1 mg/L (1,000 ppb). Long term ingestion of arsenic contaminated drinking

water has been shown to increase the incidence of hyperpigmentation, hyperkeratosis and cancer of the skin (NRCC, 1978).

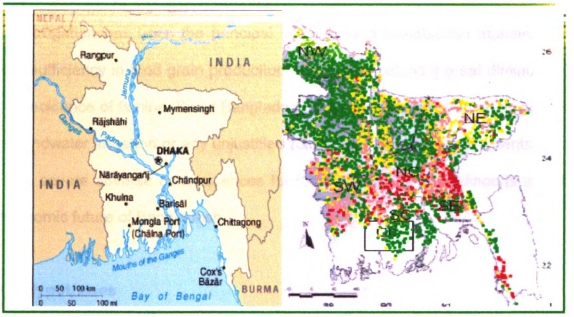

Fig.1.1: Map of Bangladesh indicating wells with arsenic levels above 50 ppb with red spots. Green and yellow spots are the tube wells containing arsenic less than 10 and 25 ppb, respectively.

1.3 Rationale

Understanding the geochemical processes that produce high arsenic (As) concentrations and the likelihood of arsenic migration in the groundwater system has a number of important benefits. Firstly, it helps to delineate safe aquifer layers for irrigating and supplying drinking water on the basis of the available shallow aquifer recharge (SAR) and redox values. Secondly, it will help in siting

new wells for irrigation development by predicting the future trends of arsenic transportation. Thirdly, of course, it is of great significance to formulating a quantitative irrigation withdrawal policy in order to continue the present pace of irrigation development.

Irrigation has been the principal factor behind Bangladesh attaining near self-sufficiency in food grain production, and hence behind a great diminution in the incidence of famine. Since Bangladesh is an agro-based country, any ban on groundwater irrigation or any unjustified rules, regulations or requirements would have severe adverse consequences for food security, rural livelihoods and the economic future of Bangladesh.

1.4 Hypotheses

Hypothesis 1

The lack of oxygenated recharging water or the shortage of dissolved oxygen (DO) at and below the water table after the extension of the unsaturated zone due to large-scale irrigation water withdrawal is the major cause of arsenic contamination in the groundwater of Bangladesh.

Rationale

Installation of large-scale irrigation wells and upstream diversion of river water promoted a rapid fall in the water table and, consequently, a shortage of oxygenated recharging groundwater. As groundwater traveled to deeper layers, a diffusive oxygen supply from the atmosphere to the aquifer could not

compensate for the oxygen consumed by the organic carbon. Therefore, the amount of dissolved oxygen concentration in the groundwater decreased.

Due to the low concentration of oxygen, the oxygen diffusion rate (ODR) also decreased. As a result, the redox potential values (p^e) decreased to a minimum and a mild reducing condition developed in the aquifer. Under mild reducing conditions, amorphous iron hydroxides are dissolved and eventually associated arsenic is released into the groundwater system. Also, the recharge from wetland cultivation would lead to a substantial increase in the dissolved organic carbon (DOC) pool in the groundwater, which would be sufficient to consume the dissolved oxygen (electron acceptors) present in the system.

Hypothesis 2

Extraction or irrigation withdrawal with a rate greater than that of aquifer recharge water and the placing of deep tube well screens at deeper layers might significantly influence the migration of arsenic into deeper layers of Bangladesh's groundwater system.

Rationale

Irrigation wells with realistic abstraction rates dramatically change the amount of surface recharge flowing through the deeper layers of the aquifer, and eventually change the groundwater flow patterns. Abstraction at a rate greater than that of aquifer recharge significantly changes the flow movements and increases the risk of arsenic contamination. As a result, arsenic can migrate from

currently contaminated layers to the uncontaminated deeper layers as an advective flow with moving groundwater.

1.5 Objectives

Overall goal

The overall goal of this research is to understand the processes that give rise to arsenic concentration in the groundwater and to develop a safe and quantitative groundwater withdrawal policy for Bangladesh.

Specific aims

- To identify the processes that produce a high concentration of arsenic in the groundwater of Bangladesh.
- To formulate a quantitative irrigation policy in order to maintain the present pace of irrigation development for the country's food production demand.
- To delineate a safe aquifer zone at the top of the summer water level where arsenic concentration should be minimal so that small-scale dug wells or shallow wells can be used to supply water for human consumption with minimal risk to human life.

2. LITERATURE REVIEW

At the emergence of the 21st century, many of the third world's countries face water quality crises because of limited and stressed water resources. The World Meteorological Organization (Obasi, 1999) predicts that the explosive growth of urban areas is rapidly depleting our water resources and detoriating its quality. By the turn of the next decade, world water demand is likely to claim almost half of the total global water runoff that is available each year. Between 1900 and 1990, the total worldwide water withdrawals increased at twice the rate of the population increase while, compared with three centuries ago, water use rose more than 35-fold (David, 1995).

In the past 45 years from 1950 to 1995, the world's population grew by about 2.2 times and the annual usage of water increased by about 2.6 times in the same period (JIID, 2003). The world population is projected to increase from the current level (near 6 billion) to 8.3 billion in 2025 and to about 10 billion in 2050 (Obasi 1997). In addition, water crises are already evident in the competition for water for industrial, domestic and agricultural irrigation uses.

2.1 Water resources and irrigation water use

It is well known that mankind, owing to its basic instinct of getting a sure and secure food supply, invented agriculture around 6500-7000 B.C. Evidence of this has been found in Neolithic sites in Iran, Iraq and Jordan. In the course of time, irrigated agriculture was invented, the origin of which can be traced to the Chalcolithic Period (3000-1000 B.C.) (Bagchi, 1995). Irrigated agriculture is by far

the biggest consumer of water worldwide. In Asia, it accounts for 86% of total annual water withdrawal, compared with 49% in North and Central America and 38% in Europe.

Table 2.1 Comparison of world water use and per capita water use in 1950 and 1995

Use of Water	1950		1995		Rate of increase	
	(1) Total Volume (km^3/yr)	(2) Per Capita (L/day)	(3) Total Volume (km^3/yr)	(4) Per Capita (L/day)	(3) / (1) (%)	(4) / (2) (%)
Agriculture	1,124	1,235	2,504	1,231	223	100
Industry	182	200	714	351	392	176
Domestic	53	58	354	174	668	300
Total	1,359	1,493	3,572	1,756	------	----
Population	2.49 billion	----	5.57 billion	-----	-----	

Source: I.A. Shiklomanov. Assessment of Water Resources and Water Availability in the World, 1996 (WMO).

On the other hand, the freshwater available for use by man is only 0.008% of all water on the planet. The annual evaporation from the ocean and land area is the same as the annual precipitation (Jones, 1992). Less than 0.027% of the total amount of water distributed over the earth is fresh and immediately available (Franks, 1972). The mean annual water loss as a crop

water use by evaporation in Bangladesh is about 142,000 million m^3 (MPO, 1987). The total global water available in different forms is described in Table 2.1.a.

Table 2.1.a. The total volume of water available in different forms on this earth

Types of Water	Volume (in 1,000s km^3)	Ratio to Total Water (%)	Ratio to Total Fresh Water (%)
* Salt Water			
Sea Water	1,338,000	96.5	—
Salty Groundwater	12,870	0.94	—
Saltwater in Lakes	65.4	0.006	—
Total Salt Water	1,350,955	97.5	—
* Fresh Water			
River Water	2.12	0.0002	0.006
Fresh Water in Lakes	91.0	0.007	0.26
Freshwater in Swamps	11.5	0.0008	0.03
Subtotal	104.62	0.0075	0.3
Fresh Groundwater	10,530	0.76	30.1
Glaciers and Snow	24,064	1.74	68.7
Soil Moisture	16.5	0.001	0.05
Underground Ice	300	0.022	0.86
Water in Living Bodies	1.12	0.0001	0.003
Atmospheric Water	12.9	0.001	0.04
Total Fresh Water	35,029	2.5	100
Total water	1,385,984	100	

Source: I.A. Shiklomanov. Assessment of Water Resources and Water Availability in the World, 1996 (WMO).

2.2 History of groundwater irrigation development projects and the arsenic contamination problem in Bangladesh

Unlike many other countries, Bangladesh mostly depends on groundwater resources as a reliable source of irrigation water, despite having large amounts of surface water. Over-pumping from aquifers presents multidimensional problems. This is the general case in large areas of India, Pakistan, Bangladesh, and Vietnam (IRRI, 1994-95). Despite all these risks, irrigation development is necessary to reduce hunger and poverty in Bangladesh.

Birth of lift irrigation on the Indo-Pak-Bangladesh subcontinent:

The birth of the lift irrigation system on the Indo-Pak-Bangladesh subcontinent took place during the period 1926 to 1935. Sir William Stampe, an irrigation engineer renowned in the earlier part of the 1920's, first conceived the idea of irrigating large dry tracts of land by using deep tube wells (Bagchi, 1995).

Use of hand tube wells (HTWs) for drinking water

In the early 1970's, most of Bangladesh's rural population obtained its drinking water from surface ponds. Nearly a quarter of a million children died each year from water-borne diseases. The provision of about 4 million hand tube wells for 97% of the rural population has been credited with bringing down the high incidence of diarrhea diseases and contributing to a halving of the infant mortality rate (WB, 1998). Paradoxically, the same wells that saved so many lives now pose a threat due to the unforeseen hazard of arsenic.

Use of shallow and deep tube wells for drinking water and irrigation

The contribution of groundwater to the total irrigated area increased from 41% in 1982/1983 to 71% in 1996/1997 with a tendency of increase in each year, while the contribution of surface water steadily declined from 59% to 29% over the same period (NMIDP, 1998). So far there have been 0.75 million deep and shallow tube wells commissioned in Bangladesh. In 2000, the number of shallow tube wells (STWs) in the country sharply rose to about 757,044 from about 635 units in 1973-74 (NMIDP, 1999; GOB, 1999). During the same period, the number of deep tube wells (DTWs) also increased nearly 20 times. Before 1970, there were no shallow tube well irrigation projects in Bangladesh.

Between 1964 and 1984, groundwater withdrawal in Bangladesh increased from about 30 million m^3/yr to over 140 million m^3/yr (MPO, 1987). During the same period, the steady state piezometric pressure head declined from around 0.7 m/year in 1970 to -7.6 m below sea level in 1984 in Dhaka City (Fig. 1). Increased withdrawal has caused an average decline of one meter of pressure for every 15 million m^3 in groundwater withdrawal (MPO, 1987).

2.3. Global perspective of arsenic contamination and groundwater use

Recent studies in groundwater from major aquifer systems around the globe have shown a large range of arsenic concentrations depending on regional hydrogeological conditions. Arsenic concentrations significantly higher than drinking water standards have been found in groundwater from large parts of

Taiwan, China, Inner Mongolia, Mexico, Chile, Argentina and the western USA where a portion of the population has been affected by arsenicosis, like Bangladesh and the eastern part of India.

Irrigation withdrawal and arsenic contamination

Abstraction from shallow aquifers created arsenic contamination in many parts of the globe. A UNICEF and EAWAG/CEC (Hanoi National University) joint research study indicated that there is a significant arsenic problem in the shallow tube wells of the aquifers of the large deltas of the Mekong and Red River in Vietnam. Concentrations of arsenic above 50 ppb have been identified in groundwater from alluvial sediment in the southern part of the Great Hungarian Plain and in part of Romania (Varsanyi et al., 1991).

Arsenic contamination under anoxic or reducing conditions

Many of the worst cases of arsenic contamination arise in anaerobic reducing aquifer conditions in the groundwater systems. Reducing aquifer systems are found in Taiwan, Inner Mongolia, China, Mexico, and the USA. The shallow aquifer of the southern Carson Desert in Nevada (USA) is highly arsenic contaminated where the upper 50 ft (15 m) of the basin is filled by sediment. The hydrologic and geochemical characteristics of the Carson Desert aquifer are similar to those of other areas of the world with high arsenic and uranium concentrations (Welch, 1998). The Hetao area of China is a district where arsenic concentrations in drinking water are elevated and about 180,000 people

have been affected (Sun et al., 1995). The depth of contaminated drinking wells ranged from 18 to 25 m, quite similar to Bangladesh

Arsenic contamination by industrial pollutants

Increased arsenic concentrations caused by mining activity have been identified in many parts of the USA. In a gold-mining district of Alaska, an arsenic concentration of about 48,000 ppb was recorded (Welch et al., 1988).

Arsenic in the natural system

Arsenic is the twentieth most abundant natural element in the earth's crust (average 2 mg/kg). Pure arsenic is a gray metal-like material that is usually found in combination with other elements such as oxygen, sulfur and chlorine. Elemental arsenic itself is not toxic, but arsenic compounds are poisons, affecting essentially all human organs (Rochette et al., 1998). Only about 125 to 150 milligrams of the chemical, half an aspirin, could kill a person in a single dose. Arsenic is also extremely hazardous if ingested in drinking water or used in cooking water in excess of the maximum permissible limit of 0.05 mg/L (the standard set by the World Health Organization) over an extended period of time. Humans generally absorb 5-15% of ingested arsenicals (NRCC, 1978). It takes anywhere between 2 to 14 years for arsenicosis to develop, depending on the amount of exposure.

2.4 Redox potential values, dissolved oxygen content, and arsenic release processes in the groundwater

Oxidation-reduction potential (ORP)

The oxidation-reduction (redox) potential of groundwater is a measure of electron activity and an indicator of the relative tendency of a solute species to accept (gain) or transfer (lose) electrons. Oxidation is defined as the loss of an electron (or electrons) from a species, while reduction is the gain of an electron (or electrons) from a species.

Thermodynamic redox potential (E_h)

Natural hydrogeochemical systems are commonly interpreted within the framework of thermodynamic equilibrium with the use of redox potential values. The redox potential (E_h) of groundwater is a measure of the relative amounts of oxidized to reduced species present in a system. In the geoscience literature prior to the 1970's, E_h was used almost exclusively to express the redox potentials of natural water. Review of the literature also suggested that redox levels in groundwater are determined essentially by the relative rate of atmospheric oxygen circulation and consumption of oxygen by aerobic and anaerobic bacteria in the aquifer system. Generally, at the surface, recharging groundwater is oxidizing and has a positive E_h value (500 to 800 mv) governed largely by their dissolved oxygen (DO) content present (up to 10 mg/L) (AECL, 1996).

Redox intensity or capacity (ρ^e)

Largely for computational and conceptual convenience, p^e has come into common use more recently (since 1970). The redox capacity p^e (eq/ L volt) at any E_h is defined as the quantity of strong reductant in the equivalent which must be added to a liter of sample solution to lower the E_h by 1 volt. Nightingale (1958) first defined the redox capacity as $P = dC_r / d(E_h)$, where dC_r is the change in concentration of reductant and $d(E_h)$ is the change in redox potential. According to Stumm & Morgan (1997), the redox capacity or intensity as $p^e = -\log \{e\}$ gives the hypothetical electron activity at equilibrium and measures the relative tendency of a solution to accept or transfer electrons. The electron activity can be expressed in p^e or in volts.

In a highly reducing solution, the tendency to donate electrons, or the hypothetical electron pressure or electron activity, is relatively large. For example, an alkaline solution has a greater tendency to accept the hydrogen ion. The activity of hypothetical electrons is very low at high p^e, just as the activity of hypothetical hydrogen ions is very low at high pH. Thus a high p^e indicates a relatively high tendency of oxidation. The review of literature suggested that the oxidation of organic matter (CH_2O) is thermodynamically possible in all ranges of p^e in surface and groundwater systems. Water in solubility equilibrium with atmospheric oxygen has a well-defined p^e value, 13.6 (open air produces a

pressure of 1 atm, and since air contains 21% oxygen, the oxygen pressure in the atmosphere, PO_2 =0.21 atm, E_h= 800 mV at pH =7 and T=25°C).

In contaminated groundwater systems, the redox gradient is often steep and the fate of redox-sensitive contaminants may be rate dependent or otherwise unpredictable (Langmuir. D, 1997). In the presence of O_2, with $p^e > 11$, aqueous iron and manganese are stable only as solid oxidized oxide (Stumm & Morgan, 1996). Such a compound, when hydrated arsenate is adsorbed with iron oxides, is called pittcite. Its hardness is 1.5 to 2 with a low specific gravity of 2.5. Stable E_h measurements are only possible in well-balanced systems (Kent et al., 1994).

2.4.1 Dissolved oxygen supply, redox potential values, and their association with arsenic release processes in groundwater

Dissolved oxygen (DO) is the most thermodynamically favored electron acceptor. When recharge water is oxidizing, it will have a significant redox buffer capacity at high E_h or p^e values. The environment is termed oxic when dissolved oxygen (DO) is greater than 30 μ M (Drever, J., 1988). Under oxidation or oxic conditions the redox potential (E_h) of groundwater is positive; reducing conditions are characterized by negative readings.

The redox potential of sedimentary groundwater generally ranges from -400 milli-Volts (mv) to +800 mv (AECL, 1996). Therefore, only mixing with oxygenated water or lacking reductant minerals or organic matter in the system can maintain the desired high oxic condition or E_h level in the groundwater.

However, it is very difficult to generalize the redox level in the groundwater because the E_h or p^e level depends very much on the time of residence of groundwater, and the time of residence varies with the groundwater velocity and length or distance of the aquifer system (Drever, J., 1988). The redox potential varies along the groundwater flow path in response to contact with reduced mineral species and organic matter (AECL, 1996). Bottomley et al. (1990) concluded that it is hard to establish a clear correlation between dissolved oxygen and E_h because E_h varies only slightly in the region where dissolved oxygen is measurable (0.01-10 mg/L).

They also found in their study that most of the groundwater E_h was not controlled by the dissolved oxygen concentrations because the E_h was less than the values expected for O_2 control (+700 to 800 mv). However, the E_h may also be quite low (<100 mv) for groundwater where dissolved oxygen (O_2) can be detected (AECL, 1996).

2.4.2 The sequence of redox process in the groundwater system

As oxygen is the most electronegative element, it has the strongest potential to accept electrons and to be reduced. Therefore, oxidation of organic matter (CH_2O) is generally observed to occur first by reduction of O_2 [p^e (W)=13.8]. Once the dissolved O_2 has been consumed, oxidation of organic matter will occur in groundwater, but more slowly. The oxidation of organic

matter, driven by microbes, will result in reduction of major and minor dissolved species in the order of NO_3, Mn (IV), Fe (III), SO_4^{2-}, HCO_3 and then NH_4-N_2 (Stumm & Morgan, 1997). Certainly this described sequence would be expected if reactions tended to occur in order of their thermodynamic possibility. These dissolved species, present in the amount of more than 10^{-5} mol/ L, are capable of controlling the redox potential E_h of groundwater (Stumm & Morgan, 1996).

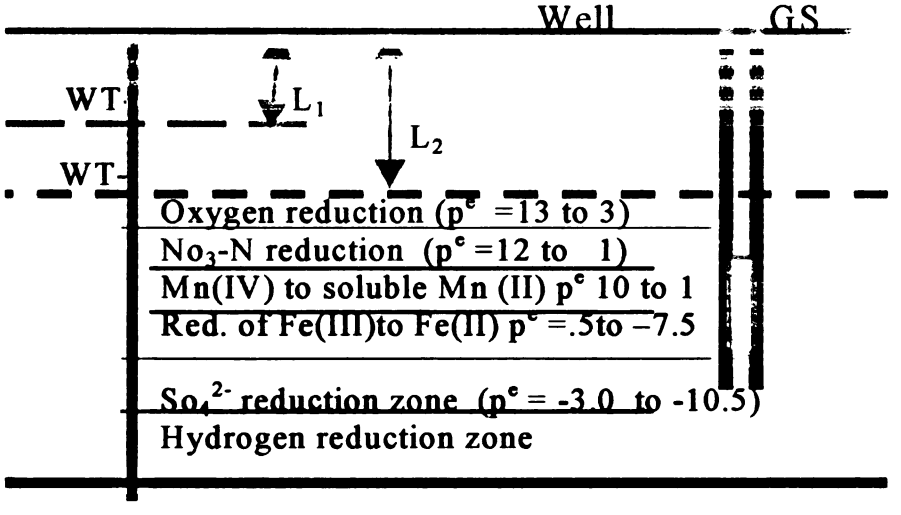

Fig. 2.1 Sequence of redox potentials in the groundwater system

2.4.3. Controlling redox potentials in the groundwater system

Grenthe et al. (1992) concluded that a low concentration of dissolved Fe^{2+}(>10^{-5} mol/L) was sufficient to control the system's redox potential values. Ross and Gascoyne (1993) also found that groundwater containing low concentrations of dissolved Fe^{2+} (typically<0.5 mg/L) has stable and reproducible

E_h values, which broadly indicate control by the Fe (II)-Fe (III) couple. In another study of groundwater where E_h has been routinely measured, Gascoyne and Kamineni (1992) found that E_h was decreasing with depth to a value close to those predicted by the Fe (II)/ Fe (III) redox couple. The extent to which E_h decreases as groundwater travels along a flow system is largely determined by the associated mineralogy of the flow system, the type and concentrations of the dissolved redox sensitive species in the groundwater and the presence of microorganisms to catalyze the reactions (AECL, 1996). Recently, the presence of dissolved oxygen has been observed in many groundwater sampled from depths up to 450 m in permeable sandstone in northern Saskatchewan (Cramer and Smellie 1994)

2.4.4 Importance of dissolved oxygen content in the recharging groundwater system

Dissolved oxygen concentration in groundwater is an important factor in terms of water quality, especially for the issue of arsenic contamination. In oxygenated waters, arsenic acid species (H_3AsO_4, H_2AsO_4, $HAsO_4^{2-}$, AsO_4^{3-}) are stable. In oxygenated water, adsorption reactions are thermodynamically favored by both enthalpy and entropy change (Stom & Morgan, 1997). In oxygenated water, dissolved Fe^{2+} is converted to Fe $(OH)_3$ (s) and anions of arsenic acids can be adsorbed onto the surface of the amorphous solid iron hydroxides.

In natural oxic groundwater and aquatic systems, sorption reactions, which are different for As (V) and As (III), strongly control the mobility of arsenic (Mok and Wai, 1994). In an oxic environment with slightly alkaline pH values, typical of most natural waters, sorption of As (V) onto Fe oxyhydroxides can transfer arsenic from the dissolved phase to the particulate phase (Xu et al., 1991; Fuller et al., 1993). A study conducted by Masscheleyn et al. (1991) also demonstrated that at low E_h (20 mv) the As (III) and dissolved iron content were the highest (Table 2.1) values. Therefore, dissolved oxygen in recharging water is an important factor in controlling arsenic release.

Table 2.2 Concentration of soluble arsenic species, Mn, and Fe^{2+} as a function of soil redox -pH condition

Days	pH	E_h (mv)	As (III) (mg/kg soil)	As(V) (mg/kg soil)	Mn (mg/kg soil)	Fe (mg/Kg soil)
0	5.6	340	1.4	5.6	1.9	17.5
3	6.7	100	46.8	3.1	20.8	15.3
6	6.8	20	76.5	6.6	21.2	72
0	5.8	440	0.9	7.9	2.4	27.3
3	6.6	80	34.3	1.2	17.4	29.5
6	7	-100	69.4	3.4	16.2	75.8

Source: Masscheleyn et al., 1991.

2.5 Existing theories of arsenic release mechanism in the groundwater of Bangladesh

There are divergent opinions regarding the arsenic release mechanism in Bangladesh's groundwater. Theories offered so far can be broadly classified into two groups, the oxidation theory of arsenic release and the reduction theory of arsenic release.

Oxidation theory of arsenic release

Increased supply of oxygen in groundwater is welcomed by the groups believing pyrite oxidation is the dominant arsenic release mechanism in Bangladesh. The cause of an increased supply of oxygen may be the development of heavy duty tube-wells known to cause extension of the vadose zone and to supply more oxygen to the groundwater (Mallick et al., 1995). Lowering the water table by pumping (Kinniburgh et al., 1997) or by nitrate pollution of the aquifer (Postma, 1991) may accelerate pyrite oxidation. In the last two decades, the Green Revolution in Bangladesh has lowered the groundwater level and, thus, the release of arsenic (Tsushima, 1999).

Arsenic is released by the oxidation of arsenical pyrites in the alluvial sediments as aquifers' drawdown permits atmospheric oxygen to invade the aquifer (Mallick & Rajagopal, 1995; Chowdhuri et.al., 1999). They suggested that the high volume extraction of groundwater in the region for irrigation has exposed

the younger deltaic sediments to air, which through oxidation reactions has caused the decomposition of iron pyrites to ferrous sulfate ($FeSO_4$), ferric sulfate ($Fe_2 (SO_4)_3$) and sulfuric acid. The process frees up arsenic, which is then oxidized into arsenite (As_2O_3) and arsenate (As_2O_5) both of which are soluble in ground water (Charkraborti et al., 1996).

Chemists belonging to this oxidation theory group have pointed out that sediments of the younger deltaic depositions (YDD) have some intermittent arsenic bearing beds or layers of arseno-pyrites and eventually arsenic can be released in the form of As_2O_3 and As_2O_5 from these sediments when they come into contact with atmospheric oxygen.

Reduction theory of arsenic release

On the contrary, investigators from the British Geological Survey (BGS, 1999), working on Bangladesh's arsenic problem, explained the arsenic release mechanism in groundwater as a reduction of arseniferous iron oxihydroxides when anoxic conditions develop during sediment burial (Nickson et al., 1998). This group also found strong evidence for and correlation between reduction of ferric oxides and hydroxides and their by-products as dissolved iron (Fe^{2+}) and (HCO^-_3) production in the groundwater. Several other studies have investigated arsenic's geochemical behavior and have pointed out the association between As (v) and Fe-oxyhydroxides by coprecipitation (Masscheleyn et al., 1991)

Dissolved iron, preliminarily present as Fe (II) in ground water, plays a very significant role in adsorbing and releasing arsenic and other trace cations and anions (Khan et al., 2000). In contact with air, Fe (II) is oxidized to Fe (III) and precipitates as Fe $(OH)_3$, hydrous ferric oxides (HFO: Fe_2O_3, Fe $(HCO_3)_2$, 2-3 H_2O). (Scott et al., 1995). It is well known that HFO binds arsenate formed during the oxidation process (Sullivan et al., 1996). Therefore, arsenic can be removed by iron species either by compound formation or by adsorption or both under oxidation conditions. On the contrary, sorbed arsenic can be released under reducing conditions from the body of HFO as a function of pH (Raven, et al, 1998).

Opinions contradicting pyrite oxidation theory

The BGS (1999) investigators strongly oppose the idea of oxidation of arsenopyrite as an arsenic release mechanism in Bangladesh. The oxidation theory of West Bengal (India), however, fails to explain the increase in arsenic level in deeper wells and anoxic conditions in part of Bangladesh (Nickson et al, 2000). Arsenic in Bangladesh's groundwater cannot derive from the presently accepted mechanism, whereby water-level drawdown from abstraction wells allows atmospheric O_2 into the aquifer and so allows the oxidation of arsenic-bearing pyrite, with concomitant release of arsenic to the groundwater (Das et al., 1995, Chowdhury, R., et al., 1999). Such a mechanism is incompatible with the

redox chemistry of the water. Arsenic produced in this way would be adsorbed to the FeOOH, the product of oxidation (Mok & Way, 1994; Thornton, 1996).

Opinions contradicting oxyhydroxide reduction theory:

In reduction theory, the correlation between iron and arsenic cannot be considered as a valid relation. Regarding the appropriateness of considering extractable iron concentration, Bridge and Husain (2000a; 2000b) noted that the correlation between extractable iron and arsenic does not necessarily imply the adsorption (oxy-hydroxide reduction hypothesis). Questions were put forward by Adel (2000) to Nickson et al. (1999) as to why the arsenic concentration was just detected in the 1990's if organic carbon has been taking oxygen for thousands of years. Adel (2000) also mentioned that, to support the reduction hypothesis, Nickson et al. (1999) showed 6% organic carbon content in the aquifer sediment, which goes beyond the boundary of scientific evidence. Scientists belonging to this group also claimed that the lack of SO_4^{-2} ions in groundwater is not a valid reason to reject the oxidation theory of arsenic release.

2.6 Lowering of the water table, ability of atmospheric oxygen access, and redox potentials of the aquifer

The oxidation and reduction potential of groundwater mainly depends on the access of atmospheric oxygen to the saturated aquifer and the amount of dissolved oxygen present in the recharge groundwater. A large percentage of soil pores are filled with water in saturated soil or aquifer systems. The water content

in the aquifer systems varies in time and space because of irrigation, flood, evaporation and infiltration. As water is replacing air (or vice versa), the change in water content generates a vertical flow of air (Refsgard et al., 1991). An exchange of gases between the soil and the atmosphere is primarily due to the mechanism of diffusion (Buckingham, 1904; Penman, 1940).

Generally, two main processes operate to effect gaseous transport within the aquifer: convection and diffusion. The dynamics of the water level are basically responsible for the convective flow of air to the soil matrix and the soil-water system. But this convective transport of oxygen in the soil-water system is at typical pore-water velocities in the unsaturated zone (1 m/year) and much more significant than diffusive transport in free water (Refsgard et al., 1991).

However, to understand the sub surface aeration system in a more comprehensive way, Mukhter et al. (1996) mentioned three well known aeration indices, namely O_2 concentration, the oxygen diffusion rate (ODR) and the redox potential (E_h) of the system. It was revealed from their study that E_h varies linearly with ODR up to a certain range, and after that, the E_h remains constant with increasing ODR. Mukter et al. (1996) also observed that, in general, an oxygen concentration of nearly 80% is required to maintain adequate ODR (above 20×10^{-8} g cm^{-2} min^{-1}) in the deeper layers.

If the oxygen concentration falls below the critical level, then ODR also decreases. In another set of experiments on depths, Mukhter et al. (1996) found that ODR varied inversely with depth (Fig. 2.2). At higher depths, oxygen

concentrations were below the critical level, so the ODR decreased. As the oxygen diffusion coefficient in water is nearly 10,000 times less than in the air (Kalita, 1999), the diffusive supply of oxygen concentration in the deeper saturated zone is smaller than that at the surface, which eventually reduces the oxygen diffusion rates (ODR)).

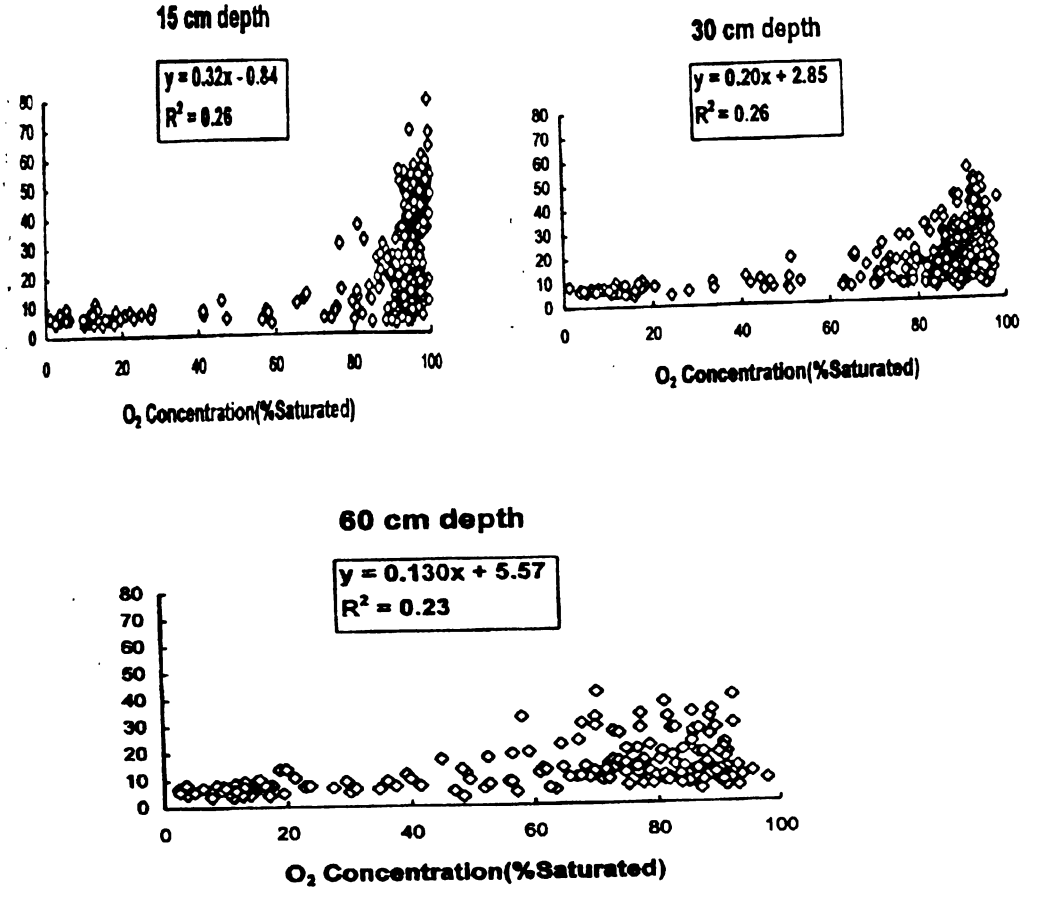

Fig. 2.2. Oxygen Diffusion Rate (ODR) decreasing over depth at 15, 30 and 60 cm below the ground surface. (Source: Mukhter et al., 1996.)

There is a common misconception that lowering of the water table provides a greater atmospheric oxygen supply to the groundwater. This may not be the real case when oxygen is consumed by organic carbon at a constant rate in the soil matrix.

2.7 Lowering of the water table, change in thermodynamic properties, and arsenic release into the groundwater system

Chemical reactions in a system take place spontaneously. The spontaneity of the chemical and physical reactions is changed by entropy. The concept of entropy is based on the second law of thermodynamics. Review of the literature indicated that when a spontaneous chemical change occurs in a system, if the total entropy change for everything were calculated, a positive value of entropy would always be obtained. The entropy is the change in enthalpy, or heat change over temperature, and can be defined by the following equation (Sawyer & McCarty (1991):

$$dS = \frac{dq_{rev}}{T} \quad \text{..... ...Entropy ...Transfer}$$

$$\nabla S = S_2 - S_1 = \int_1^2 \frac{dq_{rev}}{T}$$

where S is the entropy of the system and T is the absolute temperature. The quantity q_{rev} is the amount of heat that the system absorbs if a chemical change is brought about in an infinitely slow, reversible manner. The entropy of a substance at 0 K is zero.

$dS_{sys} = dS_{int} + dS_{sur}$

where d_{sys} is the entropy transfer to the system from its surroundings, dS_{int} is internal entropy change (zero when the system is reversible), and the entropy transfer to the system by the surroundings is dS_{Sur}, or dq/T.

If the ΔS for the whole system were positive, the reaction would occur spontaneously. This spontaneous process occurs without a change in internal energy in the container, but with an increase in entropy. In this research, both energy and entropy factors were investigated in order to determine what processes were responsible for making arsenic release reactions spontaneous in the groundwater system. Both energetic and dynamic information enables us to understand the processes.

2.8 Arsenic transportation in the groundwater system

The literature review has revealed that chemical contaminants in the natural and groundwater can be transported in particulate, or colloidal, form and in ionic form. However, it is not clear from the literature whether arsenic transportation in the deeper layers is of the colloidal form or the ionic form. When a pressure gradient is imposed on the solution in a clay-water system, water molecules can move through the pores, but ions cannot (Hanshaw and Coplen, 1973). Clay being changed behaves as a semi-permeable membrane, allowing the passage only of water, not of ions (Drever, 1988). This phenomenon is known as the anion exclusion. The membrane filtration has been suggested to be a major process affecting the composition of water trapped in the deeply

buried sedimentary rocks (Graf, 1982). Perhaps this is the reason why deep aquifers in Bangladesh are still safe and less arsenic contaminated.

Particles or colloidal transportation of arsenic

A colloidal system is defined as a system in which particles, in a finely divided state, are dispersed in a continuous medium (Benefield, 1982). Colloidal particles are not limited to any particular group or substance but are defined by size (1 nanometer to 1 micrometer). Electrophoresis phenomena indicate that colloidal particles carry electric charges. The sign and magnitude of charges depend on the nature of the colloidal materials. The stability of colloidal suspension and the ion exchange property of solids are closely related to the behavior of double layers (Drever, 1988). When a clay particle (smectite) is suspended in water, some of the cations pass into water, and the water develops a negatively charged surface and a diffuse cloud of oppositely charged ions, called a double layer or Gouy layer.

In the solution, the charged particles repel each other and do not settle. The electric charge on the surface of the particle is the primary factor responsible for colloidal stability. The electrophoretic mobility of the particle is called the Zeta potential. The magnitude of the Zeta potential is a rough measurement of the stability of the colloidal particle. A high Zeta potential suggests a strong force of separation and a stable colloidal system. Chemicals are transported in colloidal form in groundwater unless the process of coagulation overcomes the particles' strong force of separation. However, in the case of arsenic, it is poorly

understood whether arsenic moves under colloidal or ionic form in the deeper aquifer.

Ionic transportation and Retardation Factor

When any contaminants are introduced into the groundwater system, the subsequent migration is strongly influenced by the cation exchange process. When the solid adsorbs a cation, it migrates at a slower rate. If the ion exchange reaction is rapid and reversible, the rate of advance of the front of the cation is given by the following equation:

$$v_{A^+} = \frac{v}{1 + \frac{\rho}{\phi} * K_d}$$

where v_{A+} is the velocity of the contaminant profile, v is the velocity of the groundwater, ρ is the bulk density of the sediment, φ is the porosity of the sediment, and K_d is the distribution coefficient.

The expression $[1+(\rho/\varphi) * K_d]$ is called the retardation factor, which can be used to estimate how rapidly a pollutant may migrate. The value of (ρ/φ) in the groundwater sediment is typically between 5 and 20. Unless K_d is very small, the retardation factor will have a large effect on contaminant transportation. K_d is a valid representation of partitioning between liquid and solid only if the reactions that cause the partitioning are fast and reversible and only if the isotherm is linear (Freeze and Cherry, 1979).

3. DESCRIPTION OF STUDY AREA

The study area covers most of the arsenic affected area in the southwest zone of Bangladesh. The People's Republic of Bangladesh lies between latitudes 20^0 34' and 26^0 38' north and between longitudes 88^0 01' and 92^0 41' east. The country is bounded by India on the north and the west, by the Bay of Bengal on the south and by India and Burma on the east (Fig. 1). It is mostly a low and flat deltaic land, with the exception of some hilly area in the northeast and southeast and some highlands. The ground elevation is generally less than 100 meters above sea level.

Bangladesh occupies the major part of the Ganges, Brahmaputra and Meghna (GBM) river system, bounded in the east by Tripura Hill and in the north by Shilong Plateau. Fluvial-deltaic sediments, hundreds to thousands of meters thick, form highly productive, fresh water aquifers in most parts of the country.

Table 3.1 General facts about Bangladesh

Area (sq. km)	Pop.	Pop. Growth Rate	Pop. Dens.	Life Expect-ancy (yrs.)	Climate	Rain-fall (mm)	Temp. (°C)	Area Irriga-ted (Mha)
148,396	124 mil.	2.10% year	752 per sq. km	Male: 59.1 Female: 58.6	Sub – tropical with 3 seasons (winter, summer, monsoon)	2320	Min: 7.2 to 12.8, Max: 23.9 to 31.1	3.50

Data Source: 2000 Statistical Yearbook of Bangladesh

3.1 Geology of arsenic contaminated area in Bangladesh

Bangladesh lies within a geologic feature known as the Bengal Basin (Fig. 3.1). The Bengal basin was formed in the Cretaceous period, and sedimentation continues today, both in Bangladesh's sub-areas and offshore in the world's largest submarine fan complex (the Bengal Fan) (Johnson et al., 1990). The Bengal basin has four phases of deposition and erosion coinciding with four inter-glacial and glacial periods in the Quaternary time (0 to 1.6 million years ago). Prior to the recent deposition to the delta and active riverbanks, a deposition took place sometime between 25,000 and 80,000 years ago (commonly known as the younger deltaic deposition, YDD). The groundwater arsenic concentration is mostly located in the YDD.

The sediments were mainly brought by the Ganges (Mallick et al, 1996). The major part of the western alluvial delta is called the Older Deltaic Plain (ODP), developed during the Quaternary time between 80,000 and 1.6 million years ago. The ODP extends into the sub-surface below the arsenic belts in the Ganges River delta of Bangladesh. Perhaps that is why perhaps deeper aquifers under the arsenic belt (YDD) are as yet free from arsenic contamination.

3.2 Geomorphology of Bangladesh and the primary source of arsenic

Bangladesh is formed mainly from the deposit of the Ganges, Brahmaputra and Meghna (GBM) River systems (Fig. 3.2). These rivers combine in Bangladesh to produce the largest active delta in the world (Reimann, 1993). The majority of the catchments of the Ganges-Brahmaputra and Meghna (GBM)

river system lie in India, Nepal, Bhutan and China (Fig. 1.1, Fig.6.1). Fig. 3.2 shows that the deltaic and alluvial deposits of the GBM river systems underlie nearly 85% of Bangladesh. Most of Bangladesh's arsenic-affected area lies in the Quaternary alluvial plains of the Bengal Basin. Because of their position close to where the Ganges River enters Bangladesh, some authors have suggested they may be the primary source of arsenic in the Bengal alluvium (Khan, 1995).

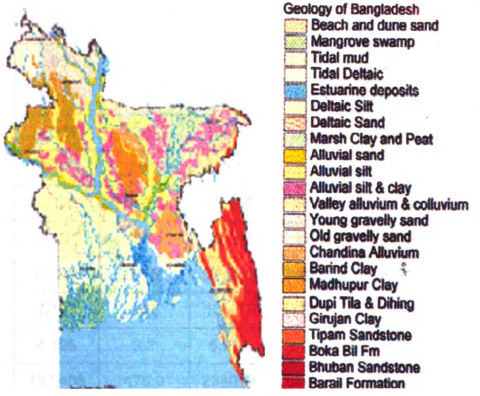

Fig. 3.1 Surface geology map of Bangladesh

Table 3.2 Average monthly discharge and sediment load in the major river system in Bangladesh

Month	Ganges (Hardinge Bridge)		Brahmaputra (Bahadurabad)		Meghna (Bhairab Bazar)	
	Flow (m^3/sec)	Sediment*	Flow (m^3/sec)	Sediment*	Flow (m^3/sec)	Sediment*
Jan.	3,113	2.0	5,194	4.0	594	0.02
Feb.	2,712	1.4	4,308	2.5	495	0.01
Mar.	2,312	0.9	4,711	3.6	635	0.06
Apr.	2,056	0.8	6,823	9.7	937	0.06
May.	1,971	0.8	15,844	36.4	1934	0.26
Jun.	4,311	3.9	32,488	87.6	3821	1.4
Jul.	17,871	48.7	44,080	121.6	7814	7.5
Aug.	37,546	168.8	45,107	163.3	8279	3.7
Sep.	36,970	156.1	36,295	117.8	8222	4.8
Oct.	17,244	81.6	21,955	42.9	6239	2.28
Nov.	7,109	10.5	10,477	12.1	3078	0.08
Dec.	4,195	3.2	6,737	5.4	990	0.01
Annual	137,408	478.9	234019	607.7	43,039	---

Data source: Coleman, 1969. * Sediment load is in million tons per annum; Ganges discharge is the pre-Farakka Barrage monthly average, taken from Rashid, 1991.

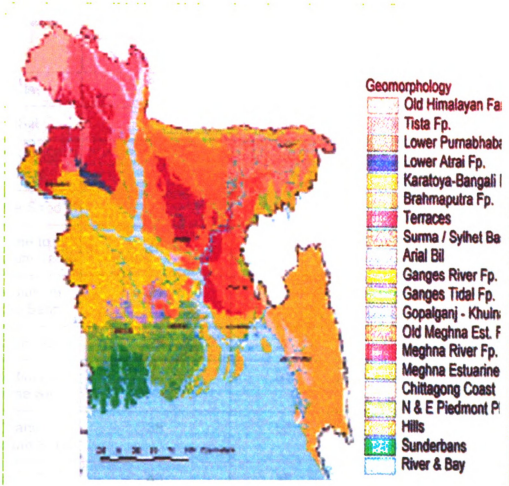

Fig. 3.2. Geomorphology of Bangladesh

3.2.1 Land and soil classifications

The majority of Bangladesh is covered with Holocene and recent fluvial and deltaic deposits from the Ganges, Brahmanaputra, Tista, Jamuna and Meghna Rivers (Fig. 3.2). The descriptions of the lithology are presented in Table 3.3.

Table 3.3 Lithology and hydraulic properties in the study area of Bangladesh

Lithology	Hydraulic Conductivity (m/day)		Specific yield (%)	
	Terrace	Flood Plains	Terrace	Flood Plains
Clay	-	-	0.5	3
Silt	-	0.4	4	5
Very Fine Sand	8	-	-	-
Fine Sand	13	12	8	16
Fine to Medium Sand	17	26	-	-
Medium to Fine Sand	21	43	-	-
Medium Sand	25	57	20	20
Medium to Coarse Sand	34	61	-	-
Coarse – Medium Sand	38	63	-	-
Coarse Sand	46	95	25	25
Gravel	25	40	30	30

Source: BGS (2001).

3.3. Hydrology and hydrostratigraphy of Bangladesh

Rainfall

Bangladesh's thirty-year national mean annual rainfall was 2320 mm, or as arranged by region in increasing order, from 1765 mm in the Southwest (SW),

1820 mm in the Northwest (NW), 2410 mm in the South-Center, (SC), and 2690 mm in the Southeast (SE), to 2830 mm in the northeast (NE) region (MPO, 1985). The mean annual volume of rainfall in Bangladesh is 326,000 million m^3, but about 81%, 264.06 billion m^3, is received during the summer humid period, from May to October (MPO, 1987). The five-year maximum two-day rainfall varies from more than 500 mm in the NE to less than 180 mm in the NW and 160 mm in the SW region.

Shallow aquifers

Groundwater in Bangladesh is mainly drawn from Quaternary strata. In parts of the country covered by major DTW projects (Deep Tube Wells), there are sufficient lithological data to permit mapping of the main lithology in the subsurface of Bangladesh. In Sylhet, two groups of aquifers exist. In the basin area, Pleistocene to Holocene sand forms exploitable aquifers in the upper 150 meters, but they tend to be thinner than those in the rest of the country (BGS & Mott MacDonald, 1999).

Deep aquifers

At present, aquifers deeper than about 150-200 m are exploited only in the coastal zone, and only for potable or industrial supply. Very deep aquifers are defined by depths greater than 350 m. In the southeast and south-center regions, fresh water extends to the coast and sometimes to the offshore islands, and it may have artesian flows. In the southwest, the saline front line lies about 20 km

north of Mongla port (Fig. 3.1). The very deepest aquifers have been tentatively identified from electric logs of oil and gas wells by Jones (1985) at depths of one to three thousand meters. However, there is no direct evidence of either the water-producing potential or water quality of these strata.

3.3.1 Aquifer properties

Transmissivity and permeability

Estimates of permeability and transmissivity were obtained from about 300 aquifer tests (UNDP, 1982; MMI, 1992) and tests on the municipal tube wells. Aquifer tests provided detailed insight into the mechanism of flow around wells, whereas because of their greater number, the DTW data showed the geographical variation of the aquifer parameters. In different regions the alluvial aquifers display confined, leaky and unconfined responses to pumping. The aquifer beneath the Holocene Flood Plains, especially along the Jamuna Flood Plain (Physiographic map in Fig. 3.1), has the highest transmissivity (2,000-5000 m^2/day) and is generally unconfined or semi-confined. Aquifer properties are presented in Table 3.4. In general, groundwater gradients over the country are low, typically between 1 m per km (1:1000) in the north of the country to as low as 0.01 m per km (1:100,000) in the south.

Table 3.4 Average aquifer properties in different geological formations and zones

Hydrological Zone	Civil District	Geological Formation	Transmissivity (m^2/day)	Storage Coefficient	Reference
Southeast (SE)	Comilla District	Chandina Formation	1,200	1.3E-03	1
	Noakhali		617		6
Northeast (NE)	Sylhet Floodplain		460	5.6E-04	4
North-Center (NC)	Dhaka	Dhamrai Formation	3,480		7
	Manikgonge		4,211		7
	Tangail		2803	2.9E-03	1
Northwest (NW)	Bogra District	Recent Alluvium	2,380	1.1E-03	1
	Dinajpur		2,755	2.8E-03	1
	Nawabganj District		3,172	6.7E-03	9
	Pabna District		4,316		1
	Rangpur District		4,384	2.6E-03	1
Southwest (SW)	Jessore District		3,660	1.9E-03	1
	Khustia		3,780	2.0E-03	1
	Khulna District		3100	1.0E-03	5
North-Center (NC)	Dhaka City	Dupi Tila Formation	1,333	8.3E-04	8
	Madhuppur Tract		1161	1.7E-03	1,3,4
Northeast (NE)	Sylhet Hills		249	1.3E-02	2
Northwest (NW)	Barind Tract		1835	1.6E-02	9

References:

1. UNDP (1982)
2. HTS (1983)
3. MMP/HTS (1983)
4. MMI (1992)
5. Rus (1985)
6. MMP (1993)
7. Barker et al. (1989)
8. MMP (1991)
9. Ahmed (1994)

Table 3.4.a Approximate wet season regional groundwater gradient

Location	Maximum Gradient (m/km)	Minimum Gradient (m/km)
North Zone	2	0.5
Central Zone	0.5	0.1
Southern Zone	0.1	0.01

Source: BWDB, 1993.

Table 3.4.b Average groundwater chemistry in different zones in Bangladesh

Region	Screen depth	T (°C)	EC (µS/cm)	pH	E_h (mv)	Mn (mg/L)	Fe (mg/L)	HCO_3 (mg/L)	SO_4 (mg/L)	Cl (mg/L)	NO_3 (mg/L)	Ref.
NC	56.9	25.9	538	6.83	108	0.38	9.0	356	4.3	20	1.3	2
NC	71.2	25.8	285	6.65	283	0.23	0.80	213	0.6	2	0.3	2
SE	18.1	25.3	792	7.39	95	0.26	4.7	452	0.4	61	7.3	2
NE	55.1	25.1	299	6.94	283	0.56	8.5	198	0.4	4	0.3	2
NW	48.0	26.0	73	6.56	--	--	3.3	54	3.0	1	0	3
NW	42.4	26.42	339	6.86	--	--	1.2	231	5.1	9	4.3	1
NW	37.8	26.7	870	6.81	--	0.16	0.8	354	2.4	96	--	1
Avg.	47.1	26.3	528	6.90	182	0.28	3.6	279	3.1	58	2.1	--

References: 1. Ahmed (1994) 2. Davies & Exley (1992) 3. Consociates (1970)

3.4 Groundwater chemistry in Bangladesh

Outside the coastal zone, groundwater is generally fresh. Bicarbonate is the dominant anion in the fresh water. Sulfate is generally absent, which contributes to the sulfate reduction.

3.5 History of irrigation development and area coverage in Bangladesh

Very little information exists on irrigation during the British colonial period in Bangladesh (1757-1947). After the recommendation of the Famine Commission of 1880, people started using farm ponds, tanks, private canals, streams and channel for irrigation purposes. By the year 1903, the Dhaka and Triveni canals of Champakaran district of Bihar were constructed. To assess the future demand of irrigation, a high-power Irrigation Commission was set up for the first time in 1905-1906, during the period of Lord Curzon (1899-1905). As per its recommendation, 50,000 miles of canals and distributaries were established to provide irrigation for 21.5 million acres of the whole British Indo-Pak-Bangladesh subcontinent.

Between 1947 and 1971, Bangladesh directed attention mostly to surface irrigation and flood control projects. After 1971, Bangladesh put her all efforts into making the Green Revolution a success. Most of the Deep Tube Well (DTW) and Shallow Tube Well (STW) projects were commissioned from 1972 to 1980 by the Bangladesh Agricultural Development Corporation (BADC). Irrigation coverage has been increasing steadily with time, as shown in Fig. 3.3.

Table 3.5. Total number of Deep Tube Wells (DTW), Shallow Tube Wells (STW), and Low Lift Pumps (LLP) (irrigation devices) used for both surface and groundwater Irrigation in Bangladesh from 1994 to 2000.

Techno-logy & Year	Hydrologic zone						Total in Bangla-desh
	SC Zone	SE Zone	NC Zone	SW Zone	NW Zone	NE Zone	
SHALLOW TUBE WELLS (STW)							
1994-95	-	13649	109614	93405	271686	515	488869
1995-96	53	14927	128064	115786	316592	826	576248
1996-97	20	16225	144423	126877	339300	1133	627978
1997-98	32	17687	152816	136033	356704	1399	664671
1998-99	29	19926	174951	152185	387101	1858	736050
1999-00	26	20875	181199	162325	390491	2128	757044
DEEP TUBE WELLS (DTW)							
1994-95	-	2613	8890	3028	11924	200	26655
1995-96	1	2461	8806	3149	12536	156	27109
1996-97	-	2260	7717	3143	11891	118	25129
1997-98	-	2312	7795	3118	12017	112	25354
1998-99	-	2448	8147	3126	12871	126	26718
1999-00	-	2291	7495	3056	12162	100	25104
LOW LIFT PUMPS (LLP)							
1994-95	4527	24115	14149	3263	5642	5349	57045
1995-96	5590	24741	14978	3654	5759	5973	60695
1996-97	5193	25208	15005	3995	6031	6962	62394
1997-98	7298	25531	15470	4384	6155	7412	66250
1998-99	8711	27221	16832	5518	6608	8028	72918
1999-00	7995	25375	16605	6243	7295	8057	71570

Source: National Minor Irrigation Development Projects (NMIDP, 1996/97). Reference: Main Report of National Minor Irrigation Census (NMIC), 1999/2000, Prepared by NMIDP & DAE Dhaka, January 2001.

3.6 Rice irrigation and rice water requirements in the SW zone study area

As a general rule, a growing rice crop needs 10 millimeters of water a day. This is equivalent to 100 tons of water per hectare. To provide 1 hectare with supplementary water, it needs a capacity of 166 liters per minute (44 US gallons per minute) if operated 10 hours per day or 70 liters per minute (18.6 gallons per minute) if operated 24 hours per day during a dry spell.

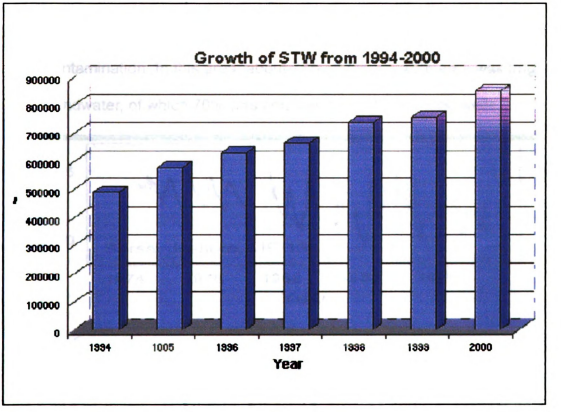

Fig. 3.3 Growth of shallow tube wells irrigation from 1994 to 2000 in Bangladesh

3.7 Groundwater level in specific study area in the southwest (SW) zone

The regional hydraulic gradient is very low, reflecting the low topographic gradient (Table 3.3.a). In the southern coastal areas, the piezometric surface in the deep aquifer is approximately 1.0-1.5 m above the mean sea level. The decline in water levels due to extraction for irrigation during the dry season through the use of shallow and deep tube wells is significant in the specific SW zone study area (Jessore and Kustia district) (Fig. 3.4). This represents the groundwater level of the specific study area in the Ganges delta area, where intensive irrigation has been practiced. Also, the groundwater is badly affected by arsenic contamination. In this area, about 77% of the irrigable area was irrigated using groundwater, of which 70% was obtained from shallow tube wells.

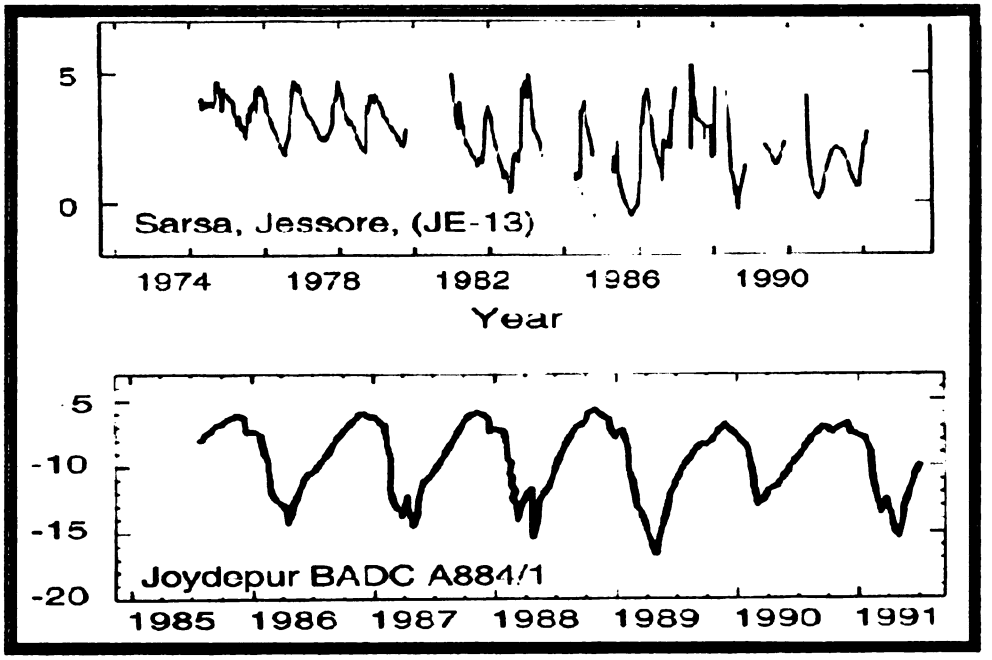

Fig. 3.4 Fluctuation of the groundwater level in the specific study area in the SW zone of Bangladesh. Source: BWDB

4. METHODOLOGY

The main hypothesis of this study is based on the idea that less oxygen is in the groundwater at and below the water table due to the extension of the unsaturated zone by overpumping of irrigation wells. Pumping at a rate greater than that of aquifer recharge causes the water table to lower farther and reduces the rate of oxygen diffusion to deeper layers. Eventually a reducing condition is developed and arsenic is released. This analysis mainly targets addressing the relationship between the arsenic concentration in groundwater and its interactions with the irrigation pumping rate and the aquifer's physical and chemical properties such as aquifer thickness, conductivity and redox potential values (P^e). The overall goal of this research is to formulate a quantitative irrigation policy to maintain the present pace of irrigation development.

4.1 Research approach and research issues

To accomplish the purpose of this research study, three analytical approaches are used: statistical, thermodynamic or geochemical, and mathematical modelings. Three objectives are presented as portions of the goal of the research. The approaches utilized to achieve these objectives are delineated below.

Objective 1

To identify the processes that produce the high arsenic concentration in Bangladesh's groundwater.

The approach to be followed under objective 1 will be to investigate the following three research questions:

1. What are the hydrologic factors that exhibit a pattern or correlation with high arsenic contamination in the groundwater system of Bangladesh?
2. What geochemical processes (such as pyrite oxidation or the oxyhydroxide reduction process) mainly control arsenic contamination in Bangladesh's groundwater system?
3. What is the interaction between the lowering of the water table position, the dissolved oxygen content in recharge water and the triggering of the arsenic contamination problem in Bangladesh's groundwater?

The first research issue will identify the hydrological and geochemical factors or activities that facilitate the arsenic contamination problem in the groundwater system. Statistical analysis (probability of exceedence, correlation analysis, and regression analysis) will be applied. The second research issue will identify the geochemical processes responsible for arsenic contamination. Thermodynamic and mathematical analysis will be done to evaluate whether oxidation or reduction processes are responsible for arsenic mobilization. The third research question will deal with the issue of the lowering water table and its influence on the ability of atmospheric oxygen to diffuse to deeper layers. A finite element analysis will address this issue.

Objective 2

To formulate a quantitative irrigation policy to maintain the present pace of groundwater irrigation development.

The following research issues will be investigated in order to achieve objective 2:

4. What is the influence of the irrigation withdrawal rate and of cropping systems on the amount of shallow aquifer recharge (SAR) available?

5. What is the influence of shallow aquifer recharge (SAR) on the groundwater flow patterns and vertical migration of arsenic from the currently contaminated layers to the uncontaminated deeper layers of the aquifer?

6. What is the influence of the placement of tube well screens at deeper layers on arsenic migration to those deeper layers?

The fourth, fifth and sixth research questions address the managerial issues in a manner that will reduce the risk of any further arsenic contamination of groundwater being caused by future irrigation development. The fourth research question is concerned with whether overpumping of groundwater did provide the conditions favorable for triggering arsenic release in Bangladesh's groundwater. The fifth and sixth research issues will address the influence of aquifer pumping rates on groundwater flow patterns and the overall arsenic contamination problem in Bangladesh's groundwater.

The IGW interactive groundwater modeling software was used to understand the influence of the pumping rate and the aquifer recharge rate on

the flow patterns and the possibility of arsenic migration. For example, if in order to avoid arsenic-contaminated layers in the aquifer, the tube well screen is placed in deeper layers with solid casing above; arsenic can migrate from the overlain top layers to deeper layers. Extraction of a greater freshwater volume than the volume of recharge (SAR) may invite salinity intrusion in the aquifer.

Objective 3

To delineate a safe aquifer zone on the top of the summer water level where arsenic concentration would be minimal so that small-scale wells can be installed for irrigation and drinking purposes.

The approach to be followed under objective 3 will be to investigate the following research question:

7. What administrative or managerial decision changes or policy changes can reduce the risk of arsenic contamination and help the installation of small-scale drinking wells?

This research issue will address the dimensions and set out the criteria that separate the aquifer safe layers from the most arsenic-contaminated layers on the basis of redox potential values. For example, new recharge water at the top of the summer water level is rich in dissolved oxygen, has higher redox potential values, and naturally would be arsenic-free and safe for drinking.

4.1.1 Data collection strategy

Despite difficulties in obtaining data, a strategy was developed that satisfied the statistical and analytical requirements for this study. There are 64 administrative districts and 453 Thana or sub-districts (second-layer administrative units in Bangladesh). Each Thana was divided into approximately 10 imaginary cells of equal area where at least 5 sample wells were likely to be available. The arsenic concentration records of those wells were collected from the reports submitted to the Government of Bangladesh (GOB) by different organizations working on the arsenic problem in Bangladesh (BGS, DPHE, etc.).

In addition to that, collection of information on surface and subsurface hydrogeology, the growth rate of deep and shallow tube wells, irrigation coverage, aquifer properties, varieties of crops grown and water management practices and policies were collected from sources like the MPO (Master Plan Organization of GOB), the DPHE, and non-governmental organizations like Mott MacDonald Ltd. (UK), the British Geological Survey (BGS), SOES (School of Environmental Studies, India), etc. The raw data are appended to this dissertation.

4.2. Analysis of research issues

In order to address the first research question, the hydrologic factors that exhibit correlation with arsenic concentrations, the following statistical analyses were conducted.

4.2.1 Statistical analysis of the arsenic distribution pattern and its relationship with surface geology, depth of the aquifer, dissolved iron content, and groundwater flow direction

On the basis of water resources and hydrogeological variations, Bangladesh was divided into six different water resources zones (MPO, 1987): northeast (NE), north-center (NC), northwest (NW), southeast (SE), south-center (SC) and southwest (SW) (Fig.4.2.b and Table 4.2.2). The distribution patterns of arsenic concentration were statistically analyzed within the boundary of each group. At first, the probability of arsenic levels exceeding 10 ppb (WHO Standard), 25 ppb (Bangladesh's target), 50 ppb (current Bangladesh standard), 100 ppb and 250 ppb was computed for each classified zone using exponential and Gumbel distribution methods. The results are presented in Fig. 4.2.a.

4.2.2 Computation of probability of arsenic concentrations exceeding threshold level in Bangladesh's groundwater

For computation of the probability of arsenic concentrations exceeding the threshold level (50 ppb), Gumbel distribution was used because the arsenic concentration distribution pattern does not satisfy the conditions of normal distribution. On the other hand, the descending exponential distribution ($p = C^* e^{-A}$) is very common in natural and hydrogeologic events such as contamination distribution and flood frequency distribution. Here, 'C' and 'A' are positive parameters and 'e' is exponential. The main advantage of the exponential

probability is that when a point on the probability density function decreases to one half the maximum value, the half value density therefore marks the point at which 50% of the data are larger and 50% of the data are smaller. For the unit area, the probability equation (4.1)

$$P = C * e^{-Ax} \tag{4.1}$$

can be expressed as follows in equation 4.2.

$$1 = C\int_{0}^{\alpha} e^{-Ax}dx = C\left(\frac{-1}{A}e^{-Ax}\right)_{0}^{\alpha} = \frac{C}{A}. \tag{4.2}$$

Unit area requires C = A.

The exponential probability function was calculated by integrating the probability equation (Eq. 4.1),

$$P = A\int_{0}^{x} e^{-Ax}dx = 1 - e^{-Ax}$$

The Gumbel or Type 1 distribution (Gumbel, 1945) is an exponential distribution form and has its skewness fixed at +1.14. The probability of exceedence of threshold arsenic levels was computed from the following Type-1 equation

$$\begin{aligned} &1 - F(x) = 1 - e^{-e^{-b}} \\ &where\ , \\ &b = \frac{1}{0.779\ *\sigma}.(x - \mu + 0.45\,\sigma) \end{aligned} \tag{4.3}$$

x = magnitude of the concentration, μ = average concentration, and σ = standard deviation.

The probability of arsenic in exceedence of the threshold level (10, 25, 50 ppb) in different hydrologic zones was computed and the results are tabulated in Table 4.2.1.

For example

The probability of arsenic exceeding the threshold level (50 ppb) in the southeast (SE) zone was computed at 71.40% (Table 4.2.1) by using Equation 4.3. The computed values of 'μ' and 'σ' were 174.13 and 199.14, respectively (Table 4.2.1). To compute the probability of exceedence of arsenic threshold level (50 ppb),

$b = (1 / 0.779 * 199.14) * (50 - 174.13 + 0.45 * 199.14 - 0.222)$ and $e^{-e-b} = 0.286$

So, the probability of exceedence of 50 ppb arsenic in water is

$$100 * [1 - F(x)] = 100 * (1 - 0.286) = 71.40.$$

Table 4.2.1 Probability of exceedence of arsenic concentrations in Bangladesh's different hydrologic zones

Hydrologic Zone	Total No. of Sampled Wells	Avg. As Conc. (ppb)	St. Dev.	Probability of exceedence (%)				
				10 ppb	25 ppb	50 ppb	100 ppb	250 ppb
Northeast (NE)	1039	34.00 (0.5-572)	67.96	58.73	48.7	34.00	14.90	<1
North-Center (NC)	192	28.64 (0.5-284)	51.43	53.99	48.08	38.90	24.4	4.98
Northwest (NW)	1072	12.25 (0.5-708)	47.17	44.93	32.74	18.15	5.00	0.30
Southeast (SE)	295	174.13 (0.5-1090)	199.14	80.13	76.26	71.40	59.55	29.14
Southwest (SW)	474	84.80 (0.5-1660)	145.00	66.26	61.41	53.30	38.74	12.00
South-Center (SC)	295	38.61 (0.5-862)	113.18	53.99	48.05	38.95	24.42	4.98

4.2.3 Distribution pattern of arsenic contamination over hydrologic zones

In Table 4.2.1, the probabilities of arsenic exceeding 10, 50, 100 and 250 ppb in the upper 150 m of the aquifer system were computed. These values were superimposed on the hydrologic zone maps of Bangladesh (Fig. 4.2.b) in order to reveal the distribution patterns of arsenic and its relationship with the hydrologic zone. The northwest (NW), northwest (NE), southwest (SW), southeast (SE), north-center (NC) and south-center (SC) zones are described in terms of surface geology and geomorphology in Table 4.2.2. Arc View spatial analyst software was used for surface interpolation and statistical data analysis.

The probability of arsenic in exceedence of the threshold value (>50) strongly correlates with hydrologic zones. The probability of arsenic exceeding the threshold level (50 ppb) was greater than 50% in the SE and SW zones and less than 50% in the northwest (NW), north-center (NC) and south-center (SC) regions of Bangladesh (Fig. 4.2.b and Table 4.2.1).

Table 4.2.2 Description of types of hydrologic zone, geomorphology and surface geology in Bangladesh

Hydrologic Zone ***(Fig. 4.2.b)***	*Types of Geomorphology* ***(Fig. 4.3.a,)***	*Surface Geology* ***(Fig. 4.3.c)***	*Types of Physiographic Units* ***(Fig. 4.3.b)***
Northeast (NE)	Brahmaputra, Surma/ Sylhet Basin	Sylhet depression, Old Brahmanputra Flood Plain (FP), Meghalaya Foothills	Old Brahmaputra Flood Plain (Fp), Sylhet depression
North-Center (NC)	Terrace and Alluvial Sand	Madhupur Tract	Ganges River FP, and Ganges Tidal FP
Northwest (NW)	Old Himalayan Fan, Tista Flood Plain (FP), Lower Purnabhaba FP, Karatoya -Bengali FP, Meghna River FP, Meghna Estuarine FP, Chittagong Coast and Hills	Tista Fan, Jamuna Flood Plain, Atrai Flood Plain, Barind	Tista Fan, Jamuna Flood Plain, Atrai Flood Plain
Southeast (SE)	Meghna River FP, Meghna Estuarine FP, Chittagong Coast and Hills	Alluvial Deposits	Tippera Surface

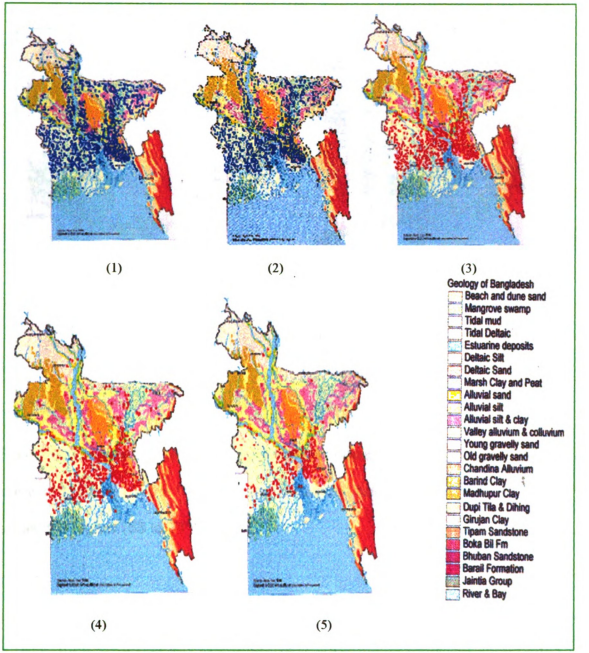

Fig. 4.2.a Blue dots on the map (1 and 2) indicate arsenic-contaminated tube wells with probability of arsenic concentrations >10 ppb and >25 ppb, respectively. Red dots on the map (3, 4, and 5) indicate wells with arsenic >50 ppb, 100 ppb, and 250 ppb, respectively.

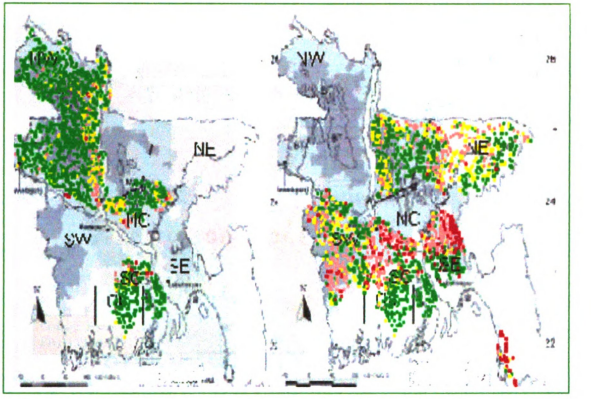

Fig 4.2 b. The probability of arsenic in exceedence of the threshold level (50 ppb) is low (18 to 39%) in the NW, NC and SC zones, but in the NE, SW and SE areas it is higher (53 to 71%).

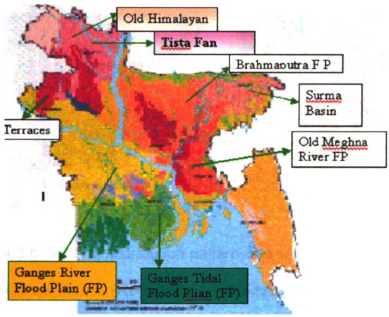

Fig. 4.3.a Geomorphology of Bangladesh

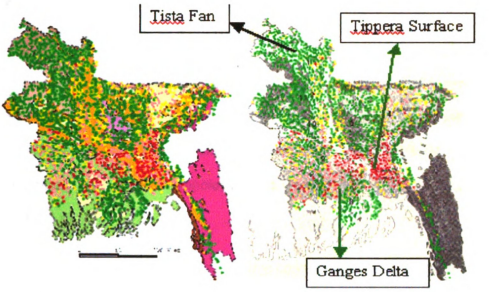

Fig. 4.3.b General distribution pattern of arsenic over surface geology and physiographic unit. (Red spots indicate arsenic >50 ppb.)

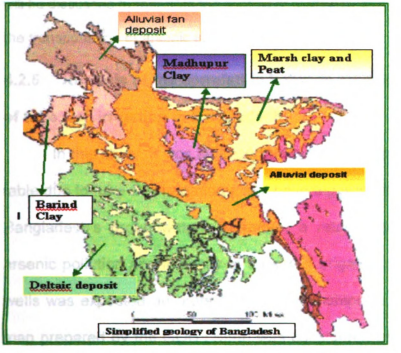

Fig. 4.3.c Surface geology (left) and the physiographic map of Bangladesh (right)

4.2.4 Correlation between arsenic pollution distribution, physiography and surface geology of Bangladesh

Despite having large variability in spatial distributions, it was found that the most arsenic contaminated area was mostly confined to the lower flood delta plains of the Ganges River in southeast (SE) and southwest (SW) region of Bangladesh (Fig.4.2.a). The dominant surface geomorphology is the Ganges flood plain and the Meghna River FP (Fig.4.3.a).

Relation between physiography and arsenic concentration in Bangladesh

The physiographic map analysis in Fig. 4.3.b clearly indicated that the highest arsenic concentration levels (>250 ppb) are mostly in the SE region where the physiograpic unit is dominated by Tippera surface (Fig.4.3.b & Table.4.2.2). This issue will be discussed further from the context of hydrology and influence of river boundary on the transportation of arsenic in the groundwater system.

4.2.5 Analysis of the correlation between arsenic pollution and intensity of tube well irrigation in Bangladesh

In this study, it was an important hypothesis that the lowering of the water table due to tube well irrigation might have triggered the arsenic contamination in Bangladesh's groundwater. Therefore, a relation between the distribution of arsenic pollution and intensity of tube well irrigation as well as the depth of the wells was expected. In order to find relationships, a groundwater irrigated area map prepared by the GOB (1999) was considered as a base map on which the highest percentage of net cultivable area irrigated by groundwater was shown by

the darkest coloration (right side of map in Fig. 4.4). Then the arsenic contamination records with tube-well coordinates were superimposed in order to establish the relation. The results showed that the most intensively irrigated areas do not coincide with the most highly arsenic-contaminated areas.

The graphical evidence in Fig. 4.4 is apparently antipathetic and does not provide any causal links or support to the relationship between arsenic pollution and tube well irrigation. However, at this stage it cannot simply be said that intensive irrigation does not contribute to the arsenic problem by observing only the area irrigated. In order to get a comprehensive idea, it is necessary to include parameters such as depth to the top of the main aquifer, specific yield, storage coefficient, recharge potential, gradients in the head, and geological and thermodynamic explanations of arsenic release in Bangladesh's groundwater.

4.2.6 Depth of irrigation wells versus arsenic concentration distribution over the aquifer's depth

The general patterns of arsenic concentration distribution over the aquifer depth were plotted for 3500 sampled wells distributed over Bangladesh (Fig. 4.5). One would expect higher R^2 values if the arsenic concentrations were related to the depths of the aquifer (0 to 50 m and 100 to 350 m of the aquifer). The main difficulty was to relate the depths with the arsenic concentrations because the concentration records are totally based on stratified random variables such as

the aquifer's depth, hydraulic conductivity, vertical permeability, storage coefficient, etc.

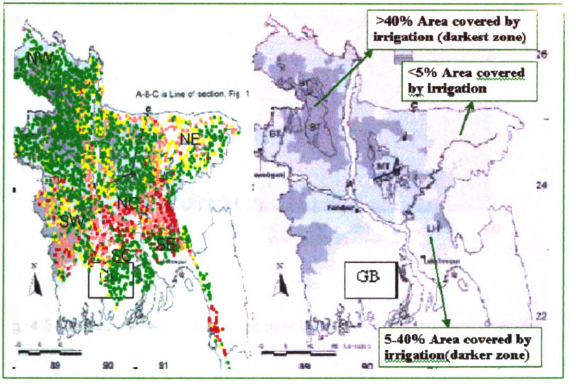

Fig. 4.4 Distribution of groundwater irrigation coverage in Bangladesh. The darkest areas use more than 40% groundwater for irrigation, darker areas use 5 to 40% and white areas use less than 5% groundwater for irrigation.

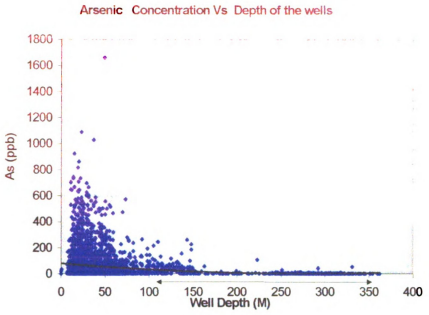

Fig. 4.5 Arsenic concentration range over the depth of Bangladesh's aquifer

To determine the relation between depth of the aquifer and arsenic concentration for the study area , a band regression analysis was performed. The average depth and arsenic concentration within the selected band or group was estimated by the method known as Ensemble Average. The main advantage of this method is that it carries the value of concentration (C) of the immediately preceding one in a particular series or group of concentration values.

The average concentration was computed as follows.

$$C_{Av_n}(x) = \frac{n-1}{n} * C_{n-1}(x) + \frac{1}{n} C_n(x) \qquad (4.4)$$

where C_{Av_n} = average concentration at any particular depth range 'x', and n = number of layers. An ensemble average value was taken for each band. A preliminary test of correlation between depth and arsenic concentration was performed and the results are presented in Table 4.2.3 and in Fig. 4.6.a and 4.6.b.

Table 4.2.3 Regression analysis between aquifer depth and arsenic pollution distribution in Bangladesh's groundwater

Zone	Depth Range (m)	Regression Equation	R^2 Value (%)
All regions (NW, NE, SW, SE)	0 to 10 m	Y=5.09 x	58
SE and SW regions	9 - 30	Y=0.3428+1.79 log (x)	60
All regions	50 -350	Y= -33.178 Ln (x)+196.29	67
(NW, NE, SW, SE)	100-350	Y= -52.64 Ln (x)+301.83	85.17

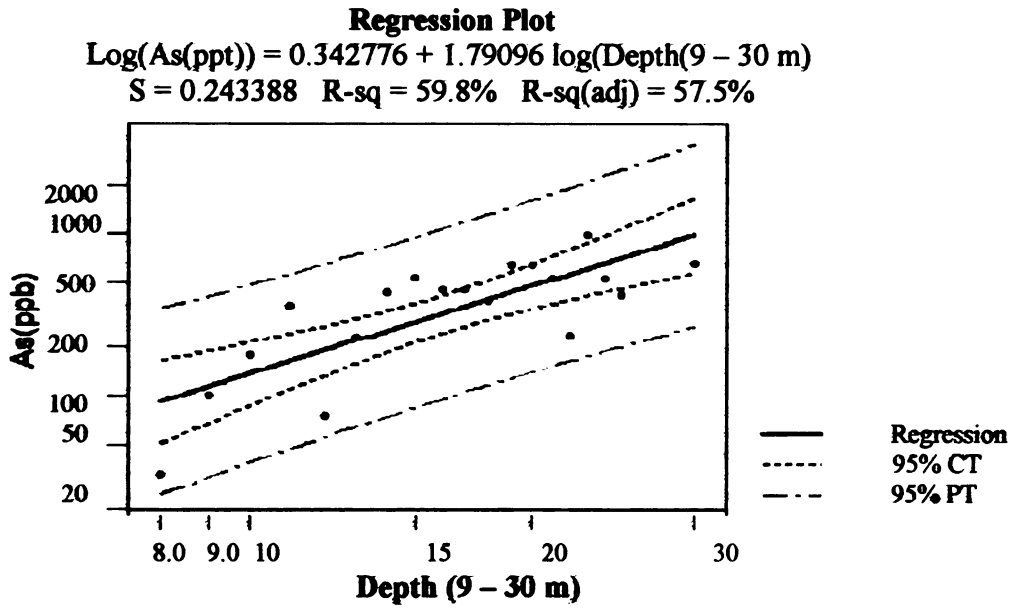

Fig. 4.6.a Arsenic content increases linearly with depth from 9 to 30 m

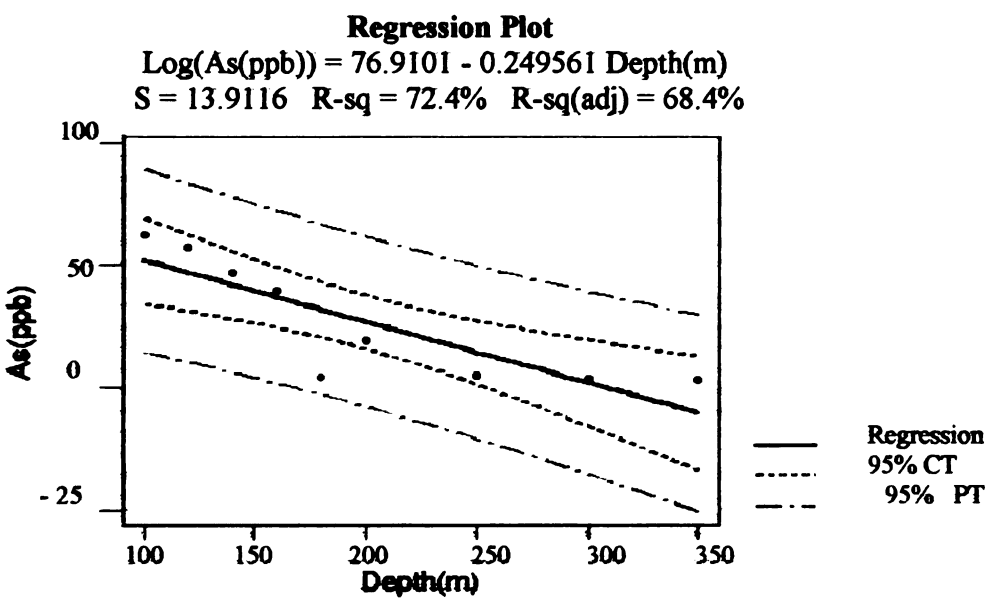

Fig. 4.6.b Arsenic content decreases linearly with depth from 100 to 350 m

4.2.7 Correlation between arsenic concentration and dissolved iron content in Bangladesh's groundwater

It was hypothesized in this study that the lack of oxygen in the vadose zone develops a reducing condition and which causes the release of arsenic into Bangladesh's groundwater. This release is associated with the amount of amorphous iron oxides and hydroxides present in the water in dissolved form. Obviously, one would consider this dissolved iron as geochemical evidence in order to support the hypothesis. If arsenic release in the groundwater is associated with the iron oxides and hydroxides at reducing condition, then one would expect higher R^2 values between arsenic species and the redox potential values or the dissolved iron in the groundwater system.

In order to reduce the spatial influence, the whole country was divided into 16 major blocks or square grids based on one-degree intervals of latitude and longitude. The advantage of a square grid system is that the geochemical evidences of arsenic released along the flow path of groundwater or along the hydraulic gradient could easily be monitored. The statistical analysis was conducted for all grids to determine the relationship between arsenic concentration and dissolved iron content for each square grid, and the results are presented in the following Figs.4.7.a and 4.7.b and also in Table 4.2.4. The grid numbers are shown in Fig. 4.8

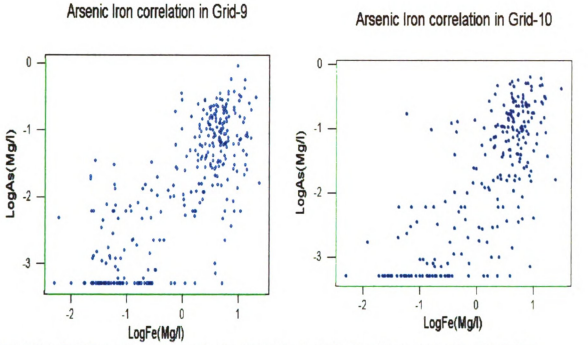

Fig.4.7.a. Relation between arsenic concentration and dissolved Iron content in the Grid-9, Grid-10 in Bangladesh

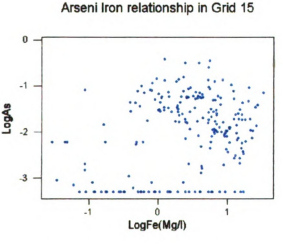

Fig.4.7.b. Relation between arsenic concentration and dissolved Iron content in the Grid-15 in Bangladesh

Table 4.2.4 Statistical relationship between arsenic and iron concentration at different grid locations (latitude/longitude) in Bangladesh.

Grid No.	Latitude (°N)	Longi-tude (°E)	No. of Well	Avg. As (III & V) (mg/L)	Avg. Iron (Fe^{2+}) Conc. (Mg/L)	R^2 (%)	Value of $\beta 1$	Value of slope $\beta 2$
1	26-26.75	88.2-89	116	0.09 0.816 - .0003	4.5 41.8 - 0.02	54	-5.46	0.49
2	25-26	88.2-89	152	0.002 0.05-0.0005	1.78 16.9-0.015	65	-2.91	0.33
3	24-25	88.2-89	200	0.021 1.66-.0005	1.06 17.2-.0005	62	-2.50	0.51
4	23-24	88.2-89	77	0.091 1.03-0.005	2.6 9.27-.006	60	-1.58	0.52
5	22-23	88.2-89-	13	0.139 0.328-.0007	3.8 7.6-0.055	99	-1.52	1
6	26-26.75	89-90	34	0.00354 0.042-.0005	3.88 28.6-0.01	37	-6.52	0.27
7	25-26	89-90	339	0.014 0.708-.0005	4.57 41.8-0.012	65	-2.58	0.54
8	24-25	89-90	369	0.021 .632-.0005	4.26 48.2-0.005	64.5	-2.40	0.67
9	23-24	89-90	328	0.07 .924-.0005	3.24 20.6-0.005	74	-1.83	0.85
10	22-23	89-90	243	0.096 .635-.0005	3.87 30.4-.005	71	-1.90	0.96
11	24-25	89-90	345	0.025 .573-.0005	1.69 15.9-.005	76	-2.12	0.86
12	23-24	90-91	411	.17 1.09-.0005	3.77 26.1-0.02	76	-1.62	1.05
13	22-23	90-91	284	0.044 .862-.0005	1.14 12.7-0.005	68	-1.99	0.9
14	24-25	91-92	344	0.025 .572-.0005	1.69 15.9-0.005	67	-2.84	0.87
15	23-24	91-91.25	411	.17 1.09-.0005	3.77 26.1-0.02	74	3.37	1.05
16	22-23	91-92	284	0.044 .86-.0005	1.14 12.7-0.005	63	-2.58	0.9

4.2.8 Correlation between arsenic distribution pattern and groundwater flow direction

The relation between arsenic distribution patterns and groundwater flow directions was analyzed by dividing the whole country into a number of square grids where arsenic concentration records and groundwater flow direction maps were available. Here a potentiometric surface and elevation map prepared by MPO (1987) was used to determine the direction of the hydraulic gradient (left side map in Fig. 4.8) . Bangladesh's whole arsenic-contaminated area was divided into 16 grids. Grids 6, 7, 8, 9, and 10 (right side map in Fig. 4.8) follow the same hydraulic gradient and direction of flow. The arsenic concentration records in those five grids showed a strong correlation between arsenic concentration and flow direction. Table 4.2.4 states that the value of the slope factors (β_2) in grids 6, 7, 8, 9, and 10 are 0.27, 0.54, 0.67, 0.85, and 0.96, respectively. The slope factor values are increasing with the grids' increasing numbering. This indicates a relationship between arsenic concentration and groundwater flow direction in Bangladesh.

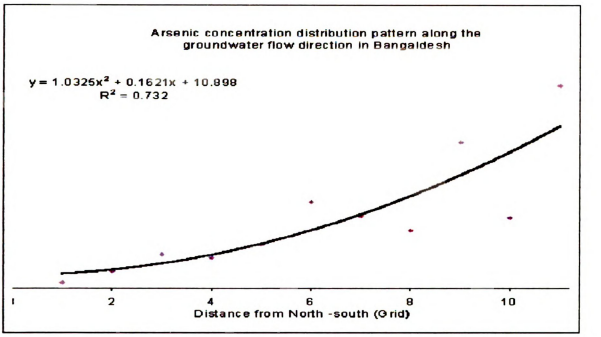

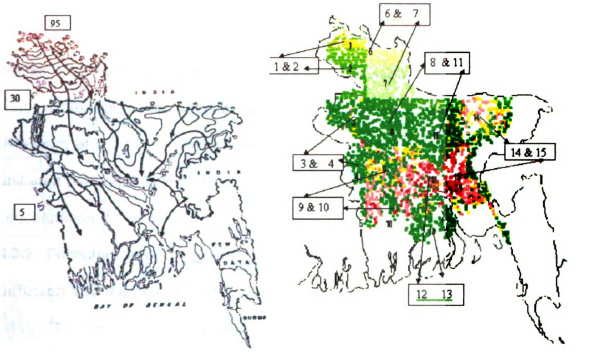

Fig. 4.8 Distribution pattern of arsenic concentration along the groundwater flow direction (left side) , considering grids 6, 7, 8, 9, and 10(right side) , where the surface elevation gradient was considered as the hydraulic gradient . .

4.3 Diffusive transportation of atmospheric oxygen to the saturated zone in the groundwater systems of Bangladesh

The statistical analysis (presented in Table 4.2.3, Fig. 4.6.a, Fig. 4.6.b, and Fig. 4.8) clearly indicates there exists a relation between arsenic pollution distribution and depth of the aquifer. On the other hand, lowering of the water table limits the diffusive supply of atmospheric oxygen to the deeper layer. The third research issue, the interactions between lowering of the water table, dissolved oxygen content in recharging water and arsenic pollution distribution in terms of oxygen accessibility in the groundwater systems will be investigated.

4.3.1 Diffusive transportation of atmospheric oxygen into the aquifer

Generally two main processes affect gaseous transportation within the aquifer: convection and diffusion. The convective transport of oxygen in the soil-water system is at typical pore-water velocities (pwv) in the unsaturated zone (Refsgard et al., 1991). Fick's law says that the flux of solute mass crossing a unit area per unit time in a given direction is proportional to the gradient of solute concentration in that direction.

4.3.2 Formulation of the governing equation for oxygen transportation by diffusion into the groundwater system

The concept of control volume was used to demonstrate how conservation of mass leads to developing a governing equation for oxygen transportation in the subsurface. A mathematical expression of Fick's law is

$$q = -D\frac{\partial C}{\partial x}. \qquad (4.3.1)$$

where q is the solute mass flux, C is the mass concentration of diffusive oxygen, D is the coefficient of proportionality (L^3/T) and the minus sign indicates that transport is from high to low concentration.

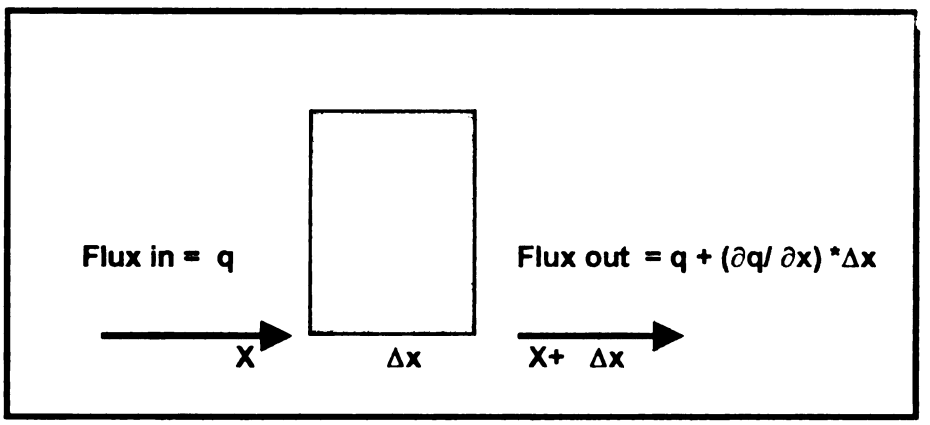

Fig. 4.9 Use of control volume to derive one-dimensional oxygen diffusion equation

Two parallel surfaces of a unit area are drawn perpendicular to the axis and separated by a distance Δx. The mass of oxygen flow in q = f (x, t) at area x is equal to the mass of oxygen flow out [q + (∂q/ ∂x) *Δx]. Let C (x, t) be the mass of oxygen concentration per unit volume at the point x at time t. There is mass C (x, t)* Δx in the line segment bounded by the parallel planes. Since molecules of oxygen are passing in and out of the volume, defined by the

boundary surface, there is a rate of change of mass in the control volume equal to $\frac{\partial C}{\partial t}\Delta x$.

This rate of change of mass must be equal to the difference in the flux, or rate of passage of oxygen molecules through each surface, in order to satisfy the law of conservation of mass. Equating these two gives us

$$\left(\frac{\partial q}{\partial x}\right)+\left(\frac{\partial C}{\partial t}\right)=0. \tag{4.3.2}$$

which yields a relationship between flux q (x, t) and concentration C (x, t). The governing equation is found by inserting the value of q (x, t) from Eq. 4.3.1 into Eq. 4.3.2.. In the presence of any source or sink, the above equation can be written as

$$\left(\frac{\partial C}{\partial t}\right)=D\left(\frac{\partial^2 C}{\partial x^2}\right)+Source.orSink.(\alpha) \tag{4.3.3}$$

Finally, the above equation (4.3.3) can be written as the governing equation describing the non-steady-state oxygen diffusion into the sub-soil aquifer system. This equation is expressed in the form of a partial differential equation as follows.

$$Dx*\frac{\partial^2 C}{\partial x^2}+(\alpha)-\frac{\partial C}{\partial t}=0$$

$$Where, \tag{4.3.4}$$

$$\alpha = Decaying..cons\tan t$$

4.3.3 Formulation of finite element technique to solve the governing equation for oxygen diffusion in the groundwater system

The above governing equation (4.3.4) can be solved both analytically and numerically, but the analytical solutions are lengthy processes. There are many numerical methods available, such as the finite difference (FD) model, the finite element (FE) model, the method of characteristics (MOC) model, and the random walk (RW) model. In this study, the finite element formulation technique was used because of its higher accuracy and adaptability to numerical solutions for physical processes like diffusion convection, pollution distribution or contaminant transportation. Many studies have shown that numerical solutions from the finite element (FE) model give satisfactory results with a wide range of boundary conditions with irregular and curved aquifer boundaries. In addition, the FE solution technique by Galerkin provides simplicity and stability of the solution (Segerlind, 1996).

Integral formulation

The integral formulation for the governing equation (4.3.4) will lead to a system of algebraic equations that can be solved for values of the field variables at each node in the mesh to obtain the variation of oxygen concentration C with time t. The weighted residual method was used in this study.

Evaluation of Weighted Residual Integral method

Galerkin's formulation of the weighted residual functions can be constructed using the shape function N_i and N_j (Segerlind, 1994). Evaluating this weighted residual integral, which is the result of integrating the product of diffusion equation (Eq. 4.3.4) and a weighting function, W (x), yields a nodal equation over the length of the element.

$$[R^e] = -\int_{x_i}^{x_j} [W_e] \left(D \frac{\partial^2 C}{\partial x^2} + \alpha + \lambda \frac{\partial C}{\partial t} \right) dx = 0 \qquad (4.3.5)$$

where $[W_e]^T = [N]^T$ is the element weighting function for node I, and is equal to the shape function or interpolation function. The finite element formulation is applied after representing the unknown concentration C by linear approximation of the form as

$$C^{(e)} = N_i C_i .. + N_j C_j .$$

or

$$C^{(e)} = \begin{bmatrix} N_i & N_j \end{bmatrix} \begin{Bmatrix} C_i \\ C_j \end{Bmatrix} = [N]\{C\} \qquad (4.3.5.a)$$

where N_i and N_j are the shape function at nodes i and j respectively, and are the values of unknown concentration C at nodes i and j.

The conventions { } and [ ] represent vector and matrix quantities, respectively, and will be represented so throughout the analysis. The shape functions N_i and N_j in equation 4.3.5.a can be expressed as follows:

$$N_i = \frac{X_j - x}{L}.and.N_j = \frac{x - X_i}{L}$$

$$N = \begin{bmatrix} N_i & N_j \end{bmatrix}.and..[N]^T = \begin{bmatrix} N_i \\ N_j \end{bmatrix}$$

In the Galerkin method, W_s, the weighted function at the S^{th} node, consists of the shape functions associated with the S^{th} node. Therefore, the transposition of the matrix of weighting function is equal to the transposition of the shape function, $[W_e]^T = [N]^T$. The above equation (4.3.5) can be written for node i & j for each element as

$$[R^e] = -\left(\int_{xi}^{xj} [N]^T \left(D \frac{\partial^2 C}{\partial x^2} + \alpha \right) dx + \int_{xi}^{xj} [N]^T \lambda \frac{\partial C}{\partial t} dx \right). = 0 \qquad \text{or}$$

$$= -\int_{xi}^{xj} \begin{bmatrix} N_i \\ N_j \end{bmatrix} .. \left(D \frac{\partial^2 C}{\partial x^2} + \alpha \right) .dx - \int_{xi}^{xj} \begin{bmatrix} N_i \\ N_j \end{bmatrix} .\lambda \frac{\partial C}{\partial t} .dx. = 0. \qquad (4.3.6)$$

After reducing terms for node i and j, equation (4.3.6) can be expressed for node i and j as

$$\{R_{(e)}\}. = \begin{Bmatrix} R_i^{(e)} \\ R_j^{(e)} \end{Bmatrix} = \begin{Bmatrix} -\int_{xi}^{xj} N_i .D. \frac{\partial^2 C}{\partial x^2} dx - \int_{xi}^{xj} N_i .. \alpha .. dx - \int_{xi}^{xj} N_i .. \lambda \frac{\partial C}{\partial t} .dx \\ -\int_{xi}^{xj} N_j .D. \frac{\partial^2 C}{\partial x^2} dx - \int_{xi}^{xj} N_{ij} \alpha .. dx - \int_{xi}^{xj} N_j .\lambda \frac{\partial C}{\partial t} .dx \end{Bmatrix}. \qquad (4.3.7)$$

Equation 4.3.7 can be rewritten as follows

The right side of the above equation (4.3.8) can be evaluated for node i, by breaking it into Part A and Part B and evaluating the time derivative in Part C.

$$Part - A = \int_{xl} N_i . D . \frac{\partial^2 C}{\partial x^2} dx$$

$$Part - C .. = . \int_{xl} N_i .. \lambda \frac{\partial C}{\partial t} . dx$$

Evaluation of the above integrals part by part follows.

Part A

$$Part - B .. = . \int_{xl} N_i .. \alpha .. dx$$

$$\text{Part A of Equation 4.3.8} = \int_{xl} N_i . D \frac{\partial^2 C}{\partial x^2} dx = D \int_{xl} N_i(x) . \frac{\partial^2 C}{\partial x^2} dx$$

Part A cannot be evaluated directly because the continuity of the function (dc/dx) is unknown. But, according to the product of two-function rule,

$$\frac{\partial}{\partial x}\left(N_i(x) \frac{dC}{dx} \right) = N_i(x) . \frac{\partial^2 C}{\partial x^2} + \frac{\partial C}{\partial x} \frac{\partial N_i(x)}{\partial x}$$

Or by rearranging, Equation 4.3.8.1(Part A) can be rewritten as

$$\int_{x_i} D.N_i(x).\frac{\partial^2 C}{\partial x^2} = D\int_{x_i} \frac{\partial}{\partial x}\left(N_i(x).\frac{\partial C}{\partial x} \right) dx - D\int_{xl} \frac{\partial C}{\partial x} \frac{\partial N_i(x)}{\partial x} . dx \quad \text{(4.3.8. Part A)}$$

The first part of RHS of Eq. 4.3.8 (Part A)

$$\int_{xl} D \frac{\partial}{\partial x}\left(N_i(x).\frac{\partial C}{\partial x} \right) dx = -DN_i(x).\frac{\partial C}{\partial x}\bigg|_{xl} = -DN_i(x).\frac{\partial C}{\partial x}\bigg|_{xl}$$

because the derivative boundary condition of i at j is equal to zero.

The second part of RHS of Eq. 4.3.8 (Part A)

$$= D \int_{x_i}^{x_j} \frac{\partial C}{\partial x} \cdot \frac{\partial N_i(x)}{\partial x} .dx \;..\; = D \int_{xi}^{xj} \frac{-1}{L} C_i \frac{-1}{L} dx \;=\; \left[\frac{D}{L^2} C_i \right]_{xi}^{xj} = \frac{D}{L} C_i$$

because the unknown oxygen concentration function $C = N_i C_i + N_j C_j$ **and**

$\frac{\partial C}{\partial x} = C_i \frac{\partial N_i}{\partial x} + 0 = \frac{-1}{L} C_i$ **as it is known that the derivative of the shape function**

$$N_i = \frac{X_i - x}{L} .and... \frac{\partial N_i}{\partial x} = \frac{-1}{L}$$

Part B

$$\int_{x_i}^{x_j} N_i \; \alpha \;..dx \;=\; \int_0^L N_i .\alpha \;.ds \;=\; \int_0^L \left(1 - \frac{s}{L}\right) .\alpha \;.ds \;=\; \alpha \;. \left[s - \frac{s^2}{2L} \right]_0^L = \alpha \;. \frac{L}{2} .$$

as ..it ..is ..known .,. in ... s..coordinate ..system ., $s. = \frac{L}{2}$*... and*

$$N_i . = \frac{X_j - (X_i + s)}{L} . = \frac{L - s}{L} = 1 - \frac{s}{L}$$

$$N_j = \frac{(X_i + s) - X_i}{L} = \frac{s}{L}$$

$$[N] = [N_i \quad N_j] = \left[1 - \frac{s}{L} \quad \frac{s}{L}\right]$$

Part C:

Evaluation of time derivative

$$\int_{x_i}^{x_j} \lambda \cdot [N]^T \cdot \frac{\partial C}{\partial t} \cdot dx = \int_0^L \lambda \cdot [N]^T [N] \{C^{(e)}\} ds$$

$$\int_0^L \lambda \cdot [N]^T \cdot [N] \cdot ds \cdot \{C^{(e)}\} = \{C_E^{(e)}\} \{C^{(e)}\}$$

where, $[C_E^{(e)}] = \int_0^L \lambda \ [N]^T [N] ds$

$C_E^{(e)}$, the element capacitance matrix, can be evaluated as

$$\left[C^{(e)}\right] = \int_0^L \lambda . \begin{bmatrix} N_i \\ N_j \end{bmatrix} . \begin{bmatrix} N_i & N_j \end{bmatrix} ds .. = \lambda \int_0^L \begin{bmatrix} N_i N_i & N_i N_j \\ N_j N_i & N_j N_j \end{bmatrix} ds .. = \frac{\lambda . L}{2} \begin{bmatrix} 1 & 0 \\ 0 & 1 \end{bmatrix}$$

where $N_i N_i = N_j N_j = 1$ and $N_i N_j = 0$,

This formulation produces a diagonal capacitance matrix. A diagonal capacitance matrix is usually referred to as a lumped formulation (Segerlind, 1996). After collecting of all terms of integral evaluation of Part A, Part B and Part C, the equation (4.3.8) can be finally expressed as the matrix-integral form of the residual equation of (4.3.5) as follows

$$\left(R^e\right) = \begin{pmatrix} .D\frac{dc}{dx}\Big].x = x_i \\ -D\frac{dc}{dx}\Big].x = x_j \end{pmatrix} + \begin{bmatrix} \frac{D}{L} & -\frac{D}{L} \\ -\frac{D}{L} & \frac{D}{L} \end{bmatrix} .. \begin{pmatrix} C_i \\ C_j \end{pmatrix} - . \begin{bmatrix} \frac{\alpha . L}{2} \\ \frac{\alpha . L}{2} \end{bmatrix} . + . \frac{\lambda L}{2} . \begin{bmatrix} 1 & 0 \\ 0 & 1 \end{bmatrix} \qquad (4.3.9)$$

The solution for a general, ordinary differential equation in a matrix-integral form of residual equation is [R] = {I} + [K] {C}-{F}, where {I}=inter elemental stiffness matrix due to derivative boundary condition, [K]= conductance matrix due to material property, and {F} is the force factor due to source and sink. The new term time derivative in Eq. 4.3.5 λ*(dc/dt) can be finally expressed as in matrix form in equation 4.3.9 as $\frac{\lambda L}{2}\begin{bmatrix}1 & 0\\ 0 & 1\end{bmatrix}$, and has to be solved by Lumped formulation method. Using the backward difference form of Lumped formulation method, the solution of the equation (4.3.9) can be written in matrix form as

$$(.[A]+\nabla t.[K])\{C\}_{t+\nabla t} = [A]\{C\}_t + \nabla t.\{F\}_{t+\nabla t} \qquad (4.3.10)$$

where A = element capacitance matrix, K = element conductance matrix,

F = force factor, C_t = concentration of oxygen at any time t, and $C_{(t+\nabla t)}$ = concentration of oxygen in the element after time step ∇t.

$$[A]=\frac{\lambda L}{2}\begin{bmatrix}1 & 0\\ 0 & 1\end{bmatrix}$$

$$[K]=\frac{D}{L}\begin{bmatrix}1 & -1\\ -1 & 1\end{bmatrix}$$

$$\{F\}^e=\frac{\alpha.L}{2}\begin{bmatrix}1\\ 1\end{bmatrix}$$ (When sources are distributed along the element)

Equation 4.3.10 gives the nodal value of oxygen concentration $\{C\}_{t+\nabla t}$, in terms of a set of known initial values $\{C\}_t$, the vector associated with source or

sink {F}, at time t and t+∇t and the ratio of θ. For the backward difference method θ =1 to get the value of the oxygen concentration C at each elemental section of 10 meter length profile with time step ∇t, software based on the finite element computer program developed by Segerlind (1997) was used to solve a system of linear equations at each node of each element. The results are presented in Fig. 4.11 and 4.12 and Table 4.3.2.

In the finite element formulation, the value of diffusion coefficient Dx = 259.2 $cm^2\ hr^{-1}$($4.166*10^{-4} m^2 s^{-1}$) and the oxygen consumption rate α= -0.002125 $cm^3 cm^{-3} h^{-1}$. The values of Dx and α are taken from the experimental findings of Kanwar (1986)and Papendick and Runkles (1965) because, in his experiment, Kanwar (1986) found a reasonably good agreement between measured and predicted oxygen concentration by using the techniques of Laplace transformation to solve the oxygen transport equation (4.3.4), although it is true that the reaction factor α varies from soil to soil as a result of the variation of organic carbon.

4.3.4 Analysis of the influence of water table lowering on oxygen concentration distribution in the deep layers of groundwater

The above equation (4.3.10) presents an oxygen transportation model with a constant oxygen consumption rate by organic carbon in the vadose zone of the aquifer. The finite element formulation model was applied to solve the equation (4.3.10) in order to understand the interaction between diffusive oxygen supply,

depth of aquifer and their relation with arsenic concentration change. It will be investigated whether lowering of water table provides a greater oxygen supply to the hypothetical arsenopyrite layer (L_6 and L_{10}) or not (Fig. 4.10).

Description of the oxygen diffusion model in deeper layers:

The model aquifer was schematically represented in Fig. 4.10. A 10 m deep aquifer was modeled by using finite element formulation. The layer numbers L_1, L_2, L_3 up to L_{10} in Fig. 4.10 represent the length of each element. Each layer is considered to be 100 cm deep. Two hypothetical layers, L_6 and L_{10}, (Fig. 4.10) were assumed to contain arsenic-rich pyrite sediment because arseno-pyrite layers can exist randomly in the aquifer at any depth and at discontinuous phase. It will be investigated whether there has been any change in the oxygen concentration of the pyretic layer (L_6 & L_{10}) before and after the introduction of well fields in Bangladesh.

Case 1 represents the situation before installation of wells when the water table position (WT-1) was at L_2, 2 m below the surface. Case 2 represents the condition after installation of 0.75 million tube wells when the water table (WT-2) was lowered to 5 m depth at L_5 (Fig. 4.10) as a result of overpumping. In this study, the change in diffusive supply of oxygen concentration at pyretic layers L_6 and L_{10} under two hypothetical conditions was investigated.

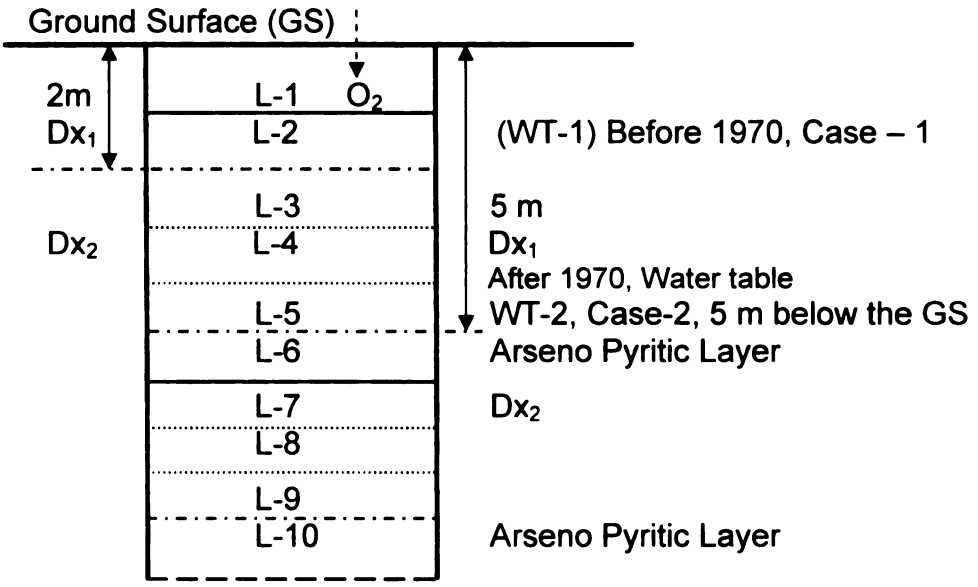

Fig. 4.10 Aquifer model cross section of a 10-meter deep layer (from L_1, L_2 to L_{10} representing ten elements).

The values of the oxygen diffusion coefficients (Dx_1 and Dx_2), oxygen consumption or decomposition rate (α) for each element length (L_1, L_2) were tabulated in Table 4.3.1. The initial oxygen concentration at the boundary of each element was 0.21 atm, except for the last one, L_{10}. After inserting all the values, pre-prepared computer software computed the values of the global conductance matrix (K), the global capacitance matrix (A), and the source or sink factor (F) in order to solve equation 4.3.10 for time steps equal to one hour and to four hours

Table 4.3.1 Number of elements, number of nodes and material properties of the aquifer material for the shallow and deep tube well system in Bangladesh

Length (cm)	Cum. Length (m)	Element No	n	Oxygen Consumption Rate (α) ($cm^3cm^{-3}h^{-1}$)	Oxygen Diffusion Coeff(Dx) (cm^2/hr)			
					Case 1		Case 2	
					D_{x1}	D_{x2}	D_{x1}	D_{x2}
L_1=100	1	1, 2	0.5	0.0021	259.2		259.2	
L_2=100	2	3, 4	0.5	0.0021	259.2		259.2	
L_3=100	3	5, 6	0.5	0.0021	*	129	259.2	
L_4=100	4	7, 8	0.5	0.0021		129	259.2	
L_5=100	5	9, 10	0.5	0.0021		129	259.2	
L_6=100	6	11, 12	0.5	0.0021		129	*	129
L_7=100	7	13, 14	0.5	0.0021		129		129
L_8=100	8	15, 16	0.5	0.0021		129		129
L_9=100	9	17, 18	0.5	0.0021		129		129
L_{10}=100	10	19, 20	0.5	0.0021		129		129

* For case 1, the water table was at 2 m depth (L_2), so the Dx_1 value was used up to 2 m, and the Dx_2 value started from L_3. (Dx_2 for saturated layers was considered to be 50% of Dx_1.) n=air fill porosity of the aquifer material

Finally, the oxygen concentration at each element was computed over the period of 500 hours. The oxygen concentration records are tabulated in Table 4.10. The graphical presentation in Fig. 4.11 indicates that lowering of the water

table about 4 m from L_2 to L_6 did not increase the oxygen concentration at L_{10} and L_6 (Fig. 4.11). The oxygen concentration in case 1 at L_6 was found 0.09 atm (3.64 mg/L) after 150 hours. But after lowering of the water table, after the same interval of time, the oxygen concentration was found to be 0.06 atm (2.39 mg/L) (Table 4.3.2).

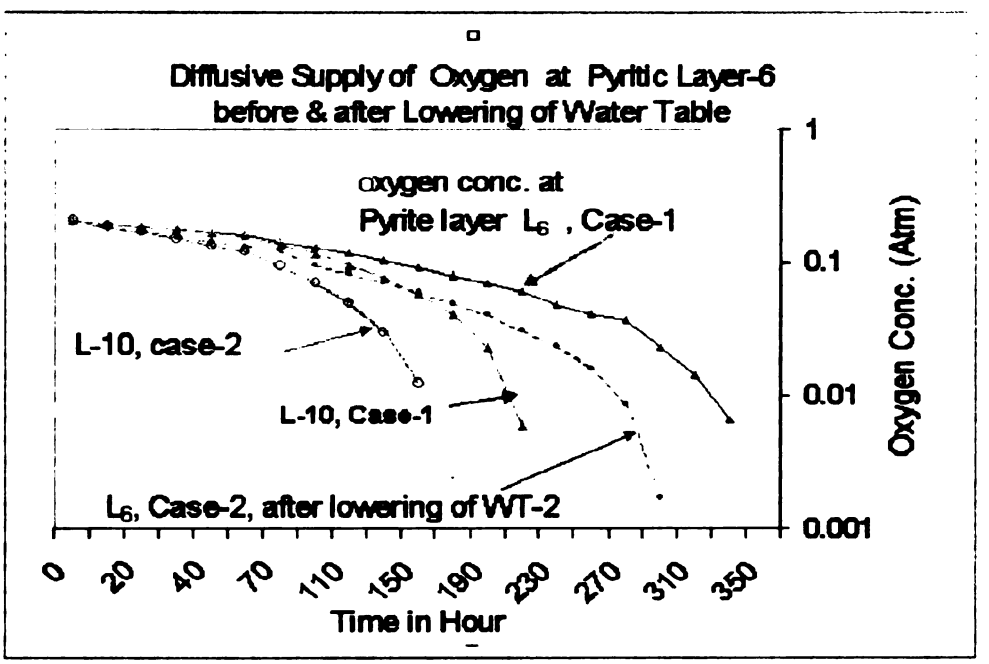

Fig. 4.11 Predicted changes in the diffusive oxygen supply at arsenic-contaminated pyretic layer L_6 and L_{10} in the aquifer.

Table 4.3.2 Diffusive oxygen concentration at pyretic layer L_6 before and after the introduction of well fields, assuming the initial O_2 concentration to be 0.21 atm for all nodes.

Time (hr)	*Oxygen conc. at layer 6 (pyretic layer at 6 m depth)*				*Oxygen conc. at layer 10 (sediment layer at 10 m depth)*			
	Case 1 (Before well intro.)		Case 2 (After well intro.)		Case 1 (Before well intro.)		Case 2 (After well intro.)	
	(atm)	(mg/L)	(atm)	(mg/L)	(atm)	(mg/L)	(atm)	(mg/L)
0	0.21	8.37	0.21	8.37	0.21	8.37	0.21	8.37
10	0.193	7.945	0.189	7.545	0.199	7.946	0.189	7.55
20	0.188	7.523	0.171	6.838	0.188	7.522	0.170	6.80
30	0.178	7.121	0.156	6.244	0.178	7.099	0.153	6.103
40	0.169	6.744	0.143	5.732	0.167	6.67	0.136	5.456
50	0.160	6.389	0.132	5.283	0.159	6.255	0.12	4.857
70	0.144	5.739	0.122	4.882	0.136	5.421	0.094	3.778
90	0.129	5.151	0.097	3.873	0.115	4.612	0.070	2.828
110	0.115	4.613	0.083	3.329	0.095	3.825	0.049	1.977
130	0.1031	4.112	0.071	2.836	0.076	3.062	0.030	1.205
150	0.0913	3.642	0.060	2.394	0.058	2.323	0.124	0.0495
170	0.0807	3.216	0.049	1.988	0.040	1.606	0	0
190	0.0690	2.778	0.0406	1.618	0.022	0.914	0	0
210	0.0599	2.391	0.031	1.235	0.006	0.240	0	0
230	0.049	1.958	0.023	0.944	0	0	0	0
250	0.040	1.618	0.0160	0.637	0	0	0	0
270	0.037	1.474	0.0087	0.346	0	0	0	0
290	0.023	0.916	0.0017	0.067	0	0	0	0
310	0.014	0.558	0	00	0	0	0	0
330	0.0066	0.263	0	0	0	0	0	0
350	0	0	0	0	0	0	0	0

4.3.5. Influence of initial boundary conditions on oxygen concentration

The influence of initial oxygen concentration at each element on the overall oxygen concentration distribution over the given depth range was also analyzed. Table 4.3.2 represents the results of oxygen concentration distribution when initial oxygen concentrations were 0.21 atm at all nodes except the last node (L_{10} = 0). Table 4.3.3 represents the results when the initial oxygen concentrations were changed from 0.21 to 0.15 atm for both case 1 and case 2. The influences of initial conditions were prominent and are discussed in detail in chapter six.

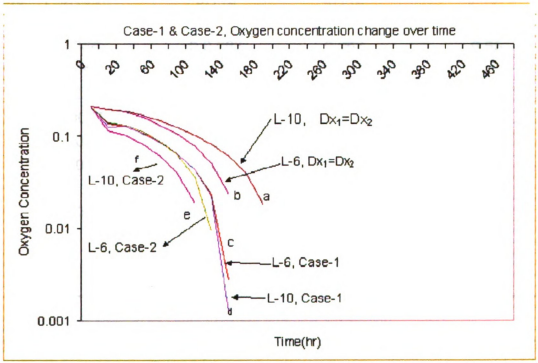

Fig. 4.12 Influence of boundary conditions on oxygen concentration (atm) before and after lowering of water table (case-1 and case -2).

Table 4.3.3 Diffusive oxygen concentration at pyretic layer 6 before and after the introduction of well fields in Bangladesh, while considering the initial O_2 concentrations of 0.15 atm for nodes in the saturated zone.

Time (hr)	*Oxygen conc. at layer 6 (pyretic layer at 6 m depth)*		*Oxygen conc. at layer 10 (sediment layer at 10 m depth)*	
	Case 1 a. (Before) (atm)	Case 2 (After) (atm)	Case 1 (Before) (atm)	Case 2 (After) (atm)
0	0.21	0.21	0.21	0.21
10	0.139	0.141	0.141	0.139
20	0.129	0.0.133	0.133	0.128
40	0.108	0.112	0.112	0.107
60	0.086	0.088	0.088	0.086
80	0.066	0.0.063	0.063	0.65
100	0.044	0.036	0.0362	0.044
120	0.024	0.009	0.009	0.023
140	0.0027	0	0	0.011
160	0	0	0	0.001
180	0	0	0	0
.				
460	0	0	0	0

a. Initial oxygen concentrations at the boundary of each element were changed to 0.15 atm at all the nodes of the saturated layers.

4.4 Computation of redox potential (p^e) values and stability analysis of arsenic (III & V) redox couples in Bangladesh's groundwater

The stability diagram of iron and arsenic redox species was constructed and evaluated in order to satisfy the second research issue, whether pyrite oxidation or reduction of iron oxyhydroxides mainly controls arsenic release in the groundwater system in Bangladesh. Literature review suggested that a mildly reducing condition (p^e= 0.5 to -3.5) is responsible for arsenic release in to groundwater. In this analysis, it will be investigated thermodynamically if mildly reducing condition could be developed after lowering of water table .The redox potential values will be computed using the activity or concentration of dissolved iron and arsenic species present in groundwater.

4.4.1 Measurement of redox potential values

Although aqueous solutions do not contain any free protons or electrons, it is nevertheless possible to define relative proton and electron activities. The pH (-log $\{H^+\}$) of a system measures a relative tendency of a solution to accept or donate protons. Similarly, the redox intensity (p^e= -log {e}) measures the tendency to accept or donate electrons in a solution.

Existing methods of measurement involve use of potential sensing inert metal electrodes or analytical determination of redox indicator species such as dissolved O_2 or Fe^2. In general, a platinum electrode responds satisfactorily to very few of the redox couples in natural and groundwater systems. In relatively

oxidizing water, E_h or p^e values measured with platinum electrodes can rarely be related to a specific redox pair (Drever,1988). Therefore the activity or concentration method is used to measure the E_h or p^e values.

The activity of electrons in a solution (hence its redox level) can be expressed in units of volts (E_h) or in units of electrons activity or p^e. The redox intensity p^e is related to redox potential (E_h) by thermodynamic equations as follows

$$p^e = \frac{F}{2.3.R.T}.E_h$$

or (4.4.1)

$$p^e = 16.9 * E_h,$$

$$E_H = 0.059 * p^e$$

Where,

R= Gas constant (8.314 *10^{-3} K.J/deg. Mol)), or R= 1.987x 10^{-3} kcal/deg.mol

T- Absolute Temperature in K.

F= Faradays' electric constant (96.42 kJ per volt gram equivalent). or in calories,

F= 23.06 kcal per volt gram equivalent, at 25 ° C, 2.3 is the conversion from natural to base 10 logarithms

4.4.2. Use of p^e as a variable to measure the iron controlled (Fe^{2+}/Fe^{3+}) redox potentials in the groundwater

The groundwater sediment contains solid amorphous Fe $(OH)_3$, and assumed that measured potential corresponds to an oxidation-reduction potential of the aquatic environment. At equilibrium Fe $(OH)_3$ (s) is in equilibrium with Fe^{2+}, the redox reaction being

$$Fe(OH)_3(s) + 3H^+ + e = Fe^{2+} + 3.H_2O.$$
$$.\log .K = 16. \qquad (4.4.2)$$

The standard state redox potential value E^0_H, can be calculated if the equilibrium constant value of log K , and standard state free energy ∇G^0 value are known.

$$E^0_h = -\frac{\nabla G^0}{n.F} = \frac{RT}{nF}.\ln .K = \frac{2.3.R.T}{nF}.\log .K$$
$$= \frac{2.3*1.98x10^{-3}(kCal)*298.(K).(volt.gramm..equivalent)}{(K.Mole)1*23.06..k.Cal}.(16) = 0.94..V \qquad (4.4.3)$$
$$or...E_{H..}.can..be..\exp ressed..in..terms..of..redox..capacity...p^e$$
$$pe^0 = \frac{E^0_h}{0.059}.. = \frac{0.94}{0.059}.. = 16.05$$

From the general redox equation , E_H or p^e for the iron redox reaction (eq. 4.4.2) can be computed as as follows

$$E_{h.(ox-red)} = E^0_{(Fe(OH)_3 - Fe^{2+})} + \frac{0.059}{n}.\log\left(\frac{\{H^+\}^3}{\{Fe^{2+}\}}\right).$$
$$or.in..terms..of..p^e \qquad (4.4.4)$$
$$p^e = p^{e^0}{}_{(Fe(OH)_3 Fe^{2+})} + \log.\left(\frac{\{H^+\}^3}{\{Fe^{2+}\}}\right)$$

Taking the value of p^{e0} from eq. 4.4.3 and substituting it in eq. 4.4.4. Assuming , [$-\log(H^+) = pH$, $-\log(Fe^{2+}) = pFe^{2+}$, and $E_H/0.059 = p^e$],gives the equation 4.4.4 as

$$p^e = 16.05 - 3 * pH + pFe^{2+} \qquad (4.4.5)$$

Using the above functional equation (eq. 4.4.4) and the average concentration of dissolved Iron (Fe^{2+}), the redox potential values can be calculated under natural pH levels in the contaminated water, and the results are presented in Table.4.4.1.

For example:

The values of dissolved Iron concentration (Fe^{2+}) in (mg/l) of different grids (as mentioned earlier) were tabulated in Table.4.2.4. The maximum iron concentration of Grid- 1 in (Table. 4.2.4) was 41.8 mg/l. The units were converted from mg/l to mol/l. As it is known, 41.8 mg/l =$7.484*10^{-4}$ mol/ l.

[by dividing iron concentration by its atomic weight 55850 mg. $\left(\frac{mg * mol * gm}{l * 55.85.gm * 1000.mg} = \frac{mg/l}{55850}\right)$ and Log ($7.484*10^{-4}$)= -3.125].

Using the redox equation (eq. 4.4.5), the minimum redox intensity at Grid .1 was computed as (-1.82) and showed in (Table.4.4.1) as follows.

p^e= 16.05-3*pH+pFe^{2+} = 16.05-3*7+3.125 = -1.82

The rest of the results are tabulated in Table (4.4.1.) exactly the same way as shown above.

Table.4.4.1 Iron controlled redox potential values at arsenic contaminated wells in different zones of Bangladesh

Location		Iron concentration in pFe^{2+} [-log(Fe^{2+}) in mol/l]			P^e @ natural water (pH =7) (Using eq.4.4.5)			No .of wells
Zone	Grid No	Max	Min	Avg	Min	Max	Avg.	
NW	1	3.12	6.44	4.09	-1.82	1.49	0.85	116
	2	3.50	6.57	4.49	-1.43	1.62	0.45	152
	3	3.51	7.04	4.72	-1.43	2.09	0.22	200
	6	3.29	6.74	4.15	-1.65	1.79	0.79	34
	7	3.12	6.66	4.08	-1.82	1.71	0.86	339
	8	3.06	7.04	4.11	-1.88	2.09	0.83	369
NE	14	3.54	7.04	4.51	-1.40	2.09	0.43	344
SW	4	3.77	6.96	4.33	-1.17	2.01	0.61	77
	5	3.86	6.93	4.16	-1.08	1.98	0.78	13
	9	3.43	7.04	4.23	-1.516	2.09	0.71	328
	10	3.26	7.04	4.15	-1.68	2.09	0.79	248
NC	11	3.54	7.04	4.52	-1.40	2.09	0.42	341
SC	13	3.64	7.04	4.69	-1.30	2.09	0.25	284
SE	15	3.33	6.44	4.17	-1.61	1.49	0.77	411

4.4.3 Computation of oxygen control red ox potential value

In natural condition, both surface and groundwater is stable at a total pressure of 1 atm. At very high p^e , the pressure of O_2 in equilibrium with liquid water will exceed 1 atm, and at very low p^e, the pressure of hydrogen in equilibrium with water will exceed 1 atm.

$$2H_2O \xrightarrow{Oxidation} O_2 + 4H^+ + 4e^-$$

The upper stability limit of water is defined above by the water oxidation reaction, and the lower stability limit of water reduction reaction is defined as

$$\frac{1}{2}O_2(g)+2e^- +2H^+ \xrightarrow{\text{Reduction}} H_2O \qquad \text{(4.4.5.a)}$$

The equilibrium constant, K_{eq}, of above water reduction reaction (eq. 4.4.5.a) can be expressed as shown in below,

$$K_{eq} = \frac{aH_2O}{\{P_{O_2}\}^{\frac{1}{2}} * \{ae^-\}^2 * \{aH^+\}^2}$$

Since the activity of liquid water, a (H_2O) =1 (pure water in standard state), after taking log on both side of K_{eq} gives as (-log (ae^-)=p^e),

$$\log\ K_{eq} = -\frac{1}{2}.\log\ .P_{O_2} + 2\,p^e + 2\,pH \qquad \text{(4.4.5.b)}$$

After rearranging the equation 4.4.5.b, the equation of P^e can be written as

$$p^e = \frac{1}{2}\log.K_{eq} + \frac{1}{4}.\log.P_{O_2} - pH \qquad \text{(4.4.6)}$$

(The standard state free energy of the reaction, $\nabla G^0_{react} = \nabla G^0(H_2O) = -237.13.kJ$ and the other standard free energy of formation are zero). Now putting the value of

∇G^0_{react} in thermodynamic equilibrium formula below, the value of log K_{eq} as

$$\log .K_{eq} = \frac{-\nabla G^0_{react}}{2.3RT} = \frac{237.13.kJ}{2.3 * 8.314 * 10^{-3}(kJ / K.mol) * 298.(K / mol)}$$

$$= \frac{237.13}{5.698} = 41.62$$

Using the value of log K= 41.61 in equation (4.4.6, the oxygen controlled redox value in the groundwater system can be computed and results are shown in

Table 4.4.2. It revealed from the results that when oxygen controls the redox potentials (p^e) value in any systems, the redox potential values were high.

Example

When the amount of dissolved oxygen is 0.05 atm (referring Table 4.4.2), the system p^e at natural water (pH=7) was computed according to the equation (4.4.6) is

$$p^e = \frac{1}{2}\log.K_{eq} + \frac{1}{4}.\log.P_{O_2} - pH = \frac{1}{2} * 41.62 + \frac{1}{4} * (-1.3) - 7 = 13.48$$

Redox values were also calculated for the oxygen concentration level as 0.00001 atm or 0.41-ppm or 410-ppb the results were tabulated in Table.4.4.2.

Table 4.4.2 Dissolved oxygen concentration available in groundwater and computation of redox potential values under natural water pH=7.

Activity of Oxygen P_{O2} (atm)	**Dissolved Oxygen (aqueous) (mg/L)**	**(ppm)**	**Redox intensity p^e**
0.21	8.66	8660	13.65
0.15	6.18	6180	13.60
0.10	4.12	4120	13.56
0.05	2.06	2060	13.48
0.01	0.41	410	13.31
0.001	0.041	41	13.06
0.0001	0.0041	4.1	12.81
0.00001	0.00041	0.41	12.31

4.4.4 Stability analysis and functional relationship among redox potential p^e, pH , and construction of p^e-pH diagram

The p^e-pH diagram is a convenient way of analysis of the stability relationships where redox reactions are involved. Analysis of the stability relationships of iron and arsenic redox species will help understand whether arsenic is released under oxic or reduced environment. Also it helps evaluating whether arsenic mobilization in groundwater occurred in dissolved form or in solid form

The upper stability limits of water

The upper stability limit of water was expressed in the equation as follows.

$$\frac{1}{2}O_2(g) + 2e^- + 2H^+ \xrightarrow{\text{Reduction}} H_2O$$
$$H_2O \xrightarrow{\text{Oxidation}} O_2 + 4H^+ + 4e^- \qquad (4.4.7)$$

The functional relationship between p^e and pH was computed by using the equation (4.4.6). For oxygen pressure, P_{O2} =0.21, indicates the upper stability limit for water. Putting log P_{O2} = 0 in equation (4.4.6), we have the functional relation as

$$p^e = 20.78 - pH \qquad (4.4.8)$$

This plots a straight line of slope -1 on the p^e-pH diagram (Line-1, in Fig. 4.13). The lower stability limit of water is conversion into Hydrogen gas, and defined by the reaction as follows.

$$H^{+} + e^{-} = \frac{1}{2} H_2(g)$$

$$K_{eq} = \frac{\{P_{H_2}\}^{\frac{1}{2}}}{aH^{+}.ae^{-}} \qquad (4.4.9)$$

$$\log .K_{eq} = \frac{1}{2} \log .P_{H_2} + p^{e} + pH = 0$$

Log(K_{eq}) of the eq (4.4.9) is zero because, the free energy of reaction involving Hydrogen is zero. Therefore, $G^{o}_{react} = 0$, so the functional relationship between p^{e} and pH is as

$$p^{e} = -\frac{1}{2}\log .P_{H_2} - pH. = -pH .....when....P_{H_2}. = 1.atm. \qquad (4.4.10)$$

At lower stability limit for water, P (H_2) =1 atm, log pH_2=0, then we have the relation of P^{e} = -pH

4.4.4.a Functional relationship among iron redox couple ($Fe(OH)_3$ & Fe^{2+}) , p^{e} and pH

As it is known that the solid amorphous Iron ($Fe(OH)_3$(s) in the arsenic contaminated groundwater system is reduced to dissolved Fe^{2+} and released arsenic. At equilibrium , ($Fe(OH)_3$(s) is in equilibrium with Fe^{2+}. The iron redox reaction was written in equation (eq 4.4.2) and the p^{e0} value was computed using eq (4.4.3) as 16.05.

$$Fe(OH_3)(s) + 3.H^{+} + e = Fe^{2+} + 3H_2O ... \& \log K = 16.$$
$$pe^{0}. = 16.05$$

Using above p^{e0} and log K values, the above equation (eq 4.4.2) gives us a functional relationship between p^e and pH and dissolved and solid iron species. The redox potential can be computed as

$$p^e = p^{e^0}{}_{(Fe(OH)_3 Fe^{2+})} + \log\left(\frac{\{H^+\}^3}{\{Fe^{2+}\}}\right)$$

or

$$p^e = 16.05 - 3pH + pFe^{2+} \qquad (4.4.11)$$

Therefore, the above equation 4.4.11 gives us a functional relationship between dissolved iron content and the associated redox potential values in the groundwater systems.

4.4.4.b Stability limit of iron and arsenic species and construction of p^e-pH diagram

In general As (V) predominates under oxidizing conditions and As (III) predominates under reducing conditions. However, the reduction of arsenate (As (V)) to arsenite (As (III)) is slow, so arsenate can be found in reducing environments, conversely arsenite can be found in oxidizing environment (Meriner et al, 1996).

The thermodynamic information obtained from the stability diagram or p^e-pH diagram describes only the systems at equilibrium and indicates the direction in which a non-equilibrium system will move. We know that arsenic is stable in

four oxidation states (+5, +3,0, -3) under E_H condition occurring in natural water. At the high E_H values encountered in oxygenated water, arsenic acid species (H_3ASO_4, $H_2ASO_4^-$, $HASO_4^{2-}$, and AsO_4^{3-}) become stable (Ferguson, 1971).

Construction of p^e-pH diagram

In groundwater system, the stability of iron and arsenic species was analyzed using p^e-pH diagram within the upper and lower boundary of water stability zone. Fig.4.13 was constructed using the following equations and indicated the simplest presentation of stability diagram of arsenic species that can be available in groundwater.

Upper stability limit of water (Line-1 in Fig.4.13)

The equation (4.4.8) was used to construct Line-1 in (Fig.4.13) indicate upper limit of water oxidation in a p^e –pH diagram.

Lower stability of limit of water (Line-2 , Fig.4.13)

Equation (4.4.10) was used to indicate lower limit of water reduction in stability or P^e-pH diagram, where, p^e=pH

Stability limit of Fe^{2+} and $Fe(OH)_3$ (s) as redox couple (Line-5, Fig.4.13)

The solid amorphous iron hydroxides are reduced to Fe^{2+} according to the following equation below.

$$Fe(OH_3)(s) + 3.H^+ + e = Fe^{2+} + 3H_2O \ldots\ldots\ldots\ldots \& \log K = 16\ldots$$
$$pe^0. = 16.05$$

The Functional relationship between p^e and pH is derived above and is expressed by the equation (4.4.12).

$$p^e = 16.05 - 3pH + pFe^{2+} \qquad (4.4.12)$$

Stability limit of Fe^{2+} and Fe_2O_3 (s) Redox Couple (Line-4, Fig.4.13)

The boundary of Fe^{2+}-Fe_2O_3 is calculated from the equation

$$Fe_2O_3 + 2.e^- + 6H^+ = 2Fe^{2+} + 3H_2O$$

$$K_{eq} = \frac{\{aFe^{2+}\}^2}{\{ae^-\}^2\{aH^+\}^6} \qquad (4.4.13)$$

The functional relation between p^e and pH of the above equation(4.4.13) can be expressed by the following equation

$$p^e = \frac{1}{2}\log.K_{eq} - \log.aFe^{2+} - 3pH \qquad (4.4.14)$$

Stability limit of arsenic acid species (Line-3 , Fig.4.13)

The p^e range within which the arsenic species are detected for each specified pH condition was shown in Fig. 4.13. The oxidation product of arsenic acid $H_3AsO_3^0$ is defined by the following equations

$$H_3AsO_3^0 + H_2O \longleftrightarrow H_2AsO_4^- + 3H^+ + 2e^-$$

$$and..the...p^e - pH....relation..is\,expressed..by$$

$$p^e = 11 - \frac{3}{2} * pH$$

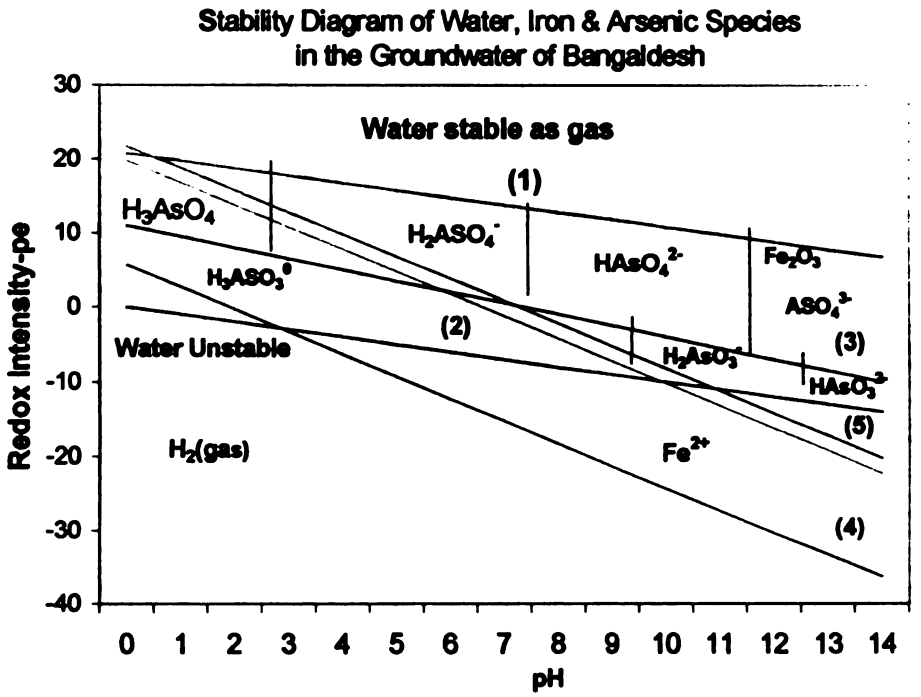

Fig.4.13 Stability diagram of water and arsenic species in the contaminated groundwater system.

4.4.5 Shifting of thermodynamic equilibrium, lowering of water table and arsenic release in groundwater of Bangladesh

This analysis was performed considering that the dissolved oxygen (DO) in recharging groundwater was in equilibrium with atmospheric oxygen before lowering the water table in Bangladesh. The abundance of DO created the hypothetical equilibrium condition (in the top left green circle in Fig.4.14) showing that the arsenic species were stable in solid state and were attached to the surface of solid amorphous Iron oxides. The redox potential values of Fe^{2+}/Fe^{3+} redox couple were calculated assuming oxygen concentration at 0.21 atm, pH was 5 and total Iron (Fe^{2+} & Fe^{3+}) concentration was 0.1 (mg/L). When these values were inserted in p^e-PH diagram, it appeared above the iron - equilibrium line-10 (Fig.4.14). This implies that redox potentials values were similar to oxygen controlled p^e values, because, the range of oxygen controlled redox values were calculated from 12.31 to 13.65 in Table 4.4.2.

But, after lowering water table, lack of DO helped develop reducing condition and reduced the p^e values. The p^e values were computed from the field records of iron concentration and inserted in Fig.4.14 against natural pH= 7. Under neutral pH of water, the p^e values of iron and arsenic appeared below their equilibrium lines (Line-3 and Line-10). It implies that thermodynamically, iron and arsenic existed as a dissolved species in ground water system of Bangladesh. The Fig.4.14 showed that the associated p^e values were within the range of mild reducing level (1.5 to -3.5). The green arrow in Fig.4.14 was used

to indicate that the hypothetical equilibrium situation had shifted from oxic to anoxic condition, and the P^e values were reduced from oxygen control range (12 to 15) to the mild reducing range (0.5 to 3.5). It is most likely due to the lowering of water table and limited access of atmospheric oxygen to the deeper aquifer.

The lines in Fig. 4.14 were constructed using the thermodynamic relations as similar to the stability diagram in Fig. 3.13.

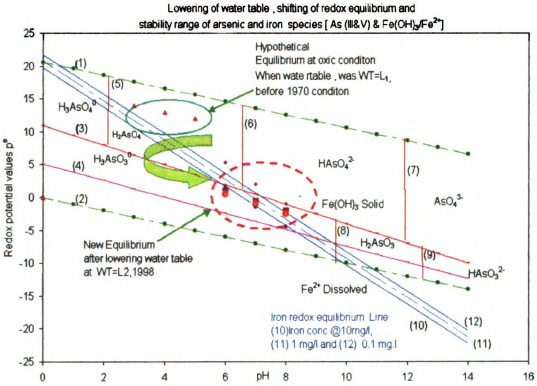

Fig. 4.14 Shifting of ground water systems from oxygenated conditions to reducing condition due to the lowering of water table in Bangladesh.

Table 4.4.3: Chemical and thermodynamic equations for p^e-pH diagram of Arsenic (III & V) and Fe $(OH)_3$ / Fe^{2+}

Line Number	Type of Equation	Chemical Equation	Thermodynamic Equation
(1)	Water Oxidation Reaction	$4H^+ + O_2(g) + 4e^- = 2H_2O$	$p^e = 20.6 - pH$
(2)	Water Reduction Reaction	$2H_2O + 2e^- = H_2(g) + 2OH^-$	$pE = - pH$
(3)	Arsenic (III) & As (v) acid species	$H_3AsO_3^0 + H_2O = H_2AsO_4^- + 3H^+ + 2e^-$	$pe = 11 - (3/2)^* pH -$
(4)	Arsenic Acid species	$As(c) + 3H_2O = H_2AsO_3^- + 4H^+ + 3e^-$	$pH + (3/4)^* pe = 3.1$
(5)	Arsenic Acid species	$H_3AsO_3^0 = H_2AsO_4^- + H^+$	$PH = 2$
(6)	Arsenic Acid species	$H_2AsO_4^- = HAsO_4^{2-} + H^+$	$PH = 6.96$
(7)	Arsenic Acid species	$HAsO_4^{2-} = AsO_4^{3-} + H^+$	$PH = 11.5$
(8)	Arsenic Acid species	$H_3AsO_3^0 = H_2AsO_3^- + H^+$	$PH = 9.2$
(9)		$H_2AsO_3^- = H_2AsO_3^{-2} + H^+$	$PH = 12.1$
(10)	$Fe(OH)_3s/Fe^{2+}$	$Fe(OH)^3(s) + 3H^+ + e^- = Fe^{2+} + 3H_2O$	$Pe = 16 - \log[Fe^{2+}] - 3pH$
(11)	$Fe(OH)_3s/Fe^{2+}$	$Fe(OH)^3(s) + 3H^+ + e^- = Fe^{2+} + 3H_2O$	$Pe = 16 - \log[Fe^{2+}] - 3pH$
(12)	H_2S/SO_4	$H_2S^0 + 4H_2O = SO_4^{2-} + 10H^+ + 8e^-$	$pH + (4/5)^* pE = 4.1$

4.5 Computation of shallow aquifer recharge (SAR) in groundwater system

Groundwater recharge is an important flux in the water balance model. The amount of groundwater extraction greatly exceeds natural recharge in many areas of Bangladesh. As a result, lowering of the water table occurs. In Bangladesh, groundwater recharge is primarily attributed through direct infiltration and percolation loss from large rainfall and floodwater. The objective of this analysis is to estimate the lower limit of the average vertical groundwater flux or vertical aquifer recharge.

Concept of groundwater recharge model

Fig. 4.15 describes a conceptual mass balance of the water cycle with precipitation (P), which strikes the ground surface to become surface water, and will either flow over the surface as runoff or infiltrate downward to the soil's unsaturated zone. Part of the infiltrated water is stored as soil moisture, some is evaporated back to the atmosphere, and the rest infiltrates downward across the water table as shallow aquifer recharge. Water that is not stored in or pumped out from the shallow aquifer sediment must flow down through the shallow aquifer system into the deeper layers of the aquifer as a recharge. Water that enters the deep aquifer system becomes part of the shallow regional aquifer system and will eventually flow laterally offsite.

4.5.1 Parameter estimation in water balance equation

In the study area, the precipitation was recorded daily from the year 1963 to 2000 in the catchment area of about 100,000 ha in the southwest zone (SW) of

Bangladesh. The potential evapotranspiration (PE) and actual evapotranspiration (AE) was calculated from the daily pan evaporation records. The daily records of permitted outflow (D_o) which is the volume of water discharge from the catchment area was measured at the main control structure of the drainage system.

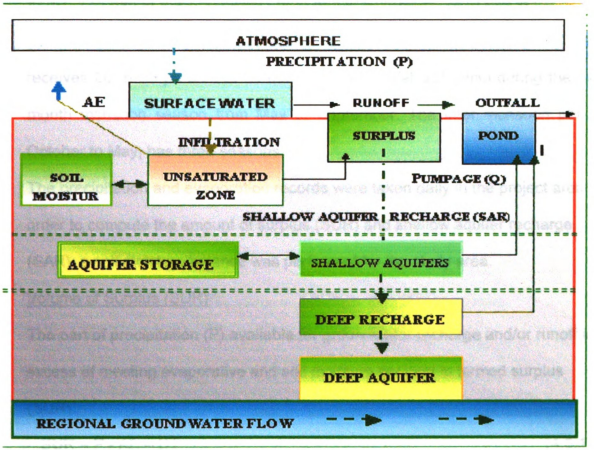

Fig. 4.15 Conceptual water balance model: rectangular areas represent reservoirs for water and arrows represent the flux.

Source of precipitation: Generally, rainfall and floodwater are the primary sources of groundwater recharge. But The major source of precipitation in Bangladesh is rainfall

Rainfall Analysis:

The thirty-year (1951-80) national mean annual rainfall is 2, 320 mm based on the analysis of 277 stations. (MPO, 1985), ranges upward by region from1, 765 mm in the Southwest, 1820 mm in Northwest, 2410 mm in the South-central, 2690 mm in the Southeast to 2830 in the Northeast. Bangladesh receives 80 to 90 percent of its mean annual rainfall 2320-mm during the five-month monsoon season from May to September. The inter monsoon period, October to May, has three seasons.

The precipitation and evaporation records were taken daily in the project area. In order to compute the amount of surplus (SUR) and shallow aquifer recharge (SAR), a soil moisture balance was performed for the study area.

Volume of Surplus (SUR)

The part of precipitation (P) available for groundwater recharge and/or runoff in excess of meeting evaporative and soil moisture demand is termed surplus (SUR).

$$SUR = P - AE - DT \qquad (4.5.1)$$

where P is precipitation, AE is the actual evapotranspiration loss, and DT is the soil moisture recharge. DT is positive when infiltration occurs and negative when soil moisture is being depleted.

4.5.2 Computation of volume of shallow aquifer recharge (SAR)

Subtracting surface runoff from the surplus (SUR) will determine the recharge of the sediments above the confining layer.

Shallow Aquifer Recharge (SAR) = [Surplus (SUR) – Surface Runoff] (4.5.2)

But it is known from Fig.4.15 that

Outflow = Surface Runoff + Pumpage (Q)

Surface Runoff = Outflow – Pumpage

Substituting the value of surface runoff into Equation 4.5.2 yields

Shallow Aquifer Recharge = Surplus (SUR) - Outflow + Pumpage (Q)

where the flux due to pumpage (Q) is unknown; we can calculate the lower limit of the shallow aquifer recharge with 33 years' average rainfall and outflow records of the study area under a rain-fed cropping system.

The lower limit of shallow aquifer recharge (SAR) = SUR – Outflow. (4.5.3)

Lower limit of shallow aquifer recharge (SAR) under rain-fed system:

A soil moisture balance analysis was conducted under the rain-fed system with the rainfall records from 1963 to 2000. The amount of SUR is computed in Appendix .A. The value of the lower limit of SAR was computed as follows. Under the rain-fed system, the amount of SUR = 716 mm, and the average outflow =435 mm. Therefore, the lower limit of shallow aquifer recharge (SAR) is

SAR = 716-435 mm =281 mm /Year

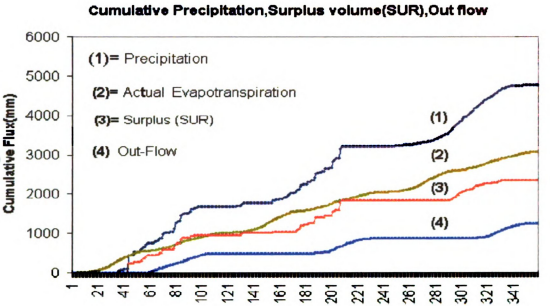

Fig. 4.16.a Cumulative sum of the surplus (SUR), outflow, and annual evaporation

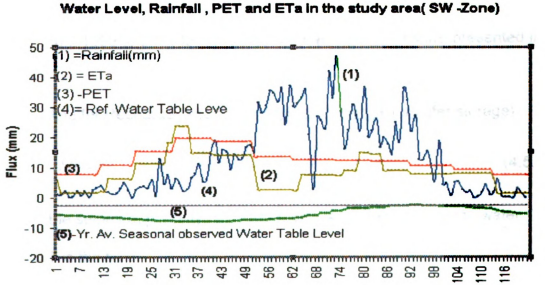

Fig.4.16.b. ET, PET and the groundwater level in the study area

4.5.3 Amount of shallow aquifer recharge(SAR) under HYV-rice irrigated system

A soil moisture balance analysis was also performed under rice irrigated system where rice was grown. The amount of SUR available under rice irrigation system was computed and the result of the shallow aquifer recharge (SAR) is presented in Appendix. B.

The amount of shallow-aquifer recharges (SAR) for the year 2001 and 2000 were computed as 470.74 and 498.1 mm, respectively.

SAR = SUR - Outflow = 964.12 mm - 493.37 mm = 470.74 mm (year 2001)

SAR = SUR - Outflow = 876.28 mm - 378.18 mm = 498.1 mm (year 2000)

The calculation of the value of SUR is presented in Appendix .B. The cumulative volume of precipitation, annual evaporation, SUR and out-flow was computed from 1999 to 2001 for the study area and the graphs are presented in Fig. 4.16.a.

Deep Aquifer Recharge = (Shallow aquifer recharge – aquifer storage)

$$Aquifer \quad ..Storage \quad = \phi .. \left(\frac{\Delta Z * [Water \quad .Table \quad)]}{\Delta T} \right) \qquad (4.5.4)$$

where ϕ is the sediment porosity, ∇ (water table) is the elevation of the water table, and T is the time.

4.5.4 Computation of SAR, SUR using soil moisture balance

A spreadsheet analysis for soil moisture balance was created in order to compute the SUR, SAR, storage opportunity, and rice water requirement for the study area. The results of SUR and SAR are presented in Appendix. A and B. For example, the amounts of surplus moisture (SUR) and soil-storage opportunity were computed as 21.20 and 100 mm, respectively, in Col. 14 and Col. 16, row marked 52 th day (Appendix .A). The 3-day cumulative amount of rainfall was 31.54 mm (Col. 6). The effective rainfall (P^e) minus the 3-day actual evaporation (AE) was calculated in Col. 10 as 25.8.

The SUR was computed according to Equation 4.5.1 (SUR = P^e - AE + DT}. The amount of excess water was (P^e – AE = 25.88) (Col.10). Soil moisture in hand on this day was equal to the moisture status on the previous day, plus the amount of excess moisture available minus the water holding capacity at AWC (150 mm). Therefore, the volume of SUR is equal to

SUR = 145.4 +25.8 – 150 = 21.2 mm.

(107.32 mm soil moisture previous day).

The storage opportunity was calculated to be 100 mm (Col. 16).

Storage Opportunity = [VMC (SAT)-VMC (WP)]* 1m - 150 mm = (0.6-0.35)* 1 m -150 mm = 100 mm.

where VMC (SAT) and VMC (WP) are volumetric moisture content at saturation and at wilting point, respectively. The amount of SUR and soil moisture computed for the study area was presented in Fig. 4.17.

Precipitation (P) or Rainfall

The rainfall distribution pattern in the study area (in the SW zone of Bangladesh) has a clear distinction between the monsoon and the non-monsoon period. Generally, May to October is regarded as the humid summer season. The rainfall records from 1967 to 2001 calculated the monthly average rainfall, and the maximum 3- day rainfall value for a two-year and five-year return period is presented in Table 4.5.1.

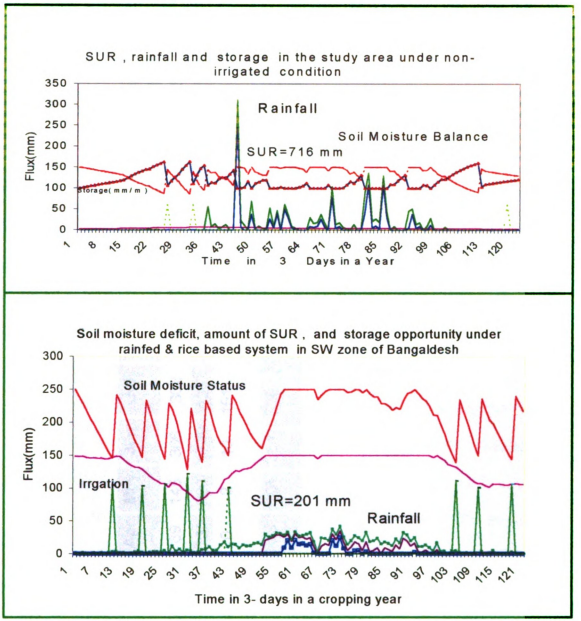

Fig. 4.17 Amount of SUR (blue lines), rainfall (solid green), and soil moisture in the SW zone study area. Blue lines (on the top & bottom graphs) are the amount of SUR (201 mm for irrigated and 716 mm for non-irrigated condition) .

Table 4.5.1 Monthly average rainfall and rainfall of 2 year and 5 year return period in the study area (SW zone of Bangladesh)(mm)

Mo.	Jan	Feb	Mar	Apr	May	Jun	Jul	Aug	Sep	Oct	Nov	Dec	Total (mm)	
Avg.	13	25	48	69	145	306	302	287	222	134	24.3	14	1588	
Max	179	358	602	730	880	1740	1357	1918	1430	1244	462	376	11316	
	T=2 yr.	0	0	0	2	40	161	186	169	98	35	0	0	691
	T=5 yr.	0	7	5.3	124	254	528	551	401	362	201	0	0	2433

5. MATHEMATICAL MODELING TO ESTIMATE GROUNDWATER MOVEMENT & LIKELIHOOD OF ARSENIC MIGRATION

The dynamics of groundwater flow movement in a system are a function of the aquifer's physical properties, the amount of aquifer recharge, the extraction rate and the boundary conditions. Under virgin conditions, the groundwater flow patterns and dynamics is a function of aquifer properties and boundary conditions, but under extraction, it is a function of pumping with a rate (Q) greater or smaller than the aquifer recharge (SAR) rate and boundary conditions.

5.1 One-dimensional analytical model to evaluate the impact of the aquifer's physical properties on arsenic concentration.

Observation well records around pumping wells in Bangladesh indicate that most of the water delivered from the water storage comes as a leakage from the top unconfined layer through the aquitard (MPO, 1987), as it is a leaky aquifer. The length of the unconfined top aquifer and the depth and vertical permeability of the aquitard basically control the flow and movements of contaminants in the aquifer.

This analysis was designed to predict the mass volume as a function of aquitard depth and vertical conductivity of the arsenic concentration in water entering a deep tube well (DTW). Fig. 5.1.a represents a common case of leaky confined aquifer in Bangladesh in which the screen of the DTW was installed at a depth ranging from 70 to 90 m. Fig. 5.1.b investigates how the aquitard depth (b') and vertical conductivity (K') of the impermeable layer (L_2) influence the arsenic

concentration of water entering a pumping well and how the results might be used to justify the theory of arsenic release by oxidation and reduction.

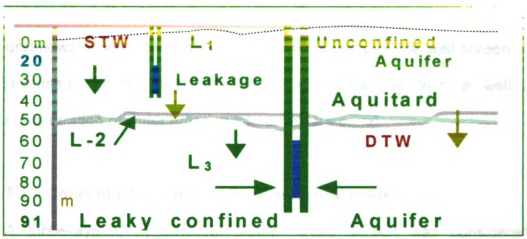

Fig. 5.1 a Schematic of a typical cross-section of aquifer in Bangladesh, where deep tube wells (DTW) and shallow tube wells (STW) were installed for irrigation.

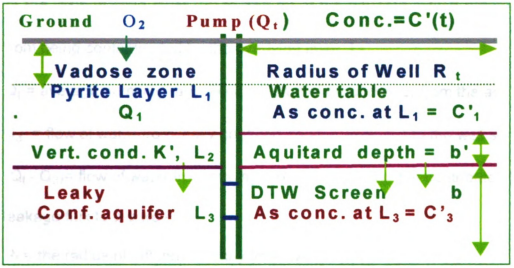

Fig. 5.1.b Conceptual model to investigate the influence of aquitard depth (b') and conductivity (K') on arsenic concentration in the water in a pumping well.

Assumptions

The first layer (L_1) was considered to be arsenic-contaminated. For the simplicity of the problem, convective flow of arsenic was assumed, as the groundwater velocity was higher near the vicinity of the well screen. It is also assumed that the concentration of water pumped from a well and the concentration of water entering into a well are equal.

5.1.1 Conceptual one-dimensional analytical model

A three-layered hypothetical aquifer cross section was considered to be investigated. Layer number three (L_3) in Fig. 5.1.b represents a leaky confined aquifer with relatively low or no arsenic contamination. Layer L_2 reflects the depth of the impermeable layer (50 to 150 m) of the aquitard, which protects layer L_3 from being contaminated by the overlying layer, L_1.

Q_t = average pumping rate (2448 m^3/day) of groundwater from the aquifer.

Q_3 = flow of water from leaky confined aquifer layer (L_3) to the well screen.

(Q_t - Q_3)= flow of water from the layer one (L_1) aquifer that contributes to Q_t as a leakage flux to the well.

R_t = the radius of influence at any time t with a pumping rate Q_t.

C'_1 = arsenic concentration (100 ppb) in unpumped layer 1 aquifer (L_1)

C'_3 = arsenic concentration in pumped leaky aquifer layer (L_3)

C'_t = resultant concentration of water entering the well at any time t,

T, n, and b are transmissivity, porosity, and depth of the pumped aquifer, respectively. Aquitard depth and hydraulic conductivity are b' and K' respectively.

When pumping starts, the concentration of water entering the well, C'_t is equal to C'_3, reflecting the aquifer's initial concentration. As pumping continues, C'_t progresses from C'_3 to C'_1, reflecting the increasing contribution of leakage to the pumped water. To determine C'_t , a mass balance of arsenic arrival to the well screen from aquifer water was considered. At any time t, the pumping rate Q_t was comprised of water derived from the leaky aquifer (Q_3) and water derived from layer one (L_1) as a leakage factor (Q_1). From mass balance, $Q_t = Q_3 + Q_1$, so it can be expressed as $Q_1 = (Q_t - Q_3)$ (Fig. 5.1.b).

According to the principle of mass balance (Ref: Fig.5.1.b), the mass of arsenic in water inflow to the well was equal to the mass of arsenic in water leaving the well. Goode et al. (1993) of the USGS derived the following equation based on the mass balance approach to a the leaky aquifer:

$C'_t * Q_t = C'_3 * Q_3 + C'_1 * (Q_t - Q_3)$, which yields

$$C'_t = C'_1 + (C'_3 - C'_1)\frac{Q_3}{Q_t} \qquad (5.1)$$

Bear (1979) derived the following formula to determine Q_3 under vertical leakage: condition through the impermeable layer.

$$Q_3 = 2\pi . b . R_t . q[R_t] = \frac{Q_t . R_t}{B} . K_1\left[\frac{R_t}{B}\right] \qquad (5.2)$$

where Q_t is the pumping rate at any time t, R_t is the radial distance from the well, $B = (T\,b'/K')^{1/2}$ is the leakage parameter, K' is the vertical hydraulic conductivity of the aquitard, K_1 is a modified Bessel function of the second kind and first order, and (ds/dr) is the hydraulic gradient. The specific discharge towards the well, q, at a radial distance R is q (R), n is the sediment porosity and the water velocity is v(R) =q (R) / n.

$$q[R_t] = \frac{T}{b}.\frac{ds}{dr}. = \frac{Q_t}{2.\pi.b.B} * K_1\frac{R_t}{B}$$

Now putting the value of q (R) and Q_3 into equation 5.1, the concentration of arsenic water entering the well at any time t (C'_t) during pumping from a well can be expressed by the following equation:

$$C_t' = C'_1 + (C_3' - C'_1) * \frac{R_t}{B}.* K_{1_1}\left[\frac{R_t}{B}\right] \qquad (5.3)$$

The concentration in the water entering the well at any time t was (C_t), computed by spreadsheet analysis considering first the radius of influence R_t and then substituting the value into Equation 5.2 to get the initial discharge (Q_3). As pumping continues, the R_t increases and ratio of partial discharge Q_3/Q_t decreases and C'_1/C'_3 increases. Then the influence of aquitard thickness (b') and conductivity (K') on the concentration of water entering into the well were computed by spreadsheet and shown in Fig. 5.2.a.

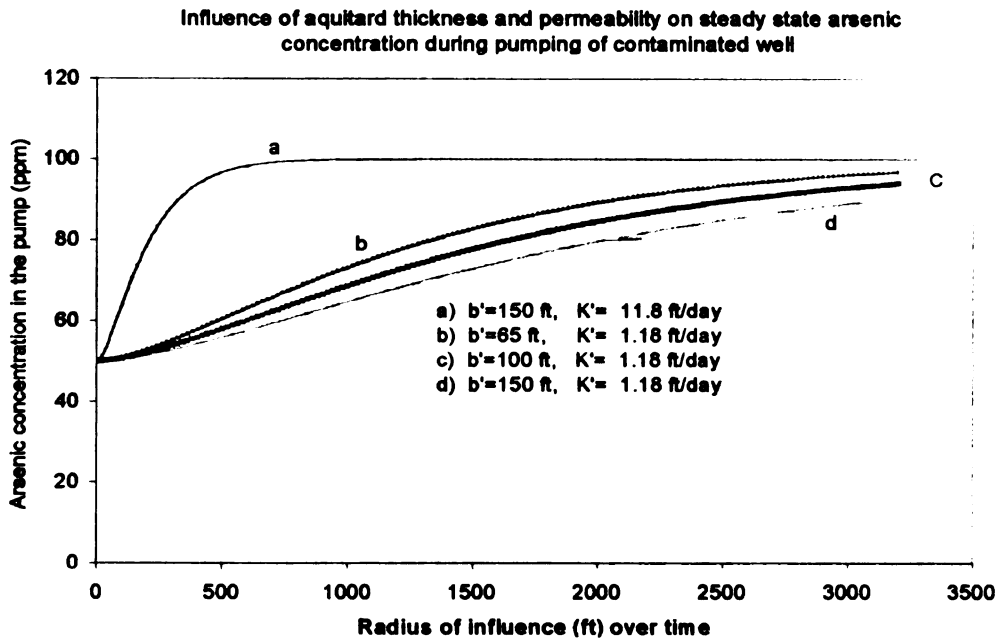

Fig. 5.2 a. Influence of aquitard thickness (b') and permeability (K') on steady state arsenic concentration of water entering in a pumping well (Q=2448m^3/day).

5.2 Three-dimensional numerical modeling to estimated shallow aquifer recharge (SAR) rate, flow components, and their impact on arsenic transportation

The arsenic transport equation derived here was based on the conservation of mass and assumed that the flow was steady state and Darcy's law was applicable. Under Darcy's assumption, the flow was described by the average linear velocity, which carried the solute by advection. The advection process, in addition to the hydrodynamic mixing process, transports non- reactive solutes. The rate of advective transport was equal to the average linear velocity

$v^*=(v/n)$, where v is the specific discharge and n is porosity. If "C" is the concentration of solute, then the mass of solute per unit volume of porous media is n C

5.2.1 Derivation of three-dimensional (3-D) transport equation

The mass of solute transport in the x direction (Fig. 5.2.b) by advection is equal to v^*_x nC dA. The mass of solute transport in the x direction by dispersion is equal to n D_x ($\partial C/ \partial x$) dA, where ($\partial C/ \partial x$) is the concentration gradient in x direction and dA is the unit area. The dispersion coefficient D_x is related to the dispersivity α_x and the diffusion coefficient D^*. v^*_x was the average linear velocity in groundwater

$$D_x=\alpha_x v_x^* + D^* \qquad (5.3.1)$$

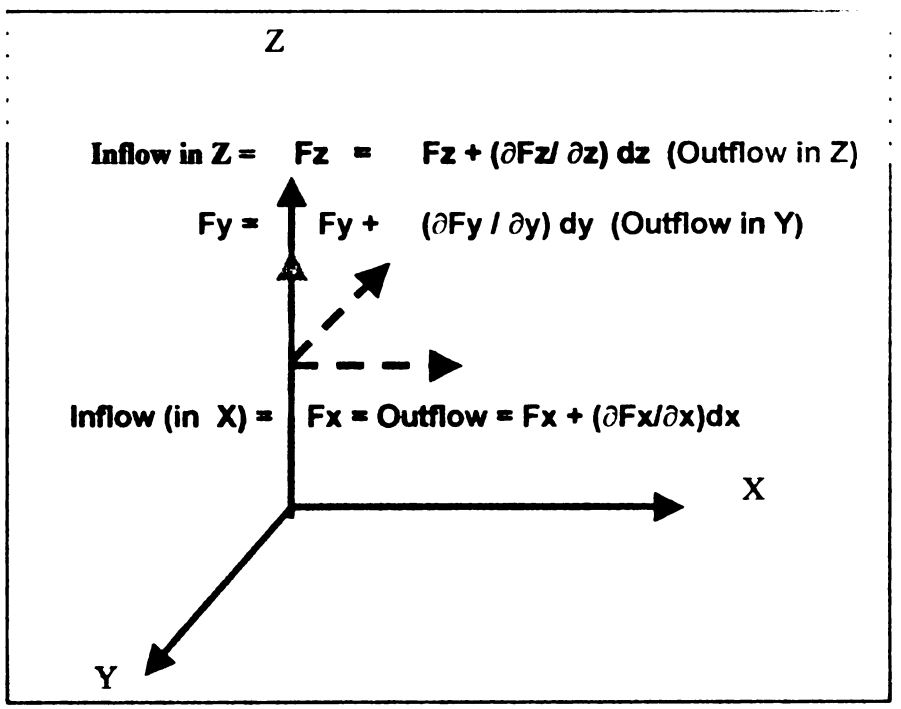

Fig. 5.2.b. Derivation of three-dimensional contaminant transportation equations

If F_x, F_y and F_z are the total mass of solute per unit cross section area (Fig. 5.2.b) transported in the x, y, and z direction per unit time, then

$$F_x = v^*_x n.C - nD_x \frac{\partial C}{\partial x} \tag{5.3.2}$$

$$F_y = v^*_y n.C - nD_y \frac{\partial C}{\partial y}. \tag{5.3.3}$$

$$F_z = v^*_z n.C - nD_z \frac{\partial C}{\partial z} \tag{5.3.4}$$

The difference in the total amount of solute entering and the total amount leaving the system is equal to the amount of solute accumulated or stored in the system.

$$\left(\frac{\partial F_x}{\partial x} + \frac{\partial F_y}{\partial y} + \frac{\partial F_z}{\partial z} \right) dx\ .dy\ .dz = -n \frac{\partial C}{\partial t} dx\ .dy\ .dz$$

The complete three dimensional (3-D) conservation of mass expressions therefore become

$$\frac{\partial F_x}{\partial x} + \frac{\partial F_y}{\partial y} + \frac{\partial F_z}{\partial z} = -n \frac{\partial C}{\partial t} \tag{5.3.5}$$

Now substituting Eq. 5.3.2, 5.3.3 and 5.3.4 into Eq. 5.3.5, canceling n from both sides, the 3-D equation for non-reactive transportation 5.3.5 becomes

$$\left[\frac{\partial}{\partial x}\left(D_x \frac{\partial C}{\partial x} \right) + \frac{\partial}{\partial y}\left(D_y \frac{\partial C}{\partial y} \right) + \frac{\partial}{\partial z}\left(D_z \frac{\partial C}{\partial z} \right) \right] - \left[\frac{\partial}{\partial x}\left(v^*_x C \right) + \frac{\partial}{\partial y}\left(v^*_y C \right) + \frac{\partial}{\partial z}\left(v^*_z C \right) \right] = \frac{\partial C}{\partial t} \tag{5.3.6}$$

The one-dimensional non-reactive transport equation then becomes

$$D_x \frac{\partial^2 C}{\partial x^2} - v^*_x \frac{\partial C}{\partial x} = \frac{\partial C}{\partial t} \tag{5.3.7}$$

The one-dimensional reactive solute transport equation was described by adding a reaction term to Eq. 5.3.7:

$$D_x \frac{\partial^2 C}{\partial x^2} - v_x \frac{\partial C}{\partial x} - \frac{\rho}{n} K_c \frac{\partial C}{\partial t} = \frac{\partial C}{\partial t} \qquad (5.3.8)$$

where $\ldots \frac{\rho}{n} K_c \frac{\partial C}{\partial t}$ *.. is .. reaction .. term*

Rearrangement gives Eq. 5.3.8 as

$$\left(1 + \frac{\rho}{n} K_c\right) \frac{\partial C}{\partial t} = D_x \frac{\partial^2 C}{\partial x^2} - v^*_x \frac{\partial C}{\partial x} \qquad (5.3.9)$$

Therefore, the advection dispersion transport equation with reactive solutes can be expressed as

$$D'_x \frac{\partial^2 C}{\partial x^2} - v'_x \frac{\partial C}{\partial x} = \frac{\partial C}{\partial t}$$

$$\text{where } \ldots D'_x = \frac{D}{1 + \frac{\rho}{n} K_c} = R \text{..(Retardation Factor)} \ldots v'_x = \frac{v}{1 + \frac{\rho}{n} K_c} \qquad (5.3.10)$$

<u>Solution to advective diffusive transport equation</u>:

The three-dimensional (3-D) advective diffusion non-reactive and reactive transport equation (Eq. 5.3.6 and Eq. 5.3.10) could be solved by traditional finite element, finite difference, method of characteristic (MOC) and random walk (RW) methods. But this study used the interactive groundwater modeling software (IGW), a new and unique method that was both computationally efficient and numerically accurate in solving the time-dependent, three-dimensional, advection-diffusion equation for application to transport in heterogeneous porous media. IGW addresses the limitations of numerical dispersions and overshooting, as found in traditional finite element (FE) and finite difference (FD) methods, by

utilizing a solution method that has no Peclet or Courant conditions, requires no time-stepping, and was relatively accurate even at large grid spacing.

Peclet Number P^e criteria

$P^e = V_x * dx / D_x$ <2, where V_x = particle velocity in x direction, dx = cell size in x direction (40 m), and D_x= dispersion coefficient.

For stability, the cell size should not be larger than twice the dispersivity

Courant Number Criteria

The time steps minimize the numerical dispersions and maximize the numerical stability of the solution.

Co = V * dt/dx (was less than 1)

5.2.2. Development of conceptual three-dimensional model for the study area

In order to determine the influence of pumping on advective and dispersive transportation of arsenic, a study area of one square kilometer was divided into 25 equal grids with sides 40 m in length. An extraction well (DTW) was installed in the center of the area (Fig. 5.2.c). Initially, a constant head boundary and no flow boundary conditions were imposed along the boundary of the study area, and later a river boundary was set in order to reflect the complexity of real field conditions.

Description of the aquifer layer (Fig. 5.2c)

a) Upper shallow aquifer (L_1): 0 to 40 m below ground level; fine sand/silt

b) Lower shallow aquifer (L_2): 40 to 140 m below ground level; medium sand

c) Deep aquifer (L_3): 140 to 400 m below ground level; silt clay

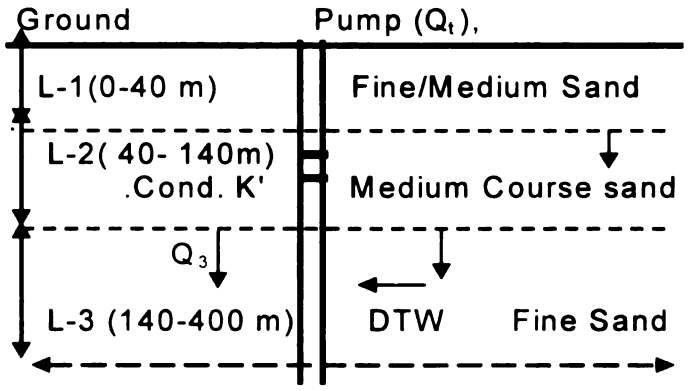

Fig. 5.2.c Cross section of a conceptual model in the study area

Types of conceptual models studied

Three types of conceptual models (M-1, M-2 and M-3) were designed in order to reflect two field conditions. Condition one, where the shallow aquifer (L_2) was more conductive than deeper layer L_3 and L_1 and was reflected in the M-2 model. Condition two was incorporated into M-3, in which deeper aquifer L_3 was more conductive than L_2 and L_2 was more conductive than L_1; it implied an upper fining sequence condition of the aquifer. Comparing the simulation results of those two models (M-2 and M-3) with those of the uniform model (M-1) would help understand the differences in flow patterns and likelihood of contaminant migration to deeper layers where aquifer properties are different. Descriptions of models are given below.

Model M-1:

and K_3 represent the conductivity values of layers L_1, L_2 and L_3, respectively). Later, the uniform model was modified to incorporate a more realistic representation of the geology as observed in the borehole log of the experimental area.

Model M-2:

This 3-layer basic model is much like M-1 but the hydraulic conductivity values are representative of condition one in which the lower shallow aquifer (L_2) is more conductive than the upper (L_1) and deeper (L_3) aquifer (K_2=50 m/day, K_1 = K_3 =15 m/day).

Model M-3:

A 3-layer model with hydraulic conductivity values representative of condition two that reflected real field conditions (upper fining sequence) in the aquifer sediments. In this model, hydraulic conductivity is set at K_1 = 15 m/day, K_2 = 50 m/day, and K_3 = 100 m/day (Fig. 5.2.c). Model M-3 differs with M-2 in terms of permeability of the deeper aquifer (L_3).

The model assumptions.

- The system is steady-state, homogeneous, and isotropic.
- The river in the study area is assumed to be the only outflow.
- The aquifer system is 400 m thick.

Table 5.1 Comparison of the layers' properties by different conceptual models

Depth (m)	Layer	Geology	Conductivity (K) (m/day)	Aquifer name
0 to 40	L_1	Silt, fine to medium sand	$K_1 = 15$	Upper shallow aquifer
40 to 140	L_2	Fine to medium sands	$K_2 = 50$	Lower shallow aquifer
140 to 400	L_3	Medium to coarse sand with gravel	$K_3 = 100$	Deeper aquifer

Justifications:

- The steady-state assumption was made as it ignored the obvious seasonality in the groundwater levels.
- The thickness of the aquifer was chosen to be 400 m to allow the bottom boundary to be deep enough so as not to influence the flow patterns.
- The hydraulic conductivity was derived from the transmissivity of the study area and thickness of the aquifer.
- A no-flow boundary was chosen for the base of the aquifer, and the lateral boundary to represent the limit of the groundwater catchments
- The net recharge was based on the soil moisture balance and checked by the observed seasonal variation of the groundwater and specific yield.

5.2.3 Computation of head distribution and flow patterns of uniform 3-D model (M-1)

In order to validate the model head gradient with the local hydraulic gradient, it was necessary to analyze the head distribution of the study area. In the study area, the actual hydraulic gradient varied from 0.15 to 0.25 m / km. The

computed gradient was 0.18 m/km and agreed with the field values. The head distribution of the top layer and the groundwater flow diagrams were presented below in Fig. 5.3 and Fig. 5.4.

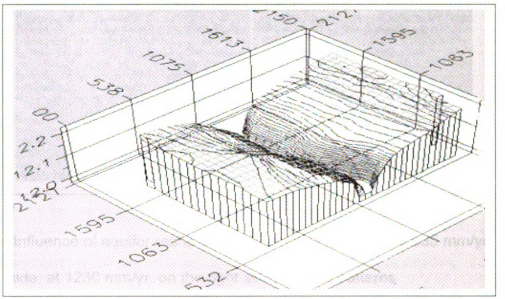

Fig. 5.3 Groundwater gradient to the river

(NB: Images in this dissertation are presented in color)

5.2.3.a Computation of flow patterns in the 3-D uniform model (M-1)

Doubling or halving the shallow aquifer recharge (SAR) rate had no or very little impact on the flow pattern as shown in Fig. 5.4. However, increasing the conductivity drew water to the deeper layers, as shown in Fig. 5.5.

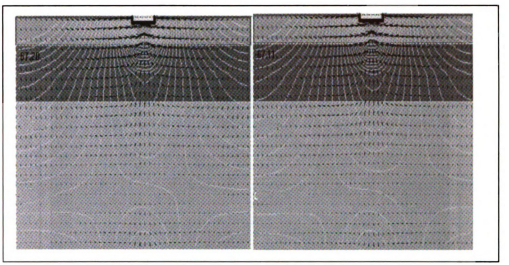

Fig. 5.4 Influence of aquifer recharge (SAR) on flow patterns (at 635 mm/yr. on the left side, at 1230 mm/yr. on the right side) on flow patterns

5.2.4 Computation of mass balance to demonstrate the impact of the extraction rate (Q) and the aquifer recharge rate (SAR) on groundwater movement and flow patterns

The mass balance computation was performed by the IGW software based on the law of mass conservation. The total inflow (in x, y and z direction) was equal to the total outflow (in x, y and z direction) at any layer (Fig. 5.2.b). The impact of average (381 mm), medium (635 mm) and high (1000 mm) shallow aquifer recharge (SAR) rates on downward flow patterns at different layers was estimated and the results are presented in Table 5.2.

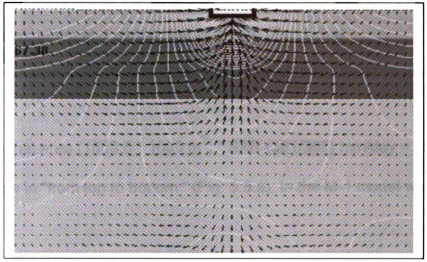

Fig. 5.5 Increasing the conductivity at L_2 drew the stream lines deeper.

Computation of total inflow and outflow components in each layer of the model (Ref. Table 5.1a and Table 5.2)

Example of mass balance computation:

Table 5.2 contains the mass balance results of the M-3 model with different aquifer recharge (SAR) rates. Table 5.1a contains mass balance results of the uniform model M-1. In Table 5.1a, using the M-1 model and the mass balance of layer one (L_1) with the SAR rate of 381 mm/yr., the total inflow is equal to the total outflow.

Total inflow 1950 m^3day^{-1} (Col. 7) = Body in (Col. 4) + Recharge (Col. 5) + Flow from top to bottom (Col. 6) = Total outflow (Col. 10 = Col. 8 + Col. 9).

Inflow =1950 (Col. 7) = 0 (Col. 4) + 1950 (Col. 5) + 0 (Col. 6) = 1950 (Col. 7)

Col. 4 = Flow coming into the layer from the lateral side as "Body in" (flow from a river or lake); in the M-1 model, this was zero (Fig. 5.5.a).

Col. 5 = Recharge in mm/day for the area for which mass balance was computed.

Cross sectional area (1869.6 * 1000 m^2) * SAR (381/365) mm/day = 1950 m^3/day

Col. 6 = Flow in "from top to bottom " (Fig. 5.5.a); in the M-1 model was also zero

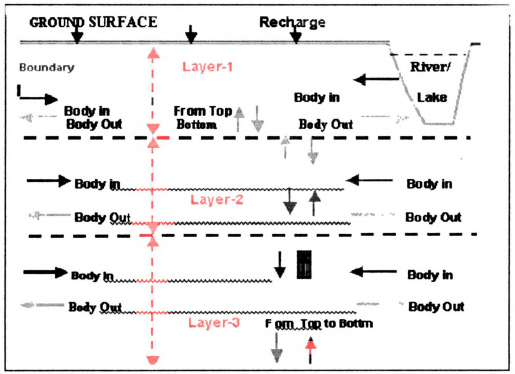

Fig. 5.5.a. Components of flow coming in and out from all directions as a part of the mass balance during model simulation.

Table 5.1. Computation of mass balance in M-1 model under natural flow condition

(1)	(2)	(3)	Flow in and flow out from different vertical layers under natural flow condition						
Model	SAR (mm/Yr)	Layer	Flow in (m^3/day)				Flow out (m^3/day)		
			(4) Body in (m^3/day)	(5) Recharge (m^3/day)	(6) From Top to Bottom	(7) Total (m^3/day)	(8) Body Out (m^3/day)	(9) From Top to Bottom	(10) Total (m^3/day)
M-1 K1=K2=K3 (15 m/day)	381	L-1	-	1950	-	1950	980	970	1950
		L-2	-	-	250	250	250	-	250
		L-3	-	-	92	92	92	-	92

Table 5.1a. Computation of mass balance in M-1 model under pumped condition

(1) Model	(2) SAR (mm/yr)	(3) Aquifer Layer	Flow in and out from different vertical layers of model M-1 with pumping rate of 5000 m^3/day							
			Flow in (m^3/day)				Flow out (m^3/day)			
			(4) Body in (m^3/day)	(5) Recharge (m^3/day)	(6) From Top to Bottom	(7) Total	(8) Body Out (m^3/day)	(9) From Top to Bottom	(10) Well Out	(11) Total (m^3/day)
M-1	381	L-1	900	1950	2150	5000	-	-	5000	5000
		L-2	900	-	-	900	-	900	-	900
		L-3	900	-	-	900	-	900	-	900

Table 5.2. Computation of mass balance in M-3 model under natural flow condition

(1)	(2)	(3)	Flow in and out from different vertical layers of models						
			Flow in (m^3/day)				Flow out (m^3/day)		
Model	SAR (mm/yr)	Aquifer Layer	(4) Body in (m^3/day)	(5) Recharge (m^3/day)	(6) From Top to Bottom	(7) Total (m^3/day)	(8) Body Out (m^3/day)	(9) From Top to Bottom	(10) Total (m^3/day)
M-3 (K3>K2>K1)	381	L-1	800	1950	-	2750	2750	-	2750
		L-2	350	-	-	350	-	350	350
		L-3	230	-	-	230	-	230	230
M-3	635	L-1	-	3220	-	3220	3220	-	3220
		L-2	13	-	-	13	-	13	13
		L-3	73	-	-	73	-	73	73
M-3	1000	L-1	-	5180	-	5180	3980	1200	5180
		L-2	-	-	440	440	440	-	440
		L-3	-	-	162	162	162	-	162

Table 5.3. Computation of mass balance in M-3 model under pumped condition with average, medium and high recharge rate

(1)	(2)	(3)	*Flow in and out from different vertical layers of models @ pumping rate of 5000 m^3/day*							
			Flow in (m^3/day)				***Flow out (m^3/day)***			
Model	***SAR (mm/yr)***	***Aquifer Layer***	**(4)** Body in (m^3/day)	(5) Recharge (m^3/day)	**(6)** From Top to Bottom	**(7)** Total	**(8)** Body Out (m^3/day)	(9) From Top to Bottom	(10) Well Out	(11) Total (m^3/day)
M-3	381	L-1	2550	1950	500	5000	-	-	5000	5000
		L-2	1700	-	-	1700	-	1700	-	1700
		L-3	1900	-	-	1900	-	1900	-	1900
M-3	635	L-1	1790	3210	-	5000	-	-	5000	5000
		L-2	1420	-	-	1420	-	1420	-	1420
		L-3	1720	-	-	1720	-	1720	-	1720
M-3	1000	L-1	-	5180	700	5880	880	-	5000	5880
		L-2	620	-	-	620	-	620	-	620
		L-3	2250	-	-	2250	-	2250	-	2250

5.3 Influence of extraction or pumping on the local hydraulic gradient and flow to and from the river

Groundwater extraction produced the following effects

Pumping had a significant influence on the flow through the deeper layers of the aquifer system. It influenced the flow through the deeper layers from three main aspects.

- In general, extraction or pumping conditions provided more flow through the deeper layers than the natural groundwater flow conditions did.
- When the extraction rate was greater than the aquifer recharge (SAR) rate, it increased the flow through the deeper layers when the aquifer was connected to the river system.
- When the aquifer recharge (SAR) rate was greater than the pumping rate, it reduced the flow through the deeper layers.

5.3.1 Impact of dispersivity and heterogeneity on arsenic migration

Adding dispersion and heterogeneity to the model reflected real field conditions. In order to see the influence of the well pumping rate on the dispersions of arsenic, a particle-tracking approach was used to trace the movement of arsenic from the surface to the well. This conceptual model was built in order to understand the influence of the ratio of the longitudinal dispersivity (D_L) to the transverse dispersivity (D_T), and the influence of the pumping rate on arsenic migration as tracer particles.

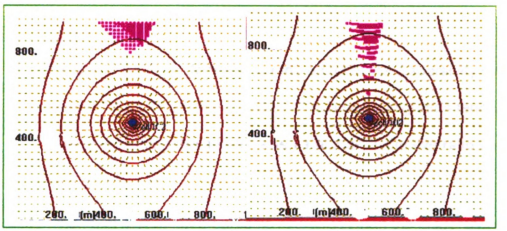

Fig. 5.6 Flow path of arsenic after 100 and 5000 days, assuming movement of arsenic particles when $D_L/D_T = 0$, Q = 2448 m^3/day

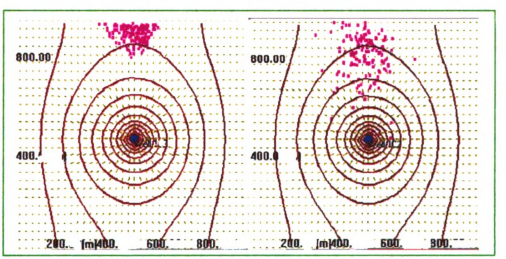

Fig. 5.7 Flow path of arsenic movement when $D_L/D_T = 5$, Q = 2448 m^3/day, after 100 and 5000 days

Impact of dispersivity ratio (D_L /D_T) on arsenic movement when pumping (Q) remains constant

Fig. 5.6 and 5.7 clearly demonstrate the effect of the dispersivity ratio on arsenic movement when Q remains constant. The arsenic migration tendency after 5000 days was found to be greater when a higher dispersive ratio was added (Fig. 5.7, $D_L/D_T = 5$).

Impact of pumping or extraction on arsenic migration when the dispersivity ratio (D_L/D_T) is fixed

Fig. 5.7 and Fig. 5.8 indicate that increasing the pumping rate had a greater influence on the arsenic transportation than reduced the pumping rate (2 CFS vs. 1 CFS) when the dispersivity ratio remained constant. Initially, no retardation of the contaminants was considered, and therefore, $K_d = 0$. A no-flow boundary was assumed around the model area.

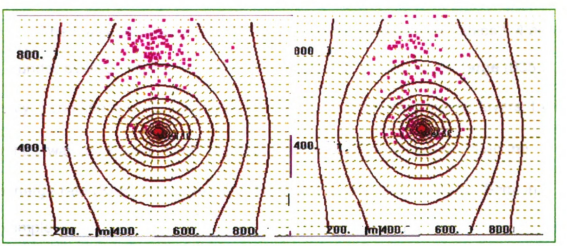

Fig. 5.8. Influence of the pumping rate on arsenic movement, when $D_L/D_T = 5$, Q = 4896 m3/day (2 CFS), and the flow path of arsenic is given after 3000 and 5000 days

By comparing the figures (Fig. 5.7 and Fig. 5.8), it is apparent that the pumping rate has a significant influence on the arsenic movement as a particle form in the groundwater system.

5.3.2 Influence of placing tube well screens in to the deeper layers on arsenic migration

It was a great concern that currently uncontaminated layers may be contaminated with arsenic as a result of groundwater movement. Placing tube well screens at deeper layers has been suggested to avoid the problem, but this practice could cause avoidably bad outcomes. This issue was investigated from the concept of mass balance results obtained by using the IGW software. The flow patterns of groundwater and local gradients to the river was used to address the issue of arsenic migration in the aquifer under the influence of placing wells at different layers.

The mass balance results of the M-2 model presented in Tables 5.4 and 5.5 under average recharge (SAR = 381 mm/yr.) and medium recharge (635 mm/yr.) conditions while placing the well screens at different aquifer layers, L_1, L_2 and L_3, was compared. It was found that pumping at a rate greater than the recharge rate (SAR) was drawing water from the river to the well as "Body in."

Example

(Table 5.4 and Table 5.5)

The component of flow as "body in" from the river was 1210 m^3/day (Col. 4, Table 5.4) when a well-screen was placed at the first layer (-20 to –26 m), with

the SAR rate at 381 mm/yr. Here, the pumping rate (Q) was greater than the recharge rate (SAR). When the SAR was increased from 381 to 635 in the M-2 model, the "body in" component from the river was reduced to 400 m^3/day from 1210 m^3/day (Table 5.5). Also, both the L_2 and the L_3 components of flow were reduced to 1520 and 660 m^3/day (Table 5.5) from 1900 and 690 m^3/day (Col. 4, Table 5.4) respectively.

Summary

It is evident from the above mass balance computation results in Table 5.4 and Table 5.5 that pumping at a rate greater than the recharge rate draws water from the river system to the well. Installation of wells at deeper layers when aquifer sediments are more transmissive results in significant amounts of water being drawn from the river, and flow through the vertical layer is increased. Therefore, it is very likely that the placing of a tube well screen at a deeper layer could result in arsenic migration with the moving groundwater induced by advective flow.

Table 5.4. Mass balance when wells are placed at different layers with recharge rate (SAR of 381mm/Yr) less than the Pumping rate Q.

(1)	(2)	(3)	*Inflows and Outflows from Different Vertical Layers of Models When a Well-screen Is Placed at the 1st and 2nd Layer*							
Model	*Well Placed at*	*Aquifer Layer*	Flow in (m^3/day)				Flow out (m^3/day)			
			(4) Body in (m^3/ day)	(5) Recharge (m^3/ day)	(6) From Top to Bottom	(7) Total	(8) Body Out (m^3/ day)	(9) From Top to Bottom	(10) Well Out	(11) Total (m^3/ day)
M-2 K2=50 K1=15 K3=15	1st layer (-20 to –26)	L_1	1210	1930	1860	5000	-	-	5000	5000
		L_2	1900	-	-	1900	-	1900	-	1900
		L_3	690	-	-	690	-	690	-	690
M-2	2nd Layer (-100 to – 120 m)	L_1	550	1930	2520	5000	-	-	5000	5000
		L_2	1400	-	-	1400	-	1400	-	1400
		L_3	490	-	-	490	-	490	-	490

Table 5.5. Mass balance when wells are placed at different layers with recharge rate of 635 mm/yr.

(1) Model	(2) Well Placed at	(3) Aquifer Layer	*Inflows and Outflows from Different Vertical Layers of Models When a Well-screen Is Placed at the 1st Layer*							
			Flow in (m^3/day)				Flow out (m^3/day)			
			(4) Body in (m^3/day)	(5) Recharge (m^3/day)	(6) From Top to Bottom	(7) Total	(8) Body Out (m^3/day)	(9) From Top to Bottom	(10) Well Out	(11) Total (m^3/day)
M-2 K2=50 K1=15 K3=15	1st layer (-6 to –20)	L_1	400	3250	1350	5000	-	-	5000	5000
		L_2	1520	-	-	1520	-	1520	-	1520
		L_3	660	-	-	660	-	660	-	660
M-2	2nd Layer (-100 to – 120 m)	L_1	-	3250	2300	5000	-	-	5000	5000
		L_2		-	660-	660	660	-	-	660
		L_3	-	-	85	85	85	-		85
M-2	3rd Layer	L_1	400	3250	1330	5000	-	-	5000	5000
		L_2	670	-		670	670	-	-	670
		L_3	480	-	-	480	-	480	-	480

Table 5.5.a Mass balance when the well screen is placed at the third layer in the M-3 model, which represented the upper fining sequence of the aquifer

(1) Model	(2) Well Placed at	(3) Layer	*Inflows and Outflows from Different Vertical Layers of Models When a Well-screen Is Placed at the 1st Layer*							
			Flow in (m^3/day)				Flow out (m^3/day)			
			(4) Body in (m^3/day)	(5) Recharge (m^3/day)	(6) From Top to Bottom	(7) Total	(8) Body Out (m^3/day)	(9) From Top to Bottom	(10) Well Out	(11) Total (m^3/day)
M-3 K2=50 K1=15 K3=100	3rd Layer (-6 to -20)	L_1	1750	3250		5000	-	-	5000	5000
		L_2	1400	-	-	1400	-	1400	-	1400
		L_3	1730	-	-	1730	-	1730	-	1730

5.4 Development of a site-specific model to predict the influence of pumping on arsenic transportation.

A site-specific conceptual model was built up in order to reflect more lithological parameters in the actual geology of the study area. The actual model cross section is shown in Fig. 5.9. It is a seven layers model study and was analyzed to predict the downward flow of arsenic through the deeper layers as a result of over extraction. This site-specific real model incorporated more realistic field complexities into the model in order to make the model results representative.

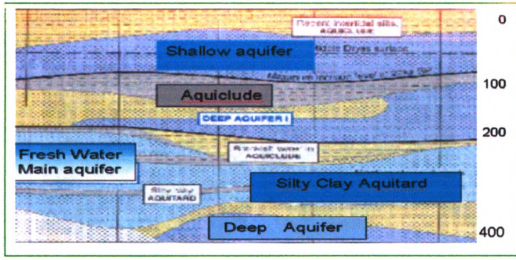

Map source: GOB(1999).

Fig. 5.9 Geological cross-section of site-specific model in the study area. Up to 400 m depth

5.4.1 Influence of pumping on vertical migration of arsenic in the models that reflected more realistic complexities in the field

Flow patterns were captured for both natural flow conditions (left side, Fig. 5.10) and extraction or pumping conditions (right side, Fig. 5.10) while simulating the site-specific model. There was significant change in the flow pattern because of extraction (Fig. 5.10). The velocity distribution was examined for each layer, and the change in velocity distribution graphs were shown in Appendix E. Site-specific model simulation showed that placing well screens at deeper layers increased the downward flow rate through the deeper layers. Therefore, it is most likely that groundwater arsenic concentration would be increased by extraction from deeper layers.

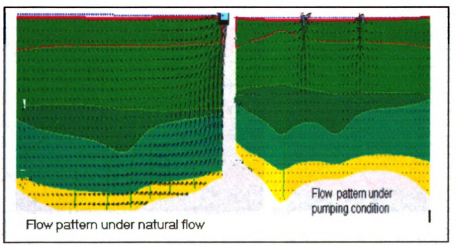

Fig. 5.10. Significant change in groundwater flow patterns due to the extraction rate in a site-specific model that reflects the real field complexity.

5.4.2 Influence of extraction on arsenic concentration migration in the site-specific real model

In order to estimate the likelihood of arsenic migration in the groundwater system, three cases of mass balance computation of arsenic concentration were designed:

1. Arsenic concentration at different layers of the site-specific model as a function of the shallow aquifer recharge (SAR) rate.

2. Arsenic concentration at different layers of the site-specific model as a function of the pumping rate (Q)

3. Arsenic concentration at different layers of the site-specific model as a function of placing well screens at L_1, L_2 and L_3.

The model results for the three cases are shown in Table 5.6.

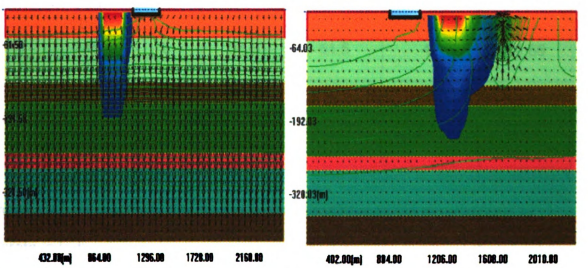

Fig.5.11. Impact of pumping on the arsenic migration under natural flow condition (left side) and pumping condition (right side) in to the deeper layer after 5000 day s without retardation.

Table 5.6. Arsenic concentration at different layers of the site-specific model as a function of SAR rate under natural groundwater flow conditions after 10000 days

Aquifer Layer	Depth (m)	Conductivity ($m\ d^{-1}$)	SAR 381 mm	SAR 762 mm	SAR 381 mm	SAR 762 mm
			Cond. (Not Pumped) (ppb)	Cond. (Not Pumped (ppb)	Cond. (Pumped) (ppb)	Cond. (Pumped) (ppb)
L_1	-10 to –40 (55)	15	1500	1500	1500	1500
L_2	-40 to –120 (80)	35	897	1049	986	728
L_3	-120 to –155 (65)	5	399	515	435	234
L_4	-155 to –245 (60)	30	124	176	162	52.2
L_5	-245 to -270	5	33.5	51.5	42	10.66
L_6	-270 to 350	100	5.52	9.7	7	1.26
L_7	-350 to -400	100	0.11	0.2	0.14	0.18

It appears from the Table 5.6 that pumping conditions helps more arsenic to migrate in to the deeper layers when the available shallow aquifer recharge rate (SAR) rate is 381 mm while comparing with the SAR at the rate 762 mm/Yr. This issue will be further discussed in section 6.6.

6. EVALUATION AND DISCUSSION OF RESULTS

Chapter six documents the results and applies results to address the research issues presented in chapter four. The results of analysis will be discussed in light of the conceptual basis or hypothesis of this study. The hypothesis is that layers at or below the water table receive less oxygenated water as a result of pumping. This study mainly investigated seven broad-based issues to achieve the overall goal and objectives. The issues are as follows:

- The geohydrologic factors that produce high arsenic in the groundwater system
- Interactions among lowering of the water table, dissolved oxygen (DO) content in the recharging water (SAR) and the likelihood of arsenic release
- Evaluation of the existing arsenic release hypotheses and establishment of logic to support the hypothesis presented in this study
- Impact of the irrigation withdrawal rate (Q) and the cropping pattern on the amount of shallow aquifer recharge (SAR)
- Influence of extraction (Q) at a rate greater than that of aquifer recharge (SAR) on groundwater movements, flow patterns and likelihood of arsenic release
- Placing of well-screens in the deeper layers of the aquifer and the likelihood of arsenic release
- Administrative and management decision variables to reduce the risk of arsenic contamination in case of further irrigation development.

Finally, recommendations are made based on the findings. The overall goal of this study was to formulate a quantitative irrigation development policy that would reduce the risk of arsenic contamination. The evaluation of this analysis is based mainly on the research issues presented in chapter four, and each research issue is discussed along with a few strategic questions.

6.1 Research issues and strategic questions

The arsenic concentration distribution analysis for different hydrologic zones was plotted in Fig. 4.2.b. Also, analyses presented in Table 4.2.1 and Figs. 4.2.a, 4.5, 4.6.a, 4.6.b, 4.7.a, and 4.7.b indicated that there were patterns or relationships between arsenic contamination and regional hydrology, geomorphology, surface geology, physiographic units, depth of the aquifer, and dissolved iron content in Bangladesh's groundwater system.

Research issues

- Hydrologic factors that correlate with high arsenic concentrations in Bangladesh's groundwater system.

Strategic questions

1. Why did the arsenic concentration exhibit patterns in hydrologic zones as shown in Figs. 4.2.b and 4.3.a, varying with the geomorphology, surface geology and physiographic units of Bangladesh?

2. Why and how is the arsenic contamination problem related to the dissolved iron content of Bangladesh's groundwater?

The fact is that the cause of arsenic contamination in the groundwater of Bangladesh is still poorly understood and a strongly debatable issue. The above strategic questions were investigated and explained by application of hydrogeochemical and thermodynamic properties. Also, the field evidence available so far justifies the explanations offered.

6.1.1 Why arsenic concentrations in groundwater exhibited correlations with the hydrologic zones, geomorphology and surface geology

Arsenic concentration analysis exhibited a correlation with the hydrologic zones as shown in Figs. 4.2.b and 4.3.a. The results will be discussed from the context of probability of arsenic exceedence in that area to explain the correlations.

Probability of arsenic concentration exceeding threshold levels was found to be highest in the southeast (SE) and southwest (SW) zones of Bangladesh

The probability of arsenic exceeding threshold levels (50 ppb) was analyzed, presented in Table 4.2.1, and pictured in Fig. 4.2.b. It appeared from the results that the southeast (SE) and southwest (SW) zones were the most arsenic-affected areas, in which the probability of arsenic exceeding threshold levels (50 ppb and 250 ppb) was found to be 71.4% and 59.55%, respectively

(Table 4.2.1), in the SE zone of Bangladesh. It was apparent from Fig. 4.2.b that there was a distinct regional pattern of arsenic contamination, with the greatest contamination in the southeast (SE) and southwest (SW) zones of the country. On the contrary, the northwest (NW), north-center (NC) and south-center (SC) zones had probabilities of arsenic exceeding threshold levels in the range of 18 to 39% (Table 4.2.1).

Alluvial deposit (in the SE) and deltaic deposit (in the SW) types of surface geology correlated with high arsenic concentration

Despite having large variability in the spatial distribution of arsenic contamination, it was found that the most highly arsenic-contaminated area was mostly confined to the lower delta flood plains of the Ganges River, which comprises the southwest (SW) region, and the Meghna River Flood Plain (FP) which built up the southeast (SE) region of Bangladesh (Table 4.2.2, Fig. 4.2.a, and Fig. 4.3.a). The young (Holocene) alluvial and deltaic deposits in the southeast (SE) and southwest (SW) zones of Bangladesh were the most affected, whereas the older alluvial sediments in the northwest (NW) and north-center (NC) regions were not (Fig. 4.3.a) as contaminated.

The least arsenic-contaminated zones were the northwest (NW) and north-center (NC) zones (Fig. 4.2.b) where the geomorphology was comprised of Old Himalayan Fan, Tista-Jamuna floodplains, and Madhupur Tract (Table 4.2.2). The geomorphologic and surface geological differences among the hydrologic zones were presented in detail in Table 4.2.2.

Physiography of the SE region (dominated by Tippera surface) strongly correlated with high arsenic concentration

The physiographic map analysis in Fig. 4.3.b clearly indicated that the highest arsenic concentration levels (>250 to 1665 ppb) were mostly confined to the SE region where the physiographic unit was dominated by Tippera surface (Fig. 4.3.b and Table 4.2.2). The red spots in Fig.4.3.b indicated the area affected by arsenic levels above 50 ppb.

Geomorphology of Ganges & Meghna River Flood Plains produced the highest sediment load and was correlated with high levels of arsenic contamination

Arsenic contamination was found mostly distributed over the Ganges - Meghna River Flood Plain (FP) (Figs. 6.1 and 4.3.a). The Ganges and Meghna River FP received sediments from the vast catchments in India and Nepal (Fig. 6.1 & Table 3.2). The combined delta of the Ganges and Meghna River FP experiences a high rate of sediment flow, about 478.9 million tons per annum (Table 3.2). It produced a greater sediment load in the SW and SE regions than in the NW and NC regions of Bangladesh.

Arsenic concentrations in the SW and SE zones were found to be greater than those in the NW and NC regions because arsenic was inherited in the sediments of that region through the development of different geomorphology.

Therefore, it seemed that the arsenic distribution pattern in the SW and SE zones highly correlated with the geomorphology of the SE and SW regions of Bangladesh.

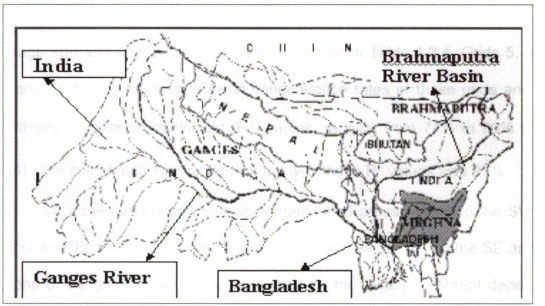

Fig. 6.1 The vast catchment area of the rivers Ganges and Meghna and Brahmaputra river basin, mostly in India and Nepal. Blue lines are the flowing river systems.

6.1.2 Explanation of why and how arsenic contamination is related to the dissolved iron content in the groundwater

The results analysis shown in Fig. 4.7.a and Fig. 4.7.b suggested that the distribution pattern of arsenic concentration in the most arsenic-contaminated aquifers offered a good correlation with the dissolved Iron (Fe^{2+}) concentration (Table 4.2.4).

Why arsenic concentration and dissolved iron content are related

In order to find a relationship between arsenic and iron, the whole country was divided into 16 grids latitudinally from 22.00 to 26.75°N and longitudinally from 88.2 to 92°E. The number of grids, respective latitudes and longitudes, and average iron and arsenic content were presented in Table 4.2.4. Grids 5, 9, 10, 12, and 15 had the highest arsenic concentration rates of these grids and also the largest regression coefficient (R^2) values, ranging from 71% to 99% (Table 4.2.4). The confidence interval associated with these R^2 values was 95%.

All of the most highly arsenic contaminated areas belong to the SW and SE zones. The reason for the high iron content in their soil is that the SE and SW regions of Bangladesh were mainly built up by the deltas' sediment deposition, and deltaic sediment contains more iron oxides as associated minerals than other types of soil (GOB, 1999).

It was found from the literature review that in sediment-water solution interactions, arsenic is strongly sorbed by the many metal oxides attached to the sediments, especially iron oxides and hydrous ferric oxides (HFO). The HFOs had a surface area an order of magnitude greater than that of the most crystalline iron minerals. The greater the surface area, the more the sorption (Dzombak and Morel, 1990). As the sediments of the SE & SW zones are rich in dissolved iron or hydrous iron content, their surface area is more inclined to adsorb arsenic. Therefore, naturally, the arsenic content in those sediments would be rich. This is how dissolved iron showed a strong correlation with arsenic in the SE and SW

regions of Bangladesh. High dissolved iron content reactions are generally microbial mediated (Lovely and Chappel, 1995).

6.1.2.a Thermodynamic explanation of the correlation between high arsenic and dissolved iron content in the groundwater system

A thermodynamic analysis was done in order to correlate the arsenic with the dissolved iron. Many reactions in nature go 100% to completion; however, the incomplete reactions are reversible, and products colloid with each other and produce reactants. When the net change in reactants and products is zero, the reaction is said to have reached equilibrium. The precipitation and dissolution reactions of ferric hydroxides are reversible reactions in the environment (Stumm and Morgan, 1997).

In this study, it was investigated how a lack of dissolved oxygen (DO) could influence iron reactions to release arsenic by shifting the chemical equilibrium condition.

Iron precipitation — Exothermic

$$4\,Fe^{2+} + O_2 + 10\,H_2O \rightleftharpoons 4\,Fe(OH)_3\,(s) + 8\,H^+ \qquad (6.1)$$

Iron dissolution — Endothermic

The above reversible reaction (6.1) is considered to be in equilibrium only when the rate of forward reaction is equal to the rate of reverse reaction. If the free energy of formation of products is equal to the free energy of formation of reactants, then the reaction is at equilibrium. Using the value of the reaction quotient (Q) and the equilibrium constant K, it is possible to understand whether the reaction in the system was in equilibrium or not. For the iron precipitation dissolution reaction (Eq. 6.1), the value of equilibrium constant K = $6.2*10^5$ = $10^{5.8}$.

$$\text{Reaction quotient (Q)} = \frac{\text{Solid } [Fe(OH)_3]^4 [H^+]^8}{[Fe^{2+}]^4 \; P[O_2] \; [H_2O]^{10}}$$

According to the thermodynamic rules, if the term Q / K equals 1, then the free energy of the reaction, ∇ G, equals zero and the system is said to be at equilibrium. If Q/K <1, ∇ G is negative and the reaction is spontaneous. In Equation 6.1, the value of the reaction quotient, Q, was calculated by considering a hypothetical system of pH = 5 and dissolved iron concentration Fe^{2+} was 0.1 mg/L ($10^{-5.5}$ mol/L), and the dissolved oxygen content was at equilibrium with the atmosphere [P_{O2} = 0.21 atm = $10^{-3.54}$ mol/L]. The reaction quotient, Q, was found to equal 10^{-31}. As the equilibrium constant K equals $10^{5.8}$, therefore, Q/K is <1, ($1 / 10^{36.8}$), implying that the equation (6.1) would favor the product and that the dissolved iron would be precipitated in solid form in the presence of dissolved

oxygen.

But when the oxygen concentration was reduced, an increased value of Q/K was found. It implies that the forward reaction rate was slowed down and the reverse reaction was powerful. For example, if the oxygen concentration decreases to 0.000002 atm ($10^{-8.58}$ mol/L), then Q = $10^{-26.42}$and Q/K = $1/10^{32.2}$ Therefore, the decreasing amount of oxygen would shift the equilibrium in the reverse direction. As a result, the dissolution of iron oxides will occur. Eventually, arsenic will be released from iron oxides. The greater the shortage of oxygen is, the more reducing conditions will prevail and the more Fe^{2+} will be dissolved and the associated arsenic will be released into the water. This is how iron and arsenic release into groundwater systems are related to each other.

6.2. Interaction between lowering of the water table, dissolved oxygen and arsenic concentration triggering

Research issue

- The second research issue was to understand the interaction between the lowering of the water table position, the dissolved oxygen content in recharging water and the triggering of the arsenic contamination problem in Bangladesh's groundwater.

Strategic questions

1. Why does the arsenic concentration vary with depth?

2. What is the role of the lowering water table on dissolved oxygen content in groundwater, redox potential values and the rise in arsenic concentration?

3. What impact did the lowering of the water table have on the dissolved oxygen concentrations of the deeper layer of the aquifer?

6.2.1 Why arsenic concentration varies with aquifer depths

With data from the real heterogenic world, one would not expect a high correlation between aquifer depths and arsenic concentration. However, an R^2 value of about 58 to 72% at a regional scale (Table 4.2.3) and about 32 to 99% in the square grid system of analysis (Table 4.2.4) was obtained.

Arsenic concentration increased from 9 to 30 m

Why arsenic concentrations vary with aquifer depth will be investigated in this section. Figs. 6.2.a and 4.6.a showed a positive correlation between arsenic concentration and aquifer depth over the depth ranging from 9 to 30 m below the ground, and the corresponding R^2 value of that layer ranged from 0.58 to 0.72.

Arsenic concentration decreased from 100 to 350 m

In contrast, a negative correlation was found between arsenic and dissolved iron from 100 to 350 m below the ground (R^2 = 0.72) (Fig. 6.2.b and Fig. 4.6.b). From 0 to 9 m and from 50 to 100 m, the correlation was poor. The above sequence of spatial variations in arsenic concentrations over the depths was also addressed from the context of thermodynamic principles. The actual redox stratification records from the field may explain the situation better.

Variation of redox values over aquifer depth

In this study, the redox potential values at different aquifer depths were computed by using the band regression method, and the analysis showed variations in redox potential values over the aquifer depths (Figs. 6.3.a and 6.3.b). Fig. 6.3.a indicated that the redox potential values decrease with increasing aquifer depth linearly from 10 to 30 m below the ground. On the contrary, the redox potential values increase with increasing aquifer depth ranging from 150 to 350 m (Fig. 6.3.b).

Analysis of the oxygen diffusion model suggests that oxygen concentration decreases with increasing aquifer depths (Figs. 4.11, 4.12, and 6.4). Comparing all these figures together (Figs. 6.3.a, 6.3.b, and 6.4), it is graphically explained that arsenic concentrations increase with decreasing redox potential values as a result of a low oxygen supply over the depths ranging from 9 to 30 m below the ground.

Why the arsenic concentration increased with depth from 9 to 30 m in Fig. 6.2.a

Arsenic concentration increases with decreasing redox potential (p^e) values (Fig. 6.3.a) and increasing aquifer depths when ranging from 9 to 30 m (Fig. 6.2.a). This is due to the fact that the oxygen concentration is decreasing as a function of depth (Fig. 6.4) and reducing conditions are simultaneously developing in the deeper layers (Fig. 6.3.a and 6.3.b). This analysis does support the working hypothesis of this study. However, it was important to find out why the arsenic concentration again decreases from 100 to 350 m below the ground (Fig. 6.2.b).

6.2.2 Why arsenic concentration again decreases over the depth ranging from 100 to 350 m (in Fig. 6.2.b)

In case of phreatic or leaky aquifer in coastal or sedimentary areas like Bangladesh, it is not always expected that the dissolved oxygen content in the deeper layers would be low, especially at the depth of 100 m below the ground. The reason is that the water below 100 m in depth may come as the regional throughflow. The regional throughflow generally is rich in dissolved oxygen content; therefore, it may cause the redox potential values to increase. Also, in deeper layers, the oxygen-consuming minerals are generally less available than in the upper layers (AECL, 1997). That is why, over the aquifer depth ranging

from 150 to 350 m, the water may be oxic and the p^e values at that depth (150 to 350 m) are found to be higher.

It is clearly understood that dissolved oxygen content is an important factor that controls the arsenic concentration of the groundwater system. However, arsenic could also be released in groundwater due to the oxidation of pyrite. The next issue to be addressed is whether lowering the water table can increase dissolved oxygen content in the aquifer.

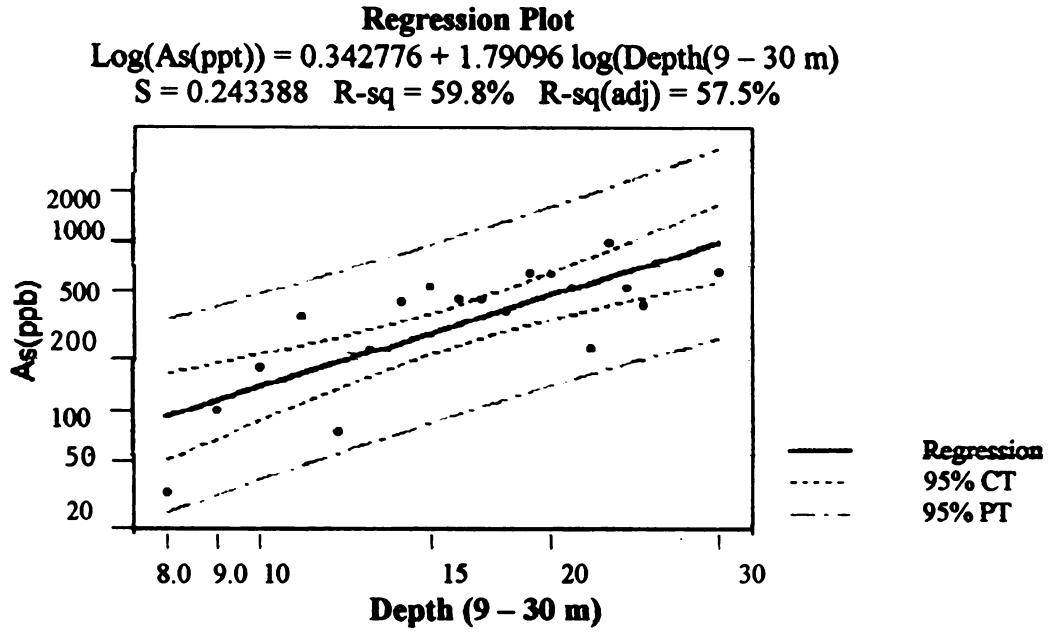

Fig. 6.2.a Arsenic content increases linearly with depth from 9 to 30 m

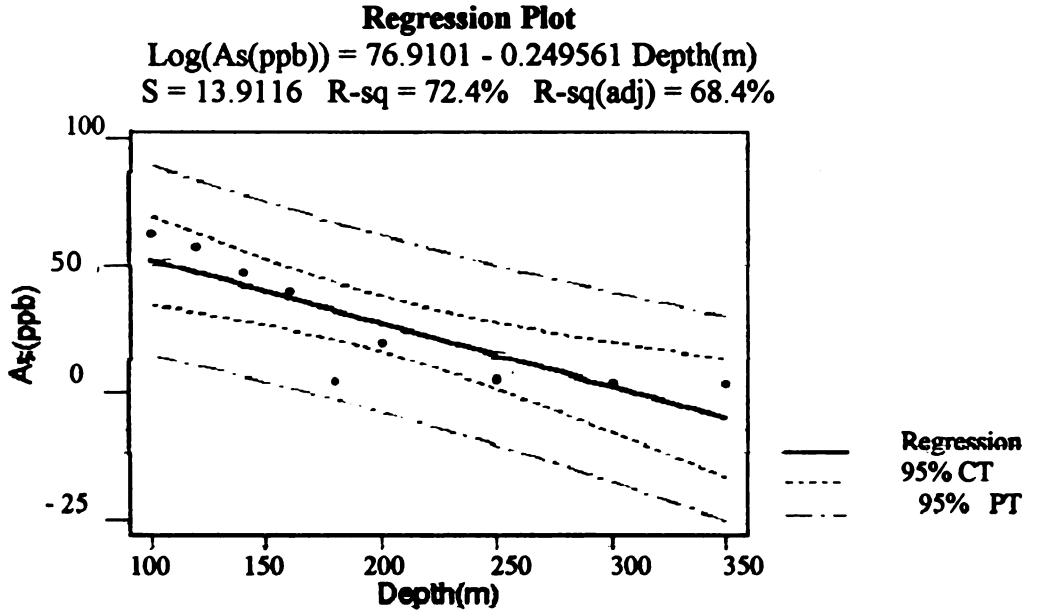

Fig. 6.2. b Arsenic content decreases linearly with depth from 100 to 350 m below the ground

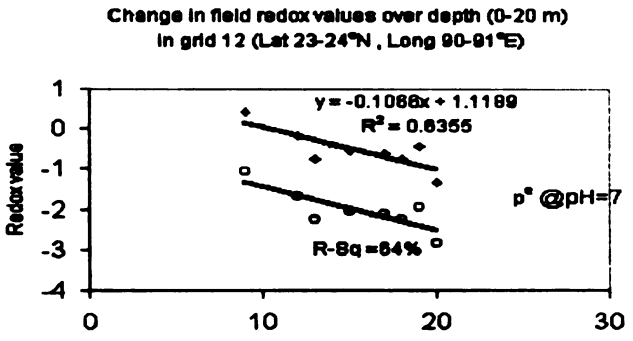

Fig.6.3.a. Redox potential values decreases over aquifer depth ranged from 10 to 30 m below the ground.

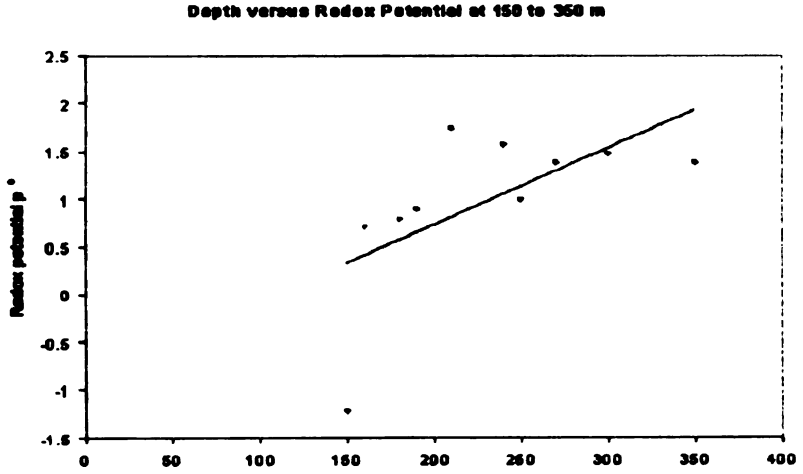

Fig.6.3.b. Redox potential values increased over depth ranging from 150 to 350 m in the most contaminated aquifer

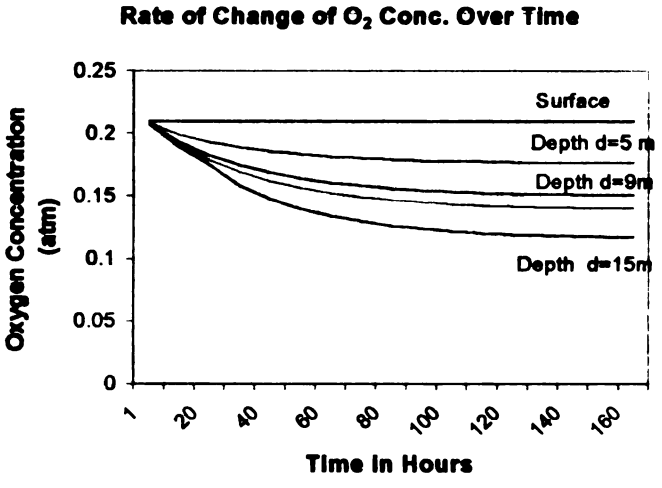

Fig.6.4. Oxygen concentration decreased with increasing aquifer depths over time.

6.2.3 What impact the lowering of the water table had on diffusive oxygen transportation to the deeper layers of the aquifer

This issue was analyzed by using the finite element model described in section 4.3.4. and Fig. 4.10. It was assumed in that model that, because of extraction, the water table was dropped about 4 m (from L_2 to L_6). The results of the lowering water table and the associated dissolved oxygen concentration values were presented in Tables 4.3.2 and 4.3.3 and graphed in Figs. 4.11 and 4.12. The results showed that a 4-meter lowering of the water table (from L_2 to L_6) did not increase the dissolved oxygen concentration at L_6 and L_{10} (Fig. 4.10).

The analysis also demonstrated that by changing the parameters' values and initial and boundary conditions, the dissolved oxygen concentration at deeper layers was increased, but these conditions are not practical in field conditions. Therefore, it could be concluded that the lowering of the water table did not increase oxygen concentration at the deeper layers.

6.3 Whether the oxidation or the reduction process mainly controls arsenic mobilization in Bangladesh's groundwater

The third research issue presented in chapter four relates to one crucial issue: whether oxidation or reduction processes caused arsenic contamination in the groundwater.

Research issues

- What geochemical processes (pyrite oxidation or oxyhydroxide reduction process) mainly control arsenic contamination in Bangladesh's groundwater system?

Strategic questions

1. Was pyrite oxidation or reduction of oxyhydroxides responsible for arsenic release?
2. What exact theory was applicable to describe the arsenic release into the groundwater of Bangladesh?

3. Why could pyrite oxidation not be considered as a principle mechanism of arsenic release, or what are the inadequacies of this theory?
4. Why is the hypothesis offered in this study a valid explanation of arsenic release that should not be rejected?
5. What are the interactions between the extraction rate, the lowering the of water table position, and the rejecting or accepting of the oxidation theory of arsenic release in groundwater?
6. Can thermodynamic principles be applied to interpret the relations among the lowering water table, the shortage of dissolved oxygen in recharging water and arsenic contamination in Bangladesh's groundwater?

6.3.1 Whether pyrite oxidation or reduction of oxyhydroxides was mainly responsible for arsenic release in the groundwater

It is still a debatable issue whether oxidation of pyrites or reduction of iron oxides controls the arsenic release mechanism in Bangladesh's groundwater. There have been divergences of views among researchers and considerable difficulties in working on the arsenic problem in Bangladesh. It was not the purpose of this analysis to focus on this debate, but discussions were had to evaluate both oxidation and reduction theory in the context of the lowering of the water table, in order to support the hypothesis offered in this study.

Opinions based on the oxidation of arseno-pyrites theory

The proponents of the oxidation theory welcome an increase in the supply of oxygen in the groundwater. There are scientists and chemists who believe pyrite oxidation was the dominant arsenic release mechanism in Bangladesh. The cause of increased oxygen supply may be due to the development of heavy duty tube-wells known to cause extension of the vadose zone and to supply more oxygen to the groundwater (Mallick et al., 1995). Oxygen-oxidized arseno-pyrite (FeAsS), and eventually arsenic, was released into the water. Pyrite oxidation may be accelerated by lowering of the water table due to overpumping (Kinniburgh et al., 1994) or to nitrate pollution of the aquifer (Postma, 1991). During the last two decades, the Green Revolution in Bangladesh has lowered the groundwater level and inadvertently caused the release of arsenic (Tsushima, 1999).

Opinions based on the reduction theory of arsenic release

The proponents of the oxyhydroxide reduction theory have rejected the explanations of the oxidation group. According to the reduction hypothesis, the origin of arsenic in groundwater is a natural process, which implies that has been present in the groundwater for thousands of years without being flushed from the delta.

The investigators in this group suggest that arsenic release was due to the reduction of arseniferous iron oxyhydroxides when anoxic conditions

developed during sediment burial (Nickson et al, 1998; Nickson & McArthur et al., 2000). Arsenic in Bangladesh's groundwater cannot drive from the presently accepted mechanism, whereby water-level draw-down from extraction wells allows atmospheric oxygen (O_2) into the aquifer and so allows the oxidation of arsenic-bearing pyrites with concomitant release of arsenic to the groundwater (Das et al., 1995; Roy Chowdhury et al., 1998). Such a mechanism is incompatible with the redox chemistry of the water. Arsenic produced in this way would be adsorbed to FeOOH, the product of oxidation (Mok & Way, 1994).

6.3.2 What theory is applicable to describe the arsenic release into the groundwater of Bangladesh

It appears from the above statements that the two theories are completely opposite to each other from the chemical point of view. However, in this study, it was hypothesized that the lack of dissolved oxygen content in recharging groundwater and the shortage of recharge due to upstream withdrawal of river water were important factors that controlled the arsenic release process in the groundwater. The hypothesis presented in this study completely opposes the pyrite oxidation theory but partially supports the reduction theory. The logic and supporting evidence to explain why the oxidation theory is inappropriate to explain the arsenic contamination problem in the groundwater of Bangladesh will be established. In order to do so, the following questions must be addressed.

6.3.2.a What was the critical difference between the reduction theory and hypothesis offered in this study?

- Like the reduction theory of arsenic release, this study also assumed that arsenic was released due to the development of reducing conditions wherein iron hydroxides scavenged arsenic during transportation. This study shows that this iron precipitation–dissolution reaction (Eq. 6.1) shifts the equilibrium due to a shortage of oxygenated recharging water in the groundwater, rather than fitting the usual explanations of microbial activity removing oxygen.
- The reduction group totally ignores surface water's contribution to the shallow aquifer recharge (SAR) and its impact on groundwater flow dynamics. This study completely analyzed the impact of SAR reduction on the groundwater flow and the likelihood of arsenic migration.

Why the hypothesis offered in this study is partially supportive of the reduction theory of arsenic release

This study also admitted that development of a reducing condition helps to release arsenic from the surface of iron oxides. But the development of a reducing condition was not found to be due to microbial activity because field studies do not support the idea that 6% organic carbon can be present at the deeper layers of the aquifer. And if organic carbon was the major cause of arsenic release, why was arsenic contamination not found in the earlier days, and why is there not any prior report of arsenic toxicity in Bangladesh?

6.3.3 Why the pyrite oxidation theory was not applicable to explain the arsenic contamination problem in Bangladesh's groundwater

The oxidation theory does not provide the geochemical evidence in the flow path of groundwater needed to support the oxidation theory. For example, if arseno-pyrite were the major cause of arsenic release, then the SO_4^{-2} ions would be dominating the groundwater flow-path. The most important oxidation reaction of arsenopyrite is as follows"

$$Fe\ As\ S + 13\ Fe^{3+} + 8\ H_2O \Rightarrow 14\ Fe^{2+} + SO_4^{2-} + 13\ H^+ + H_3\ As\ O_4 \qquad (6.3)$$

But there is no field evidence of increasing numbers of SO_4^{-2} ions along the flow-path. Rather, 3500 water quality data records (collected by BGS) indicate no relationship between arsenic and SO_4^{-2}.

If the oxidation principle is the major cause of arsenic release into the groundwater of Bangladesh, the following points must be met in the field conditions.

Point 1: Sulfate (SO_4^{2-}) contamination should be maximal only at the top of the water table if pyrite oxidation is the real cause

If arseno-pyrite is believed to be the major cause of arsenic contamination in groundwater of Bangladesh, according to the reaction in Eq. 6.3, arsenic concentrations always should be maximal at the top of the aquifer. The reason is that the dissolved oxygen (DO) should always be maximal in the upper layer of

the aquifer because of its close proximity to the surface. Arsenic must be found to be correlated with ions of SO_4^{2-} and there will be accumulation of SO_4^{2-} as a Terminal Electron Accepting (TEA) process along the flow path of groundwater. But in reality, the field evidence does not show that the top most layers were always arsenic contaminated. Rather, the top most layers were arsenic free (0 to 10 m) in almost 99% of the samples. Field evidence also did not suggest any relationship between arsenic and ions of SO_4^{2-}. In addition to that, release of SO_4^{2-} ion would also would have to be associated with increased ions of HCO_3^{-1} in the water, but water quality samples records analyses did not show any strong correlation between arsenic and bicarbonate.

Point 2: There must be a concentration gradient while pumping a deep well if the oxidation theory is valid

This study analyzed a conceptual one-dimensional model in section 5.1, and the results were presented in Fig. 5.2.a, where it was found that aquifer thickness and conductivity regulated the concentration and leakage flow of the water entering the well. If oxidation were the major cause of arsenic release, while pumping from a deep tube well, the arsenic concentration would have to vary with time because the screens of tube wells are generally placed at least 10 m below the top of the aquifer in the case of shallow tube wells (STW) and 50 to 100 m below the surface in the case of deep tube wells (DTW) (Fig. 5.1.a).

According to the pyrite oxidation theory, the top-most layers would always be more contaminated with arsenic than the deeper layers, where tube well screens are placed. It should take a long time for contaminated water to reach the well screen from the arseno-pyrite top layer. Therefore, there must be an arsenic concentration gradient while pumping water from a well. But no evidences of arsenic concentration variation were found while pumping wells in the field.

Point 3: Arsenic-contaminated water samples must be oxic and rich in redox potential values if pyrite oxidation is the real source of arsenic

If the oxidation theory is correct, the groundwater must be rich in dissolved oxygen. Most of the water samples analyzed by Nickson et al. (2000) found the arsenic-contaminated water to be anoxic or anaerobic. In addition to that, according to oxidation theory, eventually in the course of time there should not be any arsenic contamination problem in the groundwater because ultimately, the arseno-pyrite attached to the sediment will be flushed out by dissolved oxygen.

Point 4: There must be a positive correlation between the cumulative arsenic concentration and the cumulative water table decline if oxidation is the actual cause of arsenic release.

Point 5: There should be positive correlation between the maximum fall of the water table and the arsenic concentration if oxidation is the actual cause of arsenic release.

Point 6: There should be positive correlation between the most arsenic-contaminated area and the area receiving the greatest amount of recharge if oxidation is the cause of arsenic release.

Point 7: If the arseno-pyrite oxidation theory is the cause of arsenic release, the dug well waters should have been those most contaminated by arsenic

On the contrary, a study conducted by the researchers of SOES (2000) on dug wells in Bangladesh observed that out of 500 dug well samples, none of them was found with more than 50 ppb arsenic, and 86% of the water samples have arsenic levels below 10 ppb. That is why the oxidation theory is inadequate to explain the groundwater arsenic contamination problem in Bangladesh.

6.3.4 Why the hypothesis offered in this study is a valid explanation of arsenic release which should not be rejected

In order to test the hypothesis that less oxygenated recharging water at and below the water table, after extension of the vadose zone due to extraction, is the cause of arsenic release, in section 4.3.2 a conceptual oxygen diffusion model was analyzed using finite element techniques. The results indicate that the

oxygen concentration decreases with increasing aquifer depth and a 4 m lowering of the water table did not increase the diffusive oxygen supply to the deeper layers of the aquifer (Table 4.3.2 and Fig. 4.11). These results clearly demonstrate that the dissolved oxygen concentration decreases with increasing depth, supporting to the hypothesis in this study and going against oxidation theory.

A thermodynamic model was also studied in sections 4.4.5 and 6.3.6, and the results indicated that arsenic contamination release from iron oxides was caused by a shortage of dissolved oxygen. As a result, the equilibrium of the iron precipitation reaction (Eq. 6.1) had shifted to dissolution from precipitation (Fig. 6.6). That is why arsenic- contaminated groundwater is rich in dissolved iron. This analysis was completely supportive to the hypothesis offered in this study.

Unlike the other two hypotheses (oxidation and reduction), this study does not ignore the contribution of surface water recharge (SAR) to the issue of arsenic release. Three-dimensional conceptual models were analyzed in section 5.3.1 to understand the contribution of surface water recharge to groundwater movements, flow patterns, and the likelihood of arsenic migration. The model simulation results demonstrated that extraction (Q) with a rate greater than that of aquifer recharge (SAR) significantly increases downward flow through deeper layers and, thus, the risk of arsenic migration. The simulation results are supportive to the hypothesis.

Dug well samples are relatively arsenic-free, supporting the hypothesis present in this study

According to the hypothesis of this study, it is believed that groundwater in touch with atmospheric oxygen is always oxic and rich in redox potential values (p^e or E_h). As a result of oxic conditions, the dissolved arsenic contaminants in the dug well waters were adsorbed onto the solid surfaces of iron oxides. That led to groundwater having arsenic content less than 10 ppb, because dug wells are placed in close proximity to the surface and can maintain equilibrium with the atmospheric oxygen level (0.21 atm).

Moreover, the analysis of aquifer depth versus arsenic concentration (in Figs. 4.6.a and 4.6.b), aquifer depths versus oxygen concentration (Fig. 6.4), and depth versus redox potential (Figs. 6.3.a and 6.3.b) clearly demonstrates that arsenic release is due to a shortage of dissolved oxygen over the aquifer depths, which decreases the redox potential values with increasing depth. Also, a thermodynamic model was studied in order to validate the hypothesis.

Geochemical explanation of the high arsenic contamination in Bangladesh's groundwater based on the hypothesis present in this study

The sediments in the SW and SE regions contained levels of higher organic matter (Khan, 1991) than NW and NC regions; therefore, iron-reducing microbial activity enhanced the oxygen consumption rate in the sediment of the Ganges and Meghna river delta flood plains (Nickson, 2000). On contrary, the

sediment in the NW zone was coarser than that in the SW and SE zones and there was most likely less microbial activity, which is why the NW region is relatively arsenic-free.

The above explanations of the higher arsenic levels in the SE and SW regions were based on the hypothesis offered by the reduction groups, and particularly by Nickson et al. (1999), who believe that organic carbon takes oxygen from the iron hydroxides and eventually causes arsenic to be released into the groundwater. The oxidation group did not accept this geochemical explanation of arsenic release. Adel (2000) put a very logical question to the authors (Nickson et al., 1999): Why was arsenic contamination detected only in 1990 in Bangladesh if organic carbon has been taking oxygen for thousands of years? To support the reduction hypothesis, he also mentioned that Nickson et al (1999) showed 6% organic carbon in the deeper aquifer layers, which goes beyond the boundary of scientific evidence. So far, no reasonable answer has been given to his question.

This study presents the hypothesis that development of reducing conditions or low redox potential values (p^e) was responsible for the release of arsenic from the iron hydroxides. However, the development of a reducing condition was caused by the shortage of dissolved oxygen in recharging water, not by the microbial consumption of oxygen. The iron precipitation–dissolution equation (Eq. 6.1) uses thermodynamic values to find that so long as any detectable oxygen (0.41 ppb) is present in the system, the redox potential (p^e)

values do not fall below 12.31 (Table 4.4.2). This indicates that the shortage of dissolved oxygen in the recharging groundwater was mainly responsible for arsenic release under reducing conditions.

6.3.5. Interactions between shortage of dissolved oxygen, extraction rate, lowering of the water table position, and rejection or acceptance of the oxidation theory of arsenic release in groundwater

A conceptual model of oxygen diffusion was analyzed in Fig. 4.10 in order to validate the theory of arsenic release by oxidation. The predicted oxygen concentrations at hypothetical arseno-pyrite layers L_6 and L_{10} were tabulated in Table 4.3.2.

The assumptions behind the diffusion model

The water table in the model aquifer was 2 m below the ground surface (WT-1) before the introduction of wells in Bangladesh (Fig. 4.10). Dissolved oxygen in groundwater was also in equilibrium with the atmospheric oxygen concentration (0.21 atm). This was considered to be Case 1. After the introduction of well-fields into the aquifer, the water table traveled 5 m down from WT-1 to WT-2. The water table (WT-1) lowered from L_2 (2 m below ground) to L_5, which was 5 m below the ground (Fig. 4.3.1). This is Case 2.

Findings from the oxygen diffusion model

Oxygen concentration decreased with increasing water table lowering depth

It was shown in Fig 6.5.a and Fig.4.11 (derived from Table 4.3.2) that after the lowering of the water table from its original position (WT-1), the predicted oxygen concentrations at pyrite layers (L_6 and L_{10} in Fig. 4.10) were less than before the water table's lowering. Lowering of the water table did not help increase the oxygen supply rate to the pyretic layers (L_6 and L_{10}); rather, the oxygen supply rates decreased over aquifer depth and time (Fig. 6.5.a). The oxygen concentrations in the deeper layers were found to be lower than predicted (Table 4.3.2).

Why the oxygen supply rate decreased in deeper layers

The literature review also suggested that the oxygen diffusion rate (ODR) decreases with increasing depth and with the moisture content of the layer. It should be mentioned here that a minimum 80% oxygen concentration was required to maintain an adequate ODR level ($20x10^{-8}$ gm/cm^2/min) (Mukter et al., 1996). In order to predict the oxygen concentration trend, default values of the oxygen diffusion coefficient for unsaturated soil (Dx=259.2 cm^2/hr or $4.166 x10^{-4}$ m^2/sec) were used. The oxygen consumption rate (α) in the governing equation (4.3.4) was -0.002125 cm^3/cm^3/hr, which is the 1st order kinetics of oxygen consumption. In fact, the value α depends on the soil's organic matter. Using this

default value, it was found from the model that after lowering of the water table, the predicted oxygen concentrations of deeper layers were less than the concentrations of the top, over-lain layers. In another set of experiments on depth, Mukhter et al. (1996) found that ODR varied inversely with depth (Fig. 2.2).

Changing initial conditions did not increase the oxygen concentration in deeper layers

It was evident in Fig. 6.5.b that the oxygen concentration of deeper layer L_{10} could not be made higher than that of L_6 even when the following two conditions were satisfied: (1) The value of the diffusion coefficient of oxygen in unsaturated soil (Dx_1) was taken to be equal to the diffusive coefficient of oxygen in water (Dx_2), and (2) the initial oxygen concentration at L_{10} was always maintained in equilibrium pressure (0.21 atm) (Fig. 6.5.b, curve a and b). In reality, these two conditions can never be maintained because the oxygen diffusion rate through the vadose zone, Dx_1, is always greater than the oxygen diffusion rate through water, Dx_2 (Table 4.3.1).

Rejection of oxidation theory

It can be summarized from the above discussions that lowering of the water table cannot or does not provide a greater atmospheric oxygen supply to the deeper layers of the aquifer. The oxygen diffusion rate (ODR) decreases with increasing aquifer depth. If the oxygen concentration falls below the critical concentration level, then the ODR also decreases in deeper layers.

Finally, it can be concluded from this study that the oxidation theory of arsenic release is not adequate to explain the arsenic release mechanism in Bangladesh's groundwater. It does not explain why the arsenic concentration is greater in the deeper layers than at the top, while the oxygen concentration does not increase with depth.

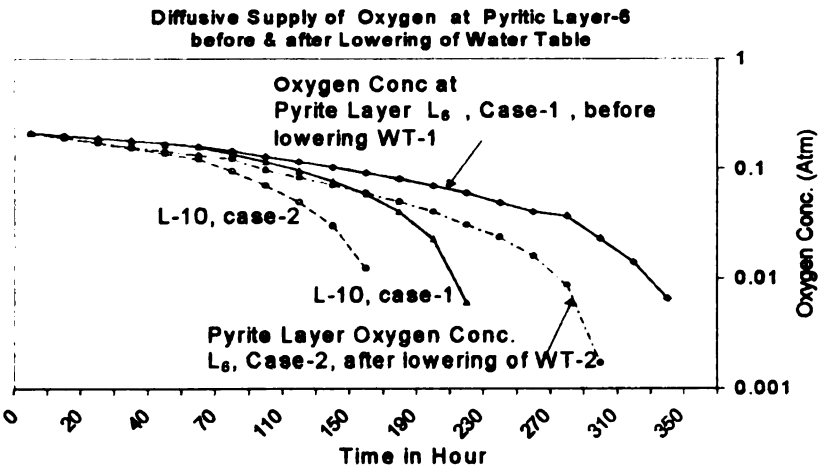

Fig.6.5.a Predicted change in the diffusive oxygen supply at arsenic contaminated pyretic layers

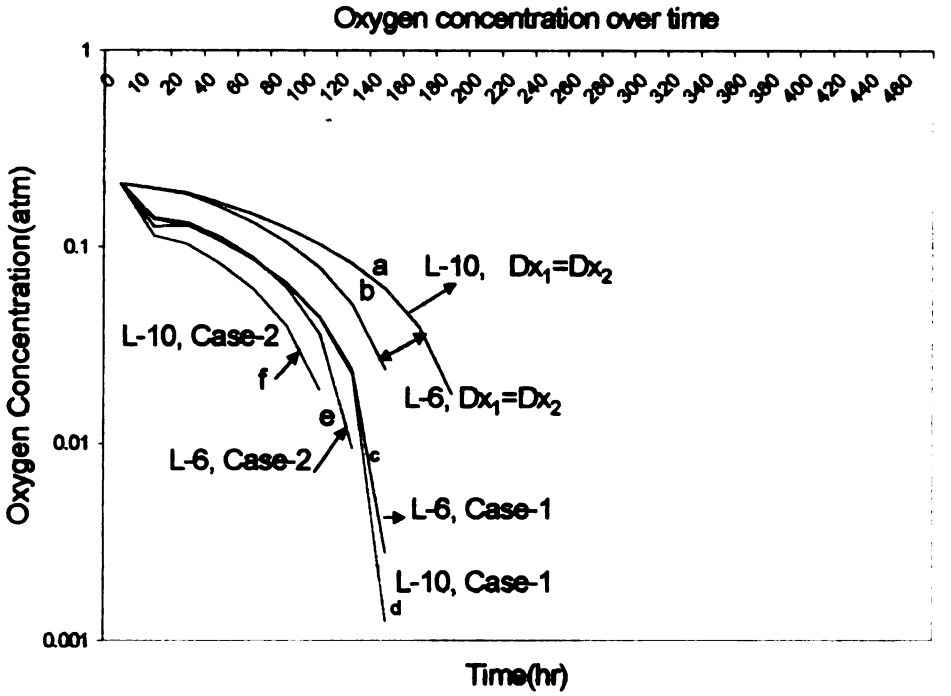

Fig.6.5.b Predicted change in dissolved oxygen concentration when the boundary conditions are changed

6.3.6 Can thermodynamic principles be applied to interpret the relations among the lowering water table, the shortage of dissolved oxygen in recharging water and arsenic contamination in the groundwater of Bangladesh

It was assumed in the hypothesis of this study that before introduction of well fields, the water table was in close proximity to the ground surface and dissolved oxygen (DO) content in groundwater was in equilibrium with atmospheric oxygen (0.21 atm). In this section, it will be discussed how thermodynamic principles support the working hypothesis presented in this study.

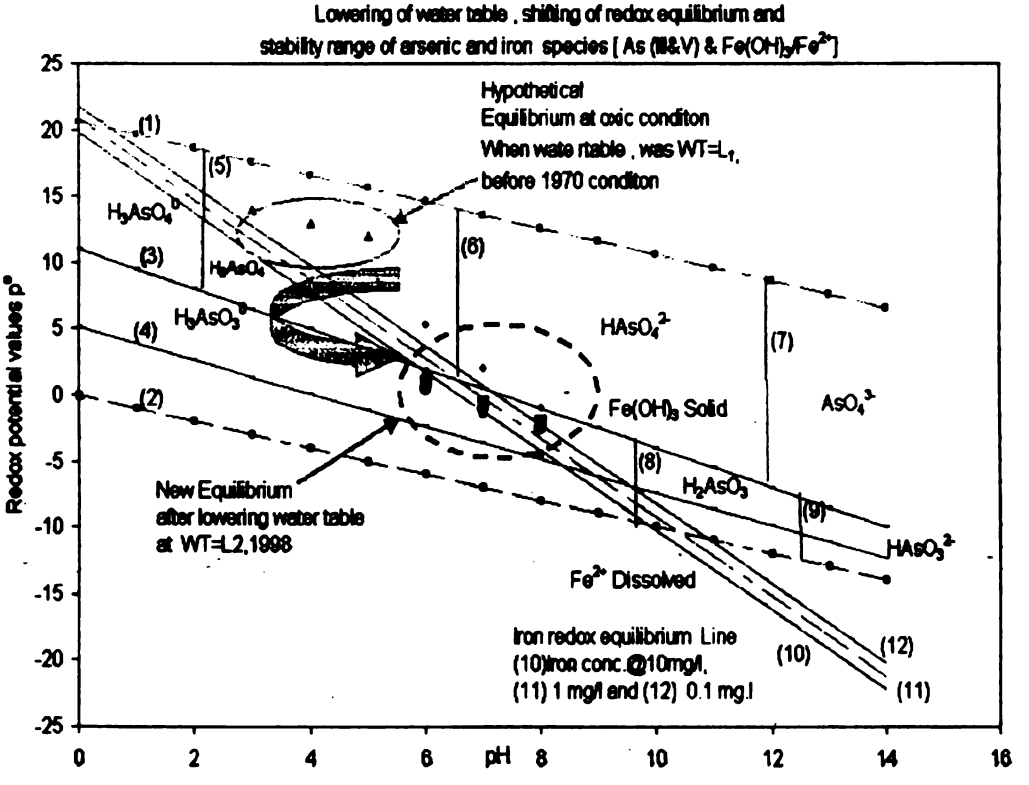

Fig. 6.6 Lowering of the water table and shifting of the equilibrium conditions

The p^e–pH diagram basically determines the stability range of the oxidized and reduced species with respect to their equilibrium lines under natural water pH levels. In Fig. 6.6, stability diagrams or p^e-pH diagrams for arsenite [As (III)] and arsenate [As (V)] redox couples (Line 3, Fig. 6.6) were drawn along with Fe (II) and Fe (III) redox equilibrium lines (Line 10 and Line 11, Fig. 6.6).

Initially, a hypothetical situation was considered before the installation of wells when the water table level was close to the ground surface and the dissolved oxygen content was in equilibrium (0.21 atm) with atmospheric oxygen. Equation 6.1 was used to determine the hypothetical equilibrium situation, marked in Fig. 6.6 at the top left with a green circle.

The p^e or redox values of the hypothetical system were computed using field maximum and minimum concentration of dissolved Fe^{2+} content in arsenic-contaminated water. Different DO content levels were assumed and those redox (p^e) values were plotted in the p^e -pH diagram in Fig. 6.6. All the p^e values under the hypothetical equilibrium condition appeared above Line 3 (the arsenic equilibrium line) and Line 10 (the iron equilibrium line) under the green circle. The computed field redox values (p^e) marked by the green circle on the top left (Fig. 6.6) ranged from 12.31 to 13.65, which implied that all p^e values were oxygen-controlled redox values. This was termed the hypothetical equilibrium condition of dissolved oxygen with atmospheric oxygen when the water table was close to the surface.

As a result of overextraction, the water table lowered and the oxygen supply to the deeper layers decreased. The maximum and minimum p^e-values were computed from the dissolved arsenic concentration in the fields and plotted in Fig. 6.6. The associated p^e values of dissolved Fe^{2+} in groundwater were also computed and plotted in Fig. 6.6. All the p^e values appeared below equilibrium line 3 and were marked with a red circle (in the middle of Fig. 6.6).

This shows that the redox potential values have decreased and the equilibrium condition has shifted from the precipitated solid iron phase (green circle) to the dissolved iron phase (red circle). The hypothetical equilibrium has shifted from an oxic to a suboxic environment In which p^e values were reduced from 1.5 to -3.5, which is a mildly reducing condition. The redox values are now controlled by dissolved iron, not by dissolved oxygen. The lowering of the water table decreased the oxygen supply rate to the deeper layers and developed the mildly reducing condition that was strongly favorable for arsenic to be released into the groundwater.

Figure 6.7 was drawn for the equilibrium redox couple SO_4^{-2} and H_2S in order to demonstrate whether arsenic was released due to the oxidation of pyrite (FeAsS) to SO_4^{-2} or the reduction of Fe^{3+} to Fe^{2+}. If pyrite were the cause of arsenic release, then Fe AsS H_2S would be oxidized to SO_4^{-2}. The water would have been rich in dissolved SO_4^{-2} ion, and the p^e values would have fallen below the equilibrium line L-12 in Fig. 6.7. However, none of the field p^e values went

arsenic release, then Fe AsS H_2S would be oxidized to SO_4^{-2}. The water would have been rich in dissolved SO_4^{-2} ion, and the p^e values would have fallen below the equilibrium line L-12 in Fig. 6.7. However, none of the field p^e values went below line-12. This proves thermodynamically that pyrite oxidation was not the process of arsenic release in Bangladesh's groundwater system because the redox potential values were not within the range of sulfate reduction.

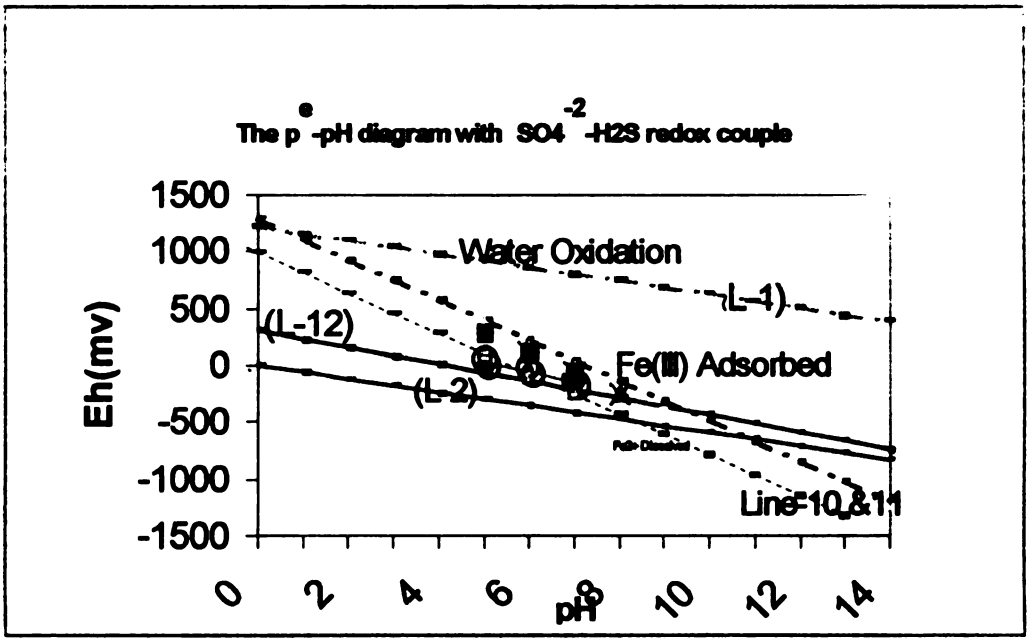

Fig. 6.7 Line 12 shows the equilibrium line of the SO_4^{-2} and H_2S redox couple; all of the p^e values fall below line 12

Summary:

It can be summarized from the above discussions that the lowering of the water table and the water's dissolved oxygen (DO) content played important roles in releasing arsenic into Bangladesh's groundwater. A smaller oxygen supply was caused by the increased depth to the water table Therefore, it appears from the thermodynamic model that the DO content was an important factor controlling arsenic release and arsenic speciation in Bangladesh's groundwater system under the original, natural conditions.

6.4 Influence of aquifer thickness on the arsenic concentration of water entering a pumping well

The fourth research issue of this study explained the influence of aquifer physical properties on the arsenic concentration of a well being pumped. It was important to understand the aquifer's influence on arsenic concentration to determine the validity of the oxidation theory of arsenic release in groundwater.

Research issue

- What is the influence of aquifer physical properties (thickness of the aquitard, conductivity) on the arsenic concentration in an irrigation well during pumping?

Strategic questions and discussions

1. What is the influence of aquitard thickness (b') on the amount of water (Q_t) entering the well screen and on the arsenic concentration in the water being pumped (C_t)?

2. What is the influence of aquitard vertical conductivity (K') on the amount of water entering the well screen and the arsenic concentration in the water being pumped?

3. How can aquifer physical properties (aquitard thickness and conductivity) and their influence be used to describe the validity of theories of arsenic release?

It is not illogical to argue that if arseno-pyrite oxidation were the source of arsenic release in Bangladesh's groundwater, the upper layer would have to be contaminated with arsenic because it was constantly in touch with atmospheric oxygen. Therefore, in the case of a leaky aquifer, the concentration of water entering a pumping well from an overlaid, arsenic-contaminated layer (L_1) (Fig. 5.1.b) must not be the same at any time as the pumped-water concentration (C_t) due to the mixing of the stratified arsenic concentration with pumped water (Q_t) of different concentrations inside the well casing.

In a leaky or semi-confined aquifer system, a deep tube-well initially extracts water from the screened aquifer's layer (L_3) where the hypothetical arsenic concentration (C'_3) may be less than the layer one (L_1) concentration (C'_1) or may even be zero (Fig. 5.1.b). When pumping starts, the concentration of water entering the well, C'_t, is to be equal to C'_3, reflecting the leaky aquifer's initial concentration. As pumping continues, the overlaid contaminated aquifer (L_1) supplies more water with a concentration of C'_1 through vertical leakage (Q_1) across the aquitard depth (b'). Eventually, C'_t progresses from C'_3 to C'_1, reflecting the increasing contribution of leakage (Q_1) to the pumped water (Q_t). As the radius of influence R_t increases over time, the ratio of partial discharge Q_3/Q_t decreases and C'_1/C'_3 increases.

From Equation 5.1 in chapter 5, it appears that when all of the pumped water Q_t comes only from the leaky aquifer layer L_3, then $Q_t = Q_3$. This implies that the arsenic concentration of the pumped water is equal to the concentration in the leaky confined aquifer (L_3) water and $C'_t = C'_3$. When no water comes from the leaky confined aquifer L_3, it implies that all water in Q_t was contributed by leakage factor Q_1 from the top layer L_1 (Fig. 5.1.b). When $Q_3 = 0$, the concentration C'_t in pumped-discharged water approaches C'_1. This means that immediately after starting to pump, the Q comes from a mixture of C_1 and C_3, but in the case of a leaky aquifer (like in Bangladesh), it takes time for Q_t to reach the equilibrium concentration with C_1. This means that there should be a concentration gradient during pumping.

6.4.1 What is the influence of aquitard thickness (b') on the amount of water entering the well screen and concentration in the pumping water?

A numerical analysis was done to illustrate the impact of aquitard thickness (b') and vertical conductivity (K') on the arsenic concentration of water entering a well being pumped (C'_t). The initial hypothetical arsenic concentration at the top layer L_1 and screened layer L_3 were assumed to be 100 and 50 ppb, respectively (Fig. 5.1.b). For the simplicity of the problem, convective flow of arsenic was assumed, as the groundwater velocity was higher near the vicinity of well screen. It was assumed that the arsenic concentration of the pumped water

and the arsenic concentration of the water entering a well were equal.

Arsenic concentration of water entering a well (C'_t) varied inversely with the thickness of the aquitard (b')

The results of this analysis were graphed in Fig. 6.8.a. It appears from that figure that the arsenic concentration of water entering into a well (C'_t) varied inversely with the thickness of the aquitard (b'). For example, while comparing graph 'b' and 'd' in Fig. 6.8, it was found that aquitard type 'b' (depth b'=65 ft.) resulted in a higher arsenic concentration (80 ppm) in pumped water (C'_t) than the aquitard type 'd' (depth b'=150 ft) where C'_t was predicted to be 65 ppb. Both K'=1.1 ft/day and R(t)=1500 ft were kept constant for aquitard types b, c and d.

The shallower the aquitard depth, the greater the rise in the arsenic concentration entering well water (C'_t) (Fig. 6.8.a). This is because in the case of a thick aquifer, more energy is required to let the leakage (Q_1) pass through the deeper layer, and as a result partial discharge Q_1 was less and eventually the ratio of Q_3/Q_t was higher to satisfy the equation of continuity. It was shown in Equation 5.1 that if the ratio of Q_3/Q_t were as high as unity, C'_t would be equal to C'_3. For a shallower depth of aquitard type ' b', the ratio of Q_3/Q_t was less and C'_t would be close to C'_1. That is how thinner aquitards cause higher arsenic concentrations in well water. Also, the concentration of water entering a well varies directly with the aquitard conductivity (Fig. 6.8).

A one-dimensional model analysis (Fig. 6.8.a) clearly demonstrates that the arsenic concentration increases directly with the conductivity. This analysis was also consistent with the results of three-dimensional models.

6.4.2. What is the influence of aquitard conductivity on the amount of water entering the well screen

While comparing graph "a" and "d" in Fig. 6.8, it was observed that the arsenic concentration in well water (C'_t) varied directly with the vertical hydraulic conductivity of the aquitard.

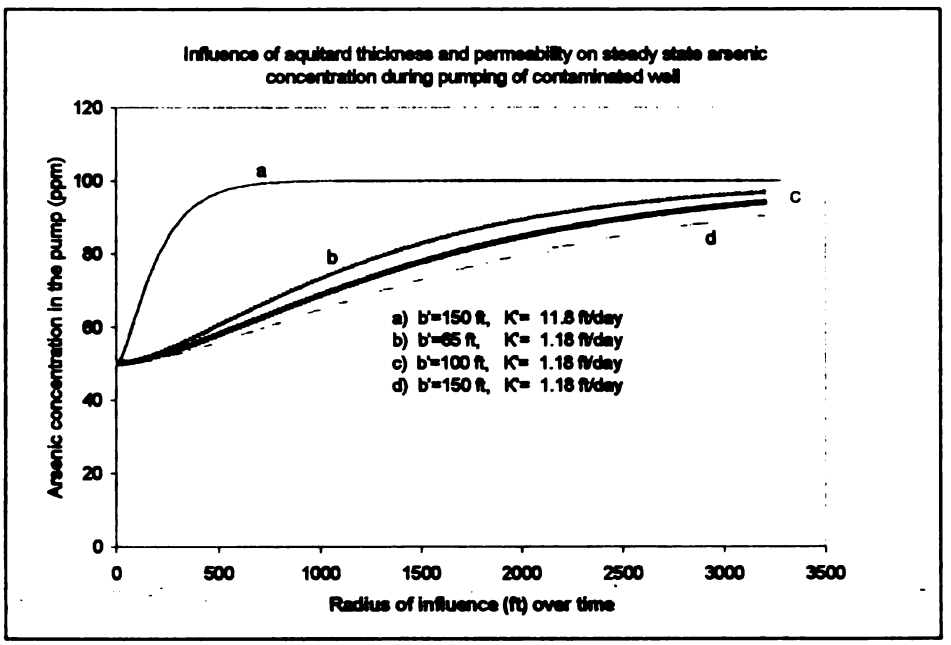

Fig. 6.8.a Influence of aquitard thickness and permeability on arsenic concentration in a well being pumped

Aquitard types "a" and "d" were of the same thickness but the conductivity 'K' of aquitard type "a" was ten times higher than that of aquitard type "d " (11.8 ft/d vs. 1.18 ft/d). As a result, the arsenic concentration in 'a' was more than that in 'd'. The results of this analysis explain why arsenic concentrations vary from layer to layer and aquifer to aquifer as a function of hydraulic conductivity and aquitard depths.

6.4.3 How aquifer physical properties (aquitard thickness and conductivity) can be used to describe the validity of oxidation theory of arsenic release.

Fig. 6.8.a shows that it will take time for the concentration of the upper aquifer to be equal to the concentration of the water entering a well, depending on the hydrologic parameters like aquitard thickness b' and conductivity K. As the radius of influence changes over time, it takes time to reach the equilibrium pumping concentration. If the pyrite oxidation theory were the real cause of arsenic release, the concentration of arsenic would always have been higher in the upper aquifer L_1 (Fig. 5.1.b). As it will take time for water from the upper aquifer to reach the well screen, there must be a concentration gradient observed while pumping for a long time in order for this theory to be an accurate description of Bangladesh's situation. The data do not show a concentration gradient, and so the reduction theory of arsenic release is more acceptable than the oxidation theory of arsenic release.

6. 5 Influence of extraction at a rate greater than that of aquifer recharge (SAR) on groundwater movements, flow patterns, and the likelihood of arsenic release

The fifth research issue of this study was to examine the relationship among aquifer recharge (SAR), groundwater movement, flow patterns, the extraction rate, and the likelihood of arsenic migration. Certainly the extraction rate (Q) and the amount of SAR available would have an impact on groundwater movement, flow patterns and the likelihood of arsenic migrating into the deeper layers of the aquifer.

Research issue

- The impact of groundwater withdrawal (Q) at a rate greater than that of shallow aquifer recharge (SAR) on the dynamics of groundwater movement, flow patterns and the likelihood of arsenic migration from the currently contaminated layers to the uncontaminated deeper layers of the aquifer.

Strategic questions:

1. What is the interaction between the extraction or pumping rate (Q) and the availability of shallow aquifer recharge (SAR) in a groundwater system?

2. What is the influence of cropping patterns on the amount of shallow aquifer recharge (SAR) available?

3. What impact do irrigation system capacities have on the potential recharge or surplus volume (SUR)?

4. What is the influence of aquifer recharge (SAR) on groundwater movement, flow patterns and the likelihood of arsenic migration?

Concept of shallow aquifer recharge (SAR)

For an aquifer with a virgin or un-pumped condition, the water balance or mass balance concept can be defined as $R_0 = D_0$, where the virgin recharge rate (R_0) is equal to the virgin discharge rate (D_0). But when wells (Q) are introduced to the system (as was done in Bangladesh), the above water balance concept is no longer true. Therefore,

$$R_0 - D_0 - Q \neq 0 \qquad (6.5.1)$$

The virgin discharge rate (D_0) remains unchanged until the pumping (Q) causes a significant change in the hydraulic gradient (h) at the boundary or periphery of the aquifer. When Q causes a significant change in the hydraulic gradient (h), then a new condition arises and the mass balance equation (6.5.1) becomes

$$(R_o + \Delta R_o) - (D_o + \Delta D_o) - Q + (dv/dt) = 0 \qquad (6.5.2)$$

where ΔR_o, ΔD_o, and (dv/dt) are the amount of change in recharge, discharge, and aquifer storage volume, respectively. As the initial recharge, R_0, is equal to D_0, Eq. 6.5.2 under an invaded condition can be expressed as

$$dv/dt = Q - \Delta R_o + \Delta D_o \quad \text{or} \quad Q = \Delta R_o - \Delta D_o + dv/dt \tag{6.5.3}$$

Here, the discharge prior to the pumping condition (ΔD_o) is termed "Capture." The mathematical definition of capture (ΔD_o) is

$$D_0 - \int^{L} Kh \frac{\partial h}{\partial s} dL = \Delta D$$

where K is hydraulic conductivity, h is the height of the water table, ($\partial h/ \partial s$) is the gradient, L is the length of the section, and D_o is the original discharge rate.

6.5.1 The interaction between the extraction or pumping rate (Q) and the availability of shallow aquifer recharge (SAR)

In the extraction situation, the pumping rate (Q) in Eq. 6.5.3 has to be balanced by three components: the aquifer recharge rate under the new pumping condition (ΔR_0), the capture or change in new discharge (ΔD_o), and the storage component (dv/dt). In order to maintain a steady-state water table and maximize the pumping limit, the storage change (dv/dt) and amount of capture (ΔD_o) must be zero.

6.5.1.a Maximum pumping limit, aquifer recharge rate (SAR) and lowering of the water table

When "capture" (ΔD_Q) is equal to zero in Eq .6.5.3, the maximum value of pumping limit Q_{max} is found to be equal to

$$Q_{max} = (dv / dt) + \Delta R_o \,. \qquad .(6.5.4)$$

In Eq. 6.5.4, Q_{max} has two components: change in storage volume (dv/dt) and change in recharge under the invaded condition (ΔR_o). So long as the volume of irrigation withdrawal (Q_{max}) remains equal to the volume of recharge in this condition of extraction (ΔR_o), there will be no withdrawal from the aquifer storage volume (dv/dt) and the water table will remain steady state over time. Whenever Q_{max} exceeds the new aquifer recharge rate (ΔR_o), that excess amount must come either from (dv/dt) or (ΔR_o). For a sustainable pumping condition, withdrawal from storage (dv/dt) must be zero. If the new aquifer recharge rate (ΔR_o) is not able to meet the excess "Q," there will be a drop in the aquifer's water table head and, over time, the water table. Therefore, pumping (Q) at a rate greater than that of aquifer recharge (SAR) will lower the water table unless the excess water comes from induced recharge sources.

6.5.1.b. The lower limit of aquifer recharge (SAR), potential recharge and amount of surplus (SUR)

In section 4.5.2, the amount of shallow aquifer recharge (SAR) was found to be

(SAR) = [Surplus (SUR) – Surface Runoff] (6.5.5)

From Fig. 4.15, it was evident that the amount of surplus (SUR) was contributing to surface runoff and shallow aquifer recharge (SAR), and

Surface Runoff = Outflow - Pumpage (Q)

Substituting this value of surface runoff into Eq. 6.5.5 yields

SAR = SUR - Outflow + Pumpage (Q) (6.5.6)

Without extraction (Q = 0), Equation 6.5.6 gives the lower limit of shallow aquifer recharge (SAR). Then, SAR is only equal to

SAR = SUR - Outflow or Surplus (SUR) = (SAR) + Outflow (6.5.7)

Potential recharge and its impact on the water table

From the irrigation development point of view, potential recharge is an important term defined as

Potential Recharge = Actual Recharge + Rejected Recharge

Potential recharge is conceptually equal to SUR and can influence the water table position.

6.5.1.c. Seasonal fluctuation of the water table and computation of shallow aquifer recharge (SAR)

The amount of SAR was computed to be 471 to 498 mm per year. The computation is presented in Appendix .B. The average of five years of water table fluctuation records in the study area (SW zone at Kustia) is shown in Fig. 6.8.b.

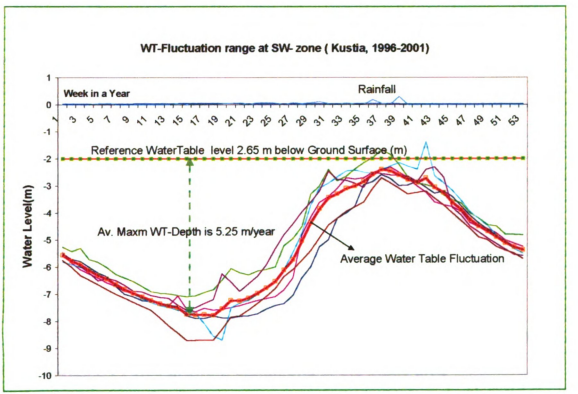

*Fig. 6.8.*b Evaluation of shallow aquifer recharge (SAR) under field conditions in the SW zone study area of Bangladesh

Validity of the shallow aquifer recharge (SAR) in the field condition:

The maximum range of seasonal lowering of groundwater in the study area was found to be 5.25 m (Fig. 6.8.b) and the computed SAR was between 478 and 498 mm per year. The actual groundwater storage coefficient in that region was 9 to 11%.The computed SAR agrees with real fluctuation levels in the field (5.25 * 1000 mm * 0.09 = 472 mm, which agrees with the lower limit of the computed SAR).

6.5.2 Influence of cropping patterns on the amount of shallow aquifer recharge (SAR) available

The amount of shallow aquifer recharge (SAR) was evaluated using Eq. 6.5.6 for the study area's irrigation system with a high-yielding variety of rice (HYV-rice) as the crop. The average seasonal fluctuation of water table records was computed from field data and the actual amount of SAR matches the computed SAR values for the study area.

6.5.2.a Estimation of the amount of surplus volume (SUR) under rain-fed and irrigated HYV-rice growing conditions in the study area

It is well known that HYV-rice consumes more water than the normal, rain-fed, local rice variety. This study suggests that growing HYV-rice decreased the amount of surplus volume (SUR) and eventually the aquifer recharge (SAR)

decreased. The surplus volume (SUR) under both rain-fed rice cropping and irrigated HYV-rice cropping systems in the study area (SW zone of Bangladesh) was evaluated.

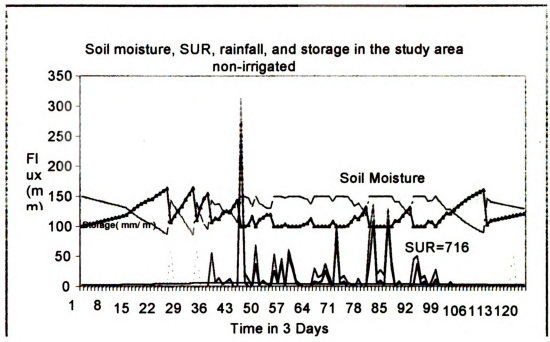

Fig. 6.9 Amount of SUR, rainfall and soil moisture balance under a rain-fed system in the SW zone of Bangladesh. The solid green line is rainfall and the blue line indicates the volume of SUR (716.26mm/yr).

HYV-rice and the amount of surplus SUR

The amount of surplus volume (SUR) was computed using the soil moisture balance. The results were presented in Appendix 4.6.4. The results indicate that growing HYV-rice decreases the amount of SUR in a system. The

amount of SUR computed with rain-fed local rice was equal to 716 mm/yr. (Fig. 6.9, Appendix. D), and the amount of SUR available under an HYV-rice irrigation system was 201 mm/yr. (Fig. 6.10, Appendix .C). The amount of SUR available under the HYV-rice irrigation system was about 72% less than that available under the rain-fed system.

The above findings show that growing crops demanding large amounts of water would reduce the amount of surplus volume (SUR). Eventually, the amount of aquifer recharge (SAR) available would be reduced in absence of any induced recharge source, and would lead to lowering of the water table. If there are no induced recharge sources (like floodwater or a river), the pumping rate (Q) must not exceed the amount of capture or ΔR_o in Eq. 6.5.4.

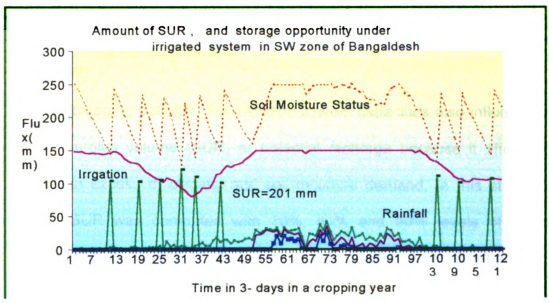

Fig. 6.10 Amount of SUR and soil moisture under an HYV-rice irrigation system. The blue line was the amount of SUR under the HYV-rice irrigated system.

6.5.3. Impact of irrigation system capacities on the potential recharge or surplus volume (SUR)

Irrigated rice, in particular, is a heavy consumer of water: Rice consumes 7650 m^3/ha and wheat consumes only 4,000 m^3/ha (David, 1995). As a general rule, a growing rice crop needs 10 millimeters of water a day. This is equivalent to 100 tons of water per hectare. To provide 1 hectare with supplementary water, a capacity of 166 liters per minute (44 US gallons per minute) is needed if operated 10 hours per day, or 70 liters per minute (18.6 gallons per minute) is needed if operated 24 hours per day. This means that the irrigation project system design capacity would be around 1.16 L/sec/ha for rice and 0.38 L/sec/ha.

6.5.3.a Design capacity of irrigation systems and its influence on surplus volume (SUR)

Like cropping patterns, the irrigation system capacities also influence the amount of surplus volume (SUR) or potential recharge because it affects the water level in excess of climatic and soil moisture demand. In this study, the amount of SUR was computed with 70%, 80% and 90% levels of system capacity. As shown in Fig. 6.11, the lowest system capacity level (70%) produced the highest amount of SUR available .It was very likely that if the supply were reduced, the balance would be reflected in the volume of SUR.

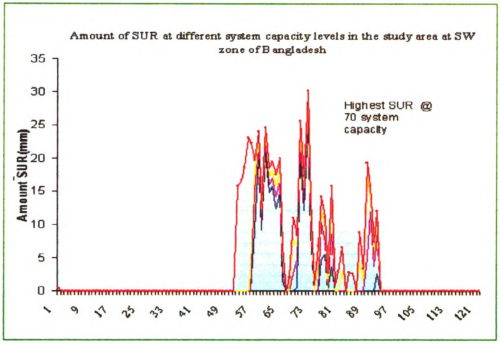

Fig. 6.11 Amount of SUR computed under different system capacity levels

What is the effect of system capacity reduction on the soil moisture balance and crop yield reduction?

Soil moisture status mainly depends upon the amount and frequency of rainfall in a n irrigation system. von Bernuth et al. (1984) investigated the relationship between soil moisture depletion and irrigation system capacity. Their results suggested that a system capacity existed above which no benefit was gained. This was known as the maximum useful system capacity. The maximum useful system capacity can be smaller or variable depending on the location and as a function of the probability of soil moisture depletion and yield reduction (von

Bernuth et al.,1984). As the irrigation system capacity is a management decision variable, the amount of SAR can be regulated through system control policy.

This demonstrates that adjusting the irrigation system capacity and cropping patterns could increase the volume of SUR or SAR. For example, growing two HYV-rice crops in a particular year reduces the available SUR to 48 mm/yr. from 211 mm/yr. when two years return period rainfall was considered (Table 6.5.1). By adjusting to crops with low water requirements, the amount of SUR can be increased.

Table 6.5. 1 Impact of cropping patterns on the amount of surplus volume

Cropping Pattern	3 Days Max (33 years)		3 Days Max (2 years return period)		3 Days Max (5 years return period)		Irrigation Withdrawal Requirement (mm)	
	Rain (mm)	SUR (mm)	Rain (mm)	SUR (mm)	Rain (mm)	SUR (mm)	33 years	2 years
Rain-fed local rice	1566	716	693	211	2481	1541	0	0
HYV Rice-HYV Rice	1566	201	693	48	2481	944	962	1632

Influence of induced recharge on water table elevation in the study area

An analysis of water table records of the study area shows that the water table level's fluctuation remained consistent (within 5 m) (Fig. 6.8.b) over the period from 1994 to 1999, despite a significant rise in the number of shallow wells to 0.62 million from 0.093 million in 1994 (Table 3.5). The number of shallow wells had increased by 58% but there was no evidence of significant decline in the water table position (Fig. 6.8). It is suggested that the study area must have been recharged by induced source such as seasonal floodwater.

It was shown (Eq. 6.5.4) that if the pumping rate (Q) increases without any change in storage volume (dv/dt), the excess water has to come from the new recharge source in order to keep the water table elevation constant. The amount of induced recharge helps maintain a consistent water table throughout the period. Now, it appears from the analysis that increasing the recharge rate (SAR) might have a significant influence on groundwater movement and the flow pattern and can increase the risk of arsenic migration into deeper layers.

6.5.4 Influence of SAR on groundwater movement, flow patterns, and likelihood of arsenic migration

The aquifer system in Bangladesh is complex in terms of sedimentological properties, both laterally and with depth. It is difficult and expensive to build a

hydrogeologic model that could incorporate all complexities to address the reality of the field conditions. However, in this study, a simple and uniform model (M-1), relatively complex models (M-2 & M-3) and a site-specific model were developed to reflect the reality of the field conditions of the study area.

Basic issues in groundwater modeling

In order to have a proper understanding of arsenic movement in the groundwater, one must understand the:

a) Influence of shallow aquifer recharge (SAR) on groundwater movement and flow patterns.

b) Influence of aquifer conductivity on downward flow through deeper layers

c) Variation in groundwater movements in response to natural groundwater flow conditions and extraction conditions

d) Impact of extraction or pumping on the depth of flow, flow patterns, dispersivity and likelihood of arsenic migration with moving water.

6.5.4.a. Influence of shallow aquifer recharge (SAR) on groundwater movement and flow patterns

This analysis was performed using the IGW-Groundwater modeling tools. Three types of conceptual models, M-1, M-2, and M-3 as previously described , were used to estimate the flow patterns and arsenic migration .

Influence of shallow aquifer recharge (SAR) on the groundwater flow pattern

Fig. 6.12 and Fig. 6.13, presented below, illustrate the simulated flow patterns obtained from the uniform model (M-1). These figures were examined to comprehend the influence of the aquifer recharge (SAR) rate on groundwater flow patterns. Basically, it gave an indication of how groundwater typically moves. It was found from the model simulation that doubling or halving the amount of aquifer recharge (SAR) had little or no impact on the groundwater flow patterns in homogeneous, uniform model M-1 (Fig. 6.12).

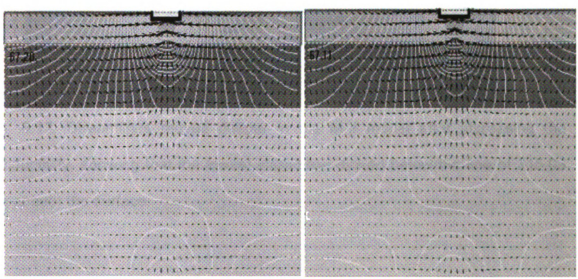

SAR=381 mm/yr. SAR=762 mm/yr.

Fig. 6.12. Doubling and halving the amount of aquifer recharge (SAR) in the uniform (M-1) model had little or no impact on the groundwater flow pattern.

However, when the conductivity at the lower shallow aquifer (L_2) in the M-2 model was increased to 50 m/day from 15 m/day, the streamlines moved deeper, just below the 315.03 level (Fig.6.13).

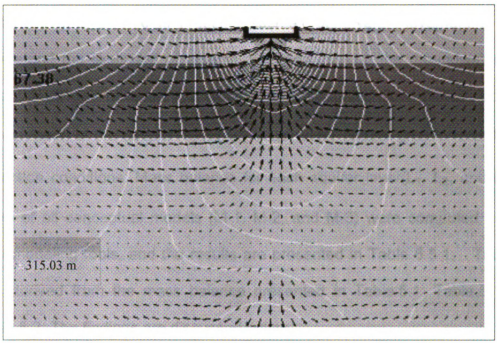

Fig. 6.13. Streamlines moved deeper in the M-2 model after increasing the conductivity, showing that the lowest streamline moved below the line of 315.03 m beneath the surface.

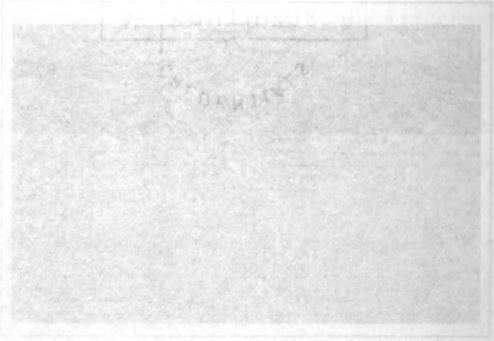

6.5.4.b. Influence of aquifer conductivity and the aquifer recharge rate (SAR) on the downward flow through deeper layers

Increasing conductivity drew water to the deeper layers (Fig. 6.13). It is a great concern in Bangladesh that presently uncontaminated layers may be contaminated by arsenic as a result of such a groundwater movement. In order to understand the likelihood of arsenic migration through the groundwater due to extraction, it was necessary to estimate the amount of flow passing downward through each of the deeper layers (L_2 & L_3) under natural groundwater flow and extraction conditions. Mass balance for each aquifer layer(L_1, L_2, and L_3) (Fig. 5.2.c) of all conceptual models (M-1, M-2, and M-3) were computed using the IGW modeling tools, and the results are presented in Table 6.5.1. Table.6.5.2 was derived from the mass balance presented in Table.5.1, Table.5.1.a, and Table.5.2. The findings are discussed below.

Model finding 1

Increasing the conductivity of deeper layers increases the downward flow rate through the deeper layers.

Simulation result of model M-2

The three-layer model (M-2) reflects a condition in which the upper shallow layer (L_1, K_1= 15) and deeper layer (L_3, K_3 = 15) were significantly less permeable than

the middle layer (L_2, K_2 = 50 m/day). This results in an increase in downward flow to the middle layer (L_2) to 15.12% under pumped conditions from 12.82% in the M-2 model under natural flow conditions (Col. 3, Table 6.5.2). This is due to the increase in conductivity of L_2 from 15 m/day to 50 m/day in M-2 model.

Simulation result of model-M-3

The conceptual model M-3 was characterized to incorporate the second condition, which reflected the upper fining sequence of aquifer system, $K_3>K_2>K_1$. The simulation results indicate that increasing the conductivity of deeper aquifer layers (in model M-3) drew more water to the deeper aquifer L_3 and L_2 under both natural flow (Col. 7, Table 5.2) and pumped conditions (Col. 7, Table 5.3).

Vertical flow of water in the deeper aquifer layer (L_3) under natural flow conditions was increased from 4.71 to 11.79% (Col. 3, Table 6.5.2). This indicates that the more highly conductive layers (L_2 & L_3) in the M-3 model drew water deeper into the aquifer under natural flow and pumped conditions.

It was found from the mass balance results presented in Table 5.2 that the downward flow (with aquifer recharge rate SAR=381 mm/yr.) passing through aquifer layers L_2 and L_3 (in model M-3) under natural flow conditions were 350 and 230 m^3/day respectively (shown in Col. 4, Table 5.2). Whatever amount of

water came as inflow to aquifer layers L_2 and L_3 (Col. 4, Table 5.2), passed vertically downward as "flow from top to bottom" at the same rate of 350 or 230 m^3/day (Col. 9, Table 5.2). The percentages of flow through each layer were computed as 17.94% (350 / 1950 * 100 = 17.94%) and 11.79% (230 / 1950 * 100 = 11.79%), respectively (Col. 3 of Table 6.5.2).

These results clearly demonstrate that higher conductivity drew water to the deeper layers in model M-3 under pumped and un-pumped conditions. It implies that upper fining sequential aquifers (M-3) are subjected to a higher risk of arsenic migration than the type of aquifer represented by M-2, because arsenic can migrate more with groundwater moving from currently contaminated layers to uncontaminated layers.

6.5.4.c. Groundwater movement variations under natural groundwater flow conditions and extraction conditions

The mass balance results presented in Table 5.1.a and Table 5.3 were used to estimate the components of flows passing through the deeper layers (L_2 and L_3) of the M-1 and M-3 models at a pumping rate of Q = 5000 m^3/day. While comparing Table 5.2 and Table 5.3, it was evident in Col. 4 and Col. 9 that the amount of flow passing downward through the aquifer layers (L_2 and L_3) in Table 5.3 was significantly higher under the influence of extraction in the M-3 model. This finding requires further investigation.

Finding 2

Extraction influences the groundwater flow dynamics in the following two areas:

1) Flow between the river and the aquifer system, and

2) Downward flow through the deeper layers

Flow between the river and the aquifer system

Comparing the simulation as run with and without the extraction rate (Col. 4 and Col. 9, Table 5.2 & Table 5.3) clearly demonstrates that

- Pumping increases the flow from the river to the aquifer when the shallow aquifer recharge (SAR) is less than the extraction rate (Q)
- Pumping decreases the flow rate from river to the aquifer system when the SAR rate is greater than the extraction rate (Q)

Under pumped or extraction conditions, the reason for increased groundwater flow from the river to the aquifer was that flow to the well required more water (5000 m^3/day) than was available from recharge (at a SAR = 381 mm/yr., the total amount of SAR was 1950 m^3/day for an area of 1.95 km^2).

Influence of extraction on downward flow through deeper layers

- Extraction generally increases the flow through deeper layers more than natural flow conditions (Table 6.5.2).

- Extraction increased the flow rate through deeper layers when the pumping rate (Q) was greater than the aquifer recharge rate (SAR).

For example, without extraction, water flow from the river to the aquifer in L_2 and L_3 was 350 and 230 m^3/day (Col. 4, Table.5.2), whereas, with extraction, the flow in L_2 and L_3 were 1700 and 1900 m^3/day, respectively (Col. 4, Table 5.3).

- Extraction proportionately decreased the flow rate through the deeper layers when aquifer recharge (SAR) rates were increased.

What happened when the extraction rate (Q) was less than the SAR?

It was found in the simulation results of model M-3 (Table 5.3) that when the extraction rate (Q = 5000 m^3/day) was less than the amount available from aquifer recharge (Col. 5, Table 5.3, SAR of 1000 mm/yr. = 5180 m^3/day for the mass balance area of 1.95 km^2), the flow from the river to the aquifer system decreased. Also, the amount of downward flow through L_2 and L_3 was proportionately decreased (Col. 9, Table 5.2).

For example, it was shown in the mass balance computation (Col. 4, Table 5.3) that when SAR=1000 mm/yr., the downward water flow rate through L_2 was 620 m^3/day, whereas the flow from the river through L_2 to the aquifer was 1700 m^3/day when the SAR=381mm/yr.

Why the increased aquifer recharge (SAR) rate decreased the downward flow rate and flow from river to the aquifer

Finding 3

The more the pumped-water share comes from the recharge source (SAR) or leakage, the less water flows from the river to the aquifer system. That condition leads to a proportionate decrease in the amount of downward flow through the deeper layers. However, in general, extraction conditions increased the downward flow to a rate higher than that of natural groundwater flow conditions (Table 6.5.2).

M-1 model simulation results

Simulation of the uniform homogeneous conductivity model (M-1), the results of which are presented in Col. 3, Table 6.5.2, indicates that the lower shallow aquifer layer (L_2) and deeper aquifer layer (L_3) receive 12.82% and 4.71% of total flow, respectively, under natural flow conditions. Under extraction conditions, with average recharge rate (SAR) equal to 381 mm, the vertical flow through L_2 and L_3 were increased to 18% (Col. 4, Table 6.5.2).

Model M-3 simulation results

Extraction also increases the downward flow through the deeper layer at L_3 .The percentage of flow increased to 38% (Col. 4, Table 6.5.2) from 11.79% (Col. 3, Table 6.5.2). The share of groundwater flow through the deeper layers is presented in Table 5.3. While comparing Table 5.3 (Col. 9) with Table 5.2 (Col. 9), it was evident that "flow from top to bottom" increased significantly under abstraction.

Finding 4

Under natural groundwater flow conditions, increasing the aquifer recharge rate (SAR) increases the downward flow through the deeper aquifer layers (L_2 & L_3) in models M-1, M-2 and M-3.

The simulation results presented in Table 6.5.2 indicate that increasing the average recharge rate (SAR) from 381 to 625 mm/yr. increases the vertical flow through the lower shallow aquifer (L_2) and deeper aquifer layer (L_3) under natural flow conditions in models M-1, M-2 and M-3 (comparing Col. 3 & Col. 5 in Table 6.5.2). Flow through L_2 and L_3 in model M-1 was increased to 15.21% from 12.82%, and in model M-2, in the same layer L_2, flow increased from 15.12 to 20.96% (Table 6.5.2).

Finding 5

- The vertical hydraulic gradient and local hydraulic gradient were also changed due to the influence of extraction.
- Extractions significantly changed the flow pattern in the groundwater system. When the pumping rate Q is more than the SAR rate, groundwater flows from the river to the aquifer, changing the local hydraulic gradient.

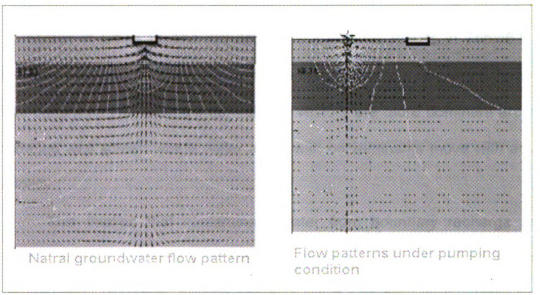

Fig. 6.14. Contrasting groundwater flow patterns between un-pumped (left side)and pumped conditions(right side)

Why pumping at a rate greater than that of shallow aquifer recharge (SAR) increases the risk of arsenic migration

The mass balance records of 3-D models indicate that pumping at a rate greater than the SAR increases flow from the river to the aquifer in order to

maintain pumping rate Q. This is also supported by the one-dimensional model analysis presented in Chapter 5.1.1. It was shown that when the ratio of the partial discharge (Q_3/Q_t in Fig. 5.1.b) is decreased, part of the pumped water Q_t comes from the boundary recharge sources from top layer L_1. When the aquitard thickness (b') is less and Q_3/Q_t is near zero, the contaminant concentrations in pumped water (C_t) becomes equal to the concentration of water in layer L_1, C_1 (as shown in Eq. 5.1). The simulated mass balance results in Table6.5.2 also demonstrated that pumping can increase the vertical flow rate more than natural flow condition. The groundwater velocity vectors are more dominant around the pumping well screen where water along with contaminants move with advective velocity.

This implies that contaminant water from boundary recharge sources moves through the layers to the well screens with the velocity of moving groundwater. Therefore, arsenic can also move with advective velocity from the contaminated upper layers to the uncontaminated deeper layers during heavy pumping. This will certainly increase the risk of arsenic migration.

Table 6.5.2 Percentage of total flow associated with each layer in the geological cross section of the conceptual model.

Types of Conceptual Models and Aquifer Depth (m)		**Flow from the surface through the layers**			
		Average Recharge (381 mm)		Medium Recharge (625 mm)	
		Natural flow conditions	Pumped conditions	Natural flow conditions	Pumped conditions
Model (1)	Layer (2)	% of total flow (3)	% of total flow (4)	% of total flow (5)	% of total flow (6)
M-1	L_1(0-40m)	100	``	100	100
	L_2 (40-140)	12.82	18	15.21	16.4
	L_3 (140-400)	4.71	18	5.81	18.6
M-2	L_1 (0-40m)	100	100	100	100
	L_2 (40-140)	15.12	27.4	20.96	18.66
	L_3 (140-400)	1.91	1.12	3.22	8.41
M-3	L_1 (0-40m)	100	100	100	100
	L_2 (40-140)	17.94	34	0.4	28.4
	L_3(140-400)	11.79	38	2	34.4

6.5.4.d. Influence of aquifer pumping and dispersivity on the vertical migration of arsenic

Migration of arsenic is influenced by the factors controlling the downward flow of groundwater. Downward flow of arsenic is influenced by the aquifer recharge rate (SAR), depth of well screens and the aquifer conductivity, dispersivity and distribution coefficient (K_d). The influence of the pumping rate on

arsenic dispersion and arsenic migration in particulate form in the no-flow boundary zone (Fig. 5.15) was analyzed.

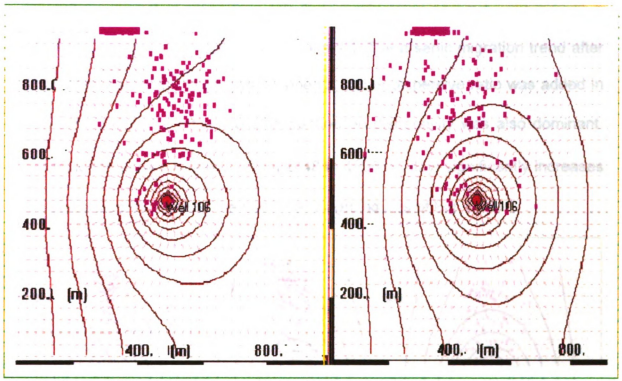

Fig. 6.15. Arsenic dispersion after 8400 days with pumping rate of 2448 m^3/day (left) and after 4250 days with 4896 m^3/day pumping rate (right).

Finding 6

Influence of extraction on arsenic migration

The above figure (Fig. 6.15) shows that arsenic migration is significantly influenced when the pumping rate (Q) is doubled (from 2448 to 4896 m^3/day) while keeping the lateral and transverse dispersion ratio (D_L/D_T =5) the same .

Influence of dispersion ratio on arsenic migration

The figure below (Fig. 6.16, middle and left) clearly demonstrates the impact on arsenic movement of increasing the dispersivity ratio(D_L/D_T) from zero to 5 when the extraction rate (Q) remains constant. The arsenic migration trend after 5000 days was found to be greater when a higher dispersive ratio was added in Fig. 5.7 (D_L/D_T =5). Influence of extraction on dispersivity was also dominant. Doubling the pumping rate Q (from 2448 to 4896 m^3/day) significantly increases the dispersion (comparing the middle and right figures of Fig. 6.16).

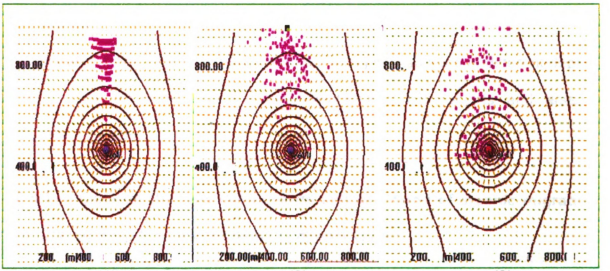

(1) (2) (3)

(1) D_L/D_T=0, Q=2448m^3/day

(2) D_L/D_T =5, Q=2448 m^3/day

(3) D_L/D_T =5, Q=4896m^3/day

Fig. 6.16. Influence of dispersivity ratio (D_L/D_T) and extraction rate (Q) on arsenic migration as a particle

6.6 Placing of tube wells screens in the deeper layers and its influence on arsenic movement from contaminated layers to the uncontaminated layers.

Research issue:

The sixth research issue of this study was to understand the impact of placing deep tube well screens at the deeper layers of the aquifer.

Strategic questions:

1. What is the impact on the components of groundwater flow in the mass balance and arsenic migration processes when placing deep tube well screens at deeper layers?

It appeared from the field experience that placing well screens at different depths might have an impact on the groundwater flow components and arsenic migration process.

6.6.1 Impact on the flow components and likelihood of arsenic migration of placing deep tube well screens at deeper layers

This issue was investigated from the computation of mass balance results presented in Table 5.4 and Table 5.5. It was necessary to analyze the components of groundwater flow and local groundwater gradients to the river to address the issue of arsenic migration in the aquifer. The results of placing well screens at different aquifer layers [L_1 (-25 to –35 m), L_2 (-100 to 120 m) and L_3 (-

300 to –320m)] of the uniform M-1 and complex site-specific models were evaluated.

Installation of wells at L_3 indicates that a significant amount of water was drawn from the river (Col. 7 of model M-3 in Table 6.6.1). While comparing the mass balance in Table 5.5 (for model M-2) and Table 5.5.a (for model M-3), it was evident that the M-3 model drew more water into the deeper layers (Col. 9, Table 5.5.a). Flow through the vertical layer was increased more in the M-3 model when aquifer sediments were more transmissive (in M-3 and M-2, in Col. 9 of Table 6.6.1). Therefore, it is very likely that the placing of a tube well screen at the deeper layer (L_3) of the study area aquifer would result in increased flow to the deeper layers, and with this moving groundwater, arsenic could migrate by the advection process. Therefore, placing well screens at deeper layers will increase the risk of arsenic migration from the currently contaminated layers to the uncontaminated layers.

Table 6.6.1 Computation of mass balance when well screens are placed at different layers with recharge rate of 635 mm/Yr.

(1) Model	(2) Well Placed at L_3	(3) Layer	Inflows and Outflows from Different Vertical Layers of Model M-3 When a Well-Screen Was Placed at the 3rd layer (L_3)							
			Flow in (m^3/day)				Flow out (m^3/day)			
			(4) Body in (m^3/day)	(5) Recharge (m^3/day)	(6) From Top to Bottom	(7) Total	(8) Body Out (m^3/day)	(9) From Top to Bottom	(10) Well Out	(11) Total (m^3/day)
M-3 K1=15 K2=50 K3=100	Layer-3 (-300 to -320 m)	L_1	1750	3250	-	5000	-	-	5000	5000
		L_2	1400	-	-	1400	-	1400	-	1400
		L_3	1730	-	-	1730	-	1730	-	1730

Conclusion

The overall conclusions are that irrigation wells with realistic extraction rates significantly and beneficially affect the flow patterns within the groundwater system. The aquifer recharge rate (SAR) also significantly induces groundwater movement and flow patterns. Extraction also significantly changed the groundwater movement and flow patterns. Placing deep tube well screens at deeper layers is not a safe approach to obtaining arsenic-free water

6.7. Administrative and management decision variables to reduce the risk of arsenic concentration in the case of further irrigation development

The seventh research issue in this study is to identify the management decision variables that can help reduce further risk of arsenic contamination in the case of groundwater irrigation development policy. There are management decision variables such as the irrigation system capacity, cropping patterns, rainwater harvesting, and soil-based arsenic-contaminated water treatment systems can help improve the availability of shallow aquifer recharge (SAR) in groundwater.

Strategic questions

1. How can irrigation system capacity reduction and adjustments in cropping patterns or seasons help increase the amount of aquifer recharge in the groundwater system?

2. How can rainwater harvesting and soil-based arsenic-contaminated groundwater treatment systems be used to reduce the risk of contamination?

6.7.1 How irrigation system capacity reduction and adjustments in cropping patterns or seasons can help increase the amount of aquifer recharge

The impact of irrigation system capacity reduction on the amount of shallow aquifer recharge available is discussed in section 6.5.3.a. Decreasing the irrigation system capacity can increase the availability of amount of SAR but it is a trade-off between yield reduction and increasing SAR.

Section 6.5.2 describes the influence of cropping patterns on the amount of SAR available. The amount of SUR available with rain-fed rice (no-pumping condition) was equal to 716 mm/yr. (Appendix D and Fig.6.9) using 33 years of average rainfall data. But when intensive HYV-rice were grown in two seasons throughout the study area, the amount of SUR was decreased from 716 to 201 mm (Appendix C, Fig. 6.10) which is about 71% less than the rain-fed condition.

This section will graphically investigate how adjusting the cropping season can help to increase SAR availability in the field.

By adjusting the cropping season, the irrigation withdrawal (Q) could be reduced from 791 to 250 mm in Kharif-1 season

By adjustment in the cropping patterns (introducing crops with low water requirements in cropping seasons Rabi, Kharif-1 and Kharif-2, starting the transplanting date earlier in the Kharif-1 season (Fig. 6.17), and maximizing the use of monsoon rainfall) , the irrigation withdrawal volume for rice can be reduced from 791 to 250 mm in the Kharif-1 season (without land preparation).

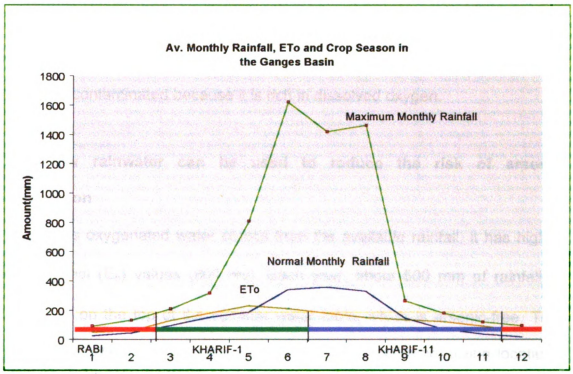

Fig. 6.17 By adjusting the cropping season and cropping patterns, the best use of rainfall can save 500 mm of pumping in a year

Therefore, by introducing crops with low water demands, 541 mm of water could be saved, and that would eventually contribute to groundwater and cause a rise

in the water table. Equation 6.5.6 indicates that, when SUR is less, outflow would be greater, and when pumpage (Q) is greater, the amount of shallow aquifer recharge (SAR) required is also higher.

6.7.2. How rainwater harvesting and soil-based arsenic-contaminated groundwater treatment systems can be used to reduce the risk of contamination

It is evident in Fig. 4.5 and the discussions in section 6.2.1 that the redox potential values decrease with depth. But the upper 0 to 10 m layer is relatively less arsenic contaminated because it is rich in dissolved oxygen.

6.7.2.1 How rainwater can be used to reduce the risk of arsenic contamination

As this oxygenated water comes from the available rainfall, it has higher redox potential (E_h) values (800 mv). Each year, about 500 mm of rainfall is accumulated on the top of the summer water table, which is arsenic-free. This 500 mm of rainwater can develop a 4 to 5 m water table head, giving locations for small-scale pumps or wells to be placed to obtain arsenic-free water.

Therefore, aquifer delineation is extremely important in terms of the supply of safe irrigation and drinking water. It is strongly suggested that the top 10 m of the aquifer be kept for installation of small scale dug wells or hand tube wells in order to ensure a long-term supply of arsenic-free water (Fig. 6.18). The upper

layer receives rainwater, which is high in redox potential values and should be safe for drinking; extraction for irrigation must be restricted.

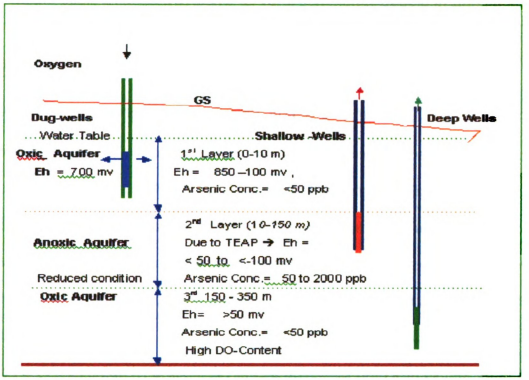

Fig. 6.18 Aquifer delineation for long-term supply of arsenic-free, safe water on the basis of redox potential values (E_h)

6.7.2.2 How soil-based arsenic-contaminated groundwater can be used to use for irrigation to reduce the risk of further arsenic contamination

With presently available technologies, contaminated water can be treated up to any trace amount. However, the low-cost arsenic removal techniques are still limited by their inability to completely remove residual As (III) from water. Adding external chemical oxidants sometimes degrades the water quality.

Therefore, this study presents two low-cost techniques as soil-based treatment systems that make use of locally available materials. These are small-scale and medium-scale treatment systems for rural community people in Bangladesh.

Arsenic-contaminated groundwater in Bangladesh is rich in dissolved iron content. Mixing of arsenic-contaminated groundwater with atmospheric oxygen would easily oxidize the dissolved iron (Fe^{2+}) to Fe $(OH)_3$ within about 20 minutes. Under this oxic condition, dissolved arsenic (V) species will be adsorbed onto iron oxides but As (III) will remain in the water in dissolved form because dissolved oxygen has no effect on the oxidation rate of As (III) (Scott and Morgan, 1995). The contaminated water will then pass through a filter bed made of low-cost ferruginous manganese ore (FMO). In order to decrease the detention time, "t", the FMO will be used to chemically oxidize the residual As (III) to As (V). Eventually, arsenic (V) will be adsorbed onto iron oxides. After laterally flowing through the filter bed, the arsenic content in effluent water will fall below the level of 10 ppb.

How does the system work?

The velocity head can easily be used to mix oxygen with contaminated water. The aerated, oxygenated water will help to form a coating of iron oxides around the sand particles and create a surface of metallic cations. Anions of arsenate (As (V)) are less mobile and stable in high oxic conditions, so they will tend to co-precipitate with metallic cations of iron oxides. Then the contaminated water will pass through the filter bed containing FMO and local river sands. The

residual arsenic (III) would be oxidized to arsenic (V) followed by adsorption on to Iron oxides. After filtration through FMO and local sands, eventually arsenic concentration will be reduced below the level recommended by the WHO (<50 ppb)

Shallow tube well-based and Subsurface Flow (SF) constructed wetland based arsenic treatment systems

In this study, two different approaches are considered for low-cost arsenic removal techniques. The shallow tube well based treatment system is for small-scale community levels and the Subsurface Flow (SF) constructed wetland system is for medium-scale communities. The design procedure is described below.

Shallow tube well-based arsenic treatment system

In order to keep the system cost low, the shallow tube well-based arsenic treatment system was considered because it is most available source of cheap energy, as well as a potential source of arsenic-contaminated water.

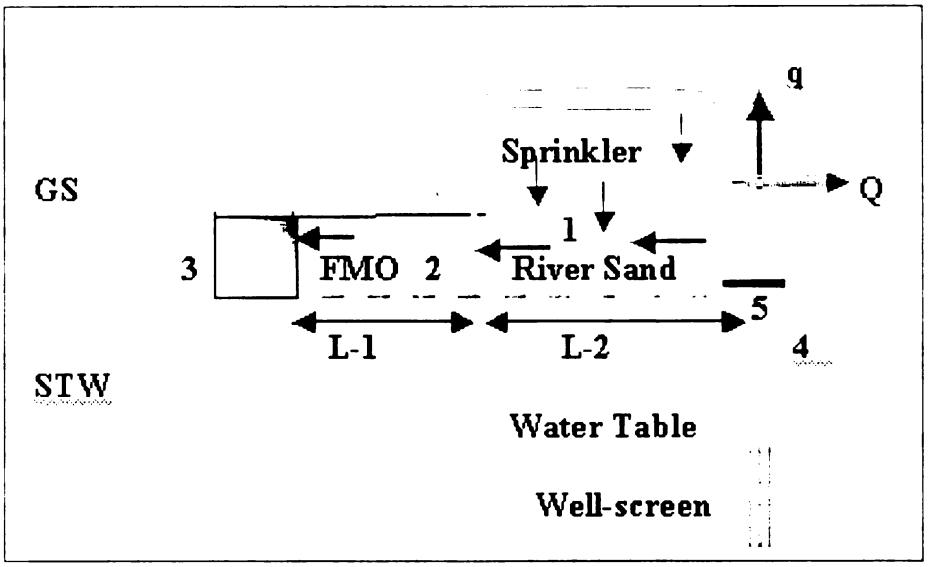

Fig. 6.19 Shallow tube well-based groundwater arsenic treatment system using locally available materials

Soil-based Subsurface–Flow (SF) constructed wetland systems for arsenic treatment

Constructed wetland systems have been popular in removing contaminants from wastewater. Generally two types of constructed wetlands are known to be developed, Free Water Surface (FWS) and Subsurface Flow (SF) constructed wetland systems (Crites et al., 1998).

Depending on topography and the availability of local materials, the SF-constructed wetland systems could be efficiently designed to accelerate the arsenic removal rate from contaminated groundwater at a low cost. The main advantage of SF–constructed wetlands is that they do increase the residual arsenic (III) removal process without adding chemical oxidants (Fig. 6.20).

Introducing aquatic weeds or bioremediation plants can also manage inorganic arsenic biologically.

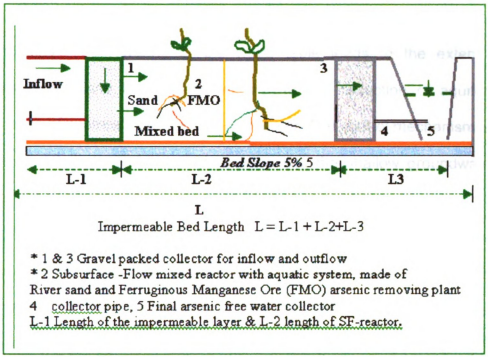

Fig. 6.20 Subsurface-Flow constructed wetland system for treating arsenic-contaminated groundwater

7. SUMMARY

This study began with several hypotheses that were based on the idea that less oxygenated water at and below the water table leads to more anoxic conditions. The lowering of the water table leads to the extension of the unsaturated zone by irrigation withdrawal and reduction of aquifer recharge because of upstream diversion of river water. The control mechanism is the lower rate of diffusion of atmospheric oxygen into the shallow groundwater and the shortage of oxygenated water in aquifer recharge.

The main objective of this study was to understand the factors that produce high levels of arsenic in Bangladesh's groundwater and to formulate a quantitative irrigation development policy so that the present pace of irrigation development could be sustained without any further risk.

This study addressed the following issues: (1) high arsenic concentration distribution and its association with geohydrologic factors; (2) interaction between lowering of the water table, the amount of dissolved oxygen (DO) available in recharging groundwater, and arsenic concentration variation over the aquifer's depths; (3) evaluation of the present theories of arsenic release; (4) the influence of the irrigation withdrawal rate and cropping systems on the amount of shallow aquifer recharge available; (5) the influence of extraction rate (Q) and shallow aquifer recharge (SAR) on groundwater movement, flow patterns, and the likelihood of arsenic migration; and (6) the impact of placing deep tube well screens at deeper layers and increasing the risk of arsenic migration to the

deeper layers of Bangladesh's groundwater. Finally, this study presents the findings and recommends administrative decision variables for quantitative irrigation development policy.

The relationship between high arsenic concentration distribution and associated geohydrologic factors.

In order to establish a relationship between high arsenic concentration and associated hydrogeologic parameters, analyses of the probability of arsenic concentrations exceeding threshold levels (50 ppb) were done initially, and the results were presented in Table 4.2.1 and pictured in Fig. 4.2.b. The southeast (SE) and southwest (SW) zones were the most arsenic-affected areas, in which the probability of arsenic exceeding threshold levels (50 ppb and 250 ppb) were found to be 71.4% and 59.55%, respectively (Table 4.2.1).

<u>High arsenic concentration distribution and its relationships with surface geology and physiography</u>

Surface geological map analysis demonstrated that the most arsenic-contaminated area was mostly confined to the lower delta flood plains of the river Ganges, which comprised the southwest (SW) region, and the Meghna River Flood Plain (FP), which built up the southeast (SE) region of Bangladesh (Fig. 4.3.a and Fig. 4.2.b). The surface geology of the SE and SW regions was alluvial deposits and deltaic deposits respectively (Table 4.2.2 and Fig. 4.2.a).

The least arsenic-contaminated zones are the northwest (NW) and north-center (NC) areas (Fig. 4.2.b) where the geomorphology is comprised of Old

Himalayan Fan, Tista-Jamuna Floodplains, and Madhupur Tract (Table 4.2.2 and Fig. 4.3.a). Arsenic concentrations in the SW and SE zones were found to be greater than those in the NW and NC regions because arsenic was inherited in the sediments of that region through the development of different geomorphological processes.

The physiographic map analysis in Fig. 4.3.b clearly indicates that high arsenic concentration levels (>250 to 1665 ppb) were mostly confined to the SE region where the physiographic unit was dominated by Tippera surface (Fig. 4.3.b and Table 4.2.2).

High arsenic concentrations offered a good correlation with dissolved iron content

Grids 5, 9, 10, 12, and 15 show the highest arsenic concentration, with R^2 values between 71% and 99% (Table 4.2.4). The confidence interval associated with these R^2 values is 95%. All of the highest arsenic contaminated areas belong to the SW and SE zones.

Arsenic concentrations increase with increasing aquifer depth from 9 to 30 m

The spatial variations of arsenic concentration distribution were analyzed using about 3500 arsenic-contaminated wells' water quality data (collected by BGS). The results indicate that the distributions of arsenic concentrations above the threshold level (>50 ppb) are mostly located between 15 m and 150 m below the surface (Fig. 4.5). Further depth analysis demonstrated that arsenic concentrations are found to increase over the depth ranging from 9 m to 30 m

below the ground surface (Fig. 6.2.a) and the correlation between arsenic concentration and depth are found to be positive (R^2=60%) (Fig. 6.2.a).

Arsenic concentrations decrease with depth from 100 m to 350 m

Arsenic concentrations decrease with depth from 100 m to 350 m below the ground (R^2=72%, Fig. 6.2.b). Arsenic concentration records at the top-most layer (within the depth ranging from 0 to 10 m) did not show any relationship with depth. The spatial variations in arsenic concentration distribution over these depths were investigated in the context of thermodynamics. The field redox potential values were computed to be within the range of 2.09 to –1.82 and are presented in Table 4.4.1.

Redox potential (p^e) values decreased linearly over aquifer depths ranging from 9 m to 30 m below the ground

The redox potential values at each depth were computed and a relationship between redox potential values and aquifer depths (Fig. 6.3.a and 6.3.b) was found. Fig. 6.3.a indicates that the redox potential values decreased linearly with increasing aquifer depth from 10 m to 30 m below the ground. On the contrary, redox potential values increase in the deeper aquifer depths ranging from 150 to 350 m (Fig. 6.3.b) and arsenic concentration values decrease below 50 ppb.

Evaluation of existing theories of arsenic release

The experts' opinions are still diverging, and there are considerable difficulties in diagnosing this problem. Proponents of oxidation theory argue that

the lowering of the water table provides atmospheric oxygen access to oxidize the arsenic-rich pyrites and eventually arsenic is released into the groundwater as desorption from iron oxides. The proponents of reduction theory believe that organic carbon takes oxygen from iron hydroxides through reductive dissolution and eventually arsenic is released.

However, the hypothesis presented in this study is in complete disagreement with the oxidation theory and partial agreement with the oxyhydroxide reduction theory of arsenic release .The hypothesis presented here states that the shortage of dissolved oxygen in the recharging groundwater is the cause of arsenic release, whereas the oxidation theory blames the exposure of arsenic rich pyrite layers to atmospheric oxygen. In addition to this, there are several vital questions that must be answered.

The critical difference between the reduction theory and hypothesis offered in this study

The reduction theory also has shortcomings. Investigators questioned why arsenic contamination was a recent phenomenon if organic carbon has been taking oxygen from iron oxides for thousands of years. Why there was not any prior report of arsenic toxicity in Bangladesh?

Like the reduction theory of arsenic release, this study indicates that arsenic is released due to development of a reducing condition. But this study does not support explanations that microbial activities derive organic carbon to remove oxygen from the iron hydroxides, releasing arsenic. Rather, this study

investigated the shortage of dissolved oxygen in the recharging water.

Lack of dissolved oxygen and / or shortage of oxygenated recharging water at and below the water table as the major cause of arsenic release in Bangladesh

This study analyzed both thermodynamic and numerical models to support the hypothesis that shortage of dissolved oxygen in the recharging groundwater is the major cause of arsenic release. Finite element simulation results show that lowering of the water table cannot increase the oxygen diffusion rate in the deeper layer of the aquifer.

Oxygen concentrations decrease with increasing aquifer depths

Analysis of the oxygen diffusion model (Table 4.3.2) suggested that oxygen concentration decreases with increasing aquifer depths (Figs. 4.11, 4.12, and 6.4). It is evident (in Fig. 6.2.a) that arsenic concentration increases with increasing depth (9 to 30 m), and the redox potential values (p^e) decrease (Fig. 6.3.a). This is due to a low oxygen supply (over the depth of 9 to 30 m below the ground) that reduces the redox potential values.

Finite element analysis of oxygen diffusion model does not support the oxidation theory

The results presented in Table 4.3.2 show that the diffusive supply of oxygen in arsenic-rich pyrite layer L_6 is decreased from 2.391 to 1.235 mg/L when the water table lowered from 2 m to 5 m below the ground surface

(Table.4.3.2). This analysis clearly demonstrates that lowering of the water table cannot accelerate arsenic-rich pyretic layer oxidation, as the dissolved oxygen content in recharging water is decreasing.

Influence of aquifer thickness (b') and conductivity on the arsenic concentration of water entering a well

It appears from the concentration model analysis (Fig. 5.1.b and Fig. 6.8.a) that the arsenic concentration of water entering a well varied inversely with the thickness of the aquifer. After increasing the aquifer thickness from 65 to 100 ft while keeping the vertical conductivity the same at 1.18 ft./day, the arsenic concentration in the water entering the well was decreased from 85 to 76 ppb (Fig. 6.8.a, curve b and c). A 54% increase in aquifer depth decreases the arsenic concentration of the well water by 8%.

The arsenic concentration in a well's water varies directly with the vertical conductivity of the aquifer. It was shown that a ten-fold increase in the conductivity value of the aquifer produced a 26% rise in the arsenic concentration of the well water.

The finite element oxygen diffusion model (Table 4.3.2) and concentration model (Fig. 6.8.a) simulation results suggested that the pyrite oxidation theory is not applicable to explain the arsenic release mechanism in the groundwater of Bangladesh.

Irrigation system capacity and planting high yielding rice varieties (HYV–rice) significantly influence the availability of shallow aquifer recharge (SAR) and potential recharge and increase the risk of arsenic migration

The amount of surplus water (SUR) and shallow aquifer recharge (SAR) water available were discussed. The virgin amount of SAR was computed as 281 mm/yr. (Section 4.5.2 and Appendix B) and under pumping conditions, the amount of SAR was computed to be in the range of 471 to 498 mm/yr. (Section 4.5.3).

Growing HYV-Rice decreases the surplus volume (SUR) by 71%

The amount of surplus volume (SUR) available was computed using the soil moisture balance. The results indicate that the amount of SUR is decreased when HYV-rice is grown. The amount of SUR available with rain-fed rice (no-pumping condition) was equal to 716 mm/yr. (Appendix D and Fig. 6.9) using 33 years of average rainfall data. But when intensive HYV-rice was grown in two seasons throughout the study area, the amount of SUR was decreased from 716 to 201 mm (Appendix C, Fig. 6.10), which is about 71% less than the rain-fed condition.

In addition to that, the irrigation requirement of HYV-rice without land preparation was computed as 637 mm. Under the improved management practice, this requirement could be reduced to 433 mm. It was shown that, by adjusting the growing season or making use of monsoon rain, the groundwater withdrawal rate (Q) could be significantly reduced.

By adjusting the cropping season, the irrigation withdrawal (Q) could be reduced from 791 to 250 mm in Kharif-1 season

By adjusting the cropping pattern, the irrigation withdrawal volume can be reduced from 791 to 250 mm in the Kharif-1 season. Therefore, by introducing crops with low water demands, 541 mm of water could be saved, which would eventually contribute to groundwater and cause the water table to rise. Equation 6.5.6 indicates that, when the SUR is smaller, outflow is greater. When the pumpage (Q) is greater, the amount of shallow aquifer recharge (SAR) to be required is also higher. This excess water for SAR has to come from an induced recharge source or from storage volume (dv/dt). If there is no induced recharge source, water comes from storage and eventually the water table drops. If irrigation development continues without developing new recharge sources, the water table will rapidly fall. If there is an induced recharge source, however, the amount of SAR will increase.

Design capacity of irrigation system and its influence on surplus volume (SUR)

Like cropping patterns, the system capacities also influenced the amount of SUR or potential recharge. In this study, the amount of SUR was computed with a 70%, 80% and 90% level of system capacity. It was evident in Fig. 6.11 that the lowest system capacity level (70%) produced the highest amount of SUR available after less than 3 day's maximum rainfall.

Influence of induced recharge on water table elevation in the study area

Analysis of the study area's water table fluctuation records in Fig. 6.8.b shows that fluctuation of the water table remained consistent (within 5 m) over the period from 1994 to 1999, despite there being a significant rise in the number of shallow wells to 0.62 million from 0.093 million in 1994 (Table 3.5). The number of shallow wells had increased by 58% but there was no evidence of significant decline in water table position (Fig. 6.8.b). This suggests that the study area must have been recharged by an induced source like seasonal floodwater.

Influence of shallow aquifer recharge (SAR) and conductivity on the groundwater flow pattern

It was found from simulation that doubling or halving the amount of aquifer recharge (SAR) had little or no impact on the groundwater flow patterns in homogeneous uniform model M-1 (Fig.6.12).

- Increasing the conductivity of deeper layers increased the downward flow rate through them.

A substantial extraction rate significantly influences the groundwater flow dynamics and increases the likelihood of arsenic migration

Extraction, or pumping, influences the groundwater flow dynamics in the following two aspects:

1) Flow between the river and the aquifer system
2) Downward flow through the deeper layers

Flow between the river and the aquifer system

A comparison of simulations with and without extraction rates (Col. 4 and Col. 9, Table 5.2 & Table 5.3) clearly demonstrates that

- Pumping increases the flow from the river to the aquifer when shallow aquifer recharge (SAR) is less than the extraction rate (Q)
- Pumping decreases the flow rate from the river to the aquifer system when the SAR rate is greater than the extracting rate (Q)

Under extraction conditions, the reason for increased groundwater flow from the river to the aquifer is that the well requires more water (5000 m^3/day) than it was available from recharge (at SAR= 381mm/yr, total amount SAR was 1950 m^3/day for an area of 1.95 km^2).

Influence of extraction on downward flow through the deeper layers

- Extraction or pumping generally increases the flow through deeper layers to a rate higher than that of natural flow conditions.
- Extraction increases the flow rate through deeper layers when the pumping rate (Q) is greater than the aquifer recharge rate (SAR). Therefore, under pumping conditions, the risk of arsenic migration to deeper layers is high.

It was also found that placing well screens at deeper layers increases the flow rate in those deeper layers. When the extraction rate is greater than the recharge rate (Q>SAR), the downward flow through the deeper layers is increased and simultaneously the risk of arsenic contamination is increased.

Mass balance analyses indicate that arsenic can migrate downward with moving groundwater's advective or hydrodynamic dispersive velocity. In order to obtain arsenic-free water in a leaky aquifer system, irrigation wells must not be placed into the deeper layers.

7.1 Conclusions

The groundwater arsenic contamination problem in Bangladesh is a complex hydrogeochemical process. The arsenic source or origin in Bangladesh is certainly natural. It appears now that arsenic release is triggered by a misguided groundwater extraction policy. Large-scale extraction and diversion of surface water from major rivers has caused a shortage of oxygenated recharging water (SAR) at and below the water table, which eventually develops reducing conditions and releases arsenic in the groundwater system.

It is still a debatable issue whether pyrite oxidation or reduction of iron oxides controls the arsenic release mechanism in the groundwater of Bangladesh. The oxidation or reduction process is a time-dependent phenomenon. Therefore, especially in a heterogeneous aquifer system, accepting or rejecting these hypotheses based on space-dependent relations cannot well be representative.

It is unfortunate that the use of groundwater for irrigation and drinking purposes and upstream diversion of surface water from the major river systems began nearly simultaneously in 1970. The simultaneous development has created confusion regarding the release mechanism of arsenic. Currently there

are two mutually exclusive theories of arsenic release: the oxidation theory and the reduction theory.

Despite divergence of opinion on the arsenic release mechanism, supporting evidence from the field and from model results is strong enough to reveal the inadequacy of the oxidation theory of arsenic release. At the same time, the suitability of the hypothesis presented in this study is strong because it is hard to deny the clear results of thermodynamic and mathematical models.

The findings of this study are contrary to the existing theories because previous theories have ignored the contribution of aquifer recharge to maintenance of the high redox values below the water table. Without knowing the influence of aquifer recharge on groundwater movement and flow patterns, it is simply a misleading approach to formulate any irrigation development policy. For example, experts working on irrigation development projects have already suggested that tube wells should be installed reaching to deeper layers in order to obtain arsenic-free water. However, models results clearly demonstrate that placing well screens at deeper layer will increase the downward flow and arsenic might move with the groundwater to the deeper layers. Also, there is evidence that extraction at a rate greater than the aquifer recharge rate (SAR) increases the downward flow through the deeper layers of the aquifer system and thus increases the risk of arsenic migration with the moving groundwater.

Similarly, cropping patterns, irrigation system capacity, and extraction rates all are management decision variables and decisions based on quantitative results can improve controls over the arsenic contamination problem. Any irrigation project must be accomplished by proper hydrogeochemical analysis. If the extraction rate Q exceeds the aquifer recharge (SAR) rate, it will endanger the groundwater ecosystem.

7.2 Findings of this study

- A distinct regional pattern of arsenic concentration was found with the greatest contamination in the southeast (SE) and southwest (SW) zone of the country. The probability of arsenic exceeding threshold values (>50 ppb) was found highest in the southeast (SE) and southwest (SW) regions, respectively and it agrees with the findings of the other field studies.
- The present theory of arsenic release by pyrite oxidation is inadequate to explain the arsenic contamination problem in Bangladesh.
- The top-most layers of the aquifer (0 to 10 m below the ground surface) were found to be relatively less arsenic-contaminated in comparison with deeper layers. This finding is supportive to the hypothesis offered in this study.
- Lowering of the water table to deeper layers after introducing well fields did not increase the oxygen concentration in water; rather it decreased the oxygen supply, because the oxygen diffusion rate (ODR) decreases with increasing aquifer depth.
- Arsenic concentration was found to increase with aquifer depth from 9 to

30 m below the ground surface but to decrease with depth from 100 to 350 m below the ground.

- The redox stratification in the most arsenic contaminated aquifers can be explained as a function of aquifer depth from 9 to 30 m (R^2=60%) and 100 to 350 m (R^2=72%) below the ground.
- Growing high yielding variety rice twice in a year in the study area has substantially reduced the surplus volume (SUR) available.
- Improved irrigation management practices can reduce the pumping requirements of the study area. It appears that by adjustments in the cropping season, the irrigation withdrawal rate can greatly be reduced. By adjustment in the cropping pattern, the irrigation withdrawal volume can be reduced about 68% in the Kharif-1 season.
- By adjusting the irrigation system capacity, the amount of surplus can be increased. The lowest system capacity level (70%) produced the highest amount of SUR available.
- The arsenic concentration of groundwater entering into a well screen increased linearly with the increasing rate of aquitard conductivity, and decreased with the increasing depth of the aquitard.
- It was found from the model simulation that doubling or halving the amount of aquifer recharge (SAR) had little or no impact on the groundwater flow patterns in a homogeneous, uniform model.
- Increasing the conductivity of deeper layers increased the downward flow

rate through the deeper layers in the aquifer system

- Pumping increased the flow from the river to the aquifer system when shallow aquifer recharge rate (SAR) was less than the extraction rate (Q).
- Pumping at the rate greater than available aquifer recharge (SAR) rate decreased the flow from the river to the aquifer systems when the SAR was proportionately greater than the abstracting rate (Q)
- Extraction increased the downward flow rate through deeper layers when the pumping rate (Q) was greater than the aquifer recharge rate (SAR).
- Pumping proportionately decreased the downward flow rate through the deeper layers when aquifer recharge (SAR) rates were greater than extraction rate (Q).
- Pumping at a rate greater than the SAR also increased the arsenic concentration to the deeper layers.
- Under natural groundwater flow conditions, increasing the aquifer recharge rate (SAR) increased the downward flow through the deeper aquifer layers.
- Vertical hydraulic gradients and local hydraulic gradients are changed by extraction patterns of the tube wells.
- Extractions or pumping significantly changed the flow pattern in the groundwater system. Extraction overall increases the downward flow rate. Placing well screens at deeper layers significantly increases the downward flow rate through deeper layers.

7.3 Recommendations

Against the backdrop of an alarming fall in the groundwater level, the optimal use of surface water in irrigation is a must for the country's sustainable development. In order to make use of the contaminated aquifer, safe layers can be delineated on the basis of redox potential values. For example, it was found that arsenic concentration varies as a function of aquifer depth. The top most layers from zero to 10 m are relatively arsenic-free. If an extraction of 500 mm/yr. or an equivalent amount can be saved, a 4 to 5 m water table could easily be developed on top of the summer water level, giving locations for small- scale pumps or wells to be placed to obtain arsenic-free water.

The aquifer delineation is extremely important in terms of supplying safe irrigation and drinking water. It is recommended that that the top 10 m of aquifer layer be kept for installation of small-scale dug wells or hand tube wells in order to ensure a long-term supply of arsenic-free water. The upper layer receives rainwater, which is high in redox potential values and should be safe for drinking; extraction for irrigation must be restricted in the top aquifer.

2. It is recommended that the placement of tube well screens at the deep layers of the aquifer should be stopped in order to reduce the risk of arsenic migration from the currently contaminated to uncontaminated deeper layers of the aquifer.

3. It will be beneficial for the aquifer system if the best use is made of runoff or surface water resources. For example, by controlling the drainage outlet

structures, residual water or floodwater can be stored or used to induce recharge. These techniques will provide oxygenated water to the aquifer and keep the redox potential values high.

4. The traditional management practices used by farmers are less efficient in terms of groundwater use. The study suggests that adjusting the cropping seasons and pattern both could reduce the volume of pumpage from the aquifer. Adjusting the transplanting dates could reduce the amount of irrigation withdrawal from 637 to 433 mm in the Kharif–1 season. Rather than growing rice twice in a year, if farmers grow wheat in the Kharif–1 season, it can save a tremendous amount of groundwater extraction. The cropping pattern "HYV–wheat in Rabi and HYV-rice in Kharif–2 " can save about 500 mm of water in a cropping year. Therefore, for the study area of the southwest zone of Bangladesh, it is recommended that this cropping pattern be followed in order to increase the level of water table.

5. It was recommended that a soil-based, low-cost arsenic removal technique could be developed using the already existing millions of shallow irrigation wells in Bangladesh. The iron reduction and oxidation theory was discussed. Laboratory studies have shown that arsenic (V) could be removed by using local materials, river sands rich in iron oxides. Cheaply available Ferruginous Manganese Ore (FMO) can adsorb arsenic (III), which otherwise can't be removed without chemical oxidants. Under oxic conditions, arsenic (V) species can be adsorbed onto the river sand rich in iron oxides.

7.3.1 Recommendations for further research

1. An important part of this study was based on the amount of dissolved oxygen available in the recharging groundwater. The oxygen diffusion model in this study was completely based on an analytical approach and is a transient simulation. This transient simulation was calculated for each of two different water table conditions. It was not a perfect approach to use a transient model to understand the complex geochemistry in the aquifer. Therefore it is suggested that field-testing of dissolved oxygen concentrations under heavy pumping condition versus limited pumping conditions would be appropriate to evaluate the amount of dissolved oxygen concentration changes over aquifer depth.

2. The pyrite oxidation theory of arsenic release and the theory of arsenic release by iron oxide reduction are both time-dependent phenomena. Thus, validation or rejection of either hypothesis on the basis of space-dependent relationships in a heterogeneous aquifer is not a reasonable representation. The final conclusion as to the validity of the hypotheses must be developed based on time-dependent relationships using more reliable field and laboratory data.

3. The exact contribution of surface water diversion to the shortage of aquifer recharge is to be estimated by reliable field data in order to demonstrate the actual impact on the groundwater flow dynamics and flow patterns.

Appendix –A:

Computation of surplus volume (SUR) and soil storage capacity for the study area in SW zone of Bangladesh

APPENDIX A

Computation of surplus (SUR) volume and soil storage capacity using soil moisture balance

Assumptions:

a. Irrigation will be applied when the daily soil moisture level falls below the Critical Water Content (CWC) level.

b. Beginning soil moisture (mm) = AWC (mm/m)
where AWC is the available water content. 150

c. Critical Water Content, CWC (mm/m) = 90

CWC=AWC*P= 90

where P is the management allowed deficit (60% of AWC)

For rice irrigation, effective rainfall=
If daily evapotranspiration is 10 mm, a three-day successive rainfall up to 70 mm is taken as effective and the excess is disregarded.
According to FAO,

For the dry season, the % taken as effective is 80%
For the wet season, the % taken as effective is 65-75%

*Computation of Storage Capacity (SC)=[VMC(SAT)-VMC(PWP)]*H=*

VMC(SAT)= 0.6

VMC(PWP)= 0.4

H=Depth of Water Table= 3

SC=(0.60-0.35)*1=250 mm/m

Storage Opportunity=SC-Stored soil moisture=250-150 mm=100 mm/m

Effective storage=Storage Opportunity-Maximum 3-day Rainfall=Col.16-col.6

The average monthly ETo of the study area in June = 4.54

The average monthly ETo of the study area in July = 4.2

1	2	3	4	5	6	7	8	9	10	11	12	13	14	15	16	17
Year/ Month	Days after	ETo (mm/day)	Kc	ETc (mm/day)	3-dayRain (mm/3-day)	Eff. Rain (mm/3-day)	ETa (mm/day)	AV Kc	Pe-Eta (mm/3-day)	Moist.Bal. (mm/3-day)	Excess Moisture	Irrg.Req. (mm)	SURPLUS Drainage	3-Day ETa(mm)	Storage Opp.	Effective storage Col 16-Col 6
3/1/00	1	2.67	0.75	2.0025	1.0625	1.009375	2.0025		-0.993125	149.006875	-0.993125		0	2.0025	100.9931	99.930625
6/1/00	2	2.67	0.21	0.5607	0.9	0.855	0.554513		-0.8085385	148.198337	-1.801663		0	1.663538	101.8017	100.9016635
9/1/00	3	2.67	0.21	0.5607	2.06	1.957	0.549476		0.30857309	148.50691	-1.49309		0	1.648427	101.4931	99.4330904
12/1/00	4	2.67	0.21	0.5607	0.12	0.114	0.551398		-1.5401941	148.966715	-3.033285		0	1.654194	103.0333	102.9132845
15/1/00	5	2.67	0.21	0.5607	0.38	0.361	0.541803		-1.2644079	145.702308	-4.297692		0	1.625408	104.2977	103.9176925
18/1/00	6	2.67	0.21	0.5607	2.16	2.052	0.533925		0.45022387	146.152531	-3.847469		0	1.601778	103.8475	101.6874686
21/1/00	7	2.67	0.21	0.5607	0.66	0.627	0.53673		-0.9831908	145.169341	-4.830659		0	1.610191	104.8307	104.1706594
24/1/00	8	2.67	0.21	0.5607	2.18	2.071	0.530805		0.47918502	145.648526	-4.351474		0	1.591815	104.3515	102.1714744
27/1/00	9	2.67	0.21	0.5607	0.09	0.0855	0.53359		-1.5152709	144.133255	-5.866745		0	1.600771	105.8667	105.7767453
30/1/00	10	2.67	0.21	0.5607	2.56	2.432	0.52415		0.85954947	144.992804	-5.007196		0	1.572451	105.0072	102.4471958
2/2/00	11	2.67	0.21	0.5607	3.41	3.2395	0.529505		1.65098449	146.643789	-3.356211		0	1.588516	103.3562	99.94621136
5/2/00	12	3.61	0.21	0.7581	4.26	4.047	0.72963		1.85751146	148.5013	-1.4987		0	2.188889	101.4987	97.23869989
8/2/00	13	3.61	0.21	0.7581	2.11	2.0045	0.745476		-0.2319279	148.269372	-1.730628		0	2.236428	101.7306	99.62062775
11/2/00	14	3.61	0.60	2.166	1.911	1.81545	2.12435		-4.5575987	143.711774	-6.288226		0	6.373049	106.2882	104.3772264
14/2/00	15	3.61	0.60	2.166	1.14	1.083	2.014663		-4.9609901	138.750784	-11.24922		0	6.04399	111.2492	110.1092165
17/2/00	16	3.61	0.60	2.166	1.52	1.444	1.895269		-4.2418066	134.508977	-15.49102		0	5.685807	115.491	113.971023
20/2/00	17	3.61	0.60	2.166	3.2	3.04	1.793183		-2.3395481	132.169429	-17.83057		0	5.379548	117.8306	114.6305712
23/2/00	18	3.61	0.60	2.166	5.11	4.8545	1.736878		-0.3561328	131.813296	-18.1867		0	5.210633	118.1867	113.0767039
26/2/00	19	3.61	0.60	2.166	2.32	2.204	1.728307		-2.96092	128.832376	-21.16762		0	5.18492	121.1676	118.8476239
29/2/00	20	3.61	0.60	2.166	0.05	0.0475	1.656566		-4.9221976	123.910179	-26.08982		0	4.969696	126.0898	126.0398215
3/3/00	21	5.10	0.75	3.825	2.71	2.5745	2.716183		-5.5740478	118.336131	-31.66387		0	8.148548	131.6639	128.9538692
6/3/00	22	5.10	0.75	3.825	3.65	3.4675	2.479286		-3.9703567	114.365774	-35.63423		0	7.437857	135.6342	131.9842259
9/3/00	23	5.10	0.75	3.825	3.88	3.686	2.310545		-3.2456362	111.120138	-38.87986		0	6.931636	138.8799	134.9998621
12/3/00	24	5.10	0.75	3.825	3.06	2.907	2.172606		-3.6108176	107.50932	-42.49068		0	6.517818	142.4907	139.4306797
15/3/00	25	5.10	0.75	3.825	5.84	5.548	2.019146		-0.5094383	106.999882	-43.00012		0	6.057438	143.0001	137.160118
18/3/00	26	5.10	0.75	3.825	0.4	0.38	1.997495		-5.612485	101.387397	-48.6126		0	5.992485	148.6126	148.212603
21/3/00	27	5.10	0.75	3.825	12.96	12.312	1.758964		7.03510688	108.422504	-41.5775		0	5.276893	141.5775	128.6174961
24/3/00	28	5.10	0.75	3.825	4.65	4.4175	2.057956		-1.7563692	106.666135	-43.33387		0	6.173869	143.3339	138.6838653
27/3/00	29	5.10	1.2	6.12	7.66	7.277	3.173297		-2.2426915	104.423243	-45.57676		0	9.519891	145.5768	137.9167568
30/3/00	30	5.10	1.2	6.12	3.18	3.021	3.020781		-6.0413416	98.3819016	-51.6181		0	9.062342	151.6181	148.4380984
2/4/00	31	6.61	1.2	7.932	6.43	6.1085	3.382725		-4.0396748	94.3422268	-55.65777		0	10.14817	155.6578	149.2277732
5/4/00	32	6.61	1.2	7.932	5.03	4.7785	3.026895		-4.3015848	90.040642	-59.95936		0	9.080085	159.9594	154.929358
8/4/00	33	6.61	1.2	7.932	2.12	2.014	2.647582		-5.9287458	84.1118963	-65.8881		0	7.942748	165.8881	163.7681037
11/4/00	34	6.61	1.2	7.932	3	2.85	2.125062		-3.5251854	80.5867109	-69.41329		0	6.375185	169.4133	166.4132891
14/4/00	35	6.61	0.75	4.9575	6.62	6.289	1.133985		2.88704602	83.4737569	-66.52624		0	3.401954	166.5262	159.9062431
17/4/00	36	6.61	0.75	4.9575	8.03	7.6285	1.293013		3.74946167	87.2232186	-62.77678		0	3.879038	162.7768	154.7467814
20/4/00	37	6.61	0.75	4.9575	11.25	10.6875	1.499546		6.18886313	93.4120817	-56.58792		0	4.498637	156.5879	145.3379183
23/4/00	38	6.61	0.75	4.9575	5.43	5.1585	1.840449		-0.3628465	93.0492352	-56.95076		0	5.521347	156.9508	151.5207648

26/4/00	39	6.61	0.75	4.9575	6.06	5.757	1.820462	0.29561388	93.3448491	-56.65515	0	5.461386	156.6552	150.5951509
29/4/00	40	6.61	0.75	4.9575	14.56	13.832	1.836745	8.32176369	101.666613	-48.33339	0	5.510236	148.3334	133.7733872
2/5/00	41	6.3	0.75	4.725	19.09	18.1355	2.187497	11.5730085	113.239621	-36.76038	0	6.562492	136.7604	117.6703787
5/5/00	42	6.3	0.75	4.725	11.54	10.963	2.79508	2.57775965	115.817381	-34.18262	0	8.38524	134.1826	122.6426191
8/5/00	43	6.3	0.75	4.725	15.9	15.105	2.930412	6.31376251	122.131143	-27.86886	0	8.791237	127.8689	111.9688586
11/5/00	44	6.3	0.75	4.725	15.18	14.421	3.261885	4.63534491	126.766488	-23.23351	0	9.785655	123.2335	108.0535117
14/5/00	45	6.3	0.75	4.725	9.51	9.0345	3.505241	-1.4812219	125.285266	-24.71473	0	10.51572	124.7147	115.2047336
17/5/00	46	6.3	0.75	4.725	14.48	13.756	3.427476	3.47357054	128.758837	-21.24116	0	10.28243	121.2412	106.761163
20/5/00	47	6.3	0.75	4.725	12.63	11.9985	3.609839	1.16898318	129.92782	-20.07218	0	10.82952	120.0722	107.4421799
23/5/00	48	6.3	0.75	4.725	13.15	12.4925	3.671211	1.47886833	131.406688	-18.59331	0	11.01363	118.5933	105.4433115
26/5/00	49	6.3	0.75	4.725	16.75	15.9125	3.748851	4.66594657	136.072635	-13.92736	0	11.24655	113.9274	97.17736497
29/5/00	50	6.3	0.75	4.725	17.69	16.8055	3.993813	4.82405998	140.896695	-9.103305	0	11.98144	109.1033	91.41330498
1/6/00	51	4.54	0.75	3.405	15.21	13.689	3.060592	4.50722512	145.40392	-4.59608	0	9.181775	104.5961	89.38607987
4/6/00	**52**	**4.54**	**0.2**	**0.908**	**31.64**	**28.386**	**0.861631**	**25.801108**	**150**	**21.20603**	**21.205028**	**2.584892**	**100**	**68.46**
7/6/00	53	4.54	0.2	0.908	28.45	25.605	0.908	22.881	150	22.881	22.881	2.724	100	71.55
10/6/00	54	4.54	0.2	0.908	30.69	27.621	0.908	24.897	150	24.897	24.897	2.724	100	69.31
13/6/00	55	4.54	0.2	0.908	35.51	31.959	0.908	29.235	150	29.235	29.235	2.724	100	64.49
16/6/00	56	4.54	0.2	0.908	34.75	31.275	0.908	28.551	150	28.551	28.551	2.724	100	65.25
19/6/00	57	4.54	0.2	0.908	31.9	28.71	0.908	25.986	150	25.986	25.986	2.724	100	68.1
22/6/00	58	4.54	0.2	0.908	36.57	32.913	0.908	30.189	150	30.189	30.189	2.724	100	63.43
25/6/00	59	4.54	0.2	0.908	24.42	21.978	0.908	19.254	150	19.254	19.254	2.724	100	75.58
28/6/00	60	4.54	0.2	0.908	37.24	33.516	0.908	30.792	150	30.792	30.792	2.724	100	62.76
1/7/00	61	4.2	0.2	0.84	30.33	27.297	0.84	24.777	150	24.777	24.777	2.52	100	69.67
4/7/00	62	4.2	0.2	0.84	31.39	28.251	0.84	25.731	150	25.731	25.731	2.52	100	68.61
7/7/00	63	4.2	0.6	2.52	33.3	29.97	2.52	22.41	150	22.41	22.41	7.56	100	66.7
10/7/00	64	4.2	0.6	2.52	36	32.4	2.52	24.84	150	24.84	24.84	7.56	100	64
13/7/00	65	4.2	0.6	2.52	21.09	18.981	2.52	11.421	150	11.421	11.421	7.56	100	78.91
16/7/00	66	4.2	0.6	2.52	2.69	2.421	2.52	-5.139	144.861	-5.139	0	7.56	105.139	102.449
19/7/00	67	4.2	0.6	2.52	26.96	24.264	2.376108	17.135676	150	11.99688	11.996676	7.128324	100	73.04
22/7/00	68	4.2	0.6	2.52	25.9	23.31	2.52	15.75	150	15.75	15.75	7.56	100	74.1
25/7/00	69	4.2	0.6	2.52	23	20.7	2.52	13.14	150	13.14	13.14	7.56	100	77
28/7/00	70	4.2	0.6	2.52	42.09	37.881	2.52	30.321	150	30.321	30.321	7.56	100	57.91
31/7/00	71	4.2	0.6	2.52	33	29.7	2.52	22.14	150	22.14	22.14	7.56	100	67
3/8/00	72	4.11	0.6	2.466	47.09	42.381	2.466	34.983	150	34.983	34.983	7.398	100	52.91
6/8/00	73	4.11	0.6	2.466	28.87	25.983	2.466	18.585	150	18.585	18.585	7.398	100	71.13
9/8/00	74	4.11	0.75	3.0825	16.09	14.481	3.0825	5.2335	150	5.2335	5.2335	9.2475	100	83.91
12/8/00	75	4.11	0.75	3.0825	22.57	20.313	3.0825	11.0655	150	11.0655	11.0655	9.2475	100	77.43
16/8/00	76	4.11	0.75	3.0825	30.78	27.702	3.0825	18.4545	150	18.4545	18.4545	9.2475	100	69.22
20/8/00	77	4.11	0.75	3.0825	27.39	24.651	3.0825	15.4035	150	15.4035	15.4035	9.2475	100	72.61
23/8/00	78	4.11	1.2	4.932	22.36	20.124	4.932	5.328	150	5.328	5.328	14.796	100	77.64
26/8/00	79	4.11	1.2	4.932	36.81	33.129	4.932	18.333	150	18.333	18.333	14.796	100	63.19
29/8/00	80	4.11	1.2	4.932	20.42	18.378	4.932	3.582	150	3.582	3.582	14.796	100	79.58
1/9/00	81	4.02	1.2	4.824	22.27	20.043	4.824	5.571	150	5.571	5.571	14.472	100	77.73

4/9/00	82	4.02	1.2	4.824	26.42	23.778	4.824	9.306	150	9.306	9.306	14.472	100	73.58
7/9/00	83	4.02	1.2	4.824	16.78	15.102	4.824	0.63	150	0.63	0.63	14.472	100	83.22
10/9/00	84	4.02	0.75	3.015	20.15	18.135	3.015	9.09	150	9.09	9.09	9.045	100	79.85
13/9/00	85	4.02	0.75	3.015	17.75	15.975	3.015	6.93	150	6.93	6.93	9.045	100	82.25
16/9/00	86	4.02	0.75	3.015	14.33	12.897	3.015	3.852	150	3.852	3.852	9.045	100	85.67
19/9/00	87	4.02	0.75	3.015	25.18	22.662	3.015	13.617	150	13.617	13.617	9.045	100	74.82
22/9/00	88	4.02	0.75	3.015	18.66	16.794	3.015	7.749	150	7.749	7.749	9.045	100	81.34
25/9/00	89	4.02	0.75	3.015	36.24	32.616	3.015	23.571	150	23.571	23.571	9.045	100	63.76
28/9/00	90	4.02	0.75	3.015	32.27	29.043	3.015	19.998	150	19.998	19.998	9.045	100	67.73
1/10/00	91	3.52	0.75	2.64	22.18	19.962	2.64	12.042	150	12.042	12.042	7.92	100	77.82
4/10/00	92	3.52	0.75	2.64	27.24	24.516	2.64	16.596	150	16.596	16.596	7.92	100	72.76
7/10/00	93	3.52	0.75	2.64	12.66	11.394	2.64	3.474	150	3.474	3.474	7.92	100	87.34
10/10/00	94	3.52	0.75	2.64	12.36	11.124	2.64	3.204	150	3.204	3.204	7.92	100	87.64
13/10/00	95	3.52	0.75	2.64	15.36	13.824	2.64	5.904	150	5.904	5.904	7.92	100	84.64
16/10/00	96	3.52	0.75	2.64	11	9.9	2.64	1.98	150	1.98	1.98	7.92	100	89
19/10/00	97	3.52	0.75	2.64	5.444	4.8996	2.64	-3.0204	146.9796	-3.0204	0	7.92	103.0204	97.5764
22/10/00	98	3.52	0.75	2.64	18.78	16.902	2.551402	9.2477952	150	6.227395	6.2273952	7.654205	100	81.22
25/10/00	99	3.52	0.75	2.64	4.3	3.87	2.64	-4.05	145.95	-4.05	0	7.92	104.05	99.75
28/10/00	100	3.52	0.75	2.64	4.87	4.383	2.5212	-3.1808	142.7694	-7.2306	0	7.5636	107.2306	102.3606
31/10/00	101	3.52	0.75	2.64	0.78	0.702	2.427902	-6.5817072	136.187693	-13.81231	0	7.283707	113.8123	113.0323072
3/11/00	102	3.15	0.85	2.6775	5.24	4.716	2.266584	-2.0637516	134.103941	-15.89606	0	6.799752	115.8961	110.6560588
6/11/00	103	3.15	0.85	2.6775	5.33	4.797	2.204592	-1.8167768	132.287164	-17.71284	0	6.613777	117.7128	112.3828355
9/11/00	104	3.15	0.85	2.6775	2.72	2.448	2.150543	-4.0036294	128.283535	-21.71646	0	6.451629	121.7165	118.996465
12/11/00	105	3.15	0.85	2.6775	1.66	1.494	2.031435	-4.6003055	123.68323	-26.31677	0	6.094306	126.3168	124.6567795
15/11/00	106	3.15	0.85	2.6775	2.09	1.881	1.894576	-3.8027282	119.880501	-30.1195	0	5.683728	130.1195	128.0294987
18/11/00	107	3.15	0.85	2.6775	0.03	0.027	1.781445	-5.3173347	114.563167	-35.43683	0	5.344335	135.4368	135.4068334
21/11/00	108	3.15	0.85	2.6775	0.33	0.297	1.623254	-4.5727626	109.990404	-40.0096	0	4.869763	140.0096	139.6795961
24/11/00	109	3.15	0.85	2.6775	1.63	1.467	1.487215	-2.9946436	106.99576	-43.00424	0	4.461644	143.0042	141.3742396
27/11/00	110	3.15	0.85	2.6775	4.45	4.005	1.398124	-0.1893716	106.806389	-43.19361	0	4.194372	143.1936	138.7436112
30/11/00	111	3.15	0.85	2.6775	0.93	0.837	1.39249	-3.3404702	103.465919	-46.53408	0	4.17747	146.5341	145.6040814
3/12/00	112	2.52	0.85	2.142	1.6	1.44	1.034489	-1.6634668	101.802452	-48.19755	0	3.103467	148.1975	146.597548
6/12/00	113	2.52	0.2	0.504	6.15	5.535	0.234094	4.83271881	106.635171	-43.36483	0	0.702281	143.3648	137.2148292
9/12/00	114	2.52	0.2	0.504	0.42	0.378	0.261157	-0.4054709	106.2297	-43.7703	0	0.783471	143.7703	143.3503001
12/12/00	115	2.52	0.2	0.504	0.3	0.27	0.258886	-0.506659	105.723041	-44.27696	0	0.776659	144.277	143.976959
15/12/00	116	2.52	0.2	0.504	0.27	0.243	0.256049	-0.5251471	105.197894	-44.80211	0	0.768147	144.8021	144.5321061
18/12/00	117	2.52	0.2	0.504	0.03	0.027	0.253108	-0.7323246	104.465569	-45.53443	0	0.759325	145.5344	145.5044307
21/12/00	118	2.52	0.2	0.504	3.06	2.754	0.249007	2.00697844	106.472548	-43.52745	0	0.747022	143.5275	140.4674523
24/12/00	119	2.52	0.2	0.504	1.39	1.251	0.260246	0.4702612	106.942809	-43.05719	0	0.780739	143.0572	141.6671911
26/12/00	120	2.52	0.2	0.504	0	0	0.26288	-0.7886392	106.15417	-43.84583	0	0.788639	143.8458	143.8458303
29/12/00	121	2.52	0.2	0.504		0	0.258463	-0.7753901	105.37878	-44.62122	0	0.77539	144.6212	144.6212203
					1566.7075	1425.01893	252.473				716.2261	751.4115		

Appendix –B:

Computation of amount of shallow aquifer recharge (SAR) for the groundwater system of the study area in SW zone of Bangladesh

APPENDIX B:

Computation of shallow aquifer recharge (SAR) in the study area was done using the soil moisture balance

From section 4.5.2 and Eq. 4.5.3
SAR = SUR - OUTFLOW + PUMPAGE(Q)

In absence of pumping records, the lower limit of shallow aquifer recharge is

SAR = SUR - OUTFLOW

Year	SUR	Outflow	SAR
	(mm/Yr)	(mm/Yr)	(mm/Yr)
2001	964.1227113	493.373592	**470.74**
2000	876.2842456	378.181872	**498.1**

NB: The Outflow and Surpus volume (SUR) of the study area was computed using the daily soil moisture balance

Appendix-C:

Computation of the amount of surplus volume (SUR) under rice irrigated condition of the study area in Bangladesh

Appendix C:

Computation of irrigation system capacity, surplus volume (SUR) under different rice-based cropping systems in the SW zone of Bangladesh

Assumptions:

1. Instead of standing water supply for rice irrigation, we assume continuous saturation and no significant rice yield loss under saturated condition. Irrigation water is to be supplied as soon as soil moisture reaches AWC (150 mm)

3.Beginning Soil Moisture (mm) at saturation, (SAT) in (mm/m) 250
Critical Water Content, CWC (mm/m) =
CWC=SAT*P= 150

4, Seepage & Percolation Rate (mm/day)= 3.3

5. Effective rainfall=
If daily water requirement or evapotranspiration is 10 mm, a three-day successive rainfall up to 70 mm is taken as effective and the excess is disregarded.
According to FAO,

For the dry season, the % taken as effective is 80%
For the wet season, the % taken as effective is 65-75%

6. Storage Capacity (SC)=[VMC(SAT)-VMC(PWP)]*H= 250
VMC(SAT)= 0.6
VMC(PWP)= 0.35
H = Depth of Water Table = 1
=(0.60-0.35)*1=250 mm/m

7. Storage Opportunity=SC-Stored soil moisture=250 -150 mm=100 mm/m

Effective storage=Storage Opportunity-Maximum 3-day Rainfall=Col.16-col.6

8. RICE WATER REQUIREMENT=ETc+Seepage and Percolation Loss(Col.10)

9. Crop Growing Season in Rice-Based Irrigation Systems

December-March (Rabi)

April-July (Kharif-1)

August-December (Kharif-2)

10. Criteria For Effective Rainfall in Rice Cultivation:
1. The effective rainfall was computed according to the FAO Irrigation and Drainage Paper, 25

using the value of the previous day's soil moisture, Etc, Deep percolation loss.

Depth of Land Submergence = (Water Stock on Hand - Water Loss) - (Permissible Water Depth for Land Submergence)

= {(Previous Day's Soil Moisture + Rainfall + Irrigation) - (Etc + Deep Percolation) - Crop Storage - Permissble Water Depth}

1	2	3	4	5	6	7	8	10	11	12	13	*14*	15	16	16	17
3-Day	ETo	Kc	ETc	3-dayRain	Depth of	Eff. Rain	*ETa*	Pe-Eta-3*S&P	*Moist.Bal.*	Excess	Irrg.Req	*SURPLUS*	3-Day	S&P Loss	Storage	Effective storage
	(mm/day)		(mm/day)	(mm/3-day)	Submergence	(mm/3-day)	(mm/day)	(mm/3-day)	(mm/3-day)	Moisture	(mm)	Drainage	ETc(mm)	(mm/day)	Opp.	Col 16-Col 6
1	2.67	0.25	0.6675	1.0625		1.009375	0.6675	0.341875	250	0.3419	0	0.341875	0.6675	3.33	50	50
2	2.67	0.21	0.5607	0.9	179.9179	0.855	0.5607	-10.8271	239.1729	-10.827	0	0	1.6821	10	51.6821	51.6821
3	2.67	0.21	0.5607	2.06	170.2508	1.957	0.52023	-9.7251	229.4478	-20.552	0	0	1.6821	10	53.33276	53.33276155
4	2.67	0.21	0.5607	0.12	158.5857	0.114	0.48388	-11.5681	217.8797	-32.12	0	0	1.6821	10	54.95257	54.95257224
5	2.67	0.21	0.5607	0.38	147.2776	0.361	0.44063	-11.3211	206.5586	-43.441	0	0	1.6821	10	56.54211	56.54210866
6	2.67	0.21	0.5607	2.16	137.7365	2.052	0.39832	-9.6301	196.9285	-53.072	0	0	1.6821	10	58.10194	58.10193665
7	2.67	0.21	0.5607	0.66	126.6064	0.627	0.36232	-11.0551	185.8734	-64.127	0	0	1.6821	10	59.63261	59.63261146
8	2.67	0.21	0.5607	2.18	117.0713	2.071	0.32099	-9.6111	176.2623	-73.738	0	0	1.6821	10	61.13468	61.13467795
9	2.67	0.21	0.5607	0.09	105.3702	0.0855	0.28507	-11.5966	164.6657	-85.334	0	0	1.6821	10	62.60867	62.60867082
10	3.61	0.21	0.7581	2.56	95.6514	2.432	0.32682	-9.8423	154.8234	-95.177	0	0	2.2743	10	64.05511	64.05511476
11	3.61	0.21	0.7581	3.41	190.8705	3.2395	0.27708	-9.0348	145.7886	-104.21	104.21	0	2.2743	10	65.47452	65.47452466
12	3.61	0.21	0.7581	4.26	78.4743	4.047	0.23142	-8.2273	241.7727	-8.2273	0	0	2.2743	10	67.35778	67.35778343
13	3.61	0.21	0.7581	2.11	172.3084	2.0045	0.71652	-10.2698	231.5029	-18.497	0	0	2.2743	10	69.19345	69.19345224
14	3.61	0.6	2.166	1.911	157.6159	1.81545	1.6989	-14.68255	216.82035	-33.18	0	0	6.498	10	74.30568	74.30568499
15	3.61	0.6	2.166	1.14	142.16235	1.083	1.68689	-15.415	201.40535	-48.595	0	0	6.498	10	79.04881	79.04881453
16	3.61	0.6	2.166	1.52	127.12735	1.444	1.46429	-15.054	186.35135	-63.649	0	0	6.498	10	83.44949	83.44949012
17	3.61	0.6	2.166	3.2	113.75335	3.04	1.24691	-13.458	172.89335	-77.107	0	0	6.498	10	87.53244	87.53243694
18	3.61	0.6	2.166	5.11	102.20535	4.8545	1.05258	-11.6435	161.24985	-88.75	0	0	6.498	10	90.65559	89.95559499
19	3.61	0.6	2.166	2.32	190.816	2.204	0.88445	-14.294	146.95585	-103.04	103.04	0	6.498	10	94.21826	94.21826103
20	3.61	0.6	2.166	0.05	71.20785	0.0475	0.67804	-16.4505	233.5495	-16.451	0	0	6.498	10	95.5287	93.42870258
21	5.1	0.75	3.825	2.71	155.4845	2.5745	3.40551	-18.9005	214.649	-35.351	0	0	11.475	10	101.1988	101.198793
22	5.1	0.75	3.825	3.65	137.524	3.4675	2.92355	-18.0075	196.6415	-53.359	0	0	11.475	10	104.7209	103.2209469
23	5.1	0.75	3.825	3.88	119.7465	3.686	2.46436	-17.789	178.8525	-71.148	0	0	11.475	10	109.219	109.2190262
24	5.1	0.75	3.825	3.06	101.1375	2.907	2.01074	-18.568	160.2845	-89.716	0	0	11.475	10	113.1436	113.1436003
25	5.1	0.75	3.825	5.84	190.992	5.548	1.53725	-15.927	144.3575	-105.64	105.64	0	11.475	10	56.56779	56.56779129
26	5.1	0.75	3.825	0.4	63.9825	0.38	1.13112	-21.095	228.905	-21.095	0	0	11.475	10	67.2054	67.2053979
27	5.1	0.75	3.825	12.96	161.09	12.312	3.28708	-9.163	219.742	-30.258	0	0	11.475	10	76.48671	76.48670967
28	5.1	0.75	3.825	4.65	143.617	4.4175	3.05342	-17.0575	202.6845	-47.316	0	0	11.475	10	83.63465	82.63465418
29	5.1	1.2	6.12	7.66	122.6845	7.277	4.18953	-21.083	181.6015	-68.399	0	0	18.36	10	95.13318	95.13318473
30	5.1	1.2	6.12	3.18	97.1215	3.021	3.32934	-25.339	156.2625	-93.738	0	0	18.36	10	104.286	104.286015
31	6.61	1.2	7.932	6.43	191.0215	6.1085	7.932	-27.6875	128.575	-121.43	121.43	0	23.796	10	113.7288	113.7287927
32	6.61	1.2	7.932	5.03	40.509	4.7785	7.932	-29.0175	220.9825	-29.018	0	0	23.796	10	60.6749	60.67489989
33	6.61	1.2	7.932	2.12	130.0065	2.014	7.932	-31.782	189.2005	-60.8	0	0	23.796	10	81.64846	81.64845636
34	6.61	1.2	7.932	3	99.1045	2.85	7.932	-30.946	158.2545	-91.746	0	0	23.796	10	97.0766	97.0766045
35	6.61	0.75	4.9575	6.62	191.031	6.289	4.9575	-18.5835	139.671	-110.33	110.33	0	14.8725	10	104.1697	104.1696956
36	6.61	0.75	4.9575	8.03	63.5285	7.6285	4.9575	-17.244	232.756	-17.244	0	0	14.8725	10	56.89065	0.890653404
37	6.61	0.75	4.9575	11.25	159.8335	10.6875	4.9575	-14.185	218.571	-31.429	0	0	14.8725	10	63.49947	55.99947293
38	6.61	0.75	4.9575	5.43	139.8285	5.1585	4.9575	-19.714	198.857	-51.143	0	0	14.8725	10	62.17619	47.47618503

39	6.61	0.75	4.9575	6.06	120.7445	5.757	4.9575	-19.1155	179.7415	-70.259	0	0	14.8725	10	71.99657	68.79657045
40	6.61	0.75	4.9575	14.56	110.129	13.832	4.9575	-11.0405	168.701	-81.299	0	0	14.8725	10	75.63414	67.63413718
41	6.3	0.75	4.725	19.09	104.316	18.1355	4.725	-6.0395	162.6615	-87.339	0	0	14.175	10	73.32676	60.22676058
42	6.3	0.75	4.725	11.54	191.277	10.963	4.725	-13.212	149.4495	-100.55	100.55	0	14.175	10	83.8278	83.82779579
43	6.3	0.75	4.725	15.9	81.8745	15.105	4.725	-9.07	240.93	-9.07	0	0	14.175	10	92.67492	92.67491795
44	6.3	0.75	4.725	15.18	172.635	14.421	4.725	-9.754	231.176	-18.824	0	0	14.175	10	60	-262
45	6.3	0.75	4.725	9.51	157.211	9.0345	4.725	-15.1405	216.0355	-33.965	0	0	14.175	10	50	27.6
46	6.3	0.75	4.725	14.48	147.0405	13.756	4.725	-10.419	205.6165	-44.384	0	0	14.175	10	52.3	39.8
47	6.3	0.75	4.725	12.63	134.7715	11.9985	4.725	-12.1765	193.44	-56.56	0	0	14.175	10	66.11275	66.11275
48	6.3	0.75	4.725	13.15	123.115	12.4925	4.725	-11.6825	181.7575	-68.243	0	0	14.175	10	50	-18.8
49	6.3	0.75	4.725	16.75	115.0325	15.9125	4.725	-8.2625	173.495	-76.505	0	0	14.175	10	61.325	58.325
50	6.3	0.75	4.725	17.69	107.71	16.8055	4.725	-7.3695	166.1255	-83.875	0	0	14.175	10	64.69131	55.1913125
51	4.54	0.75	3.405	15.21	101.8205	14.4495	3.405	-5.7655	160.36	-89.64	0	0	10.215	10	69.45885	65.25884853
52	4.54	0.2	0.908	31.54	119.876	29.963	0.908	17.239	177.599	-72.401	0	0	2.724	10	69.43389	67.03389405
53	4.54	0.2	0.908	28.45	134.025	25.605	0.908	12.881	190.48	-59.52	0	0	2.724	10	50	-3.1
54	4.54	0.2	0.908	30.69	149.146	27.621	0.908	14.897	205.377	-44.623	0	0	2.724	10	50	41.4
55	4.54	0.2	0.908	35.51	168.863	31.959	0.908	19.235	224.612	-25.388	0	0	2.724	10	50	3.5
56	4.54	0.2	0.908	34.75	187.338	31.275	0.908	18.551	243.163	-6.837	0	0	2.724	10	52.724	52.724
57	4.54	0.2	0.908	31.9	203.039	28.71	0.908	15.986	250	9.149	0	9.149	2.724	10	50	-11.5
58	4.54	0.2	0.908	36.57	214.546	32.913	0.908	20.189	250	20.189	0	20.189	2.724	10	50	13.5
59	4.54	0.2	0.908	24.42	202.396	21.978	0.908	9.254	250	9.254	0	9.254	2.724	10	50	41.4
60	4.54	0.2	0.908	37.24	215.216	33.516	0.908	20.792	250	20.792	0	20.792	2.724	10	50	45.7
61	4.2	0.2	0.84	30.33	208.51	27.297	0.84	14.777	250	14.777	0	14.777	2.52	10	52.52	52.52
62	4.2	0.2	0.84	31.39	209.57	28.251	0.84	15.731	250	15.731	0	15.731	2.52	10	54.96944	54.96944
63	4.2	0.6	2.52	33.3	206.44	29.97	2.52	12.41	250	12.41	0	12.41	7.56	10	62.11201	62.11200704
64	4.2	0.6	2.52	36	209.14	32.4	2.52	14.84	250	14.84	0	14.84	7.56	10	50	19.8
65	4.2	0.6	2.52	21.09	194.23	18.981	2.52	1.421	250	1.421	0	1.421	7.56	10	50	34.6
66	4.2	0.6	2.52	2.69	175.83	2.421	2.52	-15.139	234.861	-15.139	0	0	7.56	10	50	31.3
67	4.2	0.6	2.52	26.96	184.961	24.264	2.52	6.704	241.565	-8.435	0	0	7.56	10	50	12.7
68	4.2	0.6	2.52	25.9	190.605	23.31	2.52	5.75	247.315	-2.685	0	0	7.56	10	50	33
69	4.2	0.6	2.52	23	193.455	20.7	2.52	3.14	250	0.455	0	0.455	7.56	10	57.56	57.56
70	4.2	0.6	2.52	42.09	215.23	37.881	2.52	20.321	250	20.321	0	20.321	7.56	10	50	-53.2
71	4.2	0.6	2.52	33	206.14	29.7	2.52	12.14	250	12.14	0	12.14	7.56	10	50	37.2
72	4.11	0.6	2.466	47.09	220.392	42.381	2.466	24.983	250	24.983	0	24.983	7.398	10	50	32.4
73	4.11	0.6	2.466	28.87	202.172	25.983	2.466	8.585	250	8.585	0	8.585	7.398	10	50.918	43.718
74	4.11	0.75	3.0825	16.09	187.5425	14.481	3.0825	-4.7665	245.2335	-4.7665	0	0	9.2475	10	57.37118	54.3711755
75	4.11	0.75	3.0825	22.57	189.256	20.313	3.0825	1.0655	246.299	-3.701	0	0	9.2475	10	65.86129	65.86128722
76	4.11	0.75	3.0825	30.78	198.5315	27.702	3.0825	8.4545	250	4.7535	0	4.7535	9.2475	10	61.77904	48.77903996
77	4.11	0.75	3.0825	27.39	198.8425	24.651	3.0825	5.4035	250	5.4035	0	5.4035	9.2475	10	69.81624	69.8162436
78	4.11	1.2	4.932	22.36	188.264	20.124	4.932	-4.672	245.328	-4.672	0	0	14.796	10	81.35445	81.35445315
79	4.11	1.2	4.932	36.81	198.042	33.129	4.932	8.333	250	3.661	0	3.661	14.796	10	50	-40
80	4.11	1.2	4.932	20.42	186.324	18.378	4.932	-6.418	243.582	-6.418	0	0	14.796	10	50	-86.3

81	4.02	1.2	4.824	22.27	182.08	20.043	4.824	-4.429	239.153	-10.847	0	0	14.472	10	50	29
82	4.02	1.2	4.824	26.42	181.801	23.778	4.824	-0.694	238.459	-11.541	0	0	14.472	10	50	23
83	4.02	1.2	4.824	16.78	171.467	15.102	4.824	-9.37	229.089	-20.911	0	0	14.472	10	50	31.5
84	4.02	0.75	3.015	20.15	170.894	18.135	3.015	-0.91	228.179	-21.821	0	0	9.045	10	50	-79.5
85	4.02	0.75	3.015	17.75	167.584	15.975	3.015	-3.07	225.109	-24.891	0	0	9.045	10	50	5.5
86	4.02	0.75	3.015	14.33	161.094	12.897	3.015	-6.148	218.961	-31.039	0	0	9.045	10	59.045	59.045
87	4.02	0.75	3.015	25.18	165.796	22.662	3.015	3.617	222.578	-27.422	0	0	9.045	10	59.26098	50.4609775
88	4.02	0.75	3.015	18.66	162.893	16.794	3.015	-2.251	220.327	-29.673	0	0	9.045	10	67.37525	67.37524926
89	4.02	0.75	3.015	36.24	178.222	32.616	3.015	13.571	233.898	-16.102	0	0	9.045	10	74.67404	74.67403671
90	4.02	0.75	3.015	32.27	187.823	29.043	3.015	9.998	243.896	-6.104	0	0	9.045	10	81.2393	81.23929602
91	3.52	0.75	2.64	22.18	188.856	19.962	2.64	2.042	245.938	-4.062	0	0	7.92	10	50	4.7
92	3.52	0.75	2.64	27.24	195.958	24.516	2.64	6.596	250	2.534	0	2.534	7.92	10	50	-0.3
93	3.52	0.75	2.64	12.66	185.44	11.394	2.64	-6.526	243.474	-6.526	0	0	7.92	10	50	37
94	3.52	0.75	2.64	12.36	178.614	11.124	2.64	-6.796	236.678	-13.322	0	0	7.92	10	50	32
95	3.52	0.75	2.64	15.36	174.818	13.824	2.64	-4.096	232.582	-17.418	0	0	7.92	10	57.92	57.92
96	3.52	0.75	2.64	11	166.362	9.9	2.64	-8.02	224.562	-25.438	0	0	7.92	10	56.59304	47.09304
97	3.52	0.75	2.64	5.444	152.786	4.8996	2.64	-13.0204	211.5416	-38.458	0	0	7.92	10	50	22
98	3.52	0.75	2.64	18.78	153.1016	16.902	2.64	-1.018	210.5236	-39.476	0	0	7.92	10	57.92	57.92
99	3.52	0.75	2.64	4.3	137.6036	3.87	2.64	-14.05	196.4736	-53.526	0	0	7.92	10	65.14304	65.14304
100	3.52	0.75	2.64	4.87	124.1236	4.383	2.64	-13.537	182.9366	-67.063	0	0	7.92	10	71.73045	71.73045248
101	3.52	0.75	2.64	0.78	106.4966	0.702	2.64	-17.218	165.7186	-84.281	0	0	7.92	10	71.25817	64.05817266
102	3.15	0.85	2.6775	5.24	93.6261	4.716	2.6775	-13.3165	152.4021	-97.598	0	0	8.0325	10	77.39338	77.39338075
103	3.15	0.85	2.6775	5.33	191.233	4.797	2.6775	-13.2355	139.1666	-110.83	110.83	0	8.0325	10	82.98102	82.98102152
104	3.15	0.85	2.6775	2.72	64.5541	2.448	2.6775	-15.5845	234.4155	-15.585	0	0	8.0325	10	88.06997	88.06996535
105	3.15	0.85	2.6775	1.66	158.743	1.494	2.6775	-16.5385	217.877	-32.123	0	0	8.0325	10	92.70472	92.70472094
106	3.15	0.85	2.6775	2.09	142.6345	1.881	2.6775	-16.1515	201.7255	-48.275	0	0	8.0325	10	96.92582	96.9258246
107	3.15	0.85	2.6775	0.03	124.423	0.027	2.6775	-18.0055	183.72	-66.28	0	0	8.0325	10	100.7702	100.7701948
108	3.15	0.85	2.6775	0.33	106.7175	0.297	2.6775	-17.7355	165.9845	-84.016	0	0	8.0325	10	104.2715	104.2714549
109	3.15	0.85	2.6775	1.63	190.863	1.467	2.6775	-16.5655	149.419	-100.58	100.58	0	8.0325	10	107.4602	107.4602275
110	3.15	0.85	2.6775	4.45	76.5365	4.005	2.6775	-14.0275	235.9725	-14.028	0	0	8.0325	10	110.3644	110.3644022
111	3.15	0.85	2.6775	0.93	159.57	0.837	2.6775	-17.1955	218.777	-31.223	0	0	8.0325	10	53.00938	53.00937932
112	2.52	0.85	2.142	1.6	144.651	1.44	2.142	-14.986	203.791	-46.209	0	0	6.426	10	59.22051	59.22050964
113	2.52	0.2	0.504	6.15	139.129	5.535	0.504	-5.977	197.814	-52.186	0	0	1.512	10	60.57761	60.57760507
114	2.52	0.2	0.504	0.42	127.422	0.378	0.504	-11.134	186.68	-63.32	0	0	1.512	10	61.9119	61.91190131
115	2.52	0.2	0.504	0.3	116.168	0.27	0.504	-11.242	175.438	-74.562	0	0	1.512	10	63.22378	63.22378137
116	2.52	0.2	0.504	0.27	104.896	0.243	0.504	-11.269	164.169	-85.831	0	0	1.512	10	64.51362	64.51362184
117	2.52	0.2	0.504	0.03	93.387	0.027	0.504	-11.485	152.684	-97.316	0	0	1.512	10	65.78179	65.78179299
118	2.52	0.2	0.504	3.06	191.006	2.754	0.504	-8.758	143.926	-106.07	106.07	0	1.512	10	67.02866	67.02865887
119	2.52	0.2	0.504	1.39	74.504	1.251	0.504	-10.261	239.739	-10.261	0	0	1.512	10	68.25458	68.2545774
120	2.52	0.2	0.504	0	168.927	0	0.504	-11.512	228.227	-21.773	0	0	1.512	10	69.4599	69.4599005
121	2.52	0.2	0.504	0	157.415	0	0.504	-11.512	216.715	-33.285	0	0	1.512	10	70.64497	70.64497417
			340.976	***1566.7075***		***1427.366***	261.643				***962.7***	201.7409	1021.59	1200		

Appendix-D:

Computation of the amount of surplus volume (SUR) under rain -fed rice condition of the study area in Bangladesh

APPENDIX D

Analysis of SUR under rainfed rice-irrigation system (Part 1): Yr. 3 (2001)

Calculation of SURPLUS, soil moisture (daily) under rainfed system

Beginning Soil Moisture (mm)=AWC(mm/m) 150
Critical WaterContent, CWC(mm/m) = 90
CWC=AWC*P= 90 Water balance =

For rice irrigation, effective rainfall=
If daily evapotranspiration is 10 mm, a three-day successive rainfall up to 70 mm is taken as effective and the excess is disregarded.
According to FAO,
For the dry season, the % taken as effective is 80% **CHART 1**
For the wet season, the % taken as effective is 65-75%

150

Storage Capacity(SC)=[VMC(SAT)-VMC(PWP)]*H=
VMC(SAT)= 0.6
VMC(PWP)= 0.35
H=Depth of Water Table= 3
=(0.60-0.35)*1=250 mm/m
Storage Opportunity=SC-Stored soil moisture=250-150 mm=100 mm/m

Effective storage=Storage Opportunity-Maximum 3-day Rainfall=Col.16-col.6

The average monthly ETo of the study area in June = 4.54

The average monthly ETo of the study area in July = 4.2

1	2	3	4	5	6	7	8	9	10	11	12	13	14	15	16	17
Year/ Month	Days	ETo (mm/day)	Kc	ETc (mm/day)	3-day Rain (mm/3-day)	Eff. Rain (mm/3-day)	ETa (mm/day)	AV Kc	Pe-Eta (mm/3-day)	Moist.Bal. (mm/3-day)	Excess Moisture	Irrg.Req. (mm)	SURPLUS Drainage	3-Day ETa(mm)	Storage Opp.	Effective storage Col 16-Col 6
3/1/00	1	2.67	0.75	2.0025	1.0625	1.009375	2.0025		-0.993125	149.006875	-0.9931		0	2.0025	100.993	99.930625
6/1/00	2	2.67	0.21	0.5607	0.9	0.855	0.554513		-0.8085385	148.198337	-1.8017		0	1.66354	101.802	100.9016635
9/1/00	3	2.67	0.21	0.5607	2.06	1.957	0.549476		0.30857309	148.50691	-1.4931		0	1.64843	101.493	99.4330904
12/1/00	4	2.67	0.21	0.5607	0.12	0.114	0.551398		-1.5401941	146.966715	-3.0333		0	1.65419	103.033	102.9132845
15/1/00	5	2.67	0.21	0.5607	0.38	0.361	0.541803		-1.2644079	145.702308	-4.2977		0	1.62541	104.298	103.9176925
18/1/00	6	2.67	0.21	0.5607	2.16	2.052	0.533925		0.45022387	146.152531	-3.8475		0	1.60178	103.847	101.6874686
21/1/00	7	2.67	0.21	0.5607	0.66	0.627	0.53673		-0.9831908	145.169341	-4.8307		0	1.61019	104.831	104.1706594
24/1/00	8	2.67	0.21	0.5607	2.18	2.071	0.530605		0.47918502	145.648526	-4.3515		0	1.59181	104.351	102.1714744
27/1/00	9	2.67	0.21	0.5607	0.09	0.0855	0.53359		-1.5152709	144.133255	-5.8667		0	1.60077	105.867	105.7767453
30/1/00	10	2.67	0.21	0.5607	2.56	2.432	0.52415		0.85954947	144.992804	-5.0072		0	1.57245	105.007	102.4471958
2/2/00	11	2.67	0.21	0.5607	3.41	3.2395	0.529505		1.65098449	146.643789	-3.3562		0	1.58852	103.356	99.94621136
5/2/00	12	3.61	0.21	0.7581	4.26	4.047	0.72983		1.85751146	148.5013	-1.4987		0	2.18949	101.499	97.23869989
8/2/00	13	3.61	0.21	0.7581	2.11	2.0045	0.745476		-0.2319279	148.269372	-1.7306		0	2.23643	101.731	99.62062775
11/2/00	14	3.61	0.60	2.166	1.911	1.81545	2.12435		-4.5575987	143.711774	-6.2882		0	6.37305	106.288	104.3772264
14/2/00	15	3.61	0.60	2.166	1.14	1.083	2.014663		-4.9609901	138.750784	-11.249		0	6.04399	111.249	110.1092165
17/2/00	16	3.61	0.60	2.166	1.52	1.444	1.895269		-4.2418066	134.508977	-15.491		0	5.68581	115.491	113.971023
20/2/00	17	3.61	0.60	2.166	3.2	3.04	1.793183		-2.3395481	132.169429	-17.831		0	5.37955	117.831	114.6305712
23/2/00	18	3.61	0.60	2.166	5.11	4.8545	1.736878		-0.3561328	131.813296	-18.187		0	5.21063	118.187	113.0767039
26/2/00	19	3.61	0.60	2.166	2.32	2.204	1.728307		-2.98092	128.832376	-21.168		0	5.18492	121.168	118.8476239
29/2/00	20	3.61	0.60	2.166	0.05	0.0475	1.656566		-4.9221976	123.910179	-26.09		0	4.9697	126.09	126.0398215
3/3/00	21	5.10	0.8	3.825	2.71	2.5745	2.716183		-5.5740478	118.336131	-31.664		0	8.14855	131.664	128.9538692
6/3/00	22	5.10	0.8	3.825	3.65	3.4675	2.479286		-3.9703567	114.365774	-35.634		0	7.43786	135.634	131.9842259
9/3/00	23	5.10	0.8	3.825	3.88	3.686	2.310545		-3.2456362	111.120138	-38.88		0	6.93164	138.88	134.9998621
12/3/00	24	5.10	0.8	3.825	3.06	2.907	2.172606		-3.6108176	107.50932	-42.491		0	6.51782	142.491	139.4306797
15/3/00	25	5.10	0.8	3.825	5.84	5.548	2.019146		-0.5094383	106.999882	-43		0	6.05744	143	137.160118
18/3/00	26	5.10	0.8	3.825	0.4	0.38	1.997495		-5.612485	101.387397	-48.613		0	5.99248	148.613	148.212603
21/3/00	27	5.10	0.8	3.825	12.96	12.312	1.758964		7.03510688	108.422504	-41.577		0	5.27689	141.577	128.6174961
24/3/00	28	5.10	0.8	3.825	4.65	4.4175	2.057956		-1.7563692	106.666135	-43.334		0	6.17387	143.334	138.6838653
27/3/00	29	5.10	1.2	6.12	7.66	7.277	3.173297		-2.2428915	104.423243	-45.577		0	9.51989	145.577	137.9167568
30/3/00	30	5.10	1.2	6.12	3.18	3.021	3.020781		-6.0413416	98.3819016	-51.618		0	9.06234	151.618	148.4380984
2/4/00	31	6.61	1.2	7.932	6.43	6.1085	3.382725		-4.0396748	94.3422268	-55.658		0	10.1482	155.658	149.2277732
5/4/00	32	6.61	1.2	7.932	5.03	4.7785	3.026695		-4.3015848	90.040642	-59.959		0	9.08008	159.959	154.929358
8/4/00	33	6.61	1.2	7.932	2.12	2.014	2.647582		-5.9287458	84.1118963	-65.888		0	7.94275	165.888	163.7681037
11/4/00	34	6.61	1.2	7.932	3	2.85	2.125062		-3.5251854	80.5867109	-69.413		0	6.37519	169.413	166.4132891
14/4/00	35	6.61	0.8	4.9575	6.62	6.289	1.133985		2.88704602	83.4737569	-66.526		0	3.40195	166.526	159.9062431
17/4/00	36	6.61	0.8	4.9575	8.03	7.6285	1.293013		3.74946167	87.2232186	-62.777		0	3.87904	162.777	154.7467814
20/4/00	37	6.61	0.8	4.9575	11.25	10.6875	1.499546		6.18886313	93.4120817	-56.588		0	4.49864	156.588	145.3379183
23/4/00	38	6.61	0.8	4.9575	5.43	5.1585	1.840449		-0.3628465	93.0492352	-56.951		0	5.52135	156.951	151.5207648
26/4/00	39	6.61	0.8	4.9575	6.06	5.757	1.820462		0.29561388	93.3448491	-56.655		0	5.46139	156.655	150.5951509
29/4/00	40	6.61	0.8	4.9575	14.56	13.832	1.836745		8.32176369	101.666613	-48.333		0	5.51024	148.333	133.7733872
2/5/00	41	6.3	0.8	4.725	19.09	18.1355	2.187497		11.5730085	113.239621	-36.76		0	6.56249	136.76	117.6703787
5/5/00	42	6.3	0.8	4.725	11.54	10.963	2.79508		2.57775965	115.817381	-34.183		0	8.38524	134.183	122.6426191
8/5/00	43	6.3	0.8	4.725	15.9	15.105	2.930412		6.31376251	122.131143	-27.869		0	8.79124	127.869	111.9688566
11/5/00	44	6.3	0.8	4.725	15.18	**14.421**	3.261885		**4.63634491**	126.766488	-23.234		0	9.78566	**123.234**	**108.0536117**
14/5/00	45	6.3	0.8	4.725	9.51	9.0345	3.505241		-1.4812219	125.285266	-24.715		0	10.5157	124.715	115.2047336
17/5/00	46	6.3	0.8	4.725	14.48	13.756	3.427476		3.47357054	128.758837	-21.241		0	10.2824	121.241	106.761163
20/5/00	47	6.3	0.8	4.725	12.63	11.9985	3.609839		1.16898318	129.92782	-20.072		0	10.8295	120.072	107.4421799

23/5/00	48	6.3	0.8	4.725	13.15	12.4925	3.671211	1.47886833	131.406688	-18.593	0	11.0136	118.593	105.4433115
26/5/00	49	6.3	0.8	4.725	16.75	15.9125	3.748851	4.66594657	136.072635	-13.927	0	11.2466	113.927	97.17736497
29/5/00	50	6.3	0.8	4.725	17.69	16.8055	3.993813	4.82405998	140.896695	-9.1033	0	11.9814	109.103	91.41330498
1/6/00	51	4.54	0.8	3.405	15.21	13.689	3.060592	4.50722512	145.40392	-4.5961	0	9.18177	104.596	89.38607987
4/6/00	52	4.54	0.2	0.908	31.54	28.386	0.861631	25.801108	150	21.205	21.20503	2.58489	100	68.46
7/6/00	53	4.54	0.2	0.908	28.45	25.605	0.908	22.881	150	22.881	22.881	2.724	100	71.55
10/6/00	54	4.54	0.2	0.908	30.69	27.621	0.908	24.897	150	24.897	24.897	2.724	100	69.31
13/6/00	55	4.54	0.2	0.908	35.51	31.959	0.908	29.235	150	29.235	29.235	2.724	100	64.49
16/6/00	56	4.54	0.2	0.908	34.75	31.275	0.908	28.551	150	28.551	28.551	2.724	100	65.25
19/6/00	57	4.54	0.2	0.908	31.9	28.71	0.908	25.986	150	25.986	25.986	2.724	100	68.1
22/6/00	58	4.54	0.2	0.908	36.57	32.913	0.908	30.189	150	30.189	30.189	2.724	100	63.43
25/6/00	59	4.54	0.2	0.908	24.42	21.978	0.908	19.254	150	19.254	19.254	2.724	100	75.58
28/6/00	60	4.54	0.2	0.908	37.24	33.516	0.908	30.792	150	30.792	30.792	2.724	100	62.76
1/7/00	61	4.2	0.2	0.84	30.33	27.297	0.84	24.777	150	24.777	24.777	2.52	100	69.67
4/7/00	62	4.2	0.2	0.84	31.39	28.251	0.84	25.731	150	25.731	25.731	2.52	100	68.61
7/7/00	63	4.2	0.6	2.52	33.3	29.97	2.52	22.41	150	22.41	22.41	7.56	100	66.7
10/7/00	64	4.2	0.6	2.52	36	32.4	2.52	24.84	150	24.84	24.84	7.56	100	64
13/7/00	65	4.2	0.6	2.52	21.09	18.981	2.52	11.421	150	11.421	11.421	7.56	100	78.91
16/7/00	66	4.2	0.6	2.52	2.69	2.421	2.52	-5.139	144.861	-5.139	0	7.56	105.139	102.449
19/7/00	67	4.2	0.6	2.52	26.96	24.264	2.376108	17.135676	150	11.9967	11.99668	7.12832	100	73.04
22/7/00	68	4.2	0.6	2.52	25.9	23.31	2.52	15.75	150	15.75	15.75	7.56	100	74.1
25/7/00	69	4.2	0.6	2.52	23	20.7	2.52	13.14	150	13.14	13.14	7.56	100	77
28/7/00	70	4.2	0.6	2.52	42.09	37.881	2.52	30.321	150	30.321	30.321	7.56	100	57.91
31/7/00	71	4.2	0.6	2.52	33	29.7	2.52	22.14	150	22.14	22.14	7.56	100	67
3/8/00	72	4.11	0.6	2.466	47.09	42.381	2.466	34.983	150	34.983	34.983	7.398	100	52.91
6/8/00	73	4.11	0.6	2.466	28.87	25.983	2.466	18.585	150	18.585	18.585	7.398	100	71.13
9/8/00	74	4.11	0.8	3.0825	16.09	14.481	3.0825	5.2335	150	5.2335	5.2335	9.2475	100	83.91
12/8/00	75	4.11	0.8	3.0825	22.57	20.313	3.0825	11.0655	150	11.0655	11.0655	9.2475	100	77.43
16/8/00	76	4.11	0.8	3.0825	30.78	27.702	3.0825	18.4545	150	18.4545	18.4545	9.2475	100	69.22
20/8/00	77	4.11	0.8	3.0825	27.39	24.651	3.0825	15.4035	150	15.4035	15.4035	9.2475	100	72.61
23/8/00	78	4.11	1.2	4.932	22.36	20.124	4.932	5.328	150	5.328	5.328	14.796	100	77.64
26/8/00	79	4.11	1.2	4.932	36.81	33.129	4.932	18.333	150	18.333	18.333	14.796	100	63.19
29/8/00	80	4.11	1.2	4.932	20.42	18.378	4.932	3.582	150	3.582	3.582	14.796	100	79.58
1/9/00	81	4.02	1.2	4.824	22.27	20.043	4.824	5.571	150	5.571	5.571	14.472	100	77.73
4/9/00	82	4.02	1.2	4.824	26.42	23.778	4.824	9.306	150	9.306	9.306	14.472	100	73.58
7/9/00	83	4.02	1.2	4.824	16.78	15.102	4.824	0.63	150	0.63	0.63	14.472	100	83.22
10/9/00	84	4.02	0.8	3.015	20.15	18.135	3.015	9.09	150	9.09	9.09	9.045	100	79.85
13/9/00	85	4.02	0.8	3.015	17.75	15.975	3.015	6.93	150	6.93	6.93	9.045	100	82.25
16/9/00	86	4.02	0.8	3.015	14.33	12.897	3.015	3.852	150	3.852	3.852	9.045	100	85.67
19/9/00	87	4.02	0.8	3.015	25.18	22.662	3.015	13.617	150	13.617	13.617	9.045	100	74.82
22/9/00	88	4.02	0.8	3.015	18.66	16.794	3.015	7.749	150	7.749	7.749	9.045	100	81.34
25/9/00	89	4.02	0.8	3.015	36.24	32.616	3.015	23.571	150	23.571	23.571	9.045	100	63.76
28/9/00	90	4.02	0.8	3.015	32.27	29.043	3.015	19.998	150	19.998	19.998	9.045	100	67.73
1/10/00	91	3.52	0.8	2.64	22.18	19.962	2.64	12.042	150	12.042	12.042	7.92	100	77.82
4/10/00	92	3.52	0.8	2.64	27.24	24.516	2.64	16.596	150	16.596	16.596	7.92	100	72.76
7/10/00	93	3.52	0.8	2.64	12.66	11.394	2.64	3.474	150	3.474	3.474	7.92	100	87.34
10/10/00	94	3.52	0.8	2.64	12.36	11.124	2.64	3.204	150	3.204	3.204	7.92	100	87.64
13/10/00	95	3.52	0.8	2.64	15.36	13.824	2.64	5.904	150	5.904	5.904	7.92	100	84.64
16/10/00	96	3.52	0.8	2.64	11	9.9	2.64	1.98	150	1.98	1.98	7.92	100	89
19/10/00	97	3.52	0.8	2.64	5.444	4.8996	2.64	-3.0204	146.9796	-3.0204	0	7.92	103.02	97.5764
22/10/00	98	3.52	0.8	2.64	18.78	16.902	2.551402	9.2477952	150	6.2274	6.227395	7.6542	100	81.22
25/10/00	99	3.52	0.8	2.64	4.3	3.87	2.64	-4.05	145.95	-4.05	0	7.92	104.05	99.75
28/10/00	100	3.52	0.8	2.64	4.87	4.383	2.5212	-3.1806	142.7694	-7.2306	0	7.5636	107.231	102.3606
31/10/00	101	3.52	0.8	2.64	0.78	0.702	2.427902	-6.5817072	136.187693	-13.812	0	7.28371	113.812	113.0323072
3/11/00	102	3.15	0.9	2.6775	5.24	4.716	2.266584	-2.0837516	134.103941	-15.896	0	6.79975	115.896	110.6560588
6/11/00	103	3.15	0.9	2.6775	5.33	4.797	2.204592	-1.8167768	132.287164	-17.713	0	6.61378	117.713	112.3828355

9/11/00	104	3.15	0.9	2.6775	2.72	2.448	2.150543	-4.0036294	128.283535	-21.716	0	6.45163	121.716	118.996465
12/11/00	105	3.15	0.9	2.6775	1.66	1.494	2.031435	-4.6003055	123.68323	-26.317	0	6.09431	126.317	124.6567705
15/11/00	106	3.15	0.9	2.6775	2.09	1.881	1.894576	-3.8027282	119.880501	-30.119	0	5.68373	130.119	128.0294987
18/11/00	107	3.15	0.9	2.6775	0.03	0.027	1.781445	-5.3173347	114.563167	-35.437	0	5.34433	135.437	135.4068334
21/11/00	108	3.15	0.9	2.6775	0.33	0.297	1.623254	-4.5727626	109.990404	-40.01	0	4.86976	140.01	139.6795961
24/11/00	109	3.15	0.9	2.6775	1.63	1.467	1.487215	-2.9946436	106.99576	-43.004	0	4.46164	143.004	141.3742396
27/11/00	110	3.15	0.9	2.6775	4.45	4.005	1.398124	-0.1893716	106.806389	-43.194	0	4.19437	143.194	138.7436112
30/11/00	111	3.15	0.9	2.6775	0.93	0.837	1.39249	-3.3404702	103.465919	-46.534	0	4.17747	146.534	145.6040814
3/12/00	112	2.52	0.9	2.142	1.6	1.44	1.034489	-1.6634666	101.802452	-48.198	0	3.10347	148.198	146.597548
6/12/00	113	2.52	0.2	0.504	6.15	5.535	0.234094	4.83271881	106.635171	-43.365	0	0.70228	143.365	137.2148292
9/12/00	114	2.52	0.2	0.504	0.42	0.378	0.261157	-0.4054709	106.2297	-43.77	0	0.78347	143.77	143.3503001
12/12/00	115	2.52	0.2	0.504	0.3	0.27	0.258886	-0.506659	105.723041	-44.277	0	0.77666	144.277	143.976959
15/12/00	116	2.52	0.2	0.504	0.27	0.243	0.256049	-0.5251471	105.197894	-44.802	0	0.76815	144.802	144.5321061
18/12/00	117	2.52	0.2	0.504	0.03	0.027	0.253108	-0.7323246	104.465569	-45.534	0	0.75932	145.534	145.5044307
21/12/00	118	2.52	0.2	0.504	3.06	2.754	0.249007	2.00697844	106.472548	-43.527	0	0.74702	143.527	140.4674523
24/12/00	119	2.52	0.2	0.504	1.39	1.251	0.260246	0.4702612	106.942809	-43.057	0	0.78074	143.057	141.6671911
26/12/00	120	2.52	0.2	0.504	0	0	0.26288	-0.7886392	106.15417	-43.846	0	0.78864	143.846	143.8458303
29/12/00	121	2.52	0.2	0.504		0	0.258463	-0.7753901	105.37878	-44.621	0	0.77539	144.621	144.6212203
					1566.7075	**1425.0189**	**252.473**				**716.2261**	**751.412**		

Appendix E :

Demonstration of velocity distribution patterns of site specific non homogeneous model under natural groundwater flow and pumping condition

Appendix: E:

Vertical velocity distribution of site specific actual model actual field model under pumping condition at seven different layers.

Water moving with a up ward velocity above the Tube well screen depth (Layer-2 and Layer-3) and below the screen depth water moves downward (Layer-3 to Layer-7)

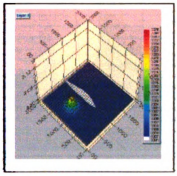

Layer-1

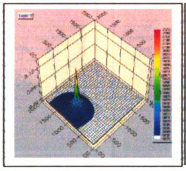

Layer-2

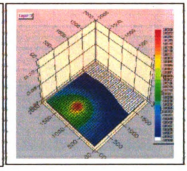

Layer-3

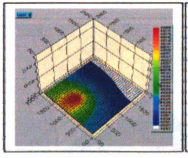

Layer-4

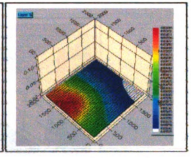

Layer-5

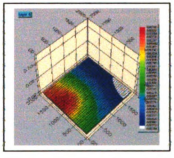

Layer-6

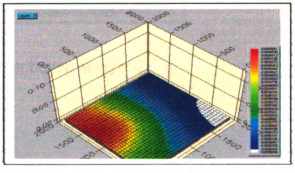

Layer-7

Appendix E-2

Velocity distribution patterns in non-homogeneous model with variation in hydraulic conductivity values under natural groundwater flow or condition

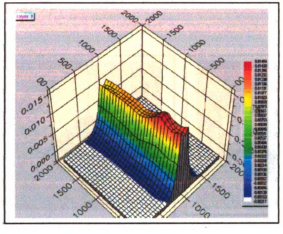

Velocity distribution at layer-1

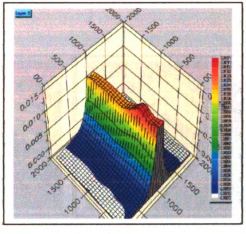

Velocity distribution at layer-2

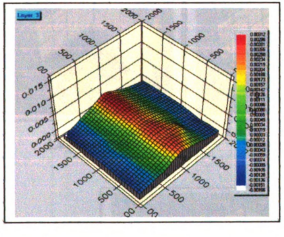

Velocity distribution at layer-3

Appendix: E:

Vertical velocity distribution of site specific actual model actual field model under pumping condition at seven different layers.

Water moving with a up ward velocity above the Tube well screen depth (Layer-2

and Layer-3) and below the screen depth water moves downward (Layer-3 to Layer-7)

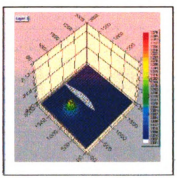

Layer-1

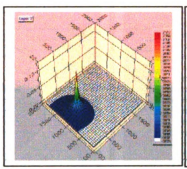

Layer-2

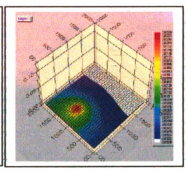

Layer-3

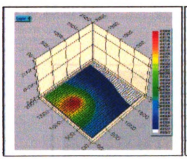

Layer-4

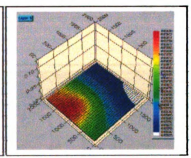

Layer-5

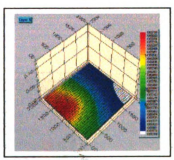

Layer-6

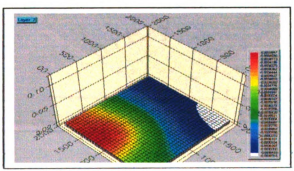

Layer-7

Appendix E-3

Variation of hydraulic conductivity values in non homogeneous model at Layer-1 , 2 and Layer-3 where conductivity at the middle layer is higer than deper layers (M-2 Model) .

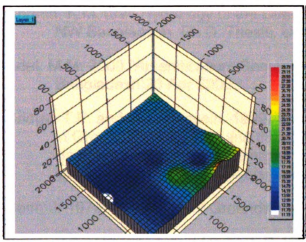

Layer-1 Conductivity varies from 11 to 25 m/day

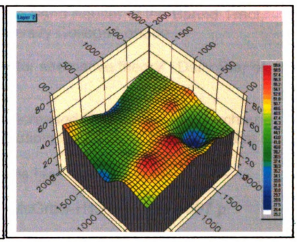

Layer-1 Conductivity varies from 25 to 50 m/day

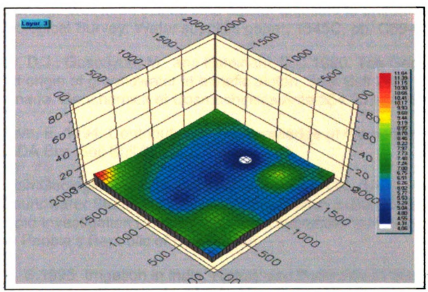

Layer-3 Conductivity values varies from 4 to 12 m/day.

REFERENCES

AECL.1996.The Evolution of Redox Conditions and Groundwater Geochemistry in Recharge-Discharge Environment of Canadian Shields. Atomic Energy of Canada Limited Report. AECL-11682.COG -96-500

Ahmed, K.M.1994.Hydrology of the Dupi Tila Sand Aquifer of the Barind Tract, NW Bangladesh. Ph.D. Thesis, University College London.

Adel, M.M. 2000."Arsenification: Searching for alternative theory". Daily Star of Bangladesh.28 Apr 2000.

Bridge, T.E. and M.T. Hussain. 1999. The Increased Draw Down and Recharge in Groundwater Aquifer and their Relationships to the Arsenic Problem in Bangladesh. http://www.dainichi-consul.co.jp/english/arsenic/arsarticles.htm

Bear, J. 1979. Hydraulics of Groundwater. McGraw-Hill, New York, 567 p

Baker, J.A., Davies, J. and Herbert, R.1989. The pilot study into optimum well design :IDA 4000 Deep Tube Wells II Project. Volume 4. Well and aquifer modeling.Part-1. A multi layer model for long term pumping tests. British Geological Survey Technical reports WD/89/11.

Brown, R.H. 1963. The cone of depression and the area of diversion around a discharge well in an infinite strip aquifer adjacent to uniform recharge, U.S. Geological Survey. Water supplies paper, 1545C, pp. C69-C85.

Bottomley, D.J., Gascoyne, M., and Kamineni, D.C.1990. The Geochemistry, age and origin of groundwater in a mafic pluton, East Bull Lake, Ontario Canada. Geochemica et Cosmochimica Acta 554,933-1008

Buckingham, E. 1994. Contribution to our knowledge of the aeration of soils. USDA Bur. Soil Bull.25

BGS (British Geological Survey and Mott MacDonald Ltd. (UK)) . 1999. Groundwater Studies of Arsenic Contamination in Bangladesh. Phase-1: Rapid Investigation Phase. Final report submitted to the Government of the People's Republic of Bangladesh.

Bagchi, K. S.1995. Irrigation in India, History and Potentials of Social Management. Published by UPALABDHI, Trust for Developmental Initiatives, 205, Kailash Hills, New Delhi-110 065.

BWDB. 1993. Hydrological map of Bangladesh. Scale 1:1,000000. Bangladesh

Water Development Board (BWDB) Dhaka.

BGS (British Geological Survey and Mott MacDonald Ltd(UK)) . 2001. Arsenic contamination of groundwater in Bangladesh. Technical report WC/00/19, volume.2.

Cramer, J.J and Smellie, J.A.T. 1994. Final report of the AECL/SKB Ciger Lake study. Atomic Energy of Canadian Limited Report, AECL-10951, COG-93-147

Charkraborti, D. 1996. Arsenic in ground waters in six districts of West Bengal, India, Environmental Geochemistry and Health, 18, 5-15, 1996

Chowdhury, T.R., Basu, G.K., Mandal, B.K., Biswas, B.K.,Samanta, G., Chowdhury, U.K., Chanda, C.R., Lodh, D., Roy, S.I., Saha, K.C., Roy, S., Kabir, S., Quamruzzaman, Q. and Chakraborty, D. 1999. Arsenic poisoning in the Ganges delta. Nature 401, 545-546.

Crites, Ron. (1998) Small and decentralized wastewater management systems

Clifford, D.A. and Zhang, Z. Arsenic chemistry and speciation. Proc.1993 Water Quality Technology Conference, AWWA, Denver, CO (1994).

Das, D., Basu, G., Chowdhury, T.R., Chakroborty, D., 1995. Brothel soil - sediment analysis of some arsenic affected areas. In Proc. Int. Conf. On Arsenic in Groundwater: Cause effect and remedy. Calcutta

Davis, J. and Exley, C. 1992. Short term BGS Pilot Project to Access the " Hydro chemical character of the main aquifer of Central and North eastern Bangladesh and Possible Toxicity of Groundwater to fish and human. Final Report. British Geological Survey. Technical Report WD/92/43R.

David, Spurgeon. 1995. Water: a looming crisis corporate report from IRRI-194-1996

Drever, James I.1988. The Geochemistry of Natural Water, Second edition. Prentice Hall, Englewood Clifts, New Jersey 07632.

Doorenbos, J. And W.O. Pruitt. 1979. FAO Irrigation and Drainage Paper No.24.

Dzombak, D.A. and Morel, M.M. 1990. Surface complexation modeling. Wiley and Sons, New York, 39 pp.

Franks, F. Ed., 1972. Water, A Comprehensive Treaty, Vol.1. New York: Plenum Publishing Corporation.

Freez, R.A. and Cherry, J.A. 1979. Groundwater. A text book published by the

PRENTICE HALL , Englewood Cliffs, NJ 07632

Ferguson, John F. and Gavis, Jerome.1972. A review of the arsenic Cycle in Natural Waters. Water Research, vol.6.pp1259-1274.

Goode, D.J.,.Hsieh, Paul .A., Shapiro, A.M.,.Wood, W.W., and Kraemer, T.F., 1993, Concentration history during pumping from a leaky aquifer with stratified initial concentration: P.29-35 in shen, H.W.,S.T.Su, and Feng Wen, (eds), Hydraulic Engineering "93, Proc.ASCE Hydraulics Div. National Conf., July 25-30,1993, Sanfrancisco, ASCE, New York

GOB (Government of the People Republic of Bangladesh), Department of International Development (UK)., 1999. Groundwater Studies for Arsenic contamination in Bangladesh, Final Review report submitted to the GOB, Vol-S1.

Graf, D. 1982. Chemical osmosis, reverse chemical osmosis, and the origin of subsurface brine. Geochim. Cosmochin.Acta, 46, 1431-1448.

Grenthe, L.W., Stumm,M., Laaksuharju, A.C., Nilsson and P.Wikberg.1992.Redox potentials and redox reactions in deep groundwater systems. Chemical Geology 98,131-150

Hanshaw, B.B., and T.B. Coplen.1973. Ul-trafication by a compacted clay membrane: II-Sodium Ion exchange at various ionic exchanges Cosmochim.Acta.37, pp 2311-2327.

JIID (Japanese Institute of Irrigation and Drainage). March, 2003. The Global Diversity of Irrigation . Pamphlet published in the 3rd World Water Forum Conference in Shiga , Japan. URL address: http://www.maff.go.jp/www/counsil/counsil_cont/nouson_sinkou/nogyo_noson_seibibukai/kikaku_syoiinkai/mizusigen.htm

Johnson, S.Y. and Alam, A.M.N. 1990. Sedimentation and Tectonics of the Sylhet Trough, Northeastern Bangladesh. United States Geological Survey. Open file report 90-313

Jones, Frank F.1992. Evaporation of water with emphasis on application and measurement text book published by Lewis publishers, Inc. 121 South Main Street, P.O.Drawer 519, Chelsea, Michigan 48118.

Kalita, Prasanta K. 1999. Transient finite element method solution of oxygen diffusion in soil, Ecological Modeling 118(1999) 227-236

Kent, D.B., J.A. Davies. 1994. Transport of chromium and Selenium in the sub-oxic zone of a shallow aquifer. Influence of redox and adsorption

reactions. Water Resources Research 30(4): 1099 -114.

Kinniburgh, D.G., Gale, I.N., Smedley, P.L. 1997. Applied. Geochemistry, 9,175-195

Khan, A.H., Rasul, S.B., and Hussain A. 2000. Appraisal of a simple arsenic removal method for groundwater of Bangladesh. J. Environmental Sci.Health, A35 (7), 1021-1041.

Khan, F.H. 1995. Geology of Bangladesh, Wiley, New Delhi

Khan, A.H., Rasul, S.B., and Munir, A.K.M.2000. Appraisal of simple arsenic removal method for groundwater of Bangladesh. J.Envron. Sc. Health.A35 (7), 1021-1041

Lovely, D.R. and Chapelle, F.H. 1995. Deep subsurface microbial process. Review of Geophysics, 33, 365-381

La Mer, V.K., and T.W. Healy. 1965. Evaporation of water: Its Retardation by Monolayers," Science 148: 36-42(1965).

Langmur, Donald. 1997. Aqueous environmental geochemistry. A text book published by Prentice Hall. Inc.

Masscheleyn, Patrick H., Delaune, Ronald D., and Patrick, William H. 1991. Effect of redox potentials and pH on arsenic speciation and solubility in a contaminated soil. Environ. Sci. Technol. Vol. 25, No.8. 1414-1419.

Mallick S. & Rajagopal, N.R. 1995.The mischief of oxygen in groundwater. Journal of Scientific and Industrial Research Vol. 54 May -June 1995, 329-330

Mallick Sukumar and Raja Opal N.R. 1996. Groundwater development in the arsenic -affected alluvial belts of West Bengal-Some questions. Current Science, Vol.70.No.11, 10 June 1996

Manning, B.A. and Goldberg, S.1997b. Arsenic (III) and arsenic (V) adsorption on threee California soils. Soil Science 162,886-895.

MPO (Master Plan Organization).1987. The groundwater resources and its availability for development. June 1987. Technical Report No.5. Submitted to the Ministry of Irrigation, Water Development and Flood Control, Government of the peoples republic of Bangladesh assisted by the United Nations Development Program(UNDP) and the World Bank.

Mok, W, M., and C.W. Wai. 1994. Distribution and mobilization of arsenic and antimony species in the Coeur D Alene river, Idaho, Env. Sci. Technlo.,

24: 102-108

Mukter, S., Baker, J.L., and Kanwar R.S. 1996. Effects of Short Term Flooding and Drainage on Soil Oxygenation. Transaction of the ASAE.Vol.39(3) 915-920.

MMI, 1992. Deep Tube well 11 Projects, Final report. Mott Macdonald International in associates with Hunting Technical Service. Report prepared for Bangladesh Agricultural Development Corporation (BADC), Dhaka, Bangladesh

Nickson, R. McArthur, J., Burgess, W., Ahmed, K.M., Ravenscroft, P., Rahman,M. 1998. Arsenic Poisoning of Bangladesh groundwater, Paper published in "Nature" Volume 395,338. (1998, September 24, page 338).

Nickson, R.T., McArthur, J.M., Ravenscroft, P., Burgess, W.G., Ahmed K.M. 2000. Mechanism of arsenic release to groundwater of Bangladesh and West Bengal, Applied Geochemistry 15 (2000) 403-413.

NRCC (National Research Council Canada). 1978. Effect of Arsenic in Canadian environment. A government report published by NRCC/CNRC, Ottawa, Canada KIA ORG. Publication No. NRCC 15391

NMIDP (National Minor Irrigation Development Projects). 2001. Main Report of National Minor Irrigation Census (NMIC), 1999/2000, Prepared by NMIDP & DAE Dhaka January 2001.

Obasi, G.O.P. 1999. The world waters: Is there enough? U.N. World Meteorological Organization, New York

Obasi, G.O.P. 1997. Saving water for the future, U.N. World Meteorological Organization, United Nations Center for Human Settlements (UN CHS/HABITAT), New York

Postma, D.; Bosen, C.; Kristiansen, H.; Larsen, F. Water Resource Research. 1991,27,2027-2045.

Pruitt, W.O. 1966. "Empirical method of estimating evapotranspiration using primarily evaporation pan". Conference proceeding. ASAE, 1966, 57-61.

Raven, K., Jain, A. and Loeppert, R. 1998. Environ. Sci.Technol., 32, 344-349

Roy Chowdhury, T., Basu, G.K., Samanta, G., Chanda, C.R., Mandal, B.K., Dhar, R.K., Chakraborti, D. 1998. In: Proceeding. Int. Conf. On Arsenic in Groundwater in Bangladesh: Causes effect and Remedies, Dhaka, 1998

Rochette, E.A., Li, G.C., and Fendorf, S.E.1998. Stability of Arsenate minerals in

soil under biotically generated reducing conditions. Soil.Sc.Soc. Am.J. 621530-1537

Ross, J.D. and M.Gascoyne.1993.Comparison of surface and down hole electrochemical measurements in research area groundwater on the Canadian Shield. Atomic Energy of Canada Limited Technical records. TR-591,COG-93-59

Refsgard J.C., Christensen T.H. & Ammentrop, H.C. 1991. A model of Oxygen Transport and consumption in the unsaturated zone. Journal of Hydrology, 129(1991) 349-369.

Scott, M.J., and Morgan, J.J.1995. Oxidation of Arsenic (III) by Synthetic Bimessite. Environ. Sci.Technol., 29, 1898-1905.

Segerlind, Larry J., 1997. Applied Finite Element Analysis. Book Published by John and Sons, New York.

Sullivan, K. A. and Aller, R. C. 1996. Digenetic cycling of arsenic in Amazon Helf sediments. Geochimica et Cosmochimica . Acta, 60,1465-1477

Stumm, Werner. and Morgan, James J.1996. Aquatic Chemistry, Chemical equilibrium and rates in natural water, 3rd Edition, Wiley Interscience.

Sun T., Wu K., Xing C. 1995. Epidemiological survey of endemic arsenic's in inner Mongolia Chinese/Endemiol (Proc. Endemic arsenic)

SOES (School Of Environmental Studies). 2002. Dug well Survey Report During February 2001. Jadavpur University, Calcutta-700 032. India. URL (http://groups.yahoo.com/group/arsenic-source/files/Chakraborti-dugwell-survey- report-during-F 8/12/01)

SOES/DCH 2000. Groundwater arsenic contamination in Bangladesh. Report of the School of Environmental Studies, Jadavpur University, Calcutta, India and Dhaka Community Hospital, Dhaka, Bangladesh.

Tsushima, Sachi. 1999. Arsenic Contamination in Ground Water in Bangladesh, Asia Arsenic Network

Thornton, I. and Farago, M.1997. The geochemistry of arsenic. In Abernethy, C.O. Calderon, R.L. and Chappell, W.R. Arsenic exposure and Health Effect Chapmann and Hall, London, 1-16.

USDHHS (United States Department of Health and Human Services). 1998. Draft Toxicological profile for arsenic. Agency for Toxic Substances and Disease registry. Division of Toxicology. 1600 Clifton Road NE, E-29.

Atlanta, Georgia 30333.

UNDP.1982. Groundwater surveys the hydrological conditions of Bangladesh. UNDP Technical Report DP

Varsanyi, L., Fodre, Z. and Bertha, A.1991. Arsenic in drinking water and mortality in the southern Great Plain, Hungary. Environmental Geochemistry and Health 13, 14-22.

Von Bernuth, R.D., Martin, Derrel L., Gilley, James R. and Watts, Darrell G. 1984. Irrigation System Capacities for Corn Production in Nebraska. Transactions of the American Society of Agricultural Engineers, 0001-2351/84/2702-0419502.00.

World Bank. 1998.Technical report on groundwater arsenic contamination problem in Bangladesh. World Bank, Bangladesh, 1998.

Welch, Alan H., and Lico, Michael S.1998. Factors controlling As and U in shallow water, southern Carson Desert, Nevada. Applied Geochemistry, vol.13, No.4.pp 521-539

Xu, H., B Allard, and Grimvall. 1991. Effect of acidification and natural organic materials on the mobility of arsenic in the environment, Water Air Soil Pollut., 57-58, 269-278, 1991